DESIGN AND REAL-TIME IMPLEMENTATION OF AN ADAPTIVE MICROGRID PROTECTION STRATEGY

BY

MUIZ MUHYEDDIN IZZAT ZABEN

A Thesis Presented to the
DEANSHIP OF GRADUATE STUDIES

KING FAHD UNIVERSITY OF PETROLEUM & MINERALS

DHAHRAN, SAUDI ARABIA

In Partial Fulfillment of the
Requirements for the Degree of

MASTER OF SCIENCE

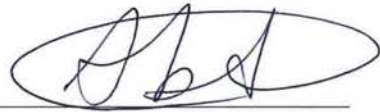In

ELECTRICAL ENGINEERING

APRIL, 2019

KING FAHD UNIVERSITY OF PETROLEUM & MINERALS

DHAHRAN- 31261, SAUDI ARABIA

DEANSHIP OF GRADUATE STUDIES

This thesis, written by**MUIZ MUHYEDDIN IZZAT ZABEN** under the direction of his

thesis advisor and approved by his thesis committee, has been presented and accepted by

the Dean of Graduate Studies, in partial fulfillment of the requirements for the degree of

MASTER OF SCIENCE IN ELECTRICAL ENGINEERING.

Prof. Mohammad AliAbido
(Advisor)

Dr. Abdallah S. Al-Ahmari
Department Chairman

Dr. Mohammad M. AlMuhaini
(Member)

Dr. Salam A. Zummo
Dean of Graduate Studies

Dr. Muhammad Khalid
(Member)

25/12/19

Date

I dedicate the work to my family

ACKNOWLEDGMENTS

First of all, I would like to thank Allah, the all Mighty, for giving me the strength and patience to complete this work.

I would like to thank my academic advisor **Prof. Mohammed A. Abido** for his unlimited support, guidance, and encouragement till completing this thesis.

I would like to send a special thanks to the Electrical Engineering Department represented by the chairman **Dr. Abdallah S. Al-Ahmari**.

I would also like to thank the committee members, **Dr. Mohammad M. AlMuhaini** and **Dr. Muhammad Khalid** for their suggestions and interest in my work.

TABLE OF CONTENTS

LIST OF TABLES

LIST OF FIGURES

LIST OF ABBREVIATIONS

AC	:	Alternating Current
APS	:	Adaptive Protection System
AVR	:	Automatic Voltage Regulator
CB	:	Circuit Breaker
CT	:	Current Transformer
DG	:	Distributed Generator
DOCR	:	Directional Overcurrent Relay
DC	:	Direct Current
DFT	:	Discrete Fourier Transform
FCL	:	Fault Current Limiter
FRT	:	Fault Ride Through
GOOSE	:	Generic Object-Oriented Substation Event
HPOTT	:	Hybrid Permissive Overreaching Transfer Trip
IBDG	:	Inverter Based Distributed Generator
IEC	:	International Electrotechnical Committee
IED	:	Intelligent Electronic Device

IEEE	:	Institute of Electronics and Electrical Engineers
LAN	:	Local Area Network
LD	:	Logical Device
LOM	:	Loss of Main
LN	:	Logical Node
LV	:	Low Voltage
MV	:	Medium Voltage
OC	:	Overcurrent
POTT	:	Permissive Overreaching Transfer Trip
PCC	:	Point of Common Coupling
POI	:	Point of Interconnection
PI	:	Proportional Integral
PLL	:	Phase Locked Loop
RBDG	:	Rotating Machine Based Distributed Generator
RTDS	:	Real-Time Digital Simulator
VSI	:	Voltage Source Inverter

ABSTRACT

Full Name   : [Muiz Muhyeddin Izzat Zaben]

Thesis Title   : [Design and real-time implementation of an adaptive microgrid protection strategy]

Major Field   : [Electrical Engineering]

Date of Degree : [April 2019]

The integration of renewable energy sources into distribution networks and the implementation of microgrids disturb the conventional protection schemes and create new protection challenges that stand against microgrid practical implementation in near future. In this thesis, a decentralized adaptive protection strategy was developed for a benchmark MV AC microgrid with high penetration of rotating machine based and inverter based distributed generators. Hybrid Permissive Overreaching Transfer Trip (HPOTT) scheme and Fast Bus Tripping (FBT) scheme are proposed to provide high speed fault clearing of distribution line and bus faults in both grid-connected and islanded modes of operation. The proposed scheme includes also the protection of distributed generators and the point of common coupling considering the voltage/frequency fault ride through requirements. A decentralized communication architecture based on IEC 61850 Generic Object-Oriented Substation Event (GOOSE) protocol is used to transfer the connection status of DGs and microgrid to every adaptive relay in the system. The relays use this information to activate the appropriate protection settings. Moreover, the same communication network is used to implement the HPOTT scheme and the FBT scheme. The proposed strategy also offers backup protection against communication network failure. A hardware-in-the-loop (HIL) test setup based on Real-Time Digital Simulator (RTDS) and commercial relays was used

to verify the operation and effectiveness of the proposed protection scheme. The study was conducted on a modified benchmark MV AC microgrid, and the results showed the effectiveness of the proposed protection strategy in clearing distribution line and bus faults at high speed under different operating scenarios.

ملخص الرسالة

الاسم الكامل: معز محي الدين عزت زين

عنوان الرسالة: تصميم وتطبيق في الوقت الحقيقي لاستراتيجية حماية متكيفة للشبكات الصغيرة

التخصص: هندسة كهربائية

تاريخ الدرجة العلمية: نيسان 2019

إن دمج مصادر الطاقة المتجددة مع شبكات التوزيع بالإضافة إلى تطبيق الشبكات الصغيرة، أدت إلى تعطيل نظم الحماية التقليدية وأدت إلى خلق مشاكل حماية جديدة قد تحول دون التطبيق العملي للشبكات الصغيرة في المستقبل القريب. في هذه الأطروحة، تم تطوير نظام حماية تكيفي لا مركزي لحماية شبكة قياسية صغيرة ذات ضغط متوسط وذات اختراق عالي من المولدات الموزعة القائمة على أساس الالات الدوارة و العواكس الكهربائية. تم اقتراح مخطط إرسال إشارة فصل متخطي هجين السماحية (HPOTT) ومخطط فصل سريع لقضبان التوصيل (FBT) لتوفير نظام فصل أخطاء عالي السرعة لخطوط التوزيع وقضبان التوصيل في الوضعين المتصل مع الشبكة والمعزول. يتضمن المخطط المقترح أيضًا حماية المولدات الموزعة ونقطة التوصيل المشتركة مع الأخذ في الاعتبار متطلبات ثبات الجهد والتردد. تم استخدام بنية اتصالات لامركزية مستندة إلى بروتوكول (Generic Object-Oriented IEC 61850 Substation Event (GOOSE) لنقل حالة اتصال المولدات الموزعة والشبكة الصغيرة إلى كل المرحلات المتكيفة.تستعمل المرحلات هذه المعلومات لتفعيل مجموعة إعدادات الحماية المناسبة. بالإضافة إلى ذلك، تم استخدام نفس شبكة الاتصالات لتنفيذ مخطط ال HPOTT ومخطط ال FBT. توفر الإستراتيجية المقترحة أيضًا حماية احتياطية ضد فشل شبكة الاتصالات. تم استخدام نظام اختبار للأجهزة داخل حلقة (HIL) بناءً على برنامج للمحاكاة في الزمن الحقيقي (RTDS) ومرحلات تجارية لاختبار عمل وفاعلية مخطط الحماية المقترح. وقد طبقت الدراسة على شبكة قياسية وأظهرت النتائج فعالية استراتيجية الحماية المقترحة في فصل أعطال خطوط التوزيع وقضبان التوصيل بسرعة عالية تحت سيناريوهات تشغيل مختلفة.

CHAPTER 1

INTRODUCTION

1.1   Motivation and Problem Statement

The increased power demand, and the threats of climate changes have accelerated the proliferation of distributed generation from sustainable energy resources and led to the concept of microgrid. The U.S. Department of Energy defines microgrid as: "*a group of interconnected loads and distributed energy resources (DERs) with clearly defined electrical boundaries that acts as a single controllable entity with respect to the grid and can connect and disconnect from the grid to enable it to operate in both grid-connected or island modes*" [1]. In recent years, the deployment of microgrid concept has increased significantly. According to a survey done by Navigant Research, the installed microgrid capacity is estimated to grow from 1.4GW in 2015 to 7.6GW by 2024 [2]. Microgrid concept offers many benefits such as increased reliability, enhanced efficiency, improved power quality, and reduced carbon emissions [3-5]. On the other hand, microgrid raises a number of technical challenges that stand against its widespread in the near future, among them is the need to design new protection strategies [6, 7].

Distribution networks are conventionally designed to operate in radial configuration where the power flows form central substations to distributed loads in one direction from upstream to downstream. The fault current magnitude in such systems is relatively high

compared to maximum load current. This structure allows protection engineers to use simple protection devices such as non-directional overcurrent relays (50/51), fuses, reclosers, and sectionalizes, etc. to protect the distribution system. These devices have low cost and can be coordinated with each other simply through proper selection of time current characteristics, pickup current settings, and time delays such that the minimum part of the distribution system will be isolated after fault clearance. The integration of distributed generators to the distribution network disturbs the radial structure and creates bidirectional fault currents. In addition, the intermittent nature of DGs combined with the changes in microgrid mode of operation (grid connected and islanded modes) and the changes in network structure cause both the non-fault and fault currents to change continuously in magnitude and direction. Consequently, conventional protection schemes with fixed protection settings become insufficient to meet protection requirement under such circumstances [8, 9]. Moreover, the presence of inverter based DGs (IBDGs) in microgrid creates additional challenges. The fault current supplied by IBDGs is limited by their control system to 1.5-2 pu [10]. This behavior challenges the sensitivity of overcurrent protection devices especially at islanded mode. Additionally, IBDGs have no stored kinetic energy, therefore, microgrids with high penetration of IBDGs will exhibit low frequency and voltage ride through [11]. Faults at islanded mode may cause instantaneous variation in frequency and voltage, consequently, the voltage and frequency protection of DGs may overtrip quickly before main protection operates [12, 13]. Accordingly, there is a need to develop new protection strategies to tackle the protection challenges imposed by DG integration and microgrid implementation at minimum cost to enable wide spread on microgrid concept in near future.

1.2 Thesis Objectives

The thesis objectives can be summarized as follows:

Objective 1: Building and simulation of a benchmark AC microgrid system in Real Time Digital Simulator (RTDS which includes rotating machine based and inverter based Distributed Energy Resources and their control system.

Objective 2: Developing a comprehensive microgrid protection strategy that covers all microgrid protection elements and is suitable for grid connected mode and islanded mode of operation.

Objective 3: Implementing and testing the proposed protection strategy in Real Time Digital Simulator (RTDS) based on Hardware In the Loop (HIL) with commercial microprocessor based relays.

1.3 Thesis Contributions

- The main contribution of this thesis is the development of a decentralized adaptive protection strategy based on Hybrid Permissive Overreaching Transfer Trip (HPOTT) for MV looped AC microgrid. Few numbers of publications have addressed the application of adaptive pilot protection schemes such as POTT to microgrid protection. The existing publications found in literature proposed POTT scheme with DOCR relays [14, 15], however, the proposed schemes used basic comparison logic that requires both terminals to pick up for forward fault to issue trip command. Such schemes will fail to trip at high speed if either terminal (not both) fail to detect the fault. Such conditions

can happen frequently in microgrids under certain conditions such as weak infeed from DGs, removal of infeed due to DG disconnection, and one circuit breaker open. Therefore, basic POTT scheme proposed in literature is not suitable for Microgird protection. In this thesis, the proposed HPOTT scheme with integrated echo logic and weak infeed logic solves this problem and allows double end disconnection under weak infeed, loss of infeed, and remote open terminal conditions. On the other hand, the existing publications were based on non-real time simulation. In this thesis, hardware-in-the-loop (HIL) test setup was developed using Real-Time Digital Simulator (RTDS) and commercial relays. Therefore, the results in this thesis is more reliable.

- The second contribution of this thesis was the development of an adaptive protection strategy based on programmable logic of modern microprocessor-based relays. The salient feature of the proposed adaptive technique is that setting adaptation is achieved using the IED's programmable logic without changing the IED group setting. The developed logic allows for larger number of change instances while making the change in protection settings instantaneous. On the other hand, the majority of proposed adaptive protection schemes [16-28] require the relay to change the setting group in response to changes in microgrid operation and topology. The drawback of this approach is not only the limited number of setting groups available in the relay, but also, the relay will be disabled for a period of time while the group is being changed. this approach therefore reduces the relay reliability and limits the number of changes that can be done. Therefore, the proposed approach in this thesis will not only increase the relay availability, but it will also increase the number of scenarios for which the relay setting can be adapted.

1.4 Thesis Organization

This thesis includes 8 chapters which are organized as follows:

Chapter 1 gives an overview of the thesis, its objectives and main contributions. It also briefly presents the methodologies and research technique to be used in the research.

Chapter 2 presents a detailed overview of the DG integration impact on conventional distribution system protection, and the microgrid protection challenges. This chapter also present a critical review and analysis of the available adaptive protection strategies for microgrids and distribution networks operating with DGs. The presented methods are critically analyzed and categorized into groups to identify the current research status and to identify the research gaps and possible future enhancements.

Chapter 3 reviews the basics of distribution system protection techniques with focus on overcurrent element, and directional element. These protection elements are the basic building blocks of the proposed protection scheme.

Chapter 4 presents a detailed modeling and simulation of MV microgrid in Real Time Digital Simulator (RTDS) including the distributed generators model, the distribution network model, and the microgrid control system.

Chapter 5 presents the proposed decentralized adaptive protection strategy using commercial off-the-shelf microprocessor-based relays to protect the MV AC microgrid with rotating based and inverter based DGs.

Chapter 6 presents the experimental setup required to for Hardware In the Loop Testing.

Chapter 7 presents the validation and testing of the proposed protection strategy in RTDS based on Hardware In the Loop (HIL) simulation with commercial protective relays.

Chapter 8 presents the conclusion, and future work.

CHAPTER 2

LITERATURE REVIEW

One of the major challenges that stands against widespread of microgrid concept in the near future is to devise a cost-effective protection strategy that can meet protection requirements under different microgrid operation modes, system configuration changes, and connection/disconnection of DGs. This chapter first reviews the impact of DG integration on conventional distribution network protection. The particular challenges related to microgrid protection are then presented. Finally, the available microgrid protection solutions are reviewed, analyzed, and research gaps are identified.

2.1 Impact of DG Integration on Conventional Distribution Network Protection

Distribution networks are conventionally designed to operate in radial configuration where the power flows form central substations to distributed loads in one direction from upstream to downstream. The fault current magnitude in such systems is relatively high compared to maximum load current. This structure allows protection engineers to use simple protection devices such as non-directional overcurrent relays (50/51), fuses, reclosers, and sectionalizes to protect the distribution system. These devices have low cost and can be coordinated with each other simply through proper selection of time current characteristics, pickup current settings, and time delays such that the minimum part of the distribution system will be isolated after fault clearance. The integration of distributed generators to the distribution network distorts the distribution network structure in several

ways. Firstly, the power generation becomes decentralized, and the fault current becomes bidirectional, this means that fault current can flow in multiple paths and directions that are not necessarily considered in conventional protection schemes. Secondly, the fault current magnitude becomes constantly changing due to the plug and play nature of DGs. Thirdly, the generated power comes not only from rotating machine distributed generation (RBDG), but also form inverter based distributed generators (IBDGs) which have different fault current characteristics. Since conventional protection devices are mostly non-directional, and have fixed protection settings, the aforementioned changes will cause sensitivity loss and/or mis-coordination of relays, fuses, and automatic reclosing schemes[29, 30] . In this section, these issues will be elaborated and explained.

2.1.1 Sympathetic Tripping

Sympathetic tripping (False tripping) refers to undesired operation of a protection relay for out of section faults. Integration of distributed generation can cause two types of sympathetic tripping:

1) Overcurrent Relay Sympathetic Tripping

In conventional distribution networks, overcurrent relays are designed to respond to the fault in one direction. Integration of distributed generation creates bidirectional power flow, therefore, reverse fault current from DGs may cause overcurrent protection devices to trip unnecessarily for faults in upstream side or in parallel feeders. Figure 2-1 shows typical radial distribution feeder. Fault at location F1 may cause the relay R3 to trip unnecessarily due to reverse fault current contribution from DG [31, 32].
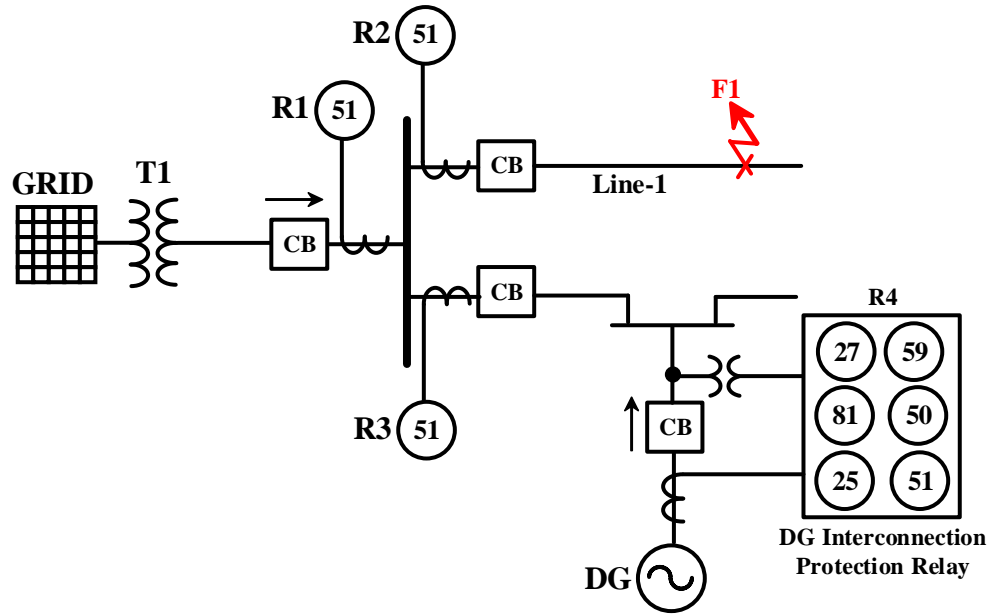
Figure 2-1: Typical Distribution Feeder with DG and Overcurrent Relays

2) DG Interconnection Relay Sympathetic Tripping

As shown in Figure 2-1, distributed generators are normally equipped with interconnection protection relays which contains protection functions such as over/under voltage (27/59), and over/under frequency (81U/O). Faults on neighboring feeders may cause the interconnection relay to operate before the main overcurrent protection clears the fault, this will lead to unnecessary disconnection of DG for a fault outside its zone of protection [33].

2.1.2 Reduction or Loss of Sensitivity

To understand the effect of DG integration on overcurrent relay sensitivity, the fault current contribution from utility and DG will be estimated for three phases bolted fault (F1) as shown in Figure 2-1. The distribution system of Figure 2-1 can be represented using the equivalent circuit o shown in Figure 2-2 where VS, and VDG represent the utility voltage, and the DG voltage respectively. ZS, ZT, ZDG, and ZL2, represent the equivalent impedance of the utility, the transformer, the DG, and the distribution line-1 respectively.

9
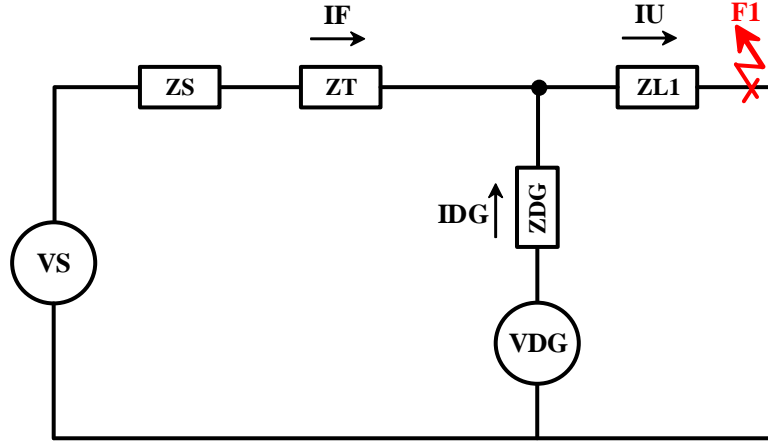
Figure 2-2: Equivalent Circuit of Typical Distribution Feeder in Figure 2-1

If the DG is considered initially unavailable, a three-phase fault current at F1 can be simply expressed as:

$$(Without\ DG) \qquad I_{F1} = \frac{V_S}{Z_S + Z_T + Z_{L1}} \qquad\qquad (2.1)$$

After adding the DG, the fault current at F1 can be written as:

$$(With\ DG) \qquad I_{F1} = \frac{V_S}{Z_{L1} + \frac{Z_{DG}.(Z_S + Z_T)}{Z_{DG} + (Z_S + Z_T)}} \qquad\qquad (2.2)$$

Accordingly, the fault current contribution from the DG can be written as:

$$I_{DG} = I_{F1}\ \frac{Z_S + Z_T}{Z_{DG} + Z_S + Z_T} \qquad\qquad (2.3)$$

and the fault current contribution from the utility source can be written as:

$$I_U = I_{F1}\ \frac{Z_{DG}}{Z_{DG} + Z_S + Z_T} \qquad\qquad (2.4)$$

It is noted from equation (2.4) that the addition of DG will always cause reduction in fault current contribution from utility source. The amount of reduction depends on the type, size,

and location of DG. This reduction will cause the overcurrent relay R1 shown in Figure 2-1 to have delayed tripping for faults on at F1 location, and therefore the selectivity between R1 and R2 will be compromised. In some cases, the fault current seen by the relay R1 may become less than its pick-up value, thus it may fail to detect the end of line fault at F1, this is referred to as blinding of protection or underreach [8, 9].

2.1.3   Reclosing Schemes Miscoordination

In distribution systems, 70%   to 80% of faults are temporary in nature [34], automatic reclosers are often used to clear temporary faults without human intervention. Moreover, reclosers are coordinated with branch fuses to prevent the fuse from blowing for transient faults on its branch, this is known as fuse saving scheme [34]. Figure 2-3 shows a typical radial distribution feeder with one line-recloser, one branch fuse, and one DG.
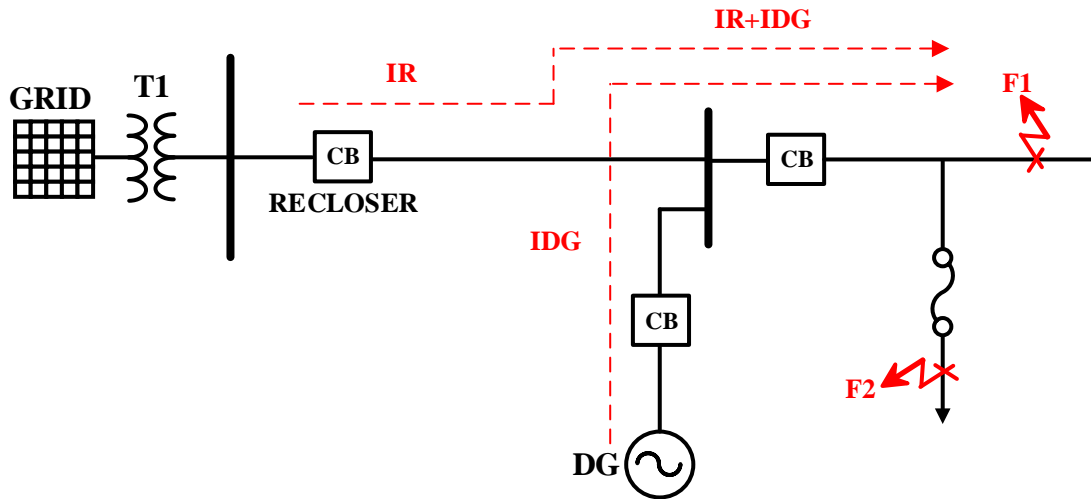
Figure 2-3: Typical Distribution Feeder with DG, Fuse, and Recloser

Assuming the DG in Figure 2-3 initially not available, the fuse and recloser are coordinated as shown in Figure 2-4. The recloser fast curve is located below the fuse Minimum Melting Time (MMT) curve, and the recloser slow curve is located above the fuse Total Clearing Time (TCT) curve. For temporary faults, the recloser trips using the fast curve and recloses

11

after time delay to allow the fault to be cleared. For permanent faults, the recloser trips using the slow curve to allow the fuse to clear the fault, and to provide backup protection in case of fuse failure, or in case the fault is not on the fuse branch. The recloser normally perform 2-3 fast tripping/time delayed reclosing attempts to ensure fault is cleared before switching to the slow curve. Fuse saving scheme is generally valid under two conditions: (a) the same fault current shall pass through the fuse and the recloser, and (b) the fault current shall not exceed the maximum and minimum values (I_{fmin}, and I_{fmax}) indicated in Figure 2-4 [35].
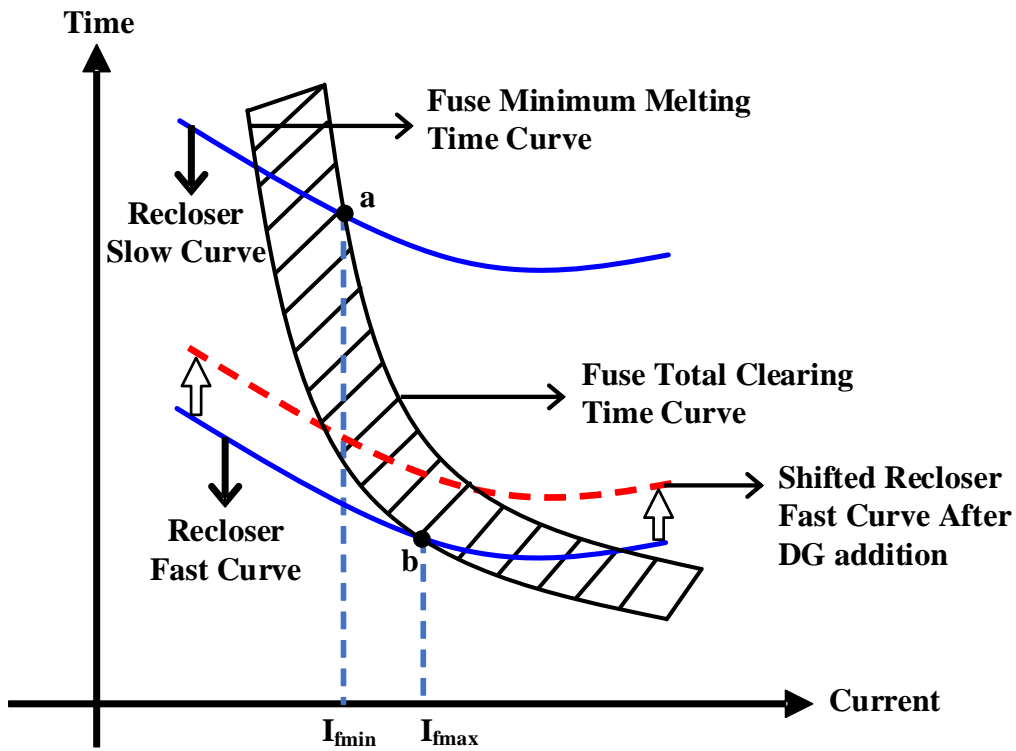
Figure 2-4: Example of fuse recloser mis-coordination due to DG Addition [33, 35]

Assuming one DG is added between the fuse and recloser as shown in Figure 2-3, the following miscoordination issues may occur:

(1) For fault at F1, the fault current contribution includes the DG fault current (IDG), and the recloser fault current (IR). However, the current that passes through the recloser is only IR, therefore, the recloser will either have slower operating time, or in the worst case, it may become blind to the fault. Accordingly, the automatic reclosing scheme will be prohibited from operating [36].

(2) For fault at F2, the DG fault current contribution causes the fuse to see higher current than the recloser. Depending on the DG rating, the fuse fault current may exceed the I_{fmax} shown in Figure 2-4, this is equivalent to shifting the characteristic of the recloser above the MMT curve of the fuse as shown in Figure 2-4, consequently, the fuse may blow before the recloser trips, and thus the fuse saving scheme collapses [35].

(3) Assuming the recloser trips before the fuse for fault at F2, during the recloser dead time, the DG fault current will sustain the fault arc and prevent it from de-ionizing. Moreover, during reclosing deadtime, the generator voltage and frequency will shift from the grid voltage and frequency due to generation and load imbalance, consequently, unsynchronized reclosing may occur upon reclosing which may cause damage to the DG and the distribution network equipment [36].

In summary, the effect of DG addition prohibits automatic reclosing, disturb the fuse saving scheme, and may cause unsynchronized reclosing.

2.1.4 Exceeding Short Circuit Level

Addition of distributed generation increases the fault current level in the network. Depending on the rating of distribution system equipment and the power rating/type of added DGs, the short circuit level may exceed the ratings of distribution equipment such as switchgears, distribution line, etc. Moreover, increased short circuit level may cause CT

saturation. To overcome these issues, the distribution network operator may need to replace the equipment or to install fault current limiters. In both cases, there will be considerable added cost [31, 32, 37].

2.1.5 Undetected Islanding

Islanding refers to the situation when part of a distribution network containing Distributed Energy Resources (DERs) is disconnected from the main utility supply while the DERs continue to energize the isolated network. Islanding can be intentional or unintentional. Unintentional islanding is an unpanned event which may occur due to disturbance on grid side such as external faults, sub-transmission system blackout, and circuit breaker failure. If unintentional islanding situation is not detected, it may cause the following [8, 38-40]:

1) DG will produce uncontrolled voltage and frequency that may exceed the permissible limits, thus causing damage to the DGs, distribution company equipment, and customer equipment.

2) Electrocution of maintenance personnel.

3) Out of phase reclosing.

To protect against unintentional islanding, DGs shall be equipped with protection relays that detected the islanding situation quickly and trip the DGs accordingly, such relays are known as Anti-Islanding relays or Loss of Main (LoM) relays. According to IEEE 1547-2018 [41], intentional islanding is a planned event in which the distribution network is designed to get energized by local DGs and can operate in parallel and disconnect from utility. Intentional islanding can be scheduled and unscheduled. Scheduled intentional islands are formed either manually through network operator or automatically through

14

operating dispatch means such as Automatic Generation Control (AGC). Unscheduled intentional islands are planned events that occurs due to abnormal conditions at the point of connection with the upstream distribution network. In this case, the islanded area is equipped with necessary detection and control means that detects the abnormal condition and initiate an automatic disconnection from utility grid rapidly [41]. From previous discussion, it is noted that "intentional islanding" described by IEEE 1547-2018 is similar to the concept of future microgrids, therefore, fast and reliable islanding detection relays would be necessary for the following reasons:

1) To enable modifying the DG control system from current control mode for example to voltage and frequency control, such that the produced voltage and frequency are controlled within the island.

2) To enable the protection relays to modify the protection settings to suite the islanded mode (if any).

2.2   Microgrid Protection Challenges

In addition to the previous issues cause by DG integration in general, there are particular protection challenges which arise when the network is intended to operate as microgrid. Firstly, there is a sharp difference in fault current level between grid connected mode and islanded mode. Secondly, the islanded microgrid will have reduced or no inertia depending on the type/number of connected DGs. Moreover, the fault current characteristics of IBDGs creates difficulties for current based protection devices [8, 9]. In this section, the microgrid protection issues will be elaborated and explained.

2.2.1   Continuous Change in pre-fault and fault currents

The intermittent nature of renewable energy based DGs combined with the change in microgrid mode of operation, and the changes in network topology (radial to looped, load shedding, feeder tripping, etc.) causes the feeder currents and short circuit levels at every relay location to change continuously both in magnitude and direction. Consequently, overcurrent-based protection schemes with fixed protection setting become insufficient to meet protection requirement under all operating scenarios [8, 14].

2.2.2   High Capital Investment in Microgrid Protection System

Considering the complex operation of microgrid, distribution networks operation becomes similar to transmission systems. Therefore, sophisticated protection schemes are required to avoid power interruptions and blackouts. In case of transmission systems, high capital investment in protection systems can be easily justified due to large affected area. However, in case of microgrids, it is difficult to justify investment in complex protection schemes as the failure does not impact large area. This issue may limit the acceptance of microgrid concept in the future unless cost effective and realistic solutions are proposed [42].

2.2.3   Impact of IBDG Fault Current Characteristic

The conventional protection relays such as overcurrent, distance, directional element, etc., were design assuming fault contribution from rotating machine based DGs. However, the fault current characteristic of IBDGs is dictated by its control system and has very different characteristic compared to RBDGs. These characteristics may not be observable at grid connected mode since the majority of fault current is contributed from main grid. However, at islanded mode with several IBDG sources, these characteristics cannot be ignored. The

16

impact of IBDGs on protection system performance and the challenges it creates can be summarized as such:

2.2.3.1 Reduction or loss of sensitivity of overcurrent relays

Unlike rotating based DGs which behaves as a voltage source during the fault, the IBDGs behaves as a current source during fault. The inverter control system normally limits the maximum fault current to 1.5-2 times the rated current to protect the power electronic switches [10]. The fault current contribution from IBDG may become becomes close to the rated of a distribution line or even more. Therefore, overcurrent detection becomes extremely difficult or impossible. Inverse time overcurrent relay will be subject to blinding of protection or slow operation time. It should be noted that such low magnitude fault current are less likely to cause damage to equipment. However, it is still dangerous for people and equipment, therefore, it must be cleared for safety purposes.

2.2.3.2 Voltage support during ground faults

Unlike RBDG, the voltage characteristic of IBDG under unbalanced faults depends on the control system design. In most cases, the IBDGs are current controlled voltage sources in which the control system tries to balance the inverter contribution to the fault as required by grid code. Consequently, the contribution will be positive sequence only, which makes fault detection more difficult. Moreover, the fast voltage control of inverter may cause (in addition to small fault current contribution) an overvoltage on healthy phases, which in turn may impact the protection sensitivity, and/or cause sympathetic tripping of DGs [43].

2.2.3.3   Mis-operation of Directional element

In reference [42], it is found that the conventional directional elements based on sequence components may mis-operate under certain conditions due to some fault current characteristics of IBDGs. Therefore, the application of directional element in IBDG dominated microgrid must be carefully studied.

2.2.3.4   Multiple control modes of operation

In reference [27], it is shown that IBDG's behaviors during fault is dependent on the inverter control mode, i.e., voltage control mode, or current control mode. It is found that the current controlled IBDGs ability to regulate their output voltage is very poor, and they depend on the connected grid. However, during grid absence at islanded mode, the current controlled IBDG becomes vulnerable to voltage drop depending on the strength of other connected sources. In contrast, voltage controlled IBDGs have better voltage control ability at islanded mode, but they have very poor current control ability which makes them vulnerable to overcurrent. The author concluded that protection requirement of voltage controlled IBDGs is different from current controlled IBDG, therefore, adaptive protection may be required when inverter operate in multiple control modes [27]. In practice however, microgrid may contain several IBDG source from different manufacturers with different control system and different fault characteristic. Since IBDG manufacturers rarely share detailed information about their control system, the fault current behavior remains ambiguous and unknown to protection system engineers.

2.2.4   The Need to Trip Faster

Distribution networks are normally connected to stiff grids. At grid connected mode, the system is characterized by high fault current contribution, high inertia, and thus stable

voltage/frequency. Overcurrent devices can operate quickly to clear the fault, and the DGs can meet the Fault Ride Through (FRT) requirements relatively easier than islanded mode. At islanded mode on the other hand, the absence of main grid creates challenges for both protection system and control system due to the following reasons:

(1) Reduction in system inertia:

At islanded mode, the inertia comes only from RBDGs. Inverter based DGs does not contribute to the inertia of the system. Therefore, faults at islanded mode causes power system frequency to change quickly. If the microgrid has only IBDG sources, the system inertia become zero. Consequently, the changes in power system frequency under any disturbance becomes instantaneous. This may cause the DG frequency protection to trip quickly before main protection operate to clear the fault [12, 13].

(2) Reduction in short circuit power

Th absence of main grid causes the short circuit level to drop sharply. Fault current contribution of DGs is relatively low compared to main grid. Consequently, faults at islanded mode causes severe voltage drop. In extreme cases when the microgrid consist only of IBDGs, the required fault current cannot be supplied due to the fault current limiting characteristic of inverters, this issue causes the voltage at the IBDG output to drop sharply leading to quick disconnection of DGs before operation of main protection.

As mentioned in section 2.2.3.1, the reduced fault current at islanded mode, and the limited fault current feeding capability of IBDGs causes overcurrent protection to underreach or to trip slowly. Comparing this behavior with fast/instantaneous variation in voltage and frequency, we found a conflicting behavior between control and protection system. The

protection system based on time overcurrent becomes slower, and the DG gets disconnected faster (have low FRT). Therefore, conventional protection methods based on inverse time overcurrent for example cannot meet the speed requirement at islanded mode. In fact, there is a need to develop new fast protection methods that can clear the fault before the frequency and voltage protection of DGs operate. These protection methods shall either be adaptive or shall be current level independent. At the same time, from control prospective, the FRT capability of DGs shall be enhanced such that DGs can withstand longer duration. The two approaches together will enhance the microgrid stability and reliability.

2.2.5 Transformer DG Grounding at islanded mode

At MV microgrid, distributed energy resources are normally coupled to the main network using interfacing transformer, the grounding method of this transformer will have significant impact on the protection system. When a microgrid gets islanded, the grounding support from utility will be disconnected, under such conditions, the system will be mainly grounded by the interfacing transformer and DG. Therefore, if the DG and interfacing transformer do not effectively ground the microgrid as shown in Figure 2-5, then ground faults at islanded mode may cause dangerous overvoltage [44]. Accordingly, suitable interconnection transformer must be considered.
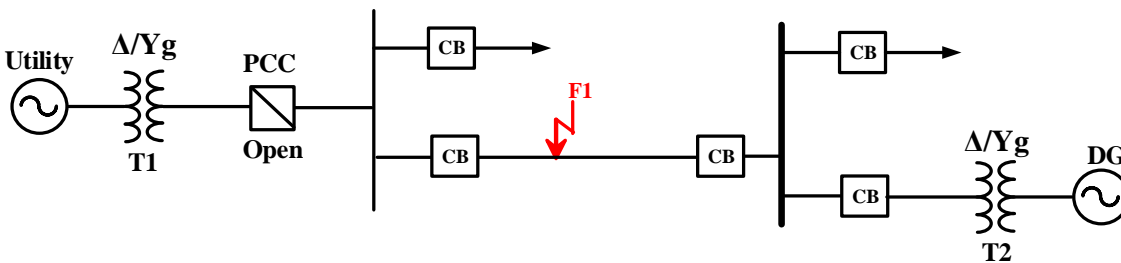
Figure 2-5: Overvoltage due to ground fault at islanded mode [45].

2.3   Fault Detection Methods and Their Application

Extensive research has been done to find proper solution to DG integration impact and microgrid protection, this section presents a thorough review of the available fault protection solutions of microgrid and active distribution networks.

2.3.1   Directional Overcurrent Protection

Conventional overcurrent relays cannot be coordinated in looped systems or in radial systems integrated with multiple DGs due to bidirectional power flow. Directional overcurrent relays (ANSI 67) restricts the overcurrent relay response to one direction, and therefore, it simplifies the coordination of time overcurrent relays and prevents sympathetic tripping. In [46], a protection strategy based on directional phase and ground over current relays was proposed to protect a biomass microgrid. In [35], a microprocessor based recloser with directional element is proposed to maintain fuse saving scheme in a distribution network integrated with DGs. Optimization techniques are often employed to solve DOCR coordination problems in meshed distribution systems. In [47-49], the coordination problem is formed as a constrained nonlinear programming problem (NLP) to determine the optimal relay settings. In [47], DOCRs with user defined characteristic is proposed. In [48], a new DOCR tripping characteristic based on current, voltage, and time is proposed to reduce the relay operating time. In [49], a dual setting DOCRs equipped with different tripping characteristic for each direction is proposed. However, all previous proposals assumed grid connected mode of operation and rotating based DGs. It can be concluded from available literature that directional overcurrent relays alone cannot provide complete solution of microgrid in both modes of operation.

2.3.2 Installing Fault Current Limiters (FCL)

Fault Current Limiter (FCL) is a device whose impedance is near zero under normal operating condition and increases to certain higher value under fault condition [50]. FCLs were initially introduced in microgrids to overcome the problem of variable fault current contribution caused by DG integration in grid connected mode. In [51], the author proposed a hybrid type FCL connected in series with every DG to limits their fault current contribution. A genetic algorithm-based overcurrent coordination technique is used to get optimal settings under transient conditions. However, the previous proposal was limited to grid connected mode of operation. The work in [52, 53] extended the concept and applied FCL in both grid connected mode and islanded mode, the FCL was connected in series between microgrid and main grid to limit the fault contribution from grid side. In [52], the FCL size and the optimal settings of directional over current relays were chosen by solving a constrained non-linear programming problem based on Genetic Algorithm (GA). In [53], a hybrid optimization technique based on Cuckoo Optimization Algorithm and Linear Programming (COA-LP) was used. However, the previous proposals [52, 53] considered rotating machine based DGs only.

2.3.3 Installing Fault Current Source (FCS)

One way to overcome the limited fault current of inverter based DGs in islanded mode of operation is to raise the fault current level by adding Fault Current Sources (FCSs) such that overcurrent relays can detect the fault easily. In [54], the author proposed adding a flywheel system to increase fault current level in islanded mode. In [55], supercapacitor energy storage system are installed at the DC link of each renewable based DER to increase its fault current injection capability. Once fault is identified, the DER closer to the fault

inject higher fault current the value of which is proportional to the measured impedance according to a droop curve. Therefore, the relay closer to the fault trips faster. In [56], super capacitor was utilized to inject fault current at islanded mode such that relays can sense the fault and clear it selectively, this happens only when the primary adaptive protection fails to switch to a low pickup setting due to failure in communication system.

2.3.4 Harmonic Based Protection

In [57], the author proposed a communication assisted protection technique for inverter dominated microgrid based on the harmonic content of inverter output voltage. Fault type is specified by monitoring the change in fundamental frequency amplitude and the Total Harmonic Distortion (THD) of all phases. Fault location is identified by communicating the sum of THD at each relay location to other relays, if the local THD is higher compared to remote THD, then fault is internal and trip command is issued accordingly. In [58], the author proposed a protection strategy for inverter based DGs in islanded microgrid. In this method, the control system of the inverter is modified such that during short circuit condition, a certain amount of fifth harmonics are injected, then a sliding window FFT based digital relay installed at the output of the inverter is used to detect these fifth harmonics and thus detecting fault condition.

2.3.5 Park Transform Based Protection

In [59], the author proposed a microgrid protection strategy based on the park transformation of three phase voltages. A disturbance signal VDIST is obtained by subtracting the measured q-axis component Vq from reference value Vqref. The disturbance signal VDIST is passed through a low pass filter and a hysteresis comparator the limits of which represent the sensitivity of fault detection. Suitable time delays are

23

assigned to ride through transient voltage sags during fault. However, since the method depends on voltage, selectivity cannot be guaranteed in small scale microgrids. In [60], a protection scheme based on park transformation of voltages combined with directional element is proposed for islanded microgrid with IBDGs. In this scheme, fault detection and fault type can be identified by monitoring the changes in the dq-components of voltage which is found to be distinct for every type of fault. Dual setting definite time grading strategy is proposed to achieve selectivity in radial feeders with multiple sections. To improve selectivity, the author in [61] proposed adding communication link between adjacent relays to share the measured values. By comparing the remote and local disturbance voltage signal VDIST at each relay location, the faulted zone can be identified and tripped accordingly. However, the authors of [62] found that as the distance between the zones gets smaller, the gradient of voltage dip becomes too small to guarantee discrimination which makes it hard to make decision on faulted zone even with communication link between them.

2.3.6 Sequence Components of Voltage and Current

In [63], the author proposed a protection strategy for LV AEP CERTS microgrid based on sequence components of current. The strategy requires the static switch at PCC to trip for any internal fault, and next, the fault is cleared at islanded mode. The microgrid is divided into zones with dedicated relays. Residual and zero-sequence overcurrent is used to protect against ground faults. Negative sequence overcurrent protection is used to protect against line-line faults. Inverse time overcurrent is proposed as primary back up protection, and under voltage protection is proposed as secondary backup protection. All zone relays are coordinated based on definite time delay with the relay at PCC tripping faster that other

relays. Other relay zones are coordinated such that downstream zones trip first to minimize the isolated portion of the network.

2.3.7   Distance Protection

Distance relays are implemented by making magnitude or phase angle comparisons between operating and polarizing quantities which are derived from the measured voltages and currents [64-66]. In [67], a two-step Mho distance protection scheme was proposed for IBDG dominated microgrid. The results showed that for ground faults, the downstream distance relays tripped unnecessarily when the downstream load is Y-connected. To overcome this problem, the work in [68] suggested adding a negative sequence impedance directional element to identify fault current direction. In [69], a three step Mho distance relay was proposed to protect a distribution feeder considering the infeed effect from RBDGs. The reach of zone 2 and 3 has been extended to account for infeed from DGs. Similar work was presented in [70] for radial microgrid with several RBDGs. The three step Mho distance relays confirmed good selectivity and sensitivity under different operating modes of microgrid, and for different types of faults. In [71], the author presented a generic procedure for setting distance relays to maintain fuse saving scheme in the presence of DGs. The under-reaching effect caused by DG integration is solved by increasing the reach of distance relays. The performance of the proposed scheme was tested using real-word event report data. In [72], a multi-zone quadrilateral distance protection scheme for long radial overhead distribution networks with fuses laterals and multiple DG integration is proposed. The author analyzed the under reaching effect of DG addition and suggested extending the relay reach accordingly, however, this requires adaptive protection and communication system to be implemented. Similar scheme is proposed in [73] for a

distribution network with DGs having mixed overhear transmission lines and underground cables. The author presented a setting procedure to provide main protection of radial feeders and back up protection for lateral fuses.

2.3.8 Inverse Time Admittance Based Protection

The concept of Inverse Time Admittance (ITA) relay has been introduced in [74] for protection of microgrids. The relay measures the apparent admittance up to the fault point using locally measured voltages and currents. The relay tripping time is calculated using the general form of inverse time tripping characteristic. Separate directional element is used to enable directionality. In [74, 75], the author proposed a multi-zone ITA relaying scheme to protect a radial microgrid having IBDGs. Similar work was presented in [76], but it was extended to protect against arcing faults. In [77], the author showed that the ITA relay can overcome the limitations of overcurrent relays protection against low fault magnitude in islanded mode. Moreover, this work included hardware implementation & validation of the ITA relay performance, in addition, the relay performance was tested in looped network microgrid. In [78], the author tested the performance of the relay in inverter dominated microgrid and the relay showed satisfactory performance.

2.3.9 Differential Protection

Differential protection is one of the most reliable solutions for Microgrid because it is independent of microgrid status, DG status, and variation in fault current magnitude. Moreover, it is inherently selective and has high fault resistance coverage. In [79], the author proposed a protection scheme based on instantaneous line current differential as primary protection, and comparative voltage as back up protection in case of communication failure. The scheme showed high performance and was able to detect high

impedance faults for currents up to 10% of nominal primary current. The authors in [12, 45, 53, 80-83] have also used line current differential for transmission line protection. In [81, 83], bus differential scheme was applied to protect busbars with three breakers. In [81], a busbar differential scheme adopted from transmission systems is used to protect the main substation bus which has double busbar arrangement. In [84], a centralized differential protection scheme for multi-terminal zone is proposed.

2.3.10 Phase Angle Comparison Protection

Phase angle comparison protection is a pilot protection scheme that involve comparing current phase angle information only. The Advantage of this method in microgrid application is its independence of fault current level. In [85], the author proposed a current phase angle pilot protection scheme for microgrid protection. In this scheme, the current phase angle is first measured locally by each relay. If the calculated phase angle belongs to the fault condition, the phase angle jump, and its rate of change are calculated. If the calculated phase angle jump exceeds a threshold value, and its rate of change indicates that the phase jump is not due to transient condition, a current direction change is declared. If a fault occurs on a transmission line, the relay on which the phase jump threshold is not exceeded sends a permissive signal to the remote end relay. If the remote end relay detects a current direction change at the same time, then a trip signal is issued.

2.3.11 Wavelet Packet Transform Based Protection

Wavelet analysis is one of the most efficient time-frequency signal processing tools which can parameterize non-periodic, and non-stationary signals. In particular, the discrete Wavelet Packet Transform (WPT) based relays have been recently attempted to protect microgrids [86, 87]. In [86], the author proposed a new signature based digital protection

relay using Wavelet Packet Transform (WPT) analysis for microgrid application. It is found that the first level high frequency sub-band of dq-axis currents yields nonzero values only for disturbances caused by faults. Therefore, the relay simply detects fault by calculating the first level WPT detail coefficient and compare its value with zero. However, in this work, relay coordination in multi-relay systems is not considered. In [87], the author extended the scope of work to include fault location, and coordination between multiple relays in a microgrid system. The author found that the WPT second level high frequency sub-band of dq-axis currents contains signature that can be used for fault location, namely, the approximate coefficient is equal to zero only at the faulted bus. This unique feature is utilized to create a coordinated trip between multiple relay in the microgrid. However, the protection relay was applied at the output of the DGs, and all faults were only applied at the DG buses, the protection did not extend to transmission line/feeder protection.

2.3.12 Time Frequency Based Differential Protection

In [88], the author proposed an S-transform based differential energy protection scheme for microgrid in both modes of operation. The proposed method is effective, fast, and can issue a trip signal within 4 cycles of fault inception. In [89], the author proposed a differential energy based protection scheme using Hilbert-Huang Transform (HHT) and compared its performance to the S-transform. In this technique, fault currents at each feeder end are measured by a relay, the relay then calculates the spectral energy content and communicate the value to the relay on the remote end. A trip decision is issued if the differential energy calculated at each side exceeds a pre-determined value.

28

2.3.13 Pattern Recognition Based Protection

In power systems, fault detection process can be viewed as a classification task whose main objective is to assign power system signals into fault or non-fault categories, and/or to classify fault types [90]. One innovative way to handle such classification problem automatically is through pattern recognition systems which can be trained to detect, classify and locate faults in power systems. The general procedure of pattern recognition system consist of three basic stages, data pre-processing stage, feature extraction and/or feature selection stage, and classification (data mining) stage [91]. In [92], a data mining approach is proposed for fault detection and location in an inverter dominated microgrid. The input features were the RMS voltage/current, sequence component of voltage/current, power factor angle, and THD of voltage/current. A hybrid feature selection technique that combines the qualities of filter and wrapper methods were used to reduce the number of features. Two statistical classifiers which are the Naive Bayes and the j48 decision trees classifiers are used to classify fault type. The results showed that decision tree method outperforms the naïve Bayes especially in fault localization. In [93, 94], the authors proposed a data mining based protection scheme that consists of two channels: fault detection, and fault type classification. In fault detection channel, the measured current is processed using wavelet transform, and a group of statistical features are generated based on the wavelet coefficients such as the standard deviation, the energy, and the Shannon entropy. The extracted features are then used as input to the classifier. In fault type classification channel, similar approach is used, but the wavelet features were derived from the negative and zero sequence current components. The author proposed the Decision Tree (DT) and the Random Forest (RF) classifiers. The classification accuracy was high

29

for both classifiers, but the RF classifier outperforms the DT classifier. In [95], the author proposed a data mining based differential protection approach for inverter dominated microgrid at islanded mode. Communication channels between relays are used to share the extracted local features among the relays. For feature extraction, a sliding window approach is used to extract several electrical features. Feature selection based on filter ranks, and Information Gain (IG) methods are used to select the most significant features. Finally, the local features and remote features transmitted via communication from other relays are combined using differential operation and used as input to the classifier. A statistical classifier based on the random forest technique is used to classify selected features into fault and non-fault category. In [96-98], a communication assisted data mining based differential protection scheme is used for transmission line protection of microgrid in both modes of operation. The extracted local features are shared between the relays at each line end via communication channel, and the differential features are computed accordingly. In [96], S-Transform is used for feature extraction, and Decision Tree (DT) based classifiers is used for fault detection and classification. In [97], the Discrete Fourier Transform (DFT) and the sequence components analysis are used for feature extraction. The Decision Tree (DT) based classifier, and Support Vector Machines (SVM) are both used for fault classification. In [98], Hilbert Huang Transform (HHT) is used for feature extraction, and three different machine learning methods (Classifiers) are proposed for fault classification and location, namely, Naïve Bayes Classifier (NBC), Support Vector Machines (SVM), and Extreme Learning Machines (ELM).

2.3.14 Travelling Wave Based Protection

Travelling Waves (TW) are high frequency transient signals generated by faults on transmission line due to sudden changes in voltage at fault point. Travelling waves propagate from fault location along the line in all directions at certain velocity that depends on the transmission line distributed inductance and capacitance [99, 100]. In [101], the author proposed a combined voltage protection and travelling wave protection scheme for microgrid application. Fault detection is based on voltage measurement and faulted zone is identified using Travelling Wave (TW) concept. In the proposed TW scheme, the measured currents are decomposed using wavelet transform up to fourth level, and the local modulus maxima of the fourth component is extracted. By comparing the first modulus maxima of each feeder, the faulted feeder can be identified to be having high magnitude and opposite polarity compared to sound feeders. In [102], the author proposed a hybrid protection strategy for microgrid based on the travelling waves as main protection, and the rate of change of current as backup protection. In the travelling wave scheme, a modified Mathematical Morphology Filter (MMF) method is use to extract the polarity information of the first two wave fronts, the method detects the fault within microseconds, and require low communication bandwidth. However, the method fails to detect faults below 5° Point on the Wave (POW), moreover, meshed configuration and single ended measurement cases are not addressed in this work. These shortcomings have been addressed in [100] where each travelling wave relay communicates with a central unit the information related to wave front polarity, time of arrival, instrument transformer number, and line number. Based on the communicated information, the central unit uses a comparison logic to identify the faulted lines and issues a trip signal accordingly.

2.3.15 State Estimation Based Protection

Estimation Based Protection - also known as "setting less protection" - has been proposed for microgrid protection in [40, 103, 104]. The method requires simple settings and eliminates the need of coordination between different protection zones. It is viewed as an evolution of current differential protection but instead of checking the validity of Kirchhoff's current law, this method extends the concept by checking the validity of any physical law that the protected zone must satisfy. This can be done systematically using State Estimation (SE). In [40], the author proposed a three phase state estimation based protection technique as a backup protection method for distribution network with high level of DG penetration. In the proposed technique, the network is first divided into protection zones. Synchronized measurements of voltage and current taken from different locations in the network are transmitted to a central computer via high speed communication network. The real time synchronized measurements taken from the zone under protection are compared against a healthy model of the protected zone. Fault detection is decided based on the goodness of fit of measurements and the heathy model. A linear three phase state estimator based on least-squares minimization is used for model checking. In [103], the author proposed a Dynamic State Estimation Based protection approach microgrid transmission line protection. In [104], a distributed dynamic state estimation (DDSE) based protection was applied to a microgrid with induction generator based wind turbines. The protection algorithm was applied to the Induction generator protection only, and was tested by applying several stator faults, external fault, and high impedance faults.

2.3.16 Directional Comparison protection

Directional comparison protection is a teleprotection scheme that employs directional protection elements and/ or distance elements at the terminals of the protected zone. Logical information about the relay status of each terminal is transmitted to the remote end(s) relay(s) or to a central processing unit. A simple comparison logic is used to make tripping decisions for internal faults. In [33], the author proposed a Permissive Overreaching Transfer Trip (POTT) scheme and Directional Comparison Blocking (DCB) scheme based on radio communications to address the problem of DG overreaching in grid connected mode of operation. In the POTT scheme, the DG instantaneous relay is allowed trip instantaneously if it has received a permissive signal from the substation direction overcurrent relay for downstream faults. In the DCB scheme, the DG trips unless it has received a blocking signal if the substation directional overcurrent relay detected a reverse fault. The DG protection is delayed to account for communication channel delay. In [105-107], an under impedance based directional comparison protection scheme is proposed for inverter dominated microgrid. In [106, 107], relays within a protected zone share status signals of fault detection and direction over a peer to peer communication channel and use a built-in comparison logic to make tripping decisions for internal faults. In [106, 107], the author used the same concept but in centralized manner, i.e., all impedance-based relays provide status information on fault detection and direction to a central unit. The central unit processes this information to locate and clear the faulted zone. Moreover, the central unit processes any topology change in the microgrid, and accordingly redefine the protection zones for suitable fault clearance. In [108], the author proposed a directional comparison pilot protection scheme for microgrid application. Fault detection is based on the

superimposed sequence components analysis. Directional element is based on the sign of Superimposed Reactive Energy (SRE) which is calculated using Hilbert Transform (HT). Moreover, the SRE coefficients are used to identify the faulted phase by comparing the SRE coefficient for each phase with threshold value. The scheme requires communication between three adjacent relays. Each relay uses a simple comparison logic to locate the faulted zone, and to take tripping action. If the fault is found to be on the same line to which the relay is connected, the relay trips instantaneously, otherwise, if the fault is located in next line, the relay trips after time delay. In [109], the author proposed a centralized protection strategy for small scale LV microgrid. Fault detection is based on comparing the dq-components (park transform) of main bus voltage with reference values. Directional element that uses the pre-bus voltage information has been proposed. The information on fault status, fault direction, and CB connection status are reported to a central unit which performs comparison logic to locate and isolate the fault. In [110], the author proposed a centralized directional comparison scheme for MV microgrid. Fault detection is based on directional under voltage at islanding mode, and a combination of directional inverse/definite time overcurrent at grid connected mode. In addition, high impedance fault detection scheme is proposed based on the fault-imposed components analysis combined with third harmonic meter. Each communication enabled relay sends the status of fault detection and fault direction to the central processing unit, which then uses a built-in directional comparison logic to located faulted zone and to make tripping decisions with coordinated time delay. Breaker failure scheme is used to send signals to neighboring breaker in case the fault is not cleared. If communication system failed, the author proposed

34

switching the protection strategy to the same method proposed in [111] which does not require communication to operate.

2.3.17 Multiagent Based Protection

Multi Agent System (MAS) is a distributed management & control system composed of multiple autonomous computational entities referred to as "Agents" that communicate with each other to perform a global task. In this methodology, the global problem is broken down into smaller tasks, and each task is assigned to an agent. Communication between the agents is the key that enables each agent to make better decisions in achieving its designated task. Primarily, Multi agent systems have been introduced to microgrid protection & control to overcome the drawback of having a sophisticated, expensive, central unit that need to communicate with every component in the power system and represents a single point of failure. In multi-agent system, each agent can autonomously operate within its environment and can make decision independently, therefore, multi agents are more flexible, cooperative, and does not represent a single point of failure to the whole system [23, 112-114]. In [113], the author proposed a multi-agent-based technique for protection against transmission lines faults in microgrid. In this scheme, one section relay agent is placed at the center of the transmission line. The relay agent acquires current phase angle measurements from each line end using phasor measurement units (PMU) located at each line end. The section agent calculates the phase angle difference and compares it with a certain threshold. If the threshold is exceeded, fault detection is declared, and the relay sends a trip signal to circuit breakers at each line end to isolate the fault. A power restoration process commences after fault isolation which involves coordination and communication between relay agent, load agent, DG agent, and restoration agent. The

objective of this process is to take necessary actions that bring the system to stable operation after disturbance. In [114], a multi-agent based protection scheme based on N-Version programming has been proposed. In this work, N refer to the number of protection principles programmed inside the agent unit. Three protection principles are considered inside each relay which are: overcurrent protection, Clark's transformation protection, and protection based on positive sequence phase differential scheme. Fault identification is based on a polling logic that takes fault detection result of the three protection schemes used. If one scheme fails to detect the fault, other modules can provide a sort of redundancy. The agents communicate with each other via a dedicated module based on IEC 61850. The same module can also be used for fault location and service restoration.

2.3.18 Adaptive Protection

Adaptive protection was originally introduced in the 1980's for transmission systems. Adaptive protection System (APS) allows the protection setting to be changing in real-time in response to external changes in power system. Although most adaptive protection systems require communication with external entities to identify the changes in power system conditions, it is possible to implement adaptive protection based on local measurements only. Accordingly, adaptive protection can be broadly classified as: Local information-based APS, and communication-based APS.

1) Local information-based APS

This type of APS uses the normal relay input measurements such as voltage, current, and digital/analogue inputs in combination with advanced algorithms/signal processing techniques to automatically adjust its protection functions and/or protection settings in

response to changes in power system conditions. In microgrid protection, local based APS has been introduced as a low-cost and reliable solution for microgrid protection. Local based APS does not require communication infrastructure. Moreover, failure within a relay will be confined to the relay and does not impact other relays in the system. In [115], a voltage restrained overcurrent protection scheme was proposed for islanded microgrid as a form on non-communication APS to overcome the selectivity problems in voltage based schemes. However, the scheme considered only islanded operation, and small scale microgrid. In [116], an adaptive inverse time overcurrent protection technique is proposed. Protection settings for different microgrid configuration and operating scenarios were studied offline and stored in the relay's group settings. A state detection algorithm was implemented inside each relay to predict the change in microgrid conditions. The algorithms consist of an islanding detection technique adopted from [117], and a grid restoration detection technique adopted from [118] to identify changes in microgrid mode of operation. Moreover, the measured fault current and the inverse time tripping characteristic of downstream relays are used to predict which relay has operated first, and which DG get disconnected. Accordingly, the relay used these state detection algorithms to update the group settings. However, the method cannot identify when the DG is reconnected, moreover, it considered radial microgrid with RBDGs. In [119], the author proposed an adaptive technique using sequence component quantities to maintain coordination between primary and backup overcurrent relays in a radial microgrid. In this method, the inverse time delay equation is made as function of an adaptive fault current parameter. The calculation of this parameter involves sequence component quantities and an impact factor quantity. The impact factor is calculated such that it scales the adaptive

fault current to a level that prevents coordination loss between main and backup relays. The impact factor is calculated for each relay locally based on the superimposed positive sequence current and the negative sequence current. However, since the impact factor calculation depends on the type of DGs available, communication system is required to inform the relay about available DGs and their status, therefore, the method can be implemented without communication only if all DGs are of same type. In [120], the author presented and adaptive pilot protection technique for protection of an islanded ring microgrid. In this work, fault detection algorithm is based on the magnitude and phase angle of park transform of line voltages. Fault direction algorithm is based on the sign and magnitude of the change in power flow (ΔP). Communication between relays is required to decide on suitable tripping action. To achieve adaptive tripping thresholds with changing load conditions, the author proposed using non-intrusive load monitoring which detects the operational status of loads in real time without communication. It is noted in this work that communication is not used for adaptive protection purpose but for relay coordination.

2) Adaptive Protection with centralized decision making

In the centralized approach, each relay communicates with a Central Protection Unit (CPU) as shown in Figure 2-6. This topology is supported by many communication protocols such as: MODBUS, DNP3, or IEC 61850. Regarding physical layer, this topology can be implemented using serial communication, bus communication, Power Line Carrier (LCR) and ethernet [121]. There are many centralized adaptive protection techniques proposed in the literature, these methods differ from each other in many aspects, such as fault detection strategy, relays setting calculation (online or offline), and the method of updating the relay setting.
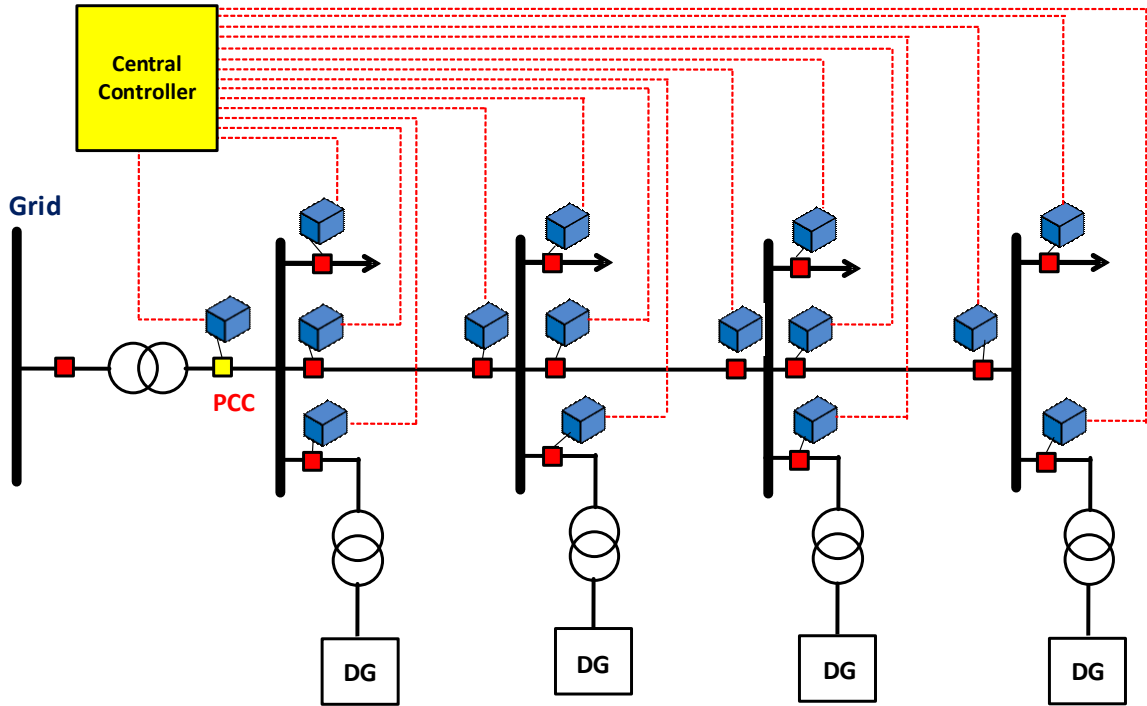
Figure 2-6: Centralized Adaptive Protection System

B) Centralized APS with offline setting calculation

In this approach, all microgrid operating scenarios will be identified offline considering all possible operational and topological changes such as MG mode of operation, load status, CB status, and DG status. For every operating mode, load flow and short circuit analysis considering all types of fault, and all fault locations will be studied offline using computer simulation tools. The simulation results are then used to select the appropriate protection settings for every operating scenario. The settings are then grouped together and saved in the memory of IED or memory of special controller. Some examples using this technique will be briefly presented here: In [16, 18], a centralized adaptive directional overcurrent protection strategies are proposed for protection of distribution network with DGs. The optimal protection settings are obtained offline by solving the coordination problem using optimization techniques. In [16], Artificial Bee Colony (ABC) optimization algorithm is

39

used, whereas in [18], the relay coordination problem has been formulated as a non-linear programming (NLP) optimization problem and two optimization solvers were used to obtain the solution, namely, (Ipopt) open-source software and (Baron) commercial optimization software. The resulting optimal relay settings are stored in separate groups within the relay's memory. During online operation, the central controller monitors the circuit breaker status to identify the prevailing network configuration. Accordingly, it sends a command to the relays to update their group settings. However, both methods were limited to grid connected mode of operation. In [20], a comprehensive centralized adaptive protection strategy for a MV Microgird at Hailuoto island is proposed. Fault detection is based on non-directional over current for protection at PCC, directional overcurrent for main feeder relay, and zero sequence voltage for diesel generator. Moreover, auto-reclosing scheme is utilized at grid connected mode for main feeder relay. The author also proposed two stage under/over voltage relays to meet fault ride through requirement of DG units. The protection settings are studied offline for five scenarios: grid connected mode (with DGs and without DGs), islanded mode (stable, and black start), and intentional islanding. The resulting settings are stored in the IED's setting groups. During online operation, the CPU monitors the connection status of microgrid and DG units and updates the IED's group setting using communication network based on IEC 61850. In [122], a centralized adaptive protection strategy with multifunction relays has been suggested. Fault detection is based on a combination of protection elements that work together to cover all types of faults. The protection elements included negative and zero sequence overcurrent, voltage sequence components, and frequency relays. Moreover, a high impedance fault detection module, and single-phase event detector are used to provide extra protection. All

40

trip actions are executed via autorecolsure module to allow for temporary fault clearance. The centralized controller monitors microgrid connection status via main CB contact and updates the relay's operating currents (pre-determined offline) whenever the microgrid status change. In [123], the author proposed an adaptive directional sequence current relay for microgrid protection. The proposed method is an extension of the adaptive method presented earlier in [119]. The extension included adding superimposed directional current element to enhance the relay coordination. Moreover, a central unit with communication network to the adaptive relays has been suggested. Since the impact factor calculation depends on type of DGs, the central unit monitors the DG connection status online and updates the same to the relays to enable accurate calculation of the impact factor. In [15], a hierarchal adaptive protection scheme for a looped microgrid is proposed. At load level, adaptive directional overcurrent with auto-reclosing capability is proposed. At loop level, a Permissive Overreach Transfer Trip (POTT) scheme based on directional overcurrent relays is used. At third level, Loop feeder PDs are protected with non-directional over current relays. And finally, at microgrid level, the PCC relay clears external faults using voltage and frequency relays. Higher Level PDs are coordinated to provide back-up protection for lower level PDs. The author used time overcurrent protection at grid connected mode, and definite time overcurrent at islanded mode to enable faster tripping. The CPU monitors the connection status of microgrid, and accordingly communicates with all adaptive relays to switch their protection. In [21], the author proposed a centralized adaptive Mho distance protection scheme. A permissive under reach transfer trip (also known as PUP Z2 scheme) and direct under reach transfer trip are used to enhance tripping speed on weak lines. Moreover, a communication system based on IEC61850 Generic

Substation Events (GSE) with time synchronized measurements is adopted between IEDs and a CPU to enable adaptivity. The CPU collects all CBs status, identifies the configuration, and updates the corresponding IEDs setting group which was studied offline to meet the protection requirement. In [124], the author proposed a centralized overcurrent protection strategy for microgrid. In this scheme, relay settings are calculated offline and the results are stored in the memory of the CPU. During online operation, the CPU monitors the connection status of all CBs through communication system, and accordingly uploads the corresponding settings to the relay's memory online through communication system. To further enhance the selectivity and sensitivity in IBDG dominated microgrid, the author suggested combining the adaptive protection system with an adaptive directional interlocking scheme in which the trip units/relays shares interlocking signals over a communication channel to enable faster and selective fault clearance. The interlocking direction changes dynamically according to the detected direction of fault current.

B) Centralized APS with online setting calculation

In [125, 126], the author proposed a centralized adaptive overcurrent protection strategy for microgrid. In this method, fault detection is based on overcurrent relays with adaptive operating currents. During online operation, the central unit communicates with every relay in the system to update its operating current and to detect fault current direction. Moreover, it communicates with every DG to acquire its connection status, its rated current, and it fault current feeding capability. The CPU uses the communicated information and runs a simple algorithm in real-time to estimate the fault current contribution at each relay location. The CPI then calculates the relay's operating current and updates it to each relay on interruption basis. Upon fault detection, the relay operates independently based on the

settings received from the CPU. The author in his proposal assumed small scale and simple microgrid in which the DGs contribute their maximum fault current for any fault location. Moreover, the time delays are set manually not adaptively. To overcome these limitations, the author in [10] proposed a method to calculate the impact factor of DGs which is required to accurately estimate the DG fault current contribution at relay location. Secondly, the author introduced a bi-directional relay coordination algorithm that automatically assigns main and backup relays (in pairs) according to varying network structure and according to fault current direction (fault location). Finally, the author suggested the concept of critical relays (breakers) whose status (Open/Closed) can be used to identify the current structure of the network. Alternatively, the author proposed using graph theory algorithms such as Dijkstra's Algorithm proposed in [127] to identify the relay hierarchy. In [128], a centralized online adaptive overcurrent protection strategy is proposed. In this scheme, the CPU monitors the connection status of all CBs and DGs in the network and performs online short circuit analysis and protection setting calculation. However, before updating the new protection settings to the relays, the CPU calculates the relays response time using both the present and the new settings and compares the result against coordination rules such as operating time limits, and the grading margin, etc. The central unit updates the new setting to the relays only if the new settings have better performance compared to old settings. Similar approach is proposed in [19] in which the CPU receives operational and topological information about the network through SCADA system and performs load flow, fault analysis, and contingency analysis online. Then it runs a Differential Evolution (DE) algorithm to select the optimal values of protection settings of directional overcurrent relays. Rhe new settings are then uploaded to the relays

via communication network directly. In [11], the author proposed a centralized adaptive microgrid protection scheme in which the central unit monitors the microgrid, performs fault detection, and fault location. Fault detection is based on the state estimation protection scheme proposed in [40]. Fault location is based on directional comparison scheme adopted from [45]. In next step, the Prims algorithm is used identify the network topology, and the Dijkstra algorithm is used to identify the shortest radial path from the fault location to the nearest operating source. Finally, after identifying the shortest path, suitable time delays are adaptively assigned for the relays within the identified shortest path to clear the fault selectively. In [129], a centralized adaptive protection strategy for LV radial microgrids was proposed. In this method, loads are protected using non-directional overcurrent PDs. For DER protection, under/over voltage and under/over frequency are proposed. Communication with other relays and with central unit is required to receive trip/disconnection signals. For PCC protection, under/over voltage and under/over frequency are proposed. Moreover, communication is used to transfer the trip signal from upstream MV breaker for LoM protection, and to receive interlocking signals from other relays for selective coordination. Finally, main feeders are protected using two stage directional overcurrent in grid connected mode, and an adaptive multi-criteria protection algorithm in islanded mode. In the later one, fault detection is based on a combination of under/over voltage and directional overcurrent. The relay operation time in islanded mode is selected as function of voltage drop, whereas the pickup setting of the OC relay is changed adaptively according to the number and type of downstream connected DGs, and their current feeding capability. The same is monitored by the CPU in real time using the communication system and is used to update the pick-up setting of the relays accordingly.

44

Selectivity between main feeder relays is ensured by sharing interlocking signals. The operation curve is designed to ensure selectivity with DGs to ensure fault ride through is met. All communication with central unit and between PDs is based on IEC 61850 standard. In [112], the author proposed a centralized adaptive protection strategy for an open loop and closed loop distribution systems with wind turbines. The CPU acquires the wind turbines status, performs online short circuit calculation, calculates the overcurrent relay settings, and accordingly uploads it to the relays. For the open loop scheme, fault detection is based on non-directional inverse time overcurrent, whereas for closed loop system, directional time overcurrent is considered. To simplify the relay coordination with increasing number of wind turbines, the author proposed using Permissive overreaching transfer trip (POTT) scheme.

3) Adaptive Protection with decentralized decision making

In decentralized scheme shown in Figure 2-7, the relays communicate to each other and share topological/operational information about microgrid, and may share also real-time measurement, however, in this scheme, each relay takes the decision autonomously from other units based on the communicated information. The main advantage of this scheme is that it is not dependent on central unit, and hence, there is no single point of failure. However, implementing such scheme is more complicated, and require IEDs with advanced processing capability.
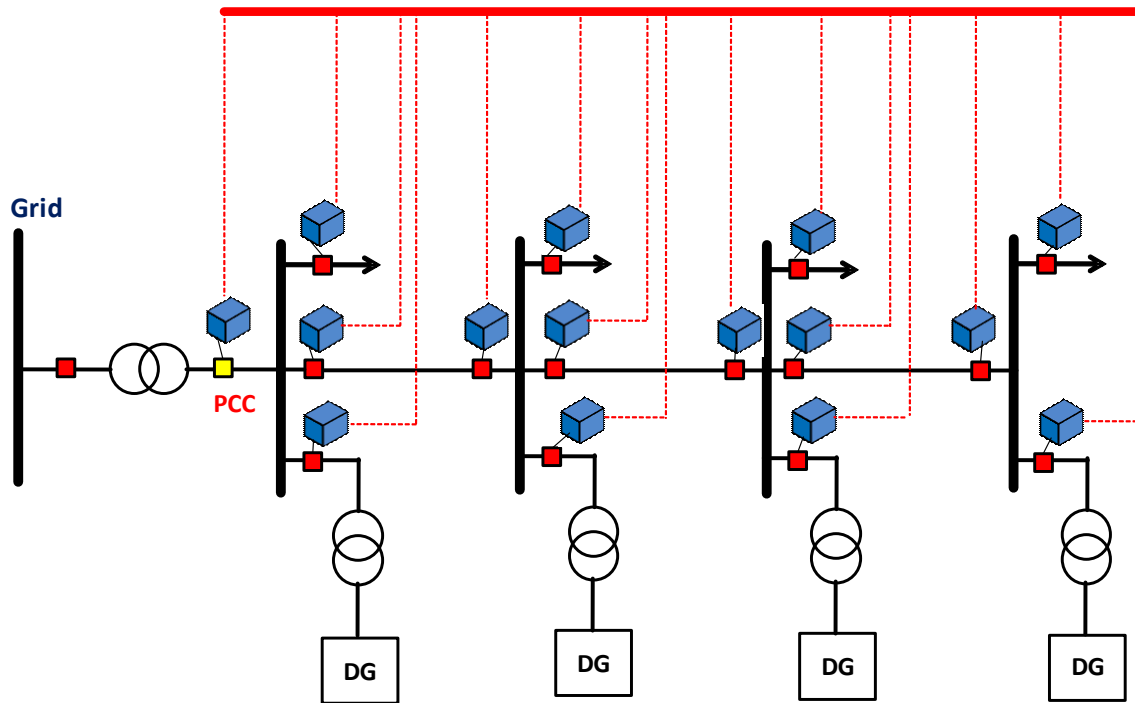
Figure 2-7: De-centralized Adaptive Protection

In [112], the author proposed a multi-agent adaptive overcurrent protection strategy for radial distribution networks with DGs. In this technique, the DG agents, breaker agents, and CT agents communicate information to the relay agent about fault current, DG status, and breaker status, the relay agent uses these-information to adjust the relay settings and the coordination strategy according to pre-studied scenarios offline. Two coordination strategies are proposed in this work, conventional overcurrent coordination when few numbers of DGs are connected, and communication-based relay to relay coordination strategy when larger number of DGs are connected, in the later, the relays determine the location of fault current (upstream or downstream) by comparing fault currents and sharing of blocking/permissive signals to maintain coordination between main and backup relay. The communication system was tested using Java agent Development Framework (JDAE) software. However, the author considered simple radial network and grid connected mode of operation. In [25], a decentralized adaptive overcurrent protection strategy is proposed

for an islanded MV maritime power system. Fault detection is based on directional overcurrent relays with high set instantaneous. The optimal relay settings for every operational status of DG and CB status were studied offline and stored in the relay's setting groups, during online operation, the DG status, and CB status are transferred to all protection relays in the power system and accordingly, the relay identifies the network topology and selects the corresponding group setting. Circuit breaker failure scheme is considered using an inter-tripping function between adjacent upstream/downstream relays. In [130], a multiagent based adaptive directional overcurrent protection strategy is proposed for microgrid protection. Fault detection is based on directional overcurrent relay with high set instantaneous. The relays are coordinated as forward-looking relays and reverse-looking relays. The optimal relay settings are studied offline for all possible configuration and stored in the relay's memory. During online operation, the connection status of DGs, and CBs are transferred to the relay agents via communication agent, accordingly, each relay identifies the prevailing network configuration and selects the corresponding setting from its memory. In post fault scenarios, the microgrid will have new configuration due to isolating some sections of the network, the monitoring process will continue, and the relays will update their settings according to the new configuration. In [23], an agent based protection scheme was proposed to solve the problem of overcurrent and frequency selectivity in autonomous microgrid. In the overcurrent selectivity scheme, the DG and load IEDs are selected as non-directional, whereas the bus routing relays are selected as directional. All relays are assigned fixed definite time delays considering the feeder characteristic and the Remedial Action Scheme (RAS) of the microgrid. Pickup values were calculated offline for different configurations and operational scenarios, and

the results are stored inside the setting groups of each IED. In real-time operation, the IEDs share status information of CBs to detect the prevailing network configuration and to activate the suitable group setting accordingly. To ensure selectivity and high-speed tripping, a logic discrimination approach is adopted, in this method, an IED sends a temporary blocking signal upon fault detection to its adjacent IEDs in the direction opposite to the direction of fault current, these blocking signals prevent other IEDs from tripping except for the IEDs closest to the fault which have not received blocking signals from other IEDs. Blocking signals and other status information are shared among IED agents using the high-speed IEC 61850 Generic Object-Oriented Substation Event (GOOSE) protocol. In the frequency adaptive protection scheme, load feeder relays are equipped with load shedding protection, and DG relays are equipped with under frequency relays, and Rate of Change of Frequency (ROCOF) relays. However, since the inertia constant depend on number of connected DG, it should be monitored online, and the frequency protection shall be adapted accordingly. A synchrophasor enable IEDs were proposed to estimate the online inertia constant by introducing a small load perturbation for a sample period. This information can then be used to adapt the frequency protection accordingly. A blocking scheme was also suggested to differentiate between pulse loads and fault, in this scheme, if the pulse load switching would excite the frequency protection, a pulse load agent would block the frequency protection whole the pulse load is on duty.

2.4   Conclusions and Identified Research Gaps

It can be seen from previous discussion that fault detection, and selective/fast tripping in microgrids is a challenging task that requires designing unconventional protection schemes like those of transmission systems, several microgrid protection solutions have been proposed in the literature.   According to the review and analysis of various technical publications, the following observations and recommendations have been drawn:

1. Protection methods that rely on local measurements without communication or adaptive settings can partially overcome microgrid protection challenges, however, integrating these methods with communication can enhance the protection speed, selectivity, and sensitivity, and can help in providing more complete solution.

2. Centralized communication architecture can give effective solution, but in case of failure of the central unit, the whole scheme may collapse, Therefore, decentralized communication schemes may be more reliable, and more flexible.

3. Many of the proposed protection solution in the literature are not comprehensive, i.e., it did not cover all protection zones of microgrids or did not address all protection issues such as islanding detection, and fault ride through requirement.

4. Most of the proposed fault detection methods are suitable for specific microgrid component or for specific microgrid configuration. Therefore, to achieve a comprehensive and generalized protection strategy, a combination of different fault detection methods shall be used.

5. It is shown that the IBDG's fault current characteristic is dependent on the control mode, i.e., voltage control mode or current control mode. However, most of proposed

solutions considered the fault current characteristic the same in both control modes. Future protection strategy shall address this issue and investigate its effect on the performance.

6. Available commercial protective relays are designed considering fault characteristic of rotating based machines. The integration of inverter based DGs alters the fault characteristic, and hence the performance of commercial protective relays needs to be re-assessed. The study done in [42] conducted a time domain simulation study to identify the performance of commercial protective relays under microgrid with several types of DG sources, the results showed that there are certain conditions under which directional overcurrent relays, distance relays, and differential relays may not perform as required, therefore, similar studies are required to be done but using physical relay testing based on real time hardware in the loop studies, such studies might help relay manufacturers in upgrading their relays to suite microgrid operation in the future.

7. Many novel protection methods such as pattern recognition methods, state estimation based methods are not only complex, but also require high investment cost, moreover, such techniques are not available as commercial products and require more investigation and hardware testing to reach such level, therefore, the application of such methods to microgrids and distribution networks in practice might not be possible in the near future.

8. In the absence of standard commercial microgrid protection relay, the only option for protection engineers is to consider the off-the-shelf transmission and distribution system protection relays, i.e., directional overcurrent, distance relay, and differential protection relays.

CHAPTER 3

OVERCURRENT PROTECTION & COORDINATION IN

DISTRIBUTION SYSTEMS

The main objective of this chapter is to cover the basic theoretical background of overcurrent coordination in radial and looped distribution networks. Firstly, this chapter present the protection requirements that must be followed during the design of protection system. After that, the overcurrent relay types, methods of coordination in distribution systems, and directional element design are covered

3.1   Protection Requirements

When designing a protection system, several requirements must be met, the most important are the selectivity, sensitivity, speed, and reliability. Other requirements can be added which includes simplicity and economy.

3.1.1 Selectivity

Selectivity implies two things. Firstly, the protection devices (PDs) shall discriminate between faulted and non-faulted conditions and shall not unnecessarily trip for non-fault conditions [131]. Secondly, when a fault occurs, the protection devices shall respond in the shortest possible time with minimum isolation of power system components. This implies that certain protection devices shall only operate to isolate the fault, these devices are called

the primary protection devices (PDs). The remaining PDs shall not trip and must provide backup protection if the primary protection fails [132].

3.1.2 Speed

Speed implies that the protection system operation time (relay operation time plus breaker operation time) shall be as fast as possible after fault inception. This is very important in maintaining power system stability, improving power quality, minimizing equipment damage, and increasing safety level [131-133].

3.1.3 Sensitivity

Sensitivity implies the level of operating quantity (current, voltage, frequency, etc.) that a protection device or a protection system can detect. The protection devices or protection system is said to be more sensitive if it can detected lower levels of operating quantities for a given fault [131-133]. The protection system designer must ensure sufficient sensitivity to detect faults [132].

3.1.4 Reliability

Reliability implies that a protection device must operate when required (dependability) and must restrain otherwise (security). For instance, the protection device shall not false trip during motor starting, transformer inrush, load switching, etc. The protection device shall maintain this behavior even after long years of installation. Based on this, reliability can be understood as the degree of certainty that a protection device will operate properly [132, 134].

3.1.5 Simplicity

Protection system shall meet the necessary protection requirement using the simplest possible design. Complicated designs may create relay setting difficulty which increases the probability of making human errors during the process.

3.1.6 Economy

The protection system cost is an important factor that must be taken into consideration. The protection scheme cost shall consider the application, for example, in transmission systems, the cost of complex protection systems and duplicate relay panels can be easily justified since the impacted area is large, and the economic loss which may result from failure is huge. However, in distribution systems feeding rural areas for example, it would be difficult to justify such complex protection system. In conclusion, it can be said that the level of protection shall be defined in accordance with the economic loss which may result in case of failure.

3.2   Overcurrent Relays and Characteristics

Overcurrent relay is designed to trip when the magnitude of measured current exceeds a specific threshold value called the pickup-current. The overcurrent relaying principle is the most commonly used type of protection in distribution systems due to its relatively simple design, and low cost.

3.2.1 Overcurrent Relay Types

Based on the operating time characteristic, overcurrent relays are classified into three categories:

1. Instantaneous Overcurrent Relay (ANSI Number 50)

In this type, the relay operates without "intentional time delay" when the measured current exceeds the pickup current setting. The instantaneous operation time ranges from 1 to 1.5 cycles. The relay characteristic is shown in Figure 3-1a, only the pickup setting is adjustable.

2. Definite Time Relay (ANSI Number 50 or 51)

In this type, the relay operates after a "fixed intentional time delay" when the measured current exceeds the pickup setting. Therefore, regardless of fault current magnitude, the relay operation time does not change. The relay characteristic is shown in Figure 3-1b. Both the time delay setting, and the pickup setting are adjustable. However, if the time delay is set to zero, the relay becomes instantaneous.

(a) (b) (c)
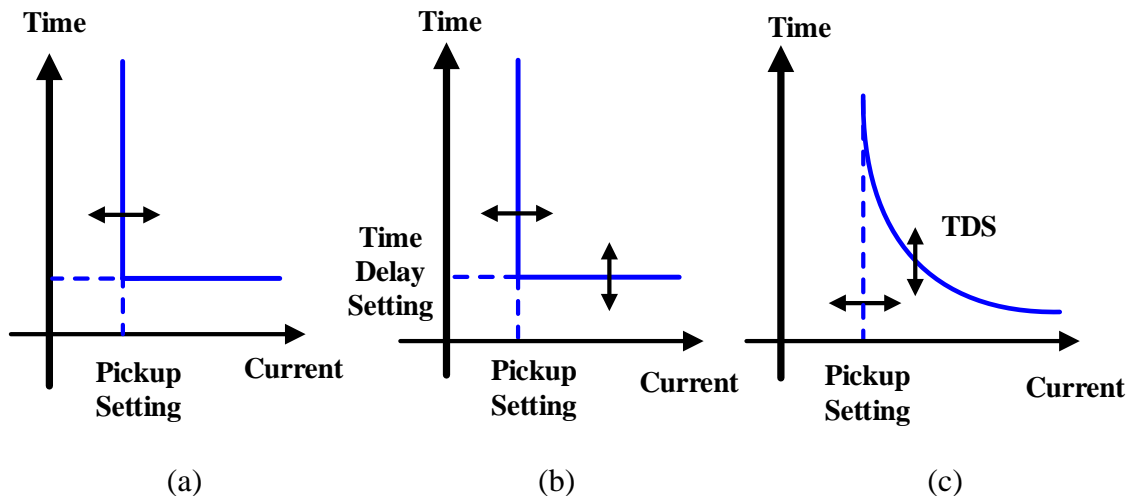
Figure 3-1: Overcurrent Relay Operating Characteristic: (a) Instantaneous, (b) Definite time, (c) Inverse time

3. Inverse Time Overcurrent Relay (51)

In this type, the relay operates after a variable time delay when the measured current exceeds the pickup setting. The time delay is inversely proportional to the input current, i.e., as the magnitude of input current gets higher, the relay tripping time becomes lower. Typical relay operation characteristic is shown in Figure 3-1c. The relay has two adjustable settings, the pickup setting, and the time dial setting (TDS). The TDS adjusts the characteristic of the relay to a predetermined trip time at a specified current. The inverse time element is described by an equation that models the behaviors of electromechanical relays. Modern microprocessor relays emulate the behavior of electrotechnical relays by applying these equations in digital format. Different equations are defined for the inverse time element by IEEE and IEC standards. Equations 3.1-3.2 below are the general form defined by IEEE C37.112-1996 standard [135]:

$$t_p = \left(\frac{A}{M^P - 1} + B \right) \times TDS \quad , M > 1 \tag{3.1}$$

$$t_r = \left(\frac{C}{1 - M^P} \right) \times TDS \quad\quad , M \leq 1 \tag{3.2}$$

Equations 3.3 is the general form defined by IEC 60255 standard:

$$t_p = \left(\frac{A}{M^P - 1} \right) \times TDS \tag{3.3}$$

Where t_p is the relay operating time in seconds; t_r is the relay reset time in second; M is the multiples of pickup current, it represents the ratio of the input current to the pickup current; *TDS* is the Time Dial Setting (typical values range from 0 to 10); A, B, and P are the parameters that determine the steepness degree of the operating time curve; and C is a

parameter that controls the steepness degree of the reset time curve. Table 3-1 shows the

parameters defining the IEEE C37.112-1996 and IEC 60225 characteristics.

Table 3-1: Parameters defining the IEEE C37.112-1996 and IEC 60225 characteristics [135]

Standard	Curve	A	B	C	P
IEEE C37.112-1996	Moderately Inverse	0.0104	0.0226	1.08	0.02
	Inverse	5.59	0.180	5.59	2.00
	Very Inverse	3.88	0.963	3.88	2.00
	Extremely Inverse	5.67	00352	5.67	2.00
	Short-Time Inverse	0.00342	0.00262	0.323	0.02
IEC 60225	Class A-Standard Inverse	0.14	*	*	0.02
	Class B-Very Inverse	13.5	*	*	2.00
	Class C-Extremely Inverse	80	*	*	2.00
	Long Time Inverse	120	*	*	2.00
	Short Time Inverse	0.05	*	*	0.04

* as specified by the manufacturer

A number of curves are defined by each standard, these curves differ from each other by

the degree of inverseness which is controlled by varying the A, B, C, and P parameters. A

family of curves can be created by controlling the TDS parameter which is normally

adjustable in the range from 0 to 10. Figure 3-2 shows a family of the IEEE Inverse time

characteristics which was created by varying the TDS parameter. Since the TDS is directly

proportional to the operating time, increasing the TDS value increases the relay operating

time by proportional amount, and vice versa. As shown in Figure 3-2, the operating

characteristic is normally expressed in terms of multiples of pickup current versus the operating time.
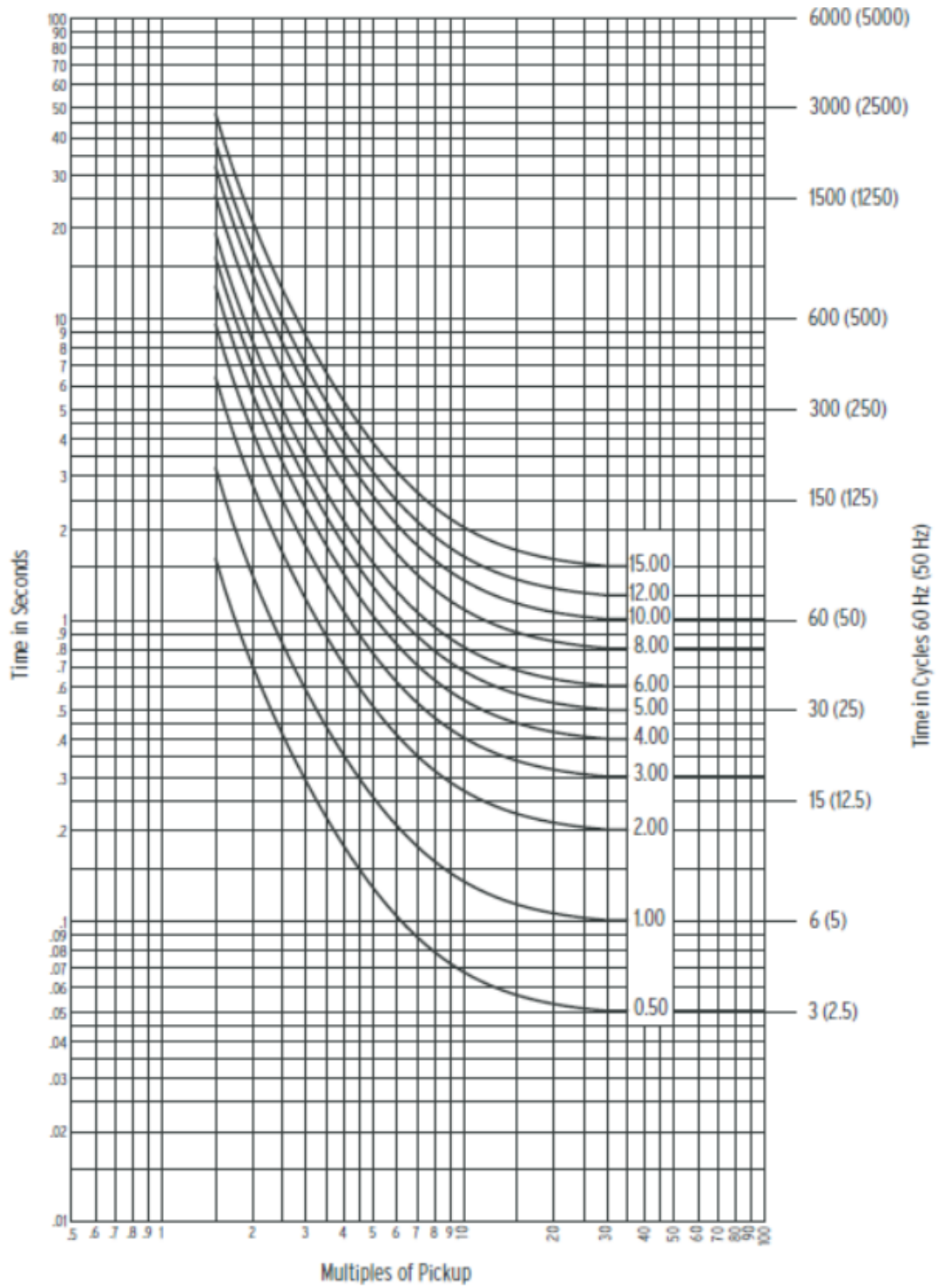
Figure 3-2: The IEEE C37.112-1996 Very Inverse Characteristic [136].

A combination of different tripping characteristics can also be used. For example, Figure 3-3a shows a combination of inverse time and instantaneous characteristics, and Figure 3-3b shows a combination of instantaneous, definite time, and inverse time characteristics. This type of characteristic is commonly found in electronic trip units of low voltage circuit breakers.

(a)   (b)
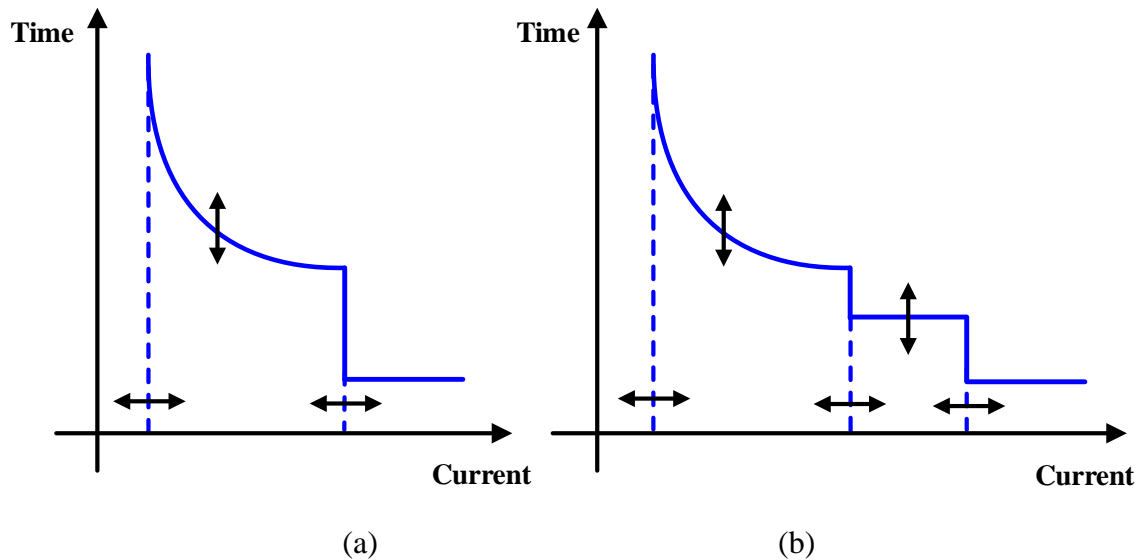
Figure 3-3: The mixed operating characteristic of the overcurrent relays: (a) instantaneous and inverse time (b) definite time, instantaneous, and inverse time.

3.2.2 Inverse Time Overcurrent Relay Coordination in Radial Lines

Figure 3-4 shows one radial feeder with multiple section breakers equipped with inverse time overcurrent relays. The current distance diagram in Figure 3-4 shows that the current decreases as distance from the source increases. Therefore, the inverse time overcurrent relay response increases as the distance from the source increases. Accordingly, coordination is done as shown in the time distance diagram shown in the bottom of Figure 3-4. In this diagram, the curve of each relay starts at the beginning of the line where the relay is located and overreach the next line to overlap with the next characteristic. Starting

from the relay farthest from the source, a Coordination Time Interval (CTI) is added between downstream and upstream relays till reaching the relay near the source. The CTI includes the circuit breaker operation time, the overtravel time (of electromechanical relay), and a safety margin. This arrangement ensures that the relay closest to the fault will trip first. Moreover, it ensures that upstream relays will provide back-up protection to downstream relays.
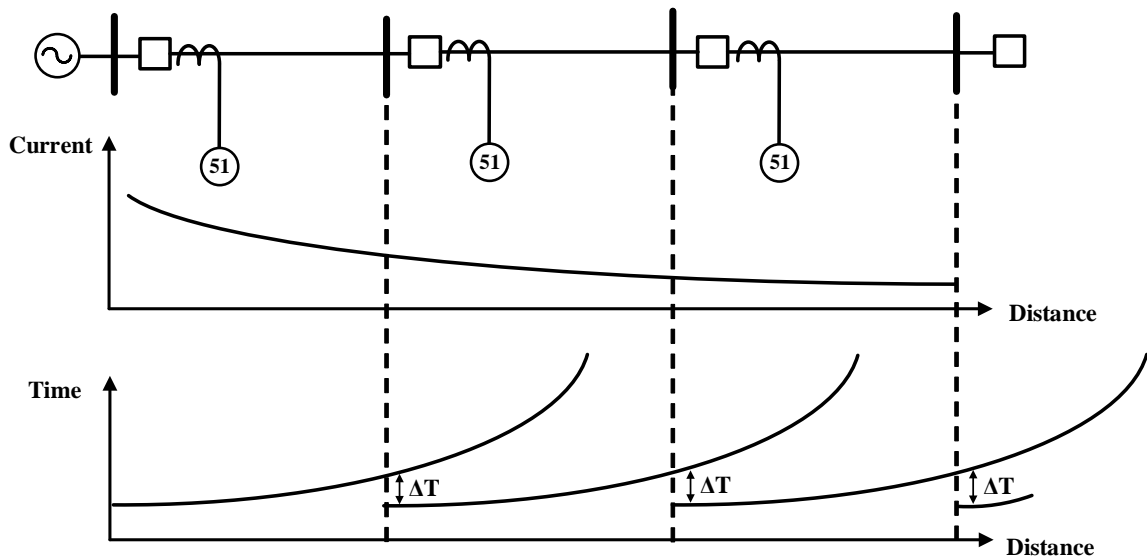
Figure 3-4: Inverse-Time Relay Coordination

Using the coordination strategy of Figure 3-4 however may result in delayed tripping for close-in faults. High fault current near the source can be harmful to the power system equipment. To solve this problem, a high set instantaneous element is combined with the inverse time overcurrent element as shown in Figure 3-5. The instantaneous element shall be set to under reach the protected line to avoid operation for faults on next line.
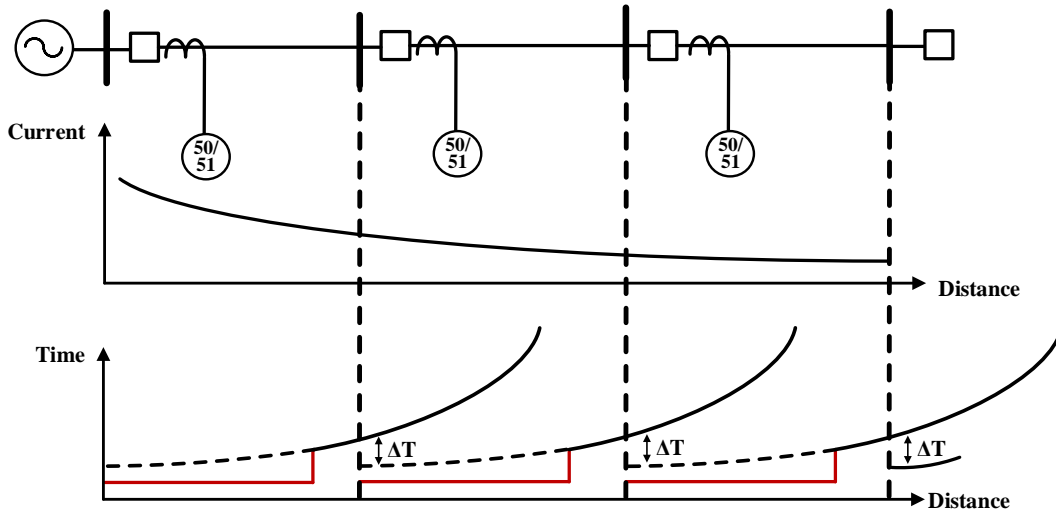
Figure 3-5: Combined Instantaneous and Inverse-Time Relay Coordination

3.2.3 Overcurrent Relay Setting in Distribution Systems

A. Phase Time Overcurrent

The common utility practice to select the pickup value of phase overcurrent element is given in the following range:

$$\frac{I_{min}^{3ph-eos}}{3} > I_{51P}^{P} > 1.3 \times I_{Lmax} \tag{3.4}$$

Where I_{51P}^{P} is the pickup setting of the phase overcurrent element, $I_{min}^{3ph-eos}$ is the minimum three phase fault at the end of line/section, and I_{Lmax} is the maximum load current. Since phase-phase fault is less than three phase faults, it should be considered as the minimum fault current.

B. Ground time overcurrent element setting rules

In contrast to the phase element, load current is not important for ground faults. However, since many distribution systems are unbalanced, the pickup setting of the ground

60

overcurrent element shall always be checked against system unbalanced to avoid false tripping. The utility practice has been to ensure that the selected pickup current is greater than one fifth the maximum load current I_{Lmax}, by doing so, 10-15% load unbalanced will be allowed. Accordingly, the pickup value selection range can be given as per equation 3.5

$$\frac{I_{min}^{1ph-eos}}{3} > I_{51N}^{P} > 0.2 \times I_{Lmax} \tag{3.5}$$

Where I_{51N}^{P} is the pickup setting of the ground overcurrent element, and $I_{min}^{1ph-eos}$ is the minimum ground fault at the end of line/section.

3.3   Directional Element

Directional element (ANSI number 32) indicates the direction of current flow with respect to a reference quantity. Directional element is a fundamental building block of many protection elements and schemes. For example, it is used to control overcurrent element, supervise distance protection, and is used in forming the quadrilateral distance characteristics. In fact, the reliability of directional comparison protection schemes such as the Permissive Overreaching Transfer Trip (POTT) is dependent on the performance of direction element [137, 138]. Conventional directional elements respond to the phase shift between a polarizing quantity and an operating quantity. Figure 3-6 shows a conventional directional element in which the phase voltage "V" is the polarizing quantity, and the phase current "I" is the operating quantity [137]. For forward fault at F1, the phase current lags the phase voltage by an angle "φ_F" which is equal to the fault loop impedance. For reverse fault at F2, the current direction reverses, and the phase current leads the phase voltage by

an angle "φ_R" which is equal to 180° minus the fault loop impedance. The directional element uses such information about phase angle difference to make directional decisions.
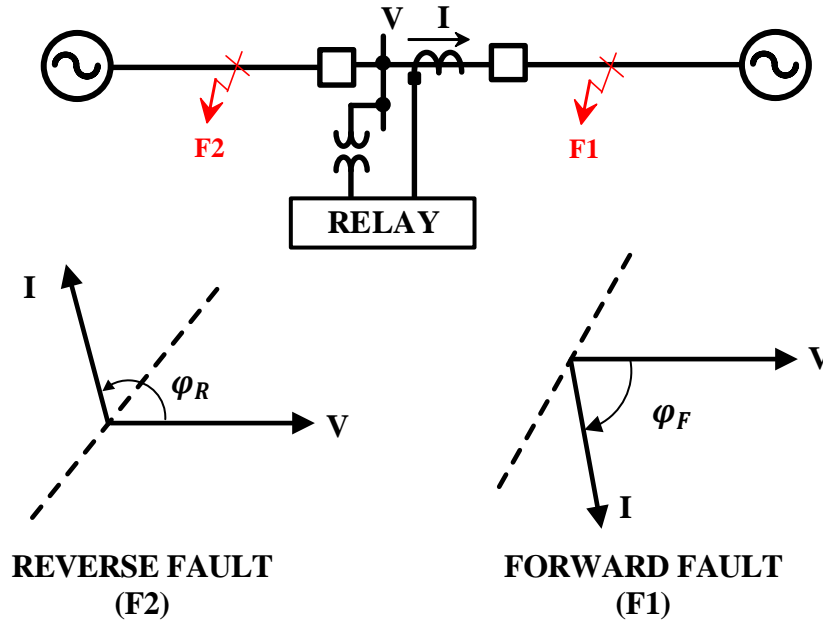
Figure 3-6: Directional Element Basic Principle of operation [137]

It is observed from Figure 3-6 that the voltage signal maintains its phase angle during fault, and therefore, it is used as a reference for the angular measurement. Voltage is the most popular polarizing quantity, but it is not the only signal. In general, the polarizing quantity is a reference signal used by the directional element to measure the change in phase angle of the operating quantity. The polarizing quantity must be stable, and reliable during faults [137]. The choice of polarizing signal depends on the type of fault and the power system topology. Generally, it can be a voltage signal or current signal or a sequence component quantity of voltage and current, or a combination of them.

Directional Relay Concepts

The initial design of directional element is done using induction (disk or cup) electromechanical relays shown in Figure 3-7. The relay has two alternating current (AC) inputs, the operating quantity (OP) and the polarizing quantity (POL). The two inputs (which can be voltage or current signals) are applied to the relay coils to produce the currents i_{m1}, and i_{m2}. The relay torque magnitude is proportional to the magnitude of coil currents and the phase angle difference between them. The relay is designed such that the torque is maximum when the produced fluxes are perpendicular, and zero when the fluxes are in phase or out of phase by 180° [134]
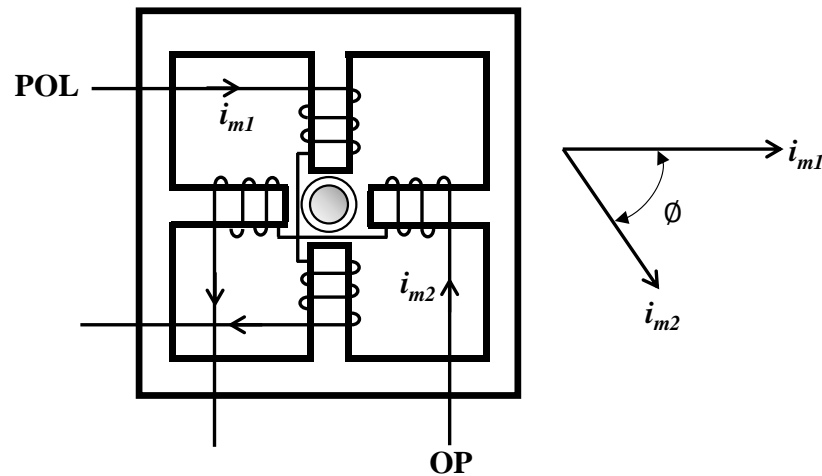
Figure 3-7: Typical electromechanical induction cup relay [137].

The general form of torque equation in terms of operating and polarizing quantities can be written as such:

$$T = k.\,|OP||POL| \cos{(\theta - \theta_{MT})} \tag{3.6}$$

Where |OP| is the magnitude of the operating quantity; |POL| is the magnitude of the polarizing quantity; θ: is the angle between the operating quantity and polarizing quantity.; and θ_{MT} is the maximum torques angle. In electromechanical relays, the maximum torque angle is defined as the angle by which the operating quantity must be displaced from the

polarizing quantity to produce the maximum torque, i.e., it is the angle at which the magnetic fluxes are perpendicular to each other. By convention, the maximum torque angle θ_{MT} is measured with reference to the polarizing quantity, and it can be defined as leading or lagging with respect to the operating quantity as defined by relay manufacturer. Equation (3.6) can be used to construct a phasor diagram to describe the relay operating characteristic. For example, if the polarizing quantity is the voltage V, the operating quantity is the current I, and θ_{MT} is defined by relay manufacturer as leading to V, a phasor diagram can be constructed as shown in Figure 3-8.
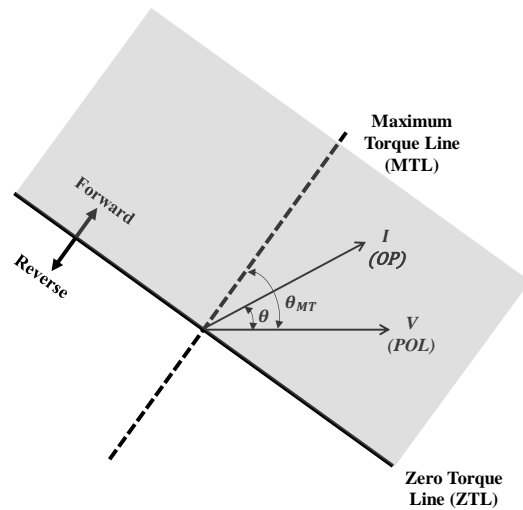
Figure 3-8: Directional Relay Operating Characteristic [139].

In this example, starting from the polarizing reference voltage and rotating by an angle θ_{MT} anti-clockwise produces what is called the Maximum Torque Line (MTL) shown as dotted line in Figure 3-8. Another important characteristic is the Zero Torque Line (ZTL) which is always perpendicular ($\pm$ 90) to the MTL, this line represents the point at which the relay torque equals zero, or equivalently, the point at which the magnetic fluxes are in phase or out of phase by 180°. The ZTL defines the relay operating regions, as shown in Figure 3-8, all operating current phasors above this line will produce positive torque and hence will

result in relay operation (in Forward Direction). On the other hand, all operating current phasors below this line produces negative torque, and hence the relay will restrain from operation.

Modern microprocessor-based relays use two approaches to implement directional element:

(1) Forming Torque-Like Quantities

In this approach, the digital relay emulates the behavior of electromechanical relays by forming a torque-like equations. The minimum torque to operate the relay, and the maximum torque angle in such relays is a relay setting not a characteristic feature. The maximum torque angle is sometimes referred to as the characteristic angle and here it represents the torque value to achieve maximum sensitivity [140, 141]. This approach has been used by earlier versions of microprocessor relay in the 1980's.

(2) Sequence Impedance Measurement

After 1993, a new operating concept has been introduced based on sequence impedance measurements has been introduced [140].

3.3.1 Phase Directional Element

3.3.1.1 Traditional Phase Directional Elements

Traditional phase directional elements were used with electromechanical relays before digital relaying technology. These relays use the line-line voltage measurements as polarizing quantities, and the phase current as operating quantity. The most commonly used polarizing line to line voltages are the 30°, 60°, and 90° connections. The angles here refer to the Relay Connection Angle (RCA) which is defined as the phase angle difference

between the operating current, and polarizing voltage at unity power factor [134]. Figure 3-9 shows the relationships between the operating current of phase-A and the corresponding polarizing voltages for every RCA type [134].
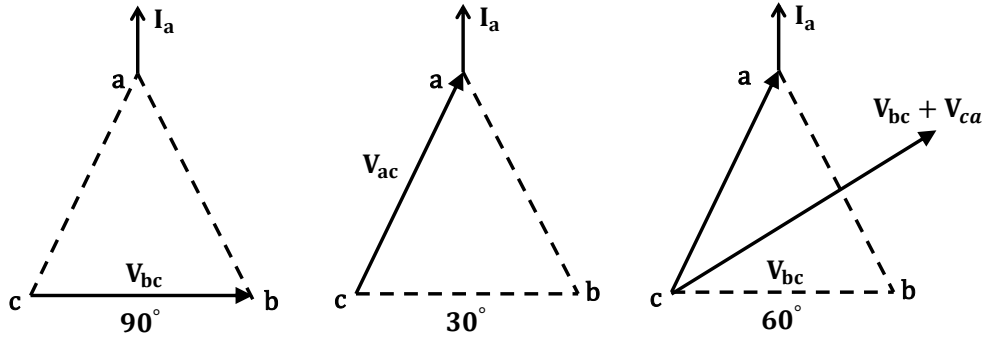
Figure 3-9: Conventional Connection of Phase Directional Relays [134].

Among the relay connection of Figure 3-9, the 90° connection or the quadrature connection has been the most popular and the mostly used connection. In this method, the polarizing line voltage is selected for any two phases, and the operating current is selected as the third phase as shown in Table 3-2.

Table 3-2: 90° Directional Element Polarizing Quantities

Phase	Polarizing Voltage	Operating current
A	VBC	IA
B	VCA	IB
C	VAB	IC

The torque expressions of each phase directional element is given as [141]:

$$TA = k.|VBC||IA| \cos\left(\theta_{,BC} - \theta_{MT}\right) \tag{3.7}$$

$$TB = k.|VCA||IB| \cos\left(\theta_{B,CA} - \theta_{MT}\right) \tag{3.8}$$

66

$$TC = k.|VAB||IC|\cos\left(\theta_{C,AB} - \theta_{MT}\right) \tag{3.9}$$

Where TA, TB, TC are the quadrature polarized relay torque of phase A, B, and C; VBC, VCA, and VAB are the line to line voltages at relay location; IA, IB, and IC, are the phase currents at relay location; $\theta_{A,BC}$, $\theta_{B,CA}$, and $\theta_{B,CA}$ are the phase angle difference between phase-phase polarizing voltages and phase operating current; and θ_{MT} is the maximum torque angle. Figure 3-10 shows a typical operating characteristic of the quadrature polarized phase directional element. Typical maximum torque angles are θMT are 30°, and 60°.
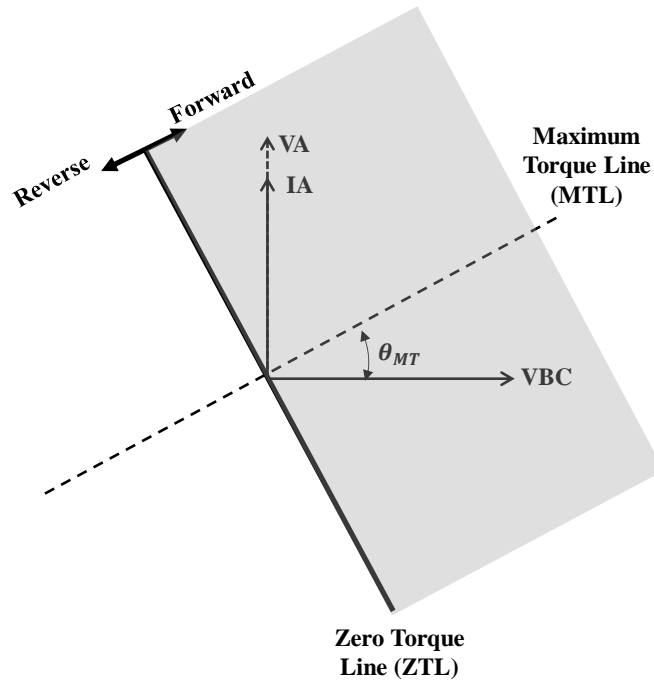
Figure 3-10: Operating characteristic of quadrature polarized phase directional element [142]

Despite of its widespread, quadrature polarized relays have inherent dis-advantage. It is found that if a reverse single line to ground fault occur while the remote infeed current is predominantly zero sequence, the healthy phase directional elements may indicate forward fault instead of reverse fault [64, 137, 141]. This disagreement may cause false tripping of

the healthy line. Possible solution to this problem are reported in [141] which include

adding supervision/blocking elements or seeking agreement between all phases before

issuing a trip command. However, these solutions have limitation as reported in [141].

Modern directional relays seek innovative ways to overcome this problem by introducing

new sequence component based directional elements. These new elements have superior

performance over the traditional 90° connected directional relay. In next section, these

methods will be explained and reviewed.

3.3.1.2   Positive Sequence Voltage-Polarized Directional Element

Positive sequence directional element is used to detect direction for three phase balanced

faults. This element can be implemented in modern microprocessor relays using two

approaches, the torque like approach and the sequence impedance-based approach. The

two methods will be briefly presented hereunder.

A. Torque Equation Approach

Since only positive sequence quantities are available under balanced load condition, this

element uses the positive sequence voltage as polarizing quantity and the positive sequence

current as operating quantity. The torque equation can be expressed as [141]:

$$T32P = |3V_1||3I_1| \cos \left(\angle 3V_1 - (\angle 3I_1 - 3Z_{L1}) \right) \qquad (3.10)$$

Where T32P is the positive sequence torque, V_1, I_1 are positive sequence voltage and at

relay location respectively, and Z_{L1} is the positive sequence line impedance. Directional

decision is based on the sign and magnitude of the torque T32P. Positive torque indicates

forward fault, and negative torque indicates reverse fault. Moreover, the magnitude of the

torque shall exceed minimum threshold to avoid nuisance tripping at condition when the polarizing and operating quantities have unreliable small values [141]. The relay operating characteristic is shown in Figure 3-11.
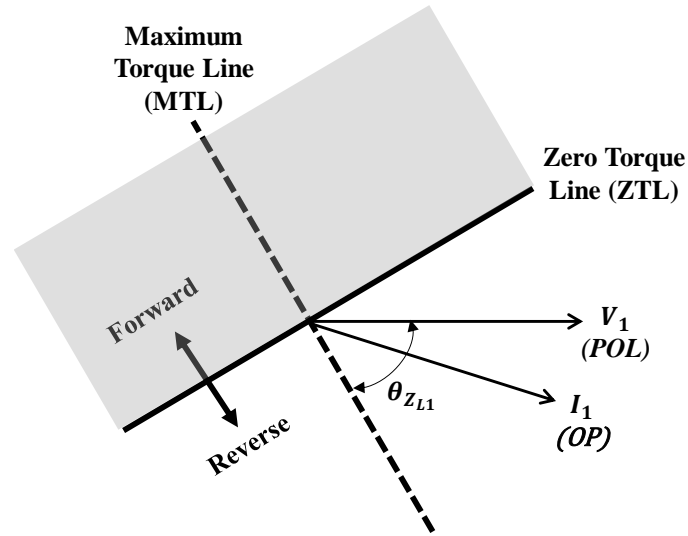
Figure 3-11: Positive Sequence Voltage Polarized Direction Element Operating characteristic (T32P)

B. Sequence Impedance Approach

An impedance based positive sequence directional element (32P) is introduced in [64]. It is based on comparing the angle of the measured positive sequence impedance against upper and lower thresholds. The fault is considered forward if measured positive sequence angle lies within the range of equation 3.11:

$$(-90° + Z1ANG) < Arg[Z1] < (90° + Z1ANG) \qquad (3.11)$$

Where Arg[Z1] is the angle of measured positive sequence impedance, and Z1ANG is the positive sequence impedance of the protected line. The operating characteristic of this element is shown in Figure 3-12.
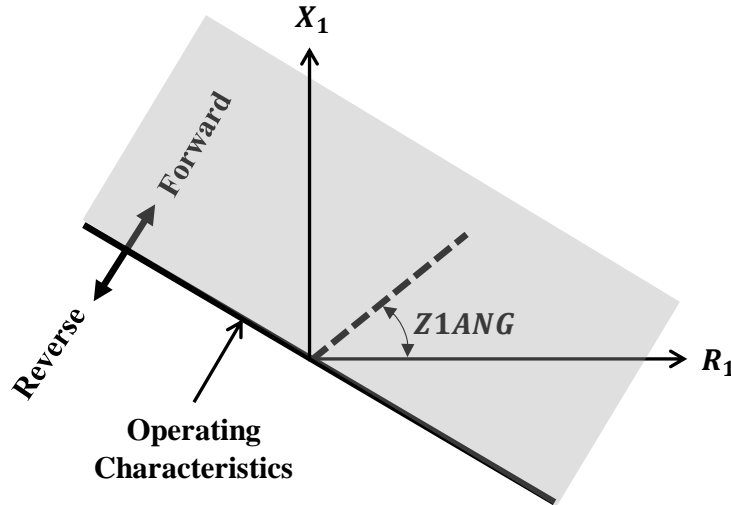
Figure 3-12: Directional Element Based on the Angle of Measured Positive Sequence Impedance [64]

3.3.2 Ground Directional Relays

3.3.3 Zero Sequence Voltage-Polarized Directional Element

This element uses the zero-sequence voltage ($3V_0$) as polarizing quantity, and the zero-sequence current ($3I_0$) as operating quantity. Figure 3-13 shows the phasor diagram of ($3V_0$) and ($3I_0$). It is noted that the phase angle difference between them is greater than $90°$, however, it was difficult to design a maximum torque angle θ_{MT} greater than $90°$ in electromechanical relays. Therefore, the polarity of either ($3V_0$) or $3(I_0)$ is normally inverted to make θ_{MT} less than $90°$ as shown in Figure 3-13.
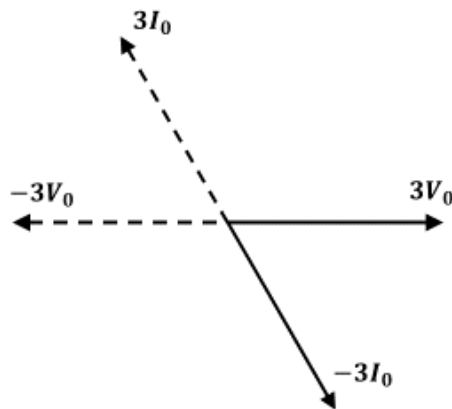
Figure 3-13: Zero Sequence Voltage Polarized Ground Directional Element Operating Characteristic

Accordingly, Table 3-3 shows the polarizing options of zero sequence voltage polarized ground directional element.

Table 3-3: Zero Sequence Voltage Polarizing Quantities

Polarizing Voltage	Operating current
3V0	-3I0
-3V0	3I0

A. Torque Equation Approach (T32V)

This element defines the torque equation based on the zero-sequence voltage as polarizing quantity, and the zero-sequence current from residual CT connection as operating quantity. Moreover, the maximum torque angle is set to equal the line zero sequence impedance. The torque expression for this directional element can be written as follows [143]:

$$T32V = |3V_0||I_R| \cos\left(\angle{-3V_0} - (\angle I_R + \angle\theta_{MT})\right) \qquad (3.12)$$

Where $T32V$ is the zero-sequence voltage polarized torque, and I_R is the zero-sequence operating current obtained from CT residual connection. Directional decision is based on the sign of the torque T32V, positive torque values indicate forward fault, whereas negative torque values indicate reverse fault. Figure 3-14 shows the operating characteristic of this directional element. The limitation of this relay is that remote faults result in very small polarizing zero sequence voltage, and hence it might be un-reliable [140]. An alternative algorithm that overcome this problem will be presented in next section.
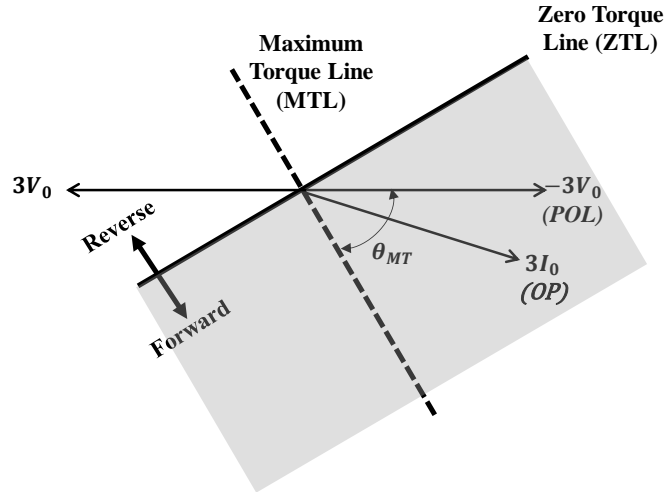
Figure 3-14: Zero Sequence Voltage Polarized Ground Direction Element Operating characteristic (T32Q) [143]

B. Sequence Impedance Based Approach

The voltage polarized zero sequence impedance (32V) directional element calculates the negative sequence impedance as shown in equation 3.13:

$$z_0 = \frac{\text{Re}[3V_0(3I_0 \cdot 1 \angle Z_{L0})]}{|3I_0{}^2|} \tag{3.13}$$

where z_0 is the zero-sequence impedance. Directional decision is based on comparing z_0 magnitude against two threshold values. If z_0 value is less than a forward fault threshold, the fault is declared forward. If z_0 is greater than a reverse fault threshold, the fault is declared as reverse. Moreover, additional supervision elements can be added to enhance the element security. In [64, 140] the directional element is supervised using two security checks:

$$I_0 > a_0 I_1 \tag{3.14}$$

$$50R > 3I_0 > 50F \tag{3.15}$$

Where a_0 is a factor selected by the user to enhance the security during current transformer (CT) saturation and line asymmetry; 50F is a forward sensitivity threshold to avoid nuisance tripping for low values of $3I_0$, and 50R is a reverse sensitivity threshold to avoid nuisance tripping for low values of 3I.

3.3.4 Zero Sequence Current Polarized Directional Element

In this element, the operating current is obtained locally using residual connection of line CTs, whereas the polarizing current is obtained from external source [141]. The relay uses this information to form the torque expression shown in equation (3.16):

$$T32I = |3I_0||I_{POL}| \cos{(\angle I_{POL} - \angle 3I_0)} \tag{3.16}$$

Where T32I is the zero-sequence current polarized torque; $3I_0$ is the zero-sequence operating obtained from residual connection of CTs, and I_{POL} is the zero-sequence polarizing current obtained from external source. The torque value is then compared against two threshold values depending on its sign. If T32I is positive and greater than the positive threshold, a forward fault is declared. Otherwise, if T32I is negative and less than the negative threshold, a reverse fault is declared [64, 140]. Additional supervision elements can be added to enhance the element security. In [140], the directional element is supervised using four security checks:

$$I_0 > a_0 I_1 \tag{3.17}$$

$$3I_0 > 50G \tag{3.18}$$

$$I_{POL} > Preset\ Threhold \tag{3.19}$$

Where a0 is a factor selected by the user to enhance the security during CT saturation and line asymmetry, and 50G is the instantaneous ground overcurrent pickup setting. In addition to above three security check, a fourth criterion is added which represent the isolation status of the zero-sequence source, the element can be disabled if the zero-sequence source is isolated.

3.3.5 Negative Sequence, Voltage Polarized Directional Element

Negative sequence element is suitable for unbalanced faults, phase to phase, phase to ground, and phase to phase to ground. This element is normally combined with the positive sequence directional element to cover all types of phase faults. Negative sequence element has many advantages over other types of ground directional elements which include [137]:

- Compared to zero sequence element, negative sequence element is not affected by zero sequence mutual coupling, and it is less affect by the neutral shift of potential transformers.
- Zero sequence polarization voltage is always available, Zero-sequence voltage or current source is not.
- For strong zero sequence sources, the negative sequence polarizing voltage is higher than the zero-sequence voltage [141].

3.3.5.1 Torque Equation Approach

The early design of negative sequence directional element uses the torque-equation approach to implement the directional element in microprocessor relays. The relay uses the negative sequence voltage as polarizing quantity (with negative sign), and the negative sequence current as operating quantity. Moreover, the maximum torque angle is selected

as the positive sequence line impedance. Accordingly, the negative sequence torque equation can be written a such [141]:

$$T32Q = |3V_2||3I_2| \cos \left(\angle -V_2 - (\angle I_2 + \angle Z_{L1}) \right) \qquad (3.20)$$

Where T32Q is the negative sequence torque, V_2 is the negative sequence voltage at relay location, I_2 is the negative sequence current at relay location, and Z_{L1} is the positive sequence line impedance (represent the setting of maximum torque angle). The element operating characteristic is shown in Figure 3-15. Directional decision is based on the sign of the negative sequence torque. Positive T32Q value is interpreted as forward fault, and negative T32Q value is interpreted as reverse fault. The Torque is maximized with negative sequence current is shifted from the voltage by an angle equals to the positive sequence impedance angle.
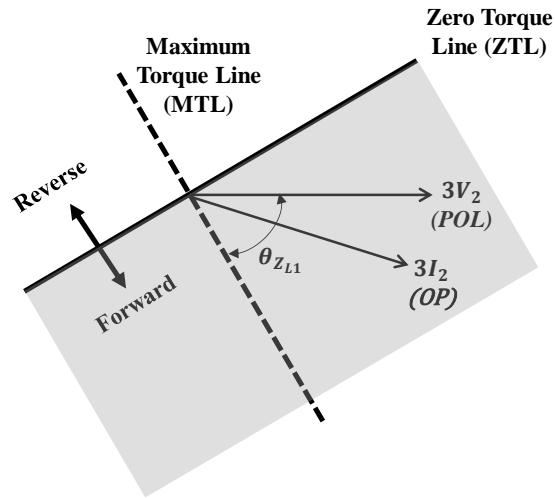

Figure 3-15: Negative Sequence Voltage Polarized Direction Element Operating characteristic (T32Q) [143]

The torque based negative sequence directional element has been implemented successfully for many years, however, it has some limitations. As reported in [141], when the source behind the relay is a strong negative sequence source, the negative sequence

voltage resulting from remote fault can be too low to ensure proper polarization. To overcome this limitation, sequence impedance based directional elements has been developed as will be shown in next section.

3.3.5.2   Sequence Impedance Approach

The voltage polarized negative sequence impedance (32Q) directional element calculates the negative sequence impedance as shown in equation 3.21:

$$z_2 = \frac{\text{Re}[V_2(I_2 \cdot 1 \angle Z_{L1})]}{|I_2{}^2|} \tag{3.21}$$

Where z_2 is the negative sequence impedance. Directional decision is based on comparing z_2 magnitude against two threshold values, if z_2 value is less than a forward fault threshold, the fault is declared forward. Otherwise, if z_2, is greater than a reverse fault threshold, the fault is declared as reverse. Moreover, additional supervision elements can be added to enhance the element security. In [64, 140], the directional element is supervised using three security checks:

$$I_2 > a_2 I_1 \tag{3.22}$$

$$I_2 > k I_0 \tag{3.23}$$

$$50R > 3I_2 > 50F \tag{3.24}$$

Where a_2 is a factor selected by the user to enhance the security during CT saturation and line asymmetry; k_2 is a preset factor selected by the user to enhance the security under unbalanced condition; 50F is the forward sensitivity threshold to avoid nuisance tripping for low values of $3I_2$; and 50R is the reverse sensitivity threshold to avoid nuisance tripping for low values of $3I_2$.

3.4 Directional Comparison Protection

Conventional protection methods such as direction overcurrent and step distance protection may result in unacceptable time delays that may compromise the stability of the power system. Communication assisted protection schemes (also known as pilot protection schemes or teleprotection schemes) are normally applied to provide high speed fault clearance, and to simplify the relay coordination [64]. Standard teleprotection schemes includes line current differential protection, current phase angle comparison protection, and directional comparison schemes [64]. Directional comparison protection is one type of teleprotection schemes that employ directional overcurrent and/or distance protection relays at both ends of the protected line with communication channel between them. Figure 3-16 show the general block diagram of directional comparison protection.
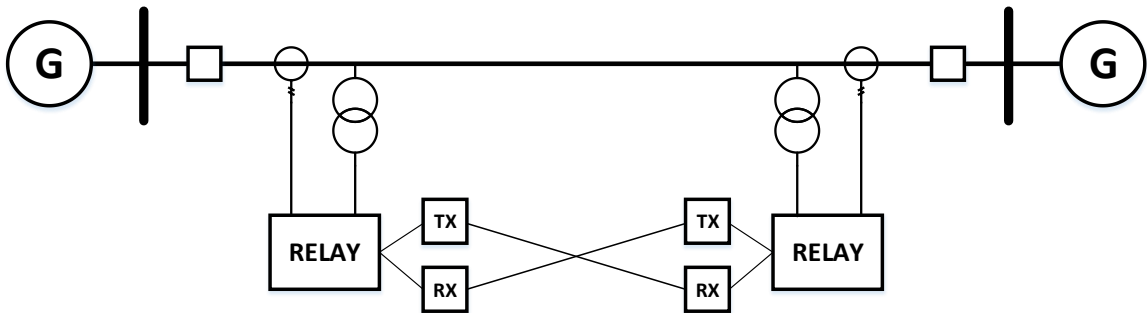
Figure 3-16: Block Diagram of Directional Comparison Protection [144]

In Figure 3-16, each relay uses a forward overreaching element and/or reverse looking element, and a comparison logic to determine whether the fault is internal or external. For internal faults, the forward elements at each line terminal operate, whereas for external faults, one forward element operates, and one reverse element operates. This information is fed to the built-in relay comparison logic to determine whether the fault is internal or external. Accordingly, the relay trips if the fault is internal and restrains otherwise [145].

In directional comparison scheme, an under reaching element is used to operate instantaneously independent of the communication scheme. A forward-looking element is set to overreach the remote line at each end with sufficient margin to cover the complete line, the operation of this element in addition to the reverse looking element is part of the communication scheme. Directional comparison scheme is based on exchanging one bit of information which represents the status of the directional or distance element at each line end. Therefore, compared to line differential for example, directional comparison requires lower channel bandwidth which makes them more cost effective. Typically, directional comparison scheme requires 0.5–1.5 kHz for analogue channels and 9.6kbps for digital channels [64]. The communicated bit between the two terminals can be either a blocking signal or a permissive signal. Accordingly, directional comparison scheme has been traditional classified as such [64]: (1) Direct Underreaching Transfer Trip (DUTT); (2) Permissive Underreaching Transfer Trip (PUTT); (3) Permissive Overreaching Transfer Trip (POTT); (4) Directional Comparison Blocking (DCB); and (5) Directional Comparison Unblocking (DCUB). Each scheme of the previous has its merits and demerits [146], however, the most prevalent directional comparison schemes are DCB and POTT. The POTT scheme is the fasters in the permissive category and is more secure compared to DCB scheme, however, the DCB is more reliable. In this thesis, a hybrid version of the POTT scheme (which combines the feature of POTT scheme (fast and secure) and DCB scheme (high reliability) [147]) will be used in this paper.

CHAPTER 4

MICROGRID MODELING

AC microgrids can operate in parallel with main grid and in islanded mode. The distributed energy resources can be either intermittent (such as photovoltaic, wind turbines, etc..) or controllable (Such as diesel/gas generators, Combined Heat and Power (CHP) generators). Therefore, the control system of DGs in microgrids depend on the type of available DGs, and the microgrid mode of operation. Some types of distributed energy resources such as photovoltaic (PV), battery banks, and fuel cells produce DC voltages and currents. On the other hand, some other types of energy sources such as wind turbines, and microturbines produce AC voltages and currents but at variable voltage and/or variable frequency. Therefore, integrating these kinds of resources to the AC distribution network requires using power electronic converters to match the prime source output voltage and frequency with that of the grid. This section presents the modeling and simulation of distributed energy resources to be used in this thesis including their control systems. Two types of distributed energy resources are targeted in this research, the first one is the diesel generator set model, and the second is a generalized model of inverter based distributed generator operating in current control mode. These models represent a rotating based DG and an inverter-based DG respectively.

4.1 Diesel Generator System Model

For decades, the diesel generators have been used mainly as a backup power source in the absence of main grid, or as a prime power source in remote areas. In microgrid application,

diesel generators play important role by regulating the system voltage and frequency in islanded mode in addition to supplying active and reactive power in both modes of operation. The modeling of diesel generator systems has been discussed in literature at different levels of details, however, for the purpose of protection system study, a simplified model based on the work presented in [148] is adopted. The model consists of synchronous generator, excitation system, automatic voltage regulator (AVR), diesel engine and speed governor.

4.1.1 Synchronous Generator

The synchronous generator model is available in RSCAD draft library, the model also includes a built-in step-up transformer to reduce the number of nodes in RTDS power system simulation. A 5.5MVA, 4.00kV, 50Hz synchronous generator model will be used in this thesis, Table 4-1 shows the synchronous machine parameters which was taken from [2].

4.1.2 Diesel Engine and Speed Governor

A simplified model for the diesel engine and its governor control system is adopted from [148], the block diagram is shown in Figure 4-1. The input to the mode is the speed deviation, and the output is the mechanical torque used to drive the synchronous generator. The speed governor is modeled as a PI controller with droop factor (R). The function of speed governor is to regulates the engine speed (frequency). The droop factor describes how the engine power changes in response to changes in load. If the speed decreases due to increase in load, then engine power increases by injecting more fuel and vice versa. The droop factor is expressed as a percentage, the lower the droop factor, the more responsive

the governor changes in speed. The diesel engine dynamics is represented by a first order transfer function with gain and time delay. Moreover, additional time delay is added to represent the delay between diesel combustion process inside the engine and torque production [148].

Table 4-1: Synchronous machine parameters [149]

| Description	Symbol	Value	Unit
Rated apparent Power	S	5.5	MVA
Rated RMS Line-to-Line Voltage	V_{LL}	4.00	kV
Base Angular Frequency	F	50	Hz
Stator resistance	R_a	0.002	pu
Stator Leakage reactance	X_a	0.13	pu
d axis unsaturated reactance	X_d	1.79	pu
d axis unsaturated transient reactance	X_d'	0.169	pu
d axis unsaturated sub−transient reactance	X_d''	0.135	pu
q axis unsaturated reactance	X_q	1.71	pu
q axis unsaturated transient reactance	X_q'	0.228	pu
q axis unsaturated sub− transient reactance	X_q''	0.2	pu
d axis unsaturated transient open time constant	T_{do}'	4.3	pu
d axis unsaturated sub−transient open time constant	T_{do}''	0.032	pu
q axis unsaturated transient open time constant	T_{qo}'	0.85	pu
d axis unsaturated sub−transient open time constant	T_{qo}''	0.05	pu
Inertia constant	H	3.03	MWs/MVA
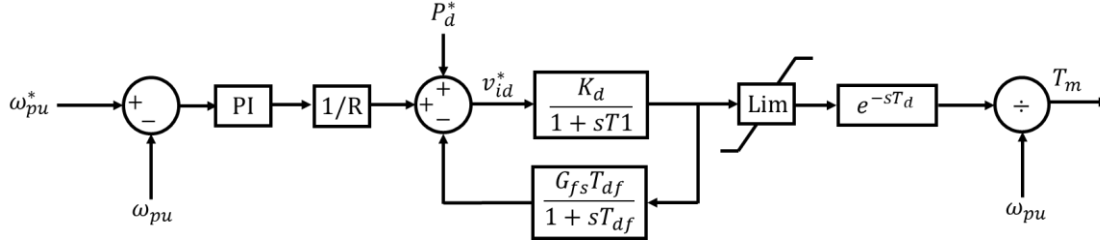
Figure 4-1: Diesel Engine and Speed Governor Model [148]

It is important to note that in grid connected mode, the system frequency is regulated by the main grid. Therefore, the diesel engine operates in speed droop mode to regulate the engine output power only. The droop factor R is set to 5%. In islanded mode, the diesel engine regulates the system frequency. Therefore, it operates in isochronous mode. In this case, the droop factor is set to 0.01%. Tuning of PI controller parameters and the gain parameters are adjusted manually in RSCAD runtime till satisfactory response is achieved.

4.1.3 Excitation System and Automatic Voltage Regulator

The excitation system supplies DC power to the rotor windings of synchronous generator to produce the magnetic field necessary for its operation. The Automatic Voltage Regulator (AVR) is used to regulate the generator's terminal voltage by controlling the exciter. Many standard models are available for the exciter and AVR. In this thesis, the IEEE Type AC4A Excitation System whose block diagram is shown in Figure 4-2 is used. This excitation system uses an ac alternator and controlled thyristor rectifier to produce the field voltage EFD needed to excite the synchronous generator field windings [150]. As shown in Figure 4-2, the inputs to the exciter are the reference voltage V_{REF}, the power system stabilizer input V_S (if any), and the voltage V_C which represent the generator measured terminal voltage and the load compensation elements (if any) measured using a voltage transducer with time constant Tr. The second block limits the voltage regulator input to values

82

between V_{IMAX} and V_{IMIN}. The third block represents a lead-lag compensator with time constants of T_B, and T_C. The fourth block represents the overall gain and time constant K_A and T_A associated with the AVR and/or the firing of the thyristors. V_{RMAX} and V_{RMIN} represent the maximum and minimum limits of regulator output voltage EF_D. These Limits can be modified to account for the loading effects by using the exciter load current and the rectifier loading factor which is proportional to the commutating reactance [150].
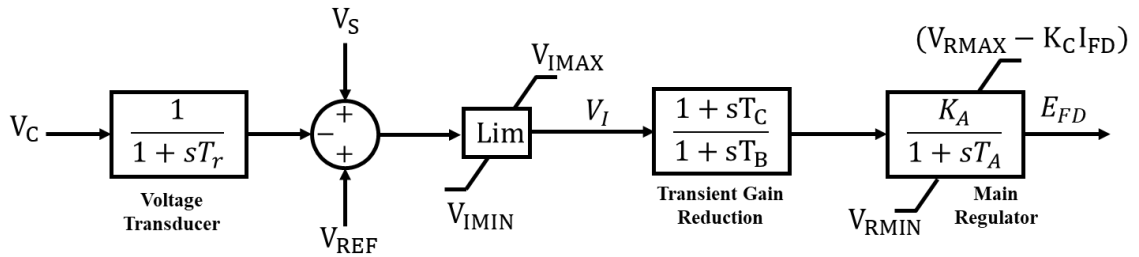

Figure 4-2: IEEE Type AC4A Excitation System Model [150].

The IEEE ACA Exciter model is available in the RTDS/RSCAD draft library and was used directly. The exciter parameters were adopted from the sample parameters provided in IEEE® standard 421.5-1992 [150]. The parameters are shown in Table 4-2.

4.2 Inverter Based Distributed Generators (IBDGs) Model

Figure 4-3 shows the general block diagram of the Inverter Based Distributed Generator (IBDG) considered in this thesis. It consists of (1) a conditioned prime energy source augmented with energy storage; (2) a DC-link capacitor; (3) a current controlled Voltage Source Inverter (VSI); (4) a three-phase low pass filter; (5) a transformer and (6) a circuit breaker (CB) to interface the IBDG with medium voltage network. The circuit element C_{DC} denote the DC bus capacitance; R_f represent the combination of filter capacitance and inverter switching losses; L_f and C_f represent the filter inductance and capacitance respectively. The circuit parameter V_{DC} denote the DC bus voltage; v_{iabc}, and i_{sabc} denote

83

the inverter output voltage and current respectively; v_{sabc}, and i_{oabc} represent the filter output voltage and current respectively. P, and Q represent the active and reactive power exchange at the Point of Interconnection (POI) between the IBDG and the microgrid.

Table 4-2:IEEE Type AC4A Excitation system Data used in simulation [150]

| Description	Symbol	Value	Unit
Voltage input transducer filter time constant	Tr	0	sec
Transient gain reduction lead/lag denominator time constant	T$_B$	12	**sec**
Transient gain reduction lead/lag numerator time constant	T$_C$	1	sec
AVR amplifier gain	K$_A$	200	-
AVR amplifier time constant	T$_A$	0.02	sec
Reference Voltage	V$_{REF}$	1	PU
Rectifier loading factor	K$_C$	0	-
Voltage regulator input upper limit	V$_{IMAX}$	10	PU
Voltage regulator input lower limit	V$_{IMIN}$	-10	PU
Voltage regulator output upper limit	V$_{RMAX}$	5.64	PU
Voltage regulator output lower limit	V$_{RMIN}$	-4.53	PU
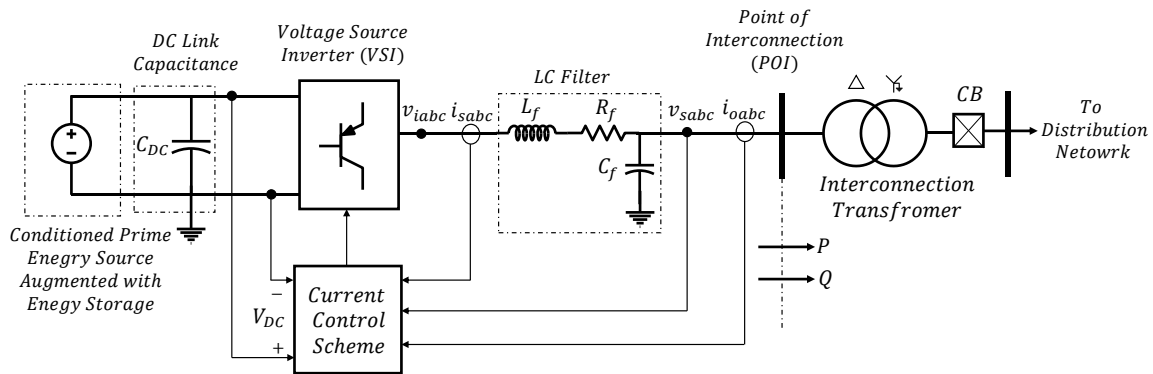
Figure 4-3: Grid Connected IBDG

4.2.1 Prime Energy Source Model

The dynamics of the DC side has secondary effect of the AC side dynamics during fault. The VSI transient behavior will have the major impact on protection system performance. Therefore, in this work, the exact modeling of the individual prime energy source such as PV or wind will not be included. Instead, the prime energy source will be modeled as DC voltage source whose value is constant during fault period. Another benefit from this assumption is the reduction of computational load on RTDS controls processor.

4.2.2 Voltage Source Inverter Model

RSCAD draft library contains detailed model for the VSI which can be used directly, however, representing the high switching dynamics of the VSI requires small time step simulation in the range of 1.4-2.5μs [151]. Therefore, simulating microgrid with multiple VSIs will occupy large portion from the RTDS processors. Considering the available RTDS rack at KFUPM LAB which has six PB5 processor cards, it would not be possible to simulate the full microgrid in real time. For that reason, the detailed VSI model will be replaced with an Average Value Model (AVM) of VSI.

For two level, and three level VSIs, two AVM methods are available, the first is the AVM in dq0 reference frame, and the second is the AVM in Phase Reference Frame [152]. In this thesis, the AVM model in phase reference frame will be used. In this method, the AC side of the VSI is represented as a three voltage-controlled sources (v_a, v_b, v_c), and the DC side of the VSC is represented as one current-controlled source (i_{dc}) as shown in Figure 4-4 [152]. The AVM in phase reference frame represents only the fundamental component of the AC voltage. High frequency harmonic content is not modeled. Moreover, the VSI

topology and the switching technique is irrelevant in this model, since it does not impact the amplitude and phase of the fundamental component [152].
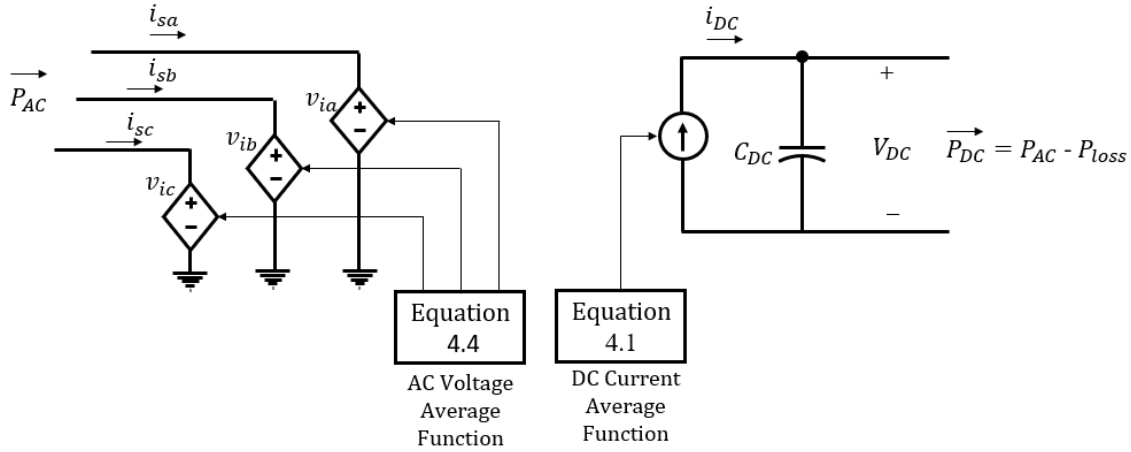

Figure 4-4: Average Value Model of VSI in phase reference frame [152].

The AVM voltage-controlled sources are represented as follows [152]:

$$\begin{bmatrix} v_{ia} \\ v_{ib} \\ v_{ic} \end{bmatrix} = \frac{V_{DC}}{2} \begin{bmatrix} m_a \\ m_b \\ m_c \end{bmatrix} \tag{4.1}$$

Where m_a, m_b, and m_c, are the inverter modulation index which are obtained using the inverse park transformation of the modulation index in dq reference frame m_d, and m_q. The AVM current-controlled-source DC current can be computed from the power balance principle using equation (4.2):

$$P_{AC} = P_{DC} + P_{Loss} \tag{4.2}$$

Where P_{AC}, P_{DC} are the average power on the AC side and the DC side of the VSI respectively. P_{Loss} is the VSI losses. In this thesis, P_{Loss} has bee omitted from equation 4.2 and lumped to the filter resistance. The resistive loss from the VSI is around 2% for two

86

level and three level converters. Accordingly, the current on the DC side of the AVM can
be computed as:

$$v_{ia}i_{sa} + v_{ib}i_{sb} + v_{ic}i_{sc} = V_{DC}I_{DC} \tag{4.3}$$

Substituting 4.1 into 4.3 yields:

$$I_{DC} = \frac{1}{2}(m_a i_{sa} + m_b i_{sb} + m_c i_{sc}) \tag{4.4}$$

RSCAD draft library contains the AVM model of the VSI in phase reference frame, and
hence it has been used directly in this thesis to reduce the number of nodes. The VSI
parameters used this thesis are shown in Table 4-3.

Table 4-3: IBDG Parameters [153]

Parameter	Symbol	Value	Unit
DC Bus Voltage	V_{DC}	2.2	kV
DC Side Filter Capacitance	C_{DC}	5000	µF
AC Side Filter Resistance	R_f	2e-3	Ω
AC Side filter Inductance	L_f	0.1	mH
AC Side Filter Capacitance	C_f	2500	µF
DC side series resistance	R_{DC}	1e-6	Ω
DC current injection resistance	R_{DC}	2e3	Ω

4.2.3 IBDG Current Control System

Various options exist for the control of IBDGs, the control option depend on the type of
DG and the microgrid mode of operation, i.e., grid connected mode or islanded mode.
Current control scheme or constant active and reactive power control scheme is used when

the IBDG is connected to a network in which the voltage and frequency control is managed by another source. The main objective of the controller is to inject active and reactive power independently. The active power is controlled by controlling the inverter d-axis current i_{sd}, and the reactive power is controlled by controlling the q-axis current i_{sq}. Figure 4-5 shows the block diagram of the current controller. It consists of phase locked loop, forward and reverse park transformation blocks, power controller, current magnitude limiter, and current controller.
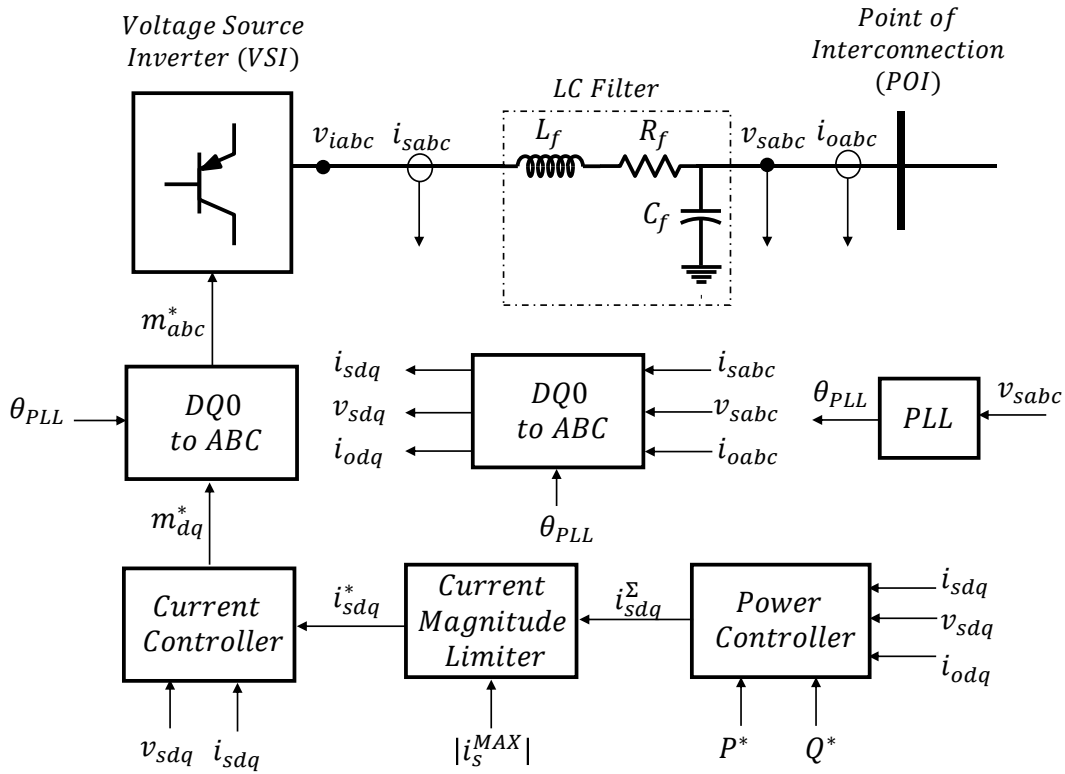

Figure 4-5: Current Control Scheme General Block Diagram

4.2.3.1   Basic Concept

In rotating reference frame, the instantaneous active and reactive powers are calculated as follows [154]:

$$P = \frac{3}{2}\left(V_{sd}i_{od} + V_{sq}i_{oq}\right) \tag{4.5}$$

$$Q = \frac{3}{2}\left(-V_{sd}i_{oq} + V_{sq}i_{od}\right) \tag{4.6}$$

where P, and Q are the active and reactive power at the point of interconnection (POI); i_{od}, and i_{oq}, are the dq components of the VSI filter output current; V_{sd}, and V_{sq} are the dq-components of the voltage at POI. If the grid space vector voltage $\hat{v}_s = v_{sd} + jv_{sq}$ is aligned with the d-axis reference, then the q-axis voltage v_{sq} would be equal to zero, and equation (4.3) and (1.4) reduces to:

$$p = \frac{3}{2}\left(V_{sd}i_{od}\right) \tag{4.7}$$

$$q = \frac{3}{2}\left(-V_{sd}i_{oq}\right) \tag{4.8}$$

From equation (4.7) and (4.8), it is noted that the instantaneous active power p, and the instantaneous reactive power q can be controlled independently by controlling the value of i_{od} and i_{oq} respectively. To achieve this, it is necessary to align the reference frame such the voltage at the POI has no q-axis component. This is achieved using PLL.

4.2.3.2 Phase Locked Loop

Phase Locked Loop (PLL) is a control system that tries to track the phase angle and frequency of a sinusoidal input signal. In this application, the PLL is used to obtain the phase angle θ_{PLL} necessary to transform the AC voltages and currents to the dq reference frame by tracking the frequency of voltages at the point of interconnection. In this study, the prebuilt Enhanced PLL control system from RSCAD draft library is used to implement the PLL controller. The enhanced PLL can be found in appendix-A. In addition to the

function of standard PLL, the enhanced PLL removes the double frequency error by estimating the amplitude of the input signal and then using it within a new loop to remove the error [155].

4.2.3.3 Power Controller

The power controller is used to obtain the reference d-axis and q-axis inverter output currents i_{sd}^{Σ} and i_{sq}^{Σ} using the active and reactive power set points (P^* and Q^*), and the measured d-axis and q-axis voltages at POI (V_{sd} and V_{sq}). The controller block diagram to be considered in this thesis is based on the contribution from [154] and is shown in Figure 4-6.
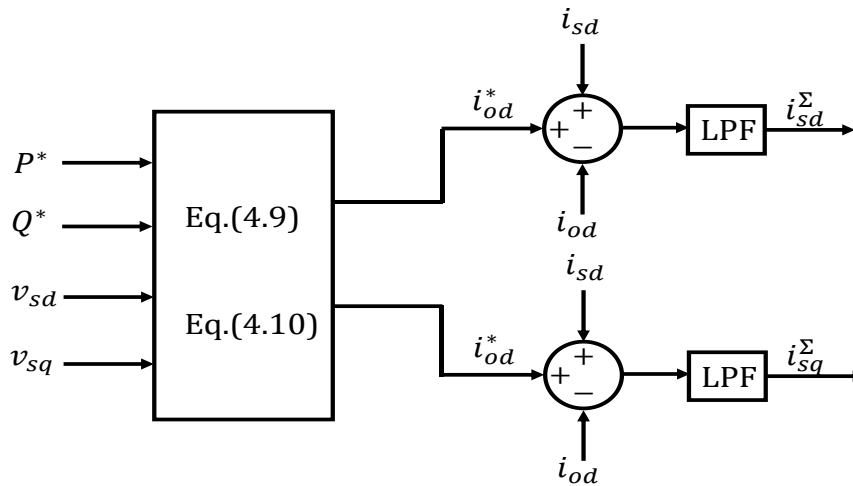

Figure 4-6: Power Controller Block Diagram

Solving for i_{od} and i_{oq} from equation 4.5 and 4.6 yields [154]:

$$i_{od}^* = \frac{2}{3}\left(\frac{V_{sd}P^* - V_{sq}Q^*}{V_{sd}^2 + V_{sq}^2}\right) \tag{4.9}$$

$$i_{oq}^* = \frac{2}{3}\left(\frac{V_{sq}P^* + V_{sd}Q^*}{V_{sd}^2 + V_{sq}^2}\right) \tag{4.10}$$

To obtain the reference current passing through the filter inductance i_{sd}^* and i_{sq}^*, equation (4.11) and (4.12) are used [154]:

$$i_{sd}^\Sigma = i_{od}^* + (i_{sd} - i_{od})$$ (4.11)

$$i_{sq}^\Sigma = i_{oq}^* + (i_{sq} - i_{oq})$$ (4.12)

A low pass filter can be used to process the reference currents to remove the harmonics and noise which may result from voltage distortion at PCC. However, since the average model of inverter is used in this thesis, the low pass filter is not used. The reference currents obtained from equation (4.11) and (4.12) are fed to the current magnitude limiter block.

4.2.3.4   Current Magnitude Limiter

To protect the inverter from short circuit currents and overloads, the inverter manufacturer normally limit the maximum fault current of the inverter, this can be achieving by adding a current magnitude limiter block which can be realized using equation (4.13):

$$|\hat{\imath}_s^*| = \sqrt{\left(i_{sd}^\Sigma\right)^2 + \left(i_{sq}^\Sigma\right)^2} < \hat{\imath}_{smax}^*$$ (4.13)

Where $|\hat{\imath}_s|$ is the magnitude of the inverter output space vector current, and $\hat{\imath}_{smax}^*$ is its maximum value which is normally in the range of 1.5-2 pu. It is noted that the ratio of $|i_{sd}^*|/|\hat{\imath}_s^*|$, and $|i_{sq}^*|/|\hat{\imath}_s^*|$ remains constant, i.e., the phase angle is not affected by the conversion [156].
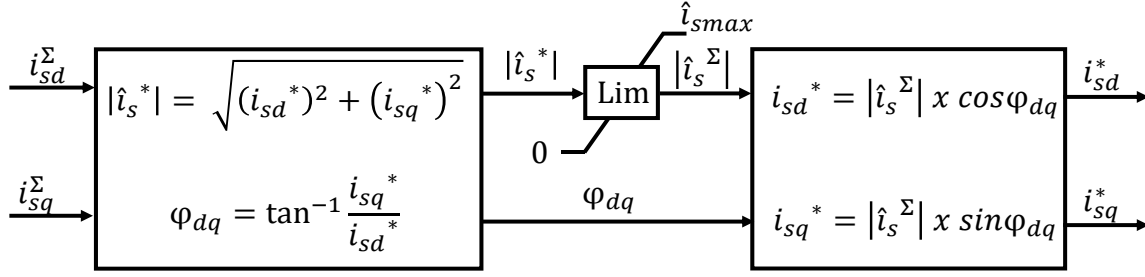
Figure 4-7: Current Magnitude Limiter Block Diagram [157]

4.2.3.5 Current Controller

From Figure 4-5 the dynamics of the inverter output current i$_{sabc}$ can be written as:

$$L_f \frac{d}{dt} i_{sabc} = -R_f i_{sabc} + V_{iabc} - V_{sabc} \tag{4.14}$$

where i$_{sabc}$ is inverter three phase output current, v$_{iabc}$ is the inverter three phase output voltage, v$_{sabc}$ is the three-phase voltage at the POI, R$_f$ is the filter resistance, and L$_f$ is the filter inductance. In synchronous rotating reference frame, equation 4.14 can be written as [158]:

$$L_f \frac{di_{sd}}{dt} = -R_f i_{sd} + L_f \omega i_{sq} + V_{id} - V_{sd} \tag{4.15}$$

$$L_f \frac{di_{sq}}{dt} = -R_f i_{sq} - L_f \omega i_{sd} + V_{iq} - V_{sq} \tag{4.16}$$

From equation 4.15, and 4.16 [158]:

- It is noted that i$_{sd}$, and i$_{sq}$ can be controlled by controlling the inverter d-axis and q-axis output voltage V$_{id}$, and V$_{iq}$. However, the POI voltages V$_{sd}$ and V$_{sq}$ also present in the equation, these terms are disturbance and shall be added to the control loop as feedforward terms to ensure closed loop stability.

92

- It is noted that a cross coupling voltage terms ($L_f \omega i_{sq}$, and $-L_f \omega i_{sd}$) are present in equation (4.15) and (4.16), therefore, it should be compensated by adding a feedforward term to the control loop similar to V_{sd} and V_{sq}.

Based on the above observations, the current controller can be simply implemented by using the scheme shown in Figure 4-8. The error signals ($i_{sd}{}^* - i_{sd}$) and ($i_{sq}{}^* - i_{sq}$) are fed to a PI controller. The feedforward compensation terms are then added to produce the final decoupled output reference voltages $V_{id}{}^*$ and $V_{iq}{}^*$.
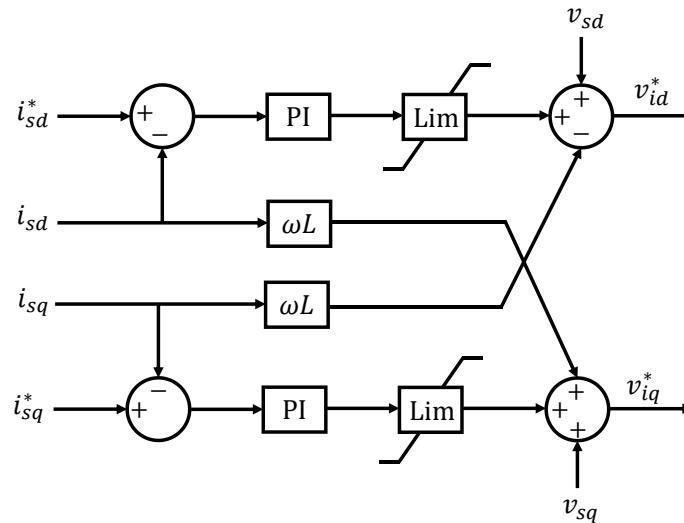

Figure 4-8: Block diagram of the current controller

4.2.3.6 Inverter modulation index calculation

Figure 4-9 shows the block diagram for generating the inverter modulation index. Assuming sinusoidal pulse width modulation (SPWM) technique is used for the voltage source inverter, the reference inverter output voltage can be written as such:

$$V_{id} = m_d \frac{VDC}{2} \tag{4.17}$$

$$V_{iq} = m_q \frac{VDC}{2} \tag{4.18}$$

where m_d and m_q are the d-axis and q-axis of the inverter modulation index, and VDC is the DC bus voltages. The m_d and m_q are passed through an inverse park transformation block to produce the abc quantities as such:

$$m_{abc}^* = \begin{bmatrix} sin\theta & cos\theta \\ sin(\theta - \frac{2\pi}{3}) & cos(\theta - \frac{2\pi}{3}) \\ sin(\theta + \frac{2\pi}{3}) & cos(\theta + \frac{2\pi}{3}) \end{bmatrix} m_{dq} \tag{4.20}$$

To keep the inverter operating in the linear modulation region, the magnitude of the modulation index shall not exceed its maximum limit which is 1 for conventional SPWM modulation, and 1.15 for SPWM with third harmonic injection [158]. The three phase modulating signals are then fed to SPWM generator to produce the firing of each power electronic switch in the inverter. Since AVM VIS model is considered in this thesis, m_{abc}^* are substituted into equation 4.1 and 4.4 introduced earlier to calculate the controlled voltage and current sources values.
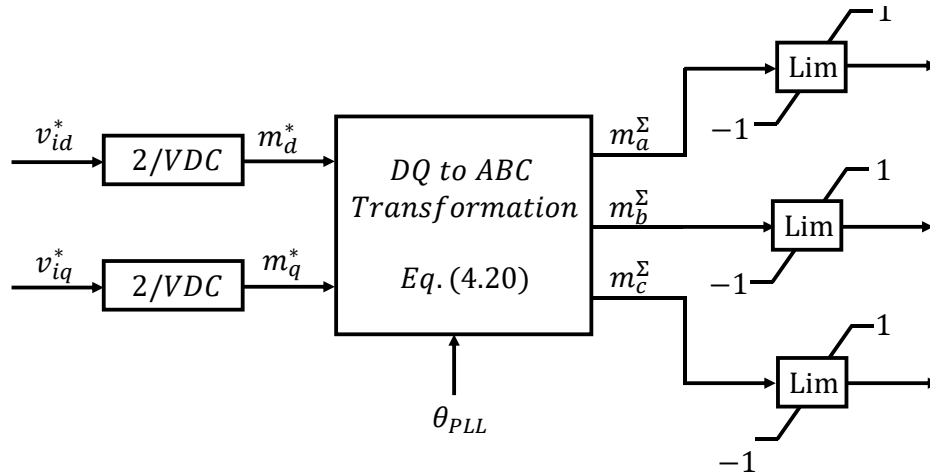

Figure 4-9: block diagram for generating the inverter modulation index

4.2.3.7   PI Controller Design

The proportional gain and the integral gain parameters k_p and k_i for the for d-axis and q-axis current control loop is selected based on the rule of thumb given in [158]:

$$k_p = \frac{L_f}{\tau_i} \qquad (4.21)$$

$$k_i = \frac{R_f}{\tau_i} \qquad (4.22)$$

where τ_i is the time constant of the closed-loop system and it is a design parameter. In this thesis, satisfactory performance has been achieved by selecting τ_i as 0.5ms. Accordingly, the resulting value k_p and k_i are 0.2, 4 respectively.

4.3   Distribution Network Model

In this thesis, the European version of the Cigrè benchmark MV distribution network has been selected. The benchmark is based on a modified version of actual distribution network in Germany that supplies small town and rural area [159]. The network parameters, line configurations, impedance calculations, and load flow results are published in [159]. The Distribution Network has two feeders separate by normally open switch. Either Feeder-1 or Feeder-2 can be used to study DER integration or both of them [159]. In this thesis, feeder-1 will be considered. However, to enable real-time simulation, the number of buses in feeder-1 is reduced from 11 buses to 6 buses while the feeder structure is almost maintained. This reduction is done due to the following limitation in RTDS:

1. The available RTDS rack at KFUPM Lab is based on PB5 processors. This model can simulate up to 72 single phase nodes on single card [151]. Considering the fact that

circuit breakers will be added as part of the protection system, the total number of nodes might be exceeded.

2. Multi-rack simulation requires using travelling wave-transmission line models. However, considering 50μs time step used in RTDS, travelling wave transmission line models require the line length to be at least 15kM [151]. However, the longest distribution line in the MV European benchmark is 7.2kM. Therefore, multi-rack simulation is not possible [151].

4.3.1 Network Topology

The single line diagram of the modified Cigrè benchmark MV European distribution network is shown in Figure 4-10. The nominal voltage of the network is 20kV, and the nominal frequency is 50Hz; the substation transformer is fed from 110kV sub-transmission system; Moreover, the network is reconfigurable by means of two normally open switches S2, and S3. Closing these switches can create looped/meshed configuration. The network parameters of the grid, transformer, and transmission lines are maintained as per the original network data published in [159].

4.3.2 Main Grid

The Sub transmission system represent the grid and its data is given in Table 4-4 [159].

<div align="center">

Table 4-4: Sub-transmission System Data [159].

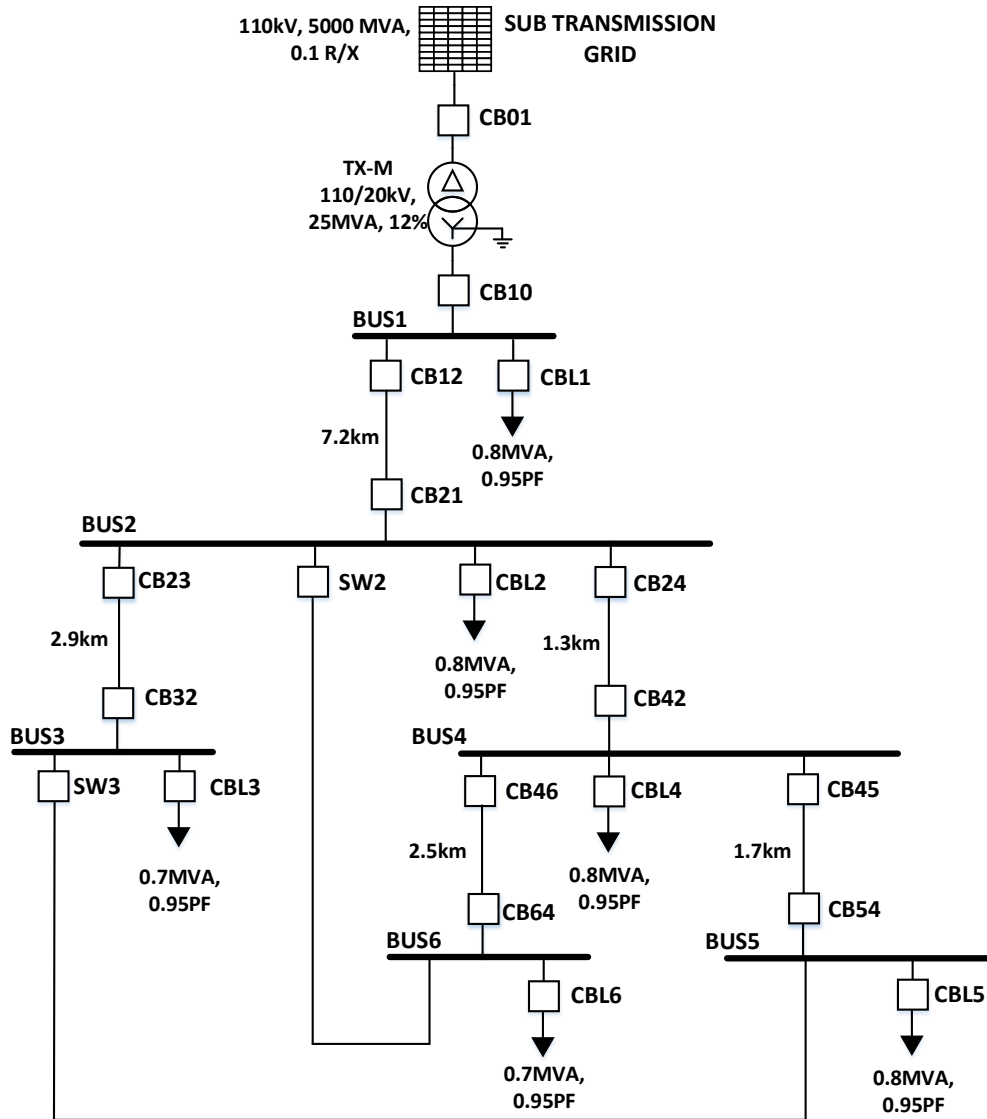| Description	Value	Unit
Nominal system voltage	*110*	*kV*
Short circuit power	5000	MVA
R/X ratio	*0.1*	-

</div>

Figure 4-10: Modified Cigrè benchmark MV IEC Distribution Network

The main grid behaves as infinite bus with respect to the distribution network, and therefore, it will be represented as an ideal voltage source behind impedance. The source model is used directly from the RSCAD library. The model requires the user to enter the positive sequence impedance and as an option, the zero-sequence impedance. However, the value of the zero-sequence impedance for the Cigrè benchmark network is not

provided. The grid source positive sequence impedance Zg is calculated from the data provided in Table 4-4 using equation (4.23).

$$|Z_g| = \frac{V_{LL}^2}{S_{sc}} = 2.42\Omega \tag{4.23}$$

Where V_{LL}, and S_{sc}, are the grid nominal system voltage and short circuit power respectively. The grid reactance and resistance X_g, and R_g can be calculated as such:

$$|Z_g| = \sqrt{X_g^2 + R_g^2} \tag{4.24}$$

Solving 4.24 for R_g and X_g yields:

$$R_g = \frac{Z_g}{\sqrt{1 + (X_g/R_g)^2}} = 0.2632\ \Omega \tag{4.25}$$

$$X_g = R_g \times (X_g/R_g) = 2.6319\ \Omega \tag{4.26}$$

Therefore, the equivalent source impedance can be represented as:

$$Z_g = 0.263 + j2.632 = 2.42\angle 84.29°\ \Omega \tag{4.27}$$

4.3.3 Substation Power Transformer

RSCAD library includes many models of power transformers, in this thesis, two winding, three-phase power transformer with tap changer is used. The transformer data is given in Table 4-5. The winding connection is configured in RSCAD to achieve dyn1 winding connection as per IEC 60076-1 standard [160]. The model contains integrated circuit breakers to reduce the number of nodes. The no load losses are estimated to be 0.1% of the transformer MVA [159], and the copper losses are considered 0.016 pu. The tap changer

98

in RTDS is modelled as idea ratio changer, i.e., changing the tap ratio is not associated with transformer windings and does not change the leakage reactance value [159]. Tap positions can be adjusted within the limits specified in Table 4-5.

Table 4-5: Transformer Data [159].

Description	Value	Unit
Connection	*3-ph Dyn1*	-
Primary Voltage	*110*	*kV*
Secondary Voltage	20	kV
Rated Power	25	*MVA*
Impedance Referred to secondary	*0.016+j1.92 (12%)*	*Ω*
Primary winding tap	*±5 % in 2.5 % increment no-load taps*	-
Secondary winding tap	±10 % in 0.625 %	-

4.3.4 Distribution Lines

RSCAD contains two models for transmission lines, the travelling wave model which is based on distributed parameter representation, and the PI section model which is based on lumped parameter representation. However, according to RTDS manual [73], if the transmission line model is shorter than 15kM, PI section can model the line more accurately. Therefore, PI section model is adopted in this thesis. The RSCAD draft model requires entering the positive and zero sequence impedances. Table 4-6 lists the transmission line parameters; R'ph, X'ph, B'ph represent the transmission line positive sequence resistance, reactance, and susceptance respectively; R'0, X'0, B'0 represent the

transmission line zero sequence resistance, reactance, and susceptance respectively; l represents the line length. These parameters are calculated in [159].

Table 4-6: Distribution Line Parameters [159]

From	To	R'ph	X'ph	B'ph	R'0	X'0	B'0	l	Installation
Bus	Bus	Ω/km	Ω/km	µS/km	Ω/km	Ω/km	µS/km	km	
1	2	0.501	0.716	47.493	0.817	1.598	47.493	7.2	Underground
2	3	0.501	0.716	47.493	0.817	1.598	47.493	2.9	Underground
2	4	0.501	0.716	47.493	0.817	1.598	47.493	1.3	Underground
4	5	0.501	0.716	47.493	0.817	1.598	47.493	1.7	Underground
4	6	0.501	0.716	47.493	0.817	1.598	47.493	2.5	Underground

4.3.5 Loads

Load is modeled using the RSCAD "Three phase RLC load with embedded breaker" which allows the user to model the load and its circuit breaker and thus reducing the total number of nodes required. The load schedule considered is presented in Table 4-7.

Table 4-7: Load values

Bus	Apparent Power			Power
	Phase A	Phase B	Phase C	Factor
	[KVA]	[KVA]	[KVA]	-
1	266.67	266.67	266.67	0.95
2	266.67	266.67	266.67	0.95
3	233.33	233.33	233.33	0.95

4	266.67	266.67	266.67	0.95
5	266.67	266.67	266.67	0.95
6	233.33	233.33	233.33	0.95

4.4 Microgrid Implementation

The study microgrid is formed by integrating the distribution network model with three distributed generators. One 5.5MV, Diesel Generator located is located at bus-2, and two 1.74MVA IBDGs located at bus-4 and bus-5 respectively. The single line diagram of the microgrid implementation in RSCAD-Runtime module is shown in Figure 4-12. The implementation details in RSCAD can be found in appendix A. The microgrid is simulated with a time step of 50μs on a one rack simulator with three PB5 processor cards. The Processor assignment for control and power system components is shown in Figure 4- 13.
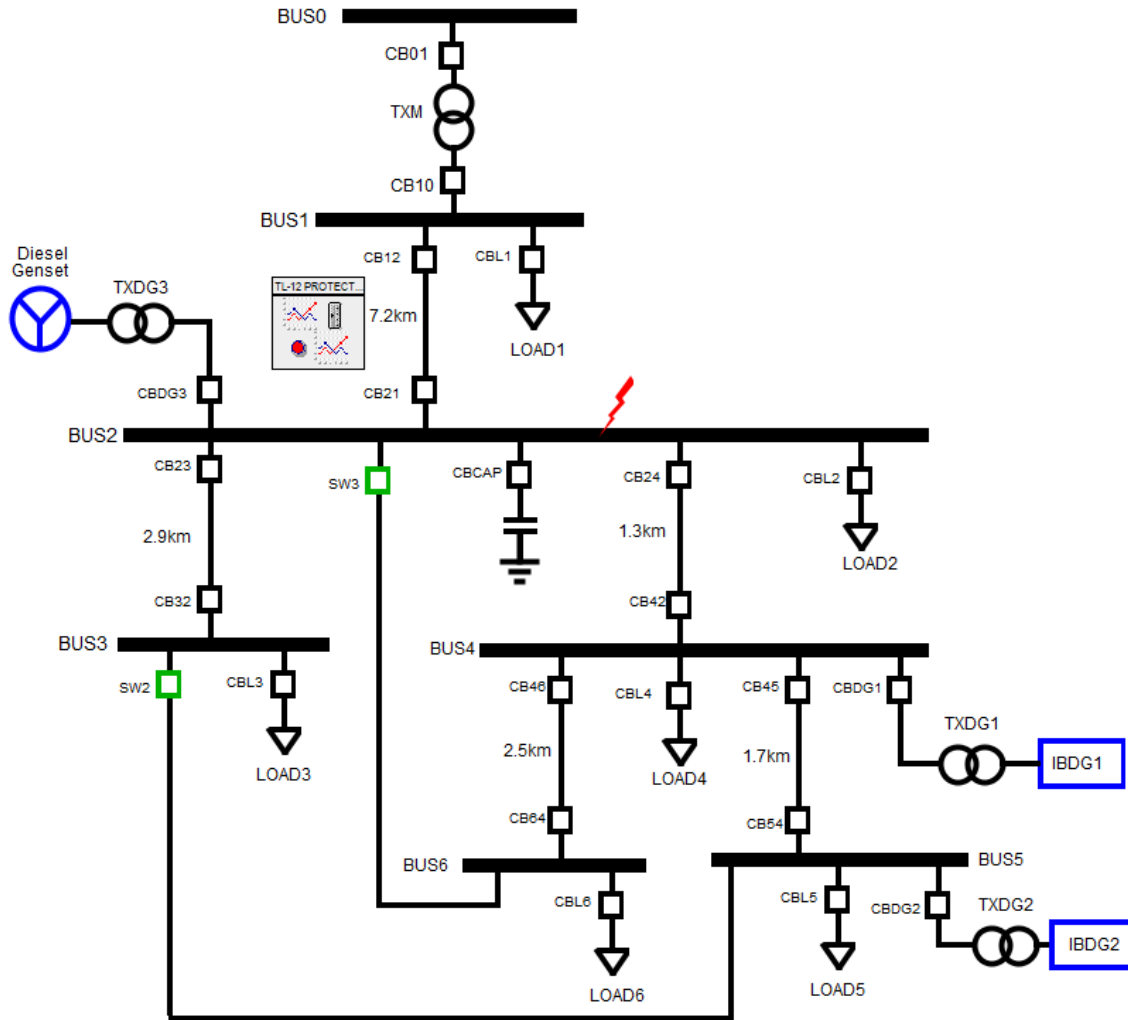
Figure 4-11: Microgrid Single Line Diagram in RSCAD Runtime module

At grid connected mode, the diesel generator operates at droop control mode, and the main grid regulates the voltage and frequency. At islanded mode, the diesel generator switches from droop control mode to isochronous mode. The diesel generator in this mode will be responsible for regulating the voltage and frequency. The IBDGs will operate at current control mode in both modes of operation.
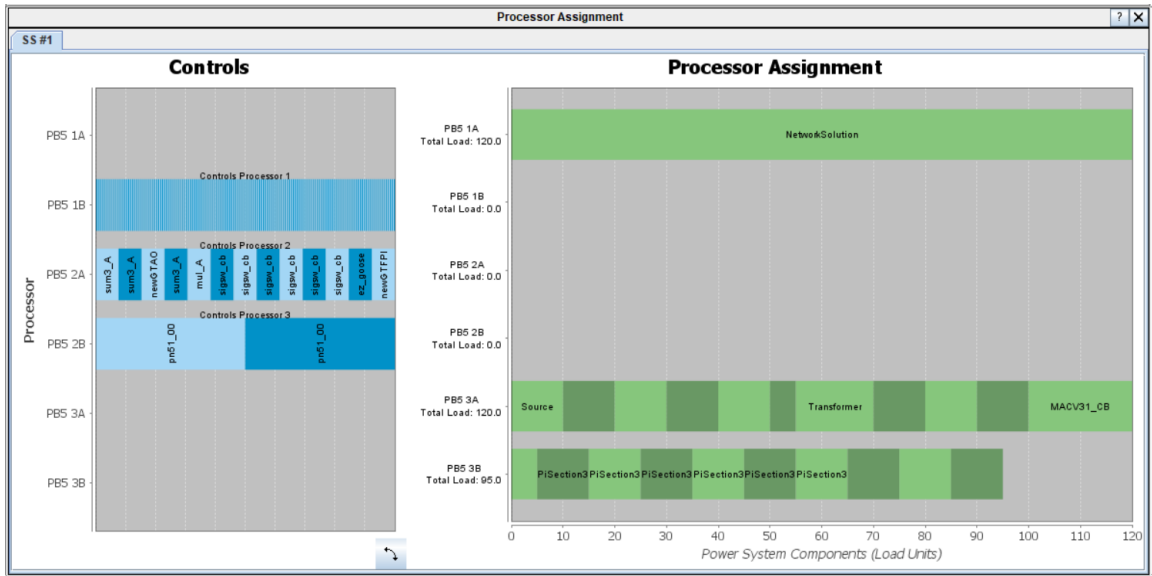
Figure 4-12: Microgrid Model Processor assignment in RSCAD/RTDS

4.5 Simulation Results

4.5.1 Grid connected Operation

In grid-connected mode, the main Circuit Breaker at PCC (CB10) is closed and the microgrid frequency is determined by the grid frequency. The IBDGs control their real and reactive power output using the current control schemes described in section 4.2.3 while the diesel generator operates in droop control to exchange real and reactive power with the grid

4.5.1.1 Steady State Bus Voltages

Table 4-8 show the steady state RMS line to line voltages on each bus for different connection states of DGs considering maximum generation and full load condition. The capacitor banks are switched on for the last three cases to obtain satisfactory bus voltage at steady state. It is noticed however that if at least two DGs are connected, there is no need for capacitor bank switching or tap changer adjustment.

103

Table 4-8: Phase-Phase RMS Bus Voltages in grid connected mode

DG Type	DG Connection Status							
DG3 (Diesel)	ON	ON	ON	ON	OFF	OFF	OFF	OFF
IBDG1	ON	OFF	ON	OFF	ON	OFF	ON	OFF
IBDG2	ON	ON	OFF	OFF	ON	ON	OFF	OFF
Phase-Phase RMS Voltage								
BUS0	109.9	109.97	109.98	109.98	109.97	110.02	110.02	110.01
BUS1	19.83	19.89	19.89	19.94	19.90	20.13	20.13	20.11
BUS2	19.97	19.85	19.85	19.71	19.65	20.13	20.13	19.80
BUS3	19.89	19.77	19.77	19.63	19.57	20.04	20.04	19.72
BUS4	19.98	19.79	19.79	19.58	19.69	20.07	20.07	19.68
BUS5	20.01	19.82	19.74	19.53	19.74	20.02	20.02	19.62
BUS6	19.91	19.72	19.72	19.51	19.61	20.00	20.00	19.60

4.5.1.2   DG Impact on Fault Current Level

To demonstrate the effect of DG integration on fault current level, a 10 cycle, 0.1Ω, three phase-fault was applied to Bus-2 before adding DGs, and after adding DGs. The increased shot circuit level due to contribution from DGs is evident from the Figure 4-14. Similar result is obtained for other buses in the system.
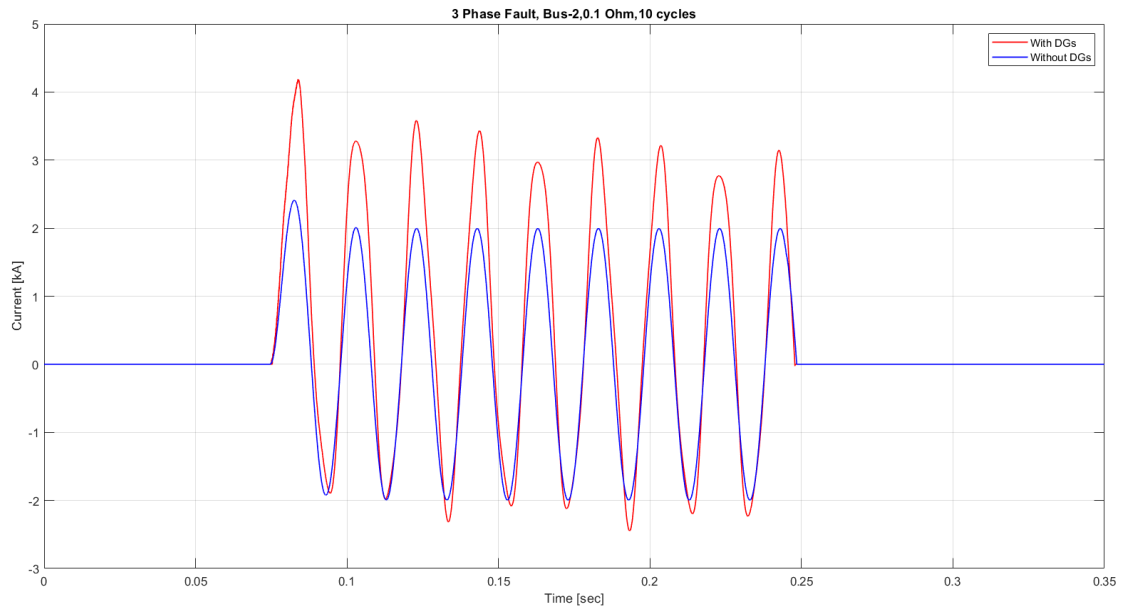
Figure 4-13: A 10 cycle, 0.1Ω, three phase at Bus-2 Before and After Adding DGs.

4.5.1.3   IBDG Fault Current Limiting

In this section, the IBDG ability to limit the magnitude of fault value will be demonstrated.

A 10 cycle, 0.1Ω, three phase faults is applied to Bus-4 to which DG1 is connected. The

maximum inverter current is set to 5kA peak. Figure 4- 15, and Figure 4-16 shows the

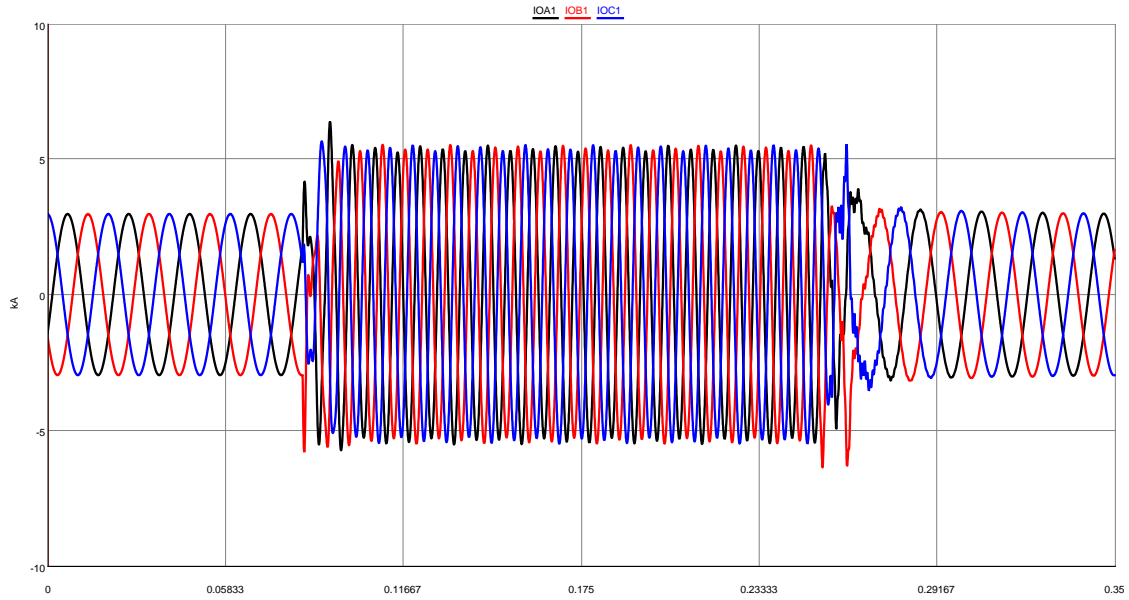IBDGs output current. It is noted that the fault current is limited to 5kA peak exactly as

expected.

Figure 4-14: IBDG1 Output Current Vs Time
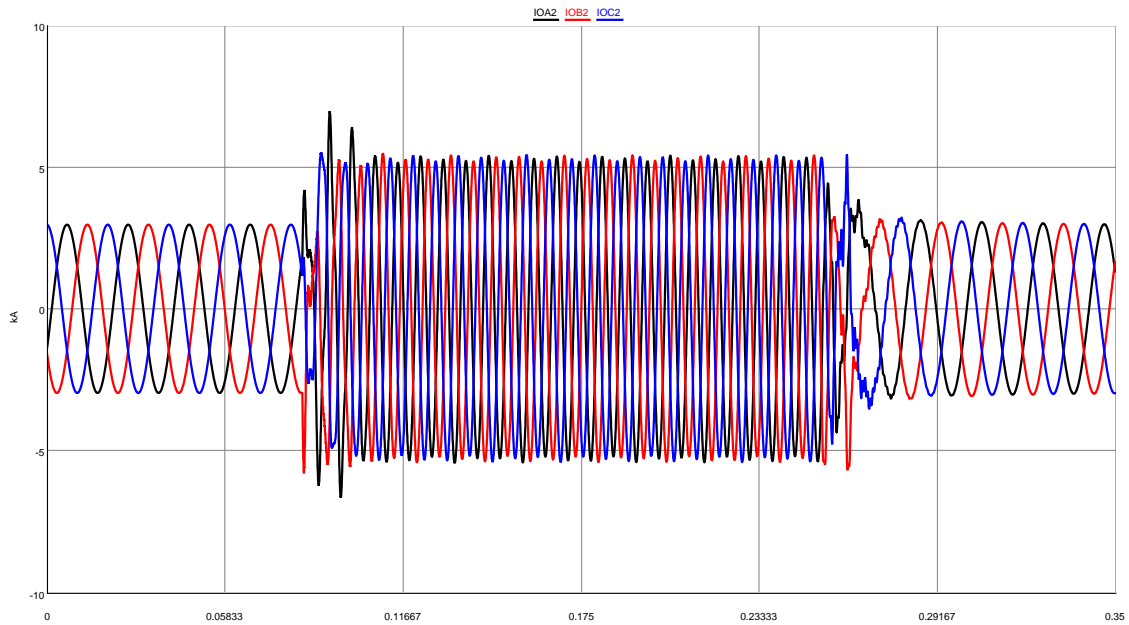
Figure 4-15: IBDG1 Output Current Vs Time

4.5.2 Islanded Mode Operation

In islanded mode of operation, the main Circuit Breaker at PCC (CB10) is open and the microgrid frequency is determined by the diesel generator. The IBDGs control their real

and reactive power output using the current control schemes described in section 4.2.3 while the diesel generator operates in isochronous mode to regulate the voltage and frequency.

4.5.2.1   Steady State Bus Voltages

Table 4-9 show the steady state RMS line to line voltages on each bus for different connection states of DGs considering maximum generation and full load condition. One capacitor banks is switched on to obtain satisfactory bus voltage at steady state for all cases.

Table 4-9: Phase-Phase RMS Bus Voltages in grid connected mode

DG Type	DG Connection Status			
DG3 (Diesel)	ON	ON	ON	ON
IBDG1	ON	OFF	ON	OFF
IBDG2	ON	ON	OFF	OFF
BUS0	110.0	110.0	110.0	110.0
BUS1	19.8	19.8	20.0	19.8
BUS2	20.0	19.9	20.2	20.0
BUS3	19.9	19.9	20.1	19.9
BUS4	20.0	19.9	20.0	19.8
BUS5	20.0	19.9	20.0	19.7
BUS6	19.9	19.8	20.0	19.7

4.5.2.2 Fault Current Level at Islanded Mode

This section demonstrates the difference between fault current level at grid connected mode and islanded mode. A 10 cycle, 0.1Ω, three phase fault is applied at Bus-2 for grid connected and islanded modes. The sharp difference in fault current level is evident from Figure 4-17. Similar results are obtained for other buses in the system but are not shown due to space limitation.
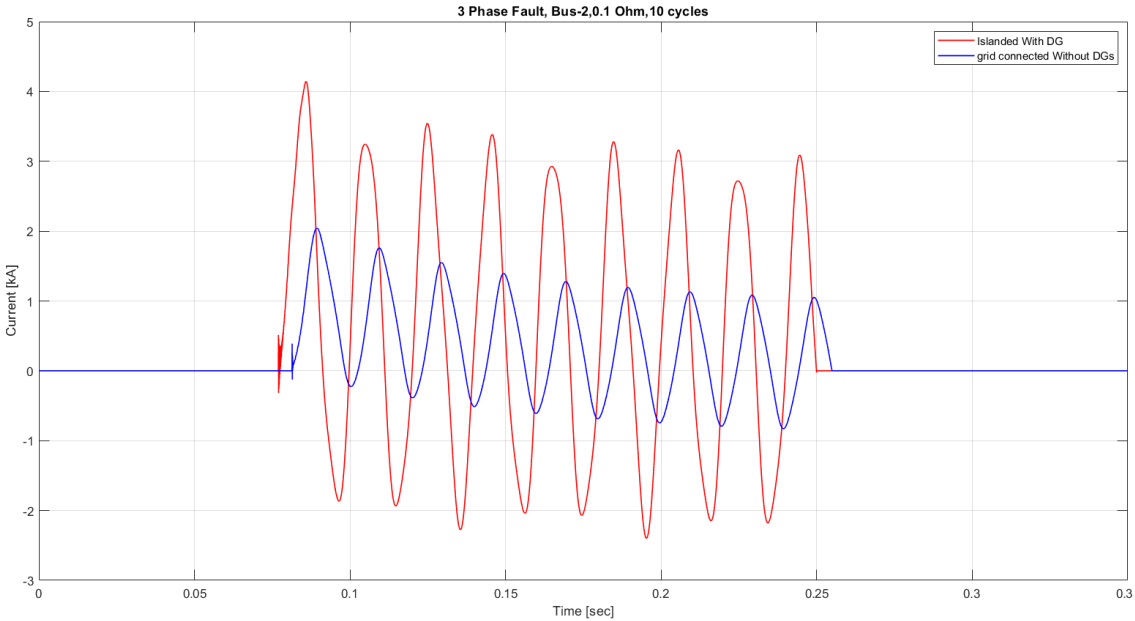

Figure 4-16: A 10 cycle, 0.1Ω, three phase at Bus-2 in grid connected mode and islanded modes

CHAPTER 5

PROPOSED ADAPTIVE PROTECTION STRATEGY

In this chapter, a decentralized pilot-based adaptive protection strategy (APS) is proposed for MV looped microgrid using off-the-shelf commercial IEDs (Intelligent Electronic Devices) and IEC 61850 GOOSE communication. The adoption of IEC 61850 with horizontal and vertical messaging structure made it possible to build a decentralized APS in which decision making is distributed over several IEDs instead of one central unit. For distribution line protection, a Hybrid Permissive Overreaching Transfer Trip (HPOTT) scheme based on DOCRs is proposed to provide high speed protection in both grid-connected and islanded modes of operation. Unlike conventional POTT logic which require both line terminals to declare forward fault, the proposed hybrid scheme with integrated echo logic, weak infeed logic, and current reversal logic allows both line terminals to trip at high speed under weak infeed, loss of infeed, and open terminal conditions. The pilot signals necessary for the HPOTT scheme are transferred using IEC 61850 GOOSE messages. The protection scheme includes also directional comparison bus protection, DG interconnection protection, and point of common coupling protection. In this section, the proposed protection scheme will be presented and explained.

5.1   Zones of protection

To achieve a generalized protection strategy that is independent of network configuration, the protection strategy is developed for each zone independently. As shown in Figure 5-1,

the microgrid is divided into five protection zones which are: (1) Distribution lines; (2) Point of common coupling; (3) Distributed generators (4) Loads; and (5) buses
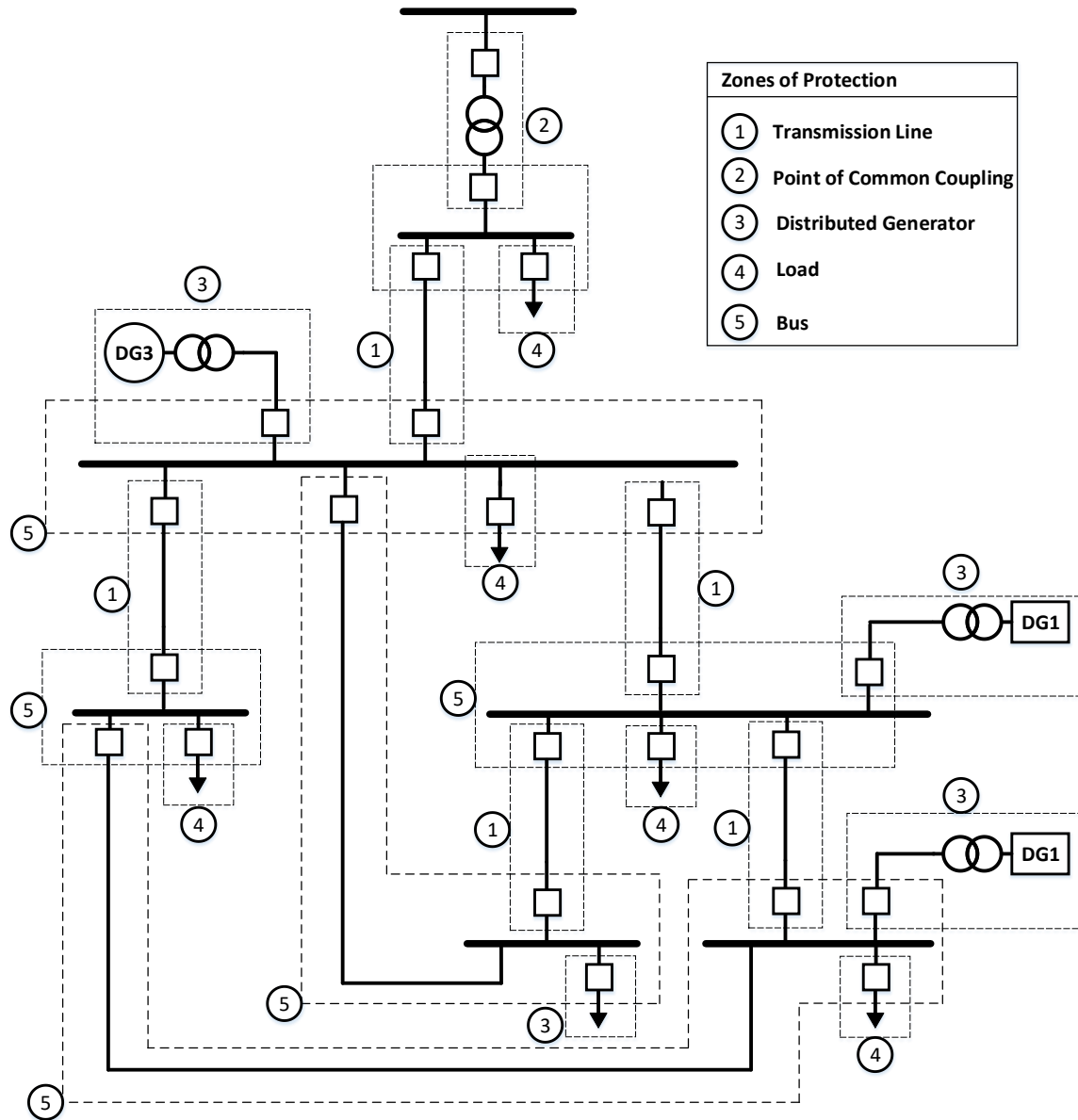

Figure 5-1: Zones of Protection

5.2 Distribution Line Protection

A communication assisted directional comparison scheme is proposed in this thesis to produce automatic and fast fault clearing of distribution line faults. In this thesis, the

scheme applied is Hybrid POTT (Permissive Overreaching Transfer Trip). Figure 5-2 shows the general arrangement of IEDs for each distribution line. Each line is equipped with one IED to enable double end disconnection. The scheme requires IEDs with directional phase and ground overcurrent elements (67P, 67G), phase undervoltage elements (27P), and zero sequence overvoltage elements (59N). Moreover, the IEDs must support IEC 61850 communication standard, and must have either a built-in hybrid POTT scheme or a programmable logic to build the scheme manually. Many off-the-shelf commercial distribution system IEDs have these specifications as standard. In the following sub-sections, the scheme logic will be explained and the criteria of protection setting will be specified.
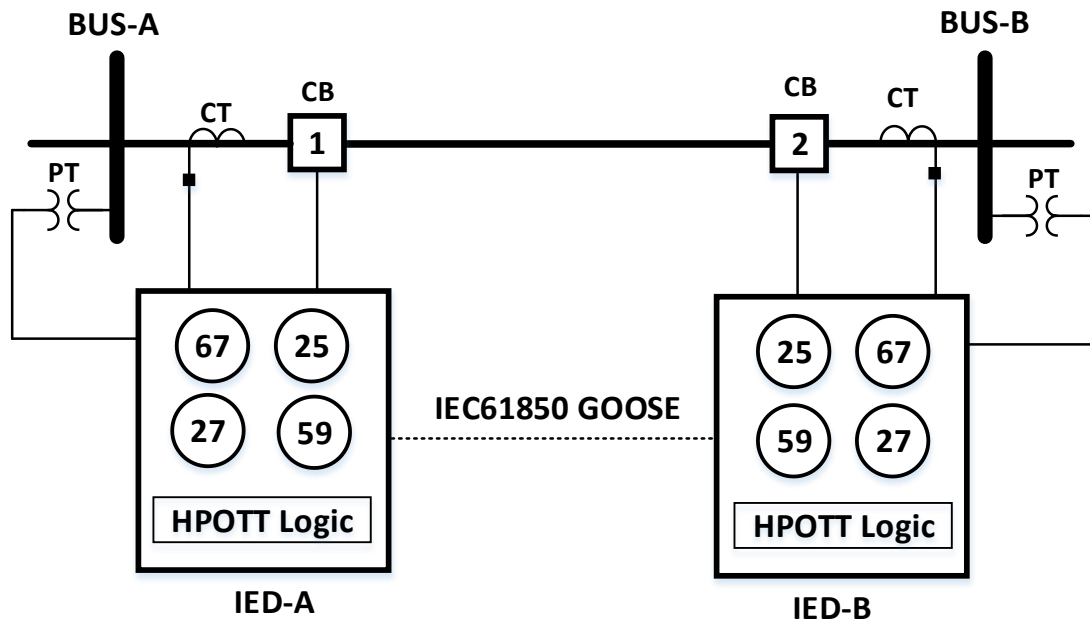
Figure 5-2: Distribution Line Protection Single Line Diagram

5.2.1 Permissive Overreaching Transfer Trip

The traditional POTT scheme operating principle is illustrated in Figure 5-3. In this scheme, one asserted overreaching protection function at each line end (marked as Level-2) is used to send a permissive signal (marked as KEY) to the remote end when a fault is detected in front of the relay. A trip command is issued to each local circuit breaker if each relay detects a fault in the forward direction and simultaneously receives a permissive trip signal (marked as PT) from the remote relay. If the fault is internal, the forward overreaching elements pick-up and both relays send a permissive signal to the remote end, this will cause the AND gate to produce an output to initiate tripping to local circuit breakers. If the fault is external, the overreaching element at only one end of the line picks up and no trip is initiated at either terminal [64, 147].
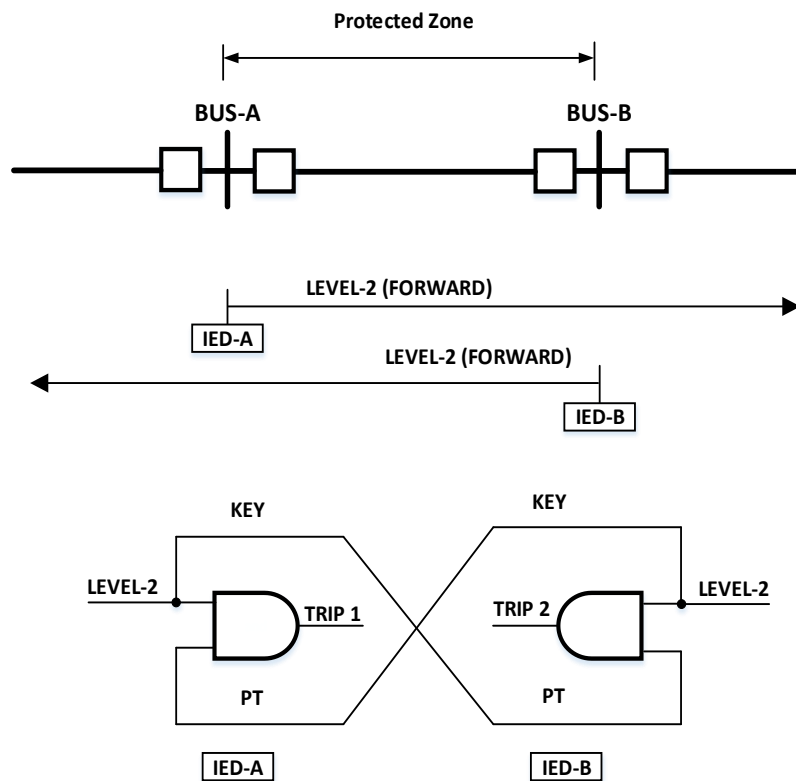
Figure 5-3: Traditional POTT relay elements and Basic Logic [64]

The forward tripping element (level-2) can be directional overcurrent and/or distance protection element that is set to overreach the protected line with enough margin to ensure the complete line is protected [64, 147]. The classical POTT scheme is simple and inherently secure against external faults. However, if either end failed to declare forward fault, high speed tripping from both ends will not occur. Weak infeed from IBDGs, loss of infeed due to plug and play nature of DGs, and remote open terminal are examples that may cause the classical POTT scheme to fail. The consequence will be fault clearance from one terminal after coordination time delay. If the other terminal is connected to weak source, sequential clearing may or may not occur depending on system transfer impedance after tripping of strong terminal. Since IBDGs maximum fault contribution is independent of system transfer impedance, the fault contribution from the weak terminal may stay below the pick-up setting, this condition leads to failure in fault detection. These limitations in traditional POTT scheme are the motivation behind proposing the hybrid POTT scheme which allows double end disconnection under weak infeed, loss of infeed, remote open terminal, and current reversal conditions.

5.2.2 Hybrid Permissive Overreaching Transfer Trip

An elementary block diagram of the hybrid POTT scheme is shown in Figure 5-4. Each relay at bus A and B has two protection elements, a permissive overreaching trip element (marked as Level-2), and a reverse blocking element (marked as Level-3). As shown in Figure 5-4, the reverse level-3 element must be set more sensitive than the remote level-2 element to avoid sympathetic tripping for out of section faults similar to the DCB scheme [64]. An under reaching directional phase and ground overcurrent element referred to as Level-1 element is normally included to provide protection against close-in high fault

currents near the relay terminals. This element operates independently from the POTT logic. The additional Level-3 element turns the classical POTT scheme into hybrid scheme (permissive and blocking scheme). The hybrid POTT scheme combines the advantage of high reliability of DCB (directional comparison blocking) scheme and high security of the pure POTT scheme [147].
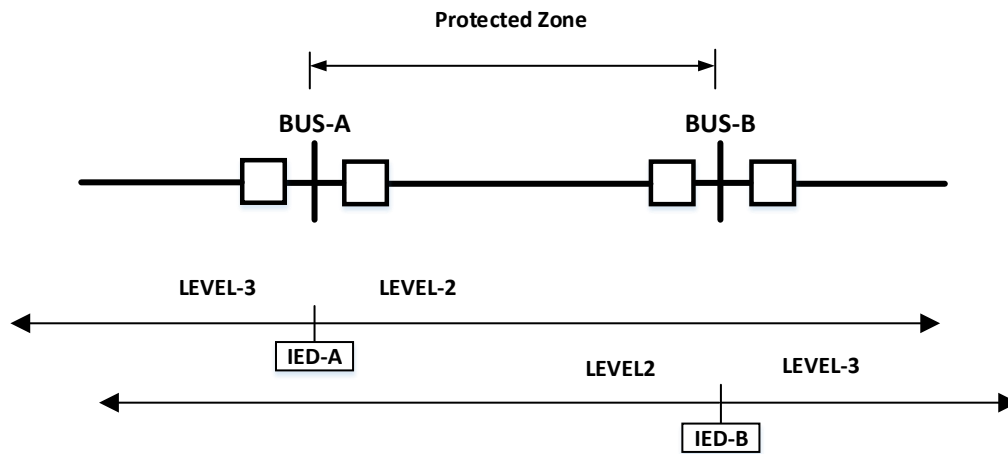

Figure 5-4: Hybrid POTT relay elements and Basic Logic [64]

In this thesis, both level-2 and level-3 will be achieved using a combination of instantaneous and phase direction overcurrent elements as shown in Figure 5-5. Level-1 element will not be used in this thesis. Such element is normally used in transmission system which has relatively longer line length compared to distribution systems.
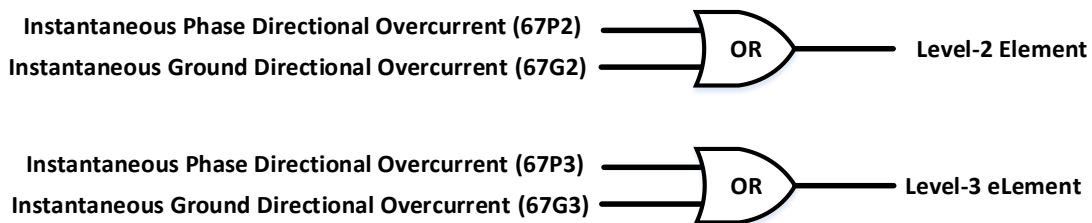
Figure 5-5: Hybrid POTT Pilot Protection Elements

In hybrid POTT scheme, the additional level-3 element is used to create three additional logic parts, the echo logic, weak infeed logic, and current reversal logic. Such logic parts are often prebuilt into modern IEDs. It is not the intention of this thesis to develop a new hybrid POTT scheme, but this thesis focusses on how commercial off-the-shelf IEDs with hybrid POTT logic can be applied to solve Microgrid protection challenges. A brief explanation of hybrid POTT logic parts will be presented below:

A- Current Reversal Logic

In parallel line applications, the fault current through a healthy line may reverse its direction due to sequential tripping in the opposite line. Such condition occurs when level-1 underreaching element operates for fault near one terminal. During current reversal, if the forward pilot tripping elements at one end asserts before the permissive trip signal from the remote end de-asserts, the POTT scheme on healthy line overtrip [145]. To overcome this problem, current reversal guard logic is added as shown in Figure 5-6. In this logic, a block extension time extends the block signal for a period of time TB to prevent the POTT from keying and tripping immediately following current reversal. The time delay TB shall be set greater than the remote overreaching element reset time plus the channel reset time plus a safety margin.
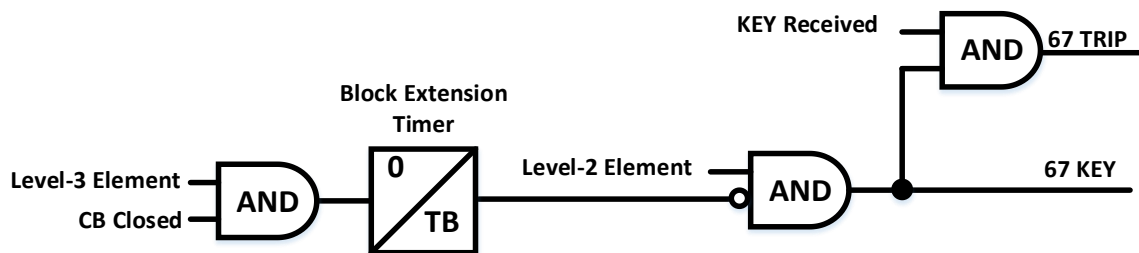

Figure 5-6: Simplified Current Reversal Logic in The Hybrid POTT scheme [145]

B- Echo Logic

The echo logic is used to allow the local terminal to trip at high speed in case the remote terminal infeed is weak, lost, or the remote terminal is open. Echo logic allows the remote relay to return (echo back) the received permissive signal to the sending terminal if no fault is detected in reverse direction. The echo signal therefore allows the sending terminal to trip at high speed. Figure 5-7 shows typical echo logic. The logic includes three timers for added security. The echo block timer extends the level-2 element pickup for a period of time TC1 to ensure echo signal is blocked during current reversal. TC1 is normally set to 10 cycles [136, 145]. The echo qualifying timer ensures that the received permissive signal must be present for a pre-specified period of time (TC2) to avoid confusion with communication channel noise, it also gives the reverse-looking elements sufficient time to operate. Typical setting of this timer is 2 cycles [136, 145]. The rising edge triggered (echo qualifying timer) is designed such that the input is ignored while the timer is running. It limits the echo signal duration to a specific time TC3 to prevent constant permissive keying (latching) between the two terminals [136, 145]. TC3 should be set greater than the echo signal transmission time plus the circuit breaker operation time, this ensures that the permissive signal will be echoed till fault is cleared. Typical setting is 4 cycles [136, 145].
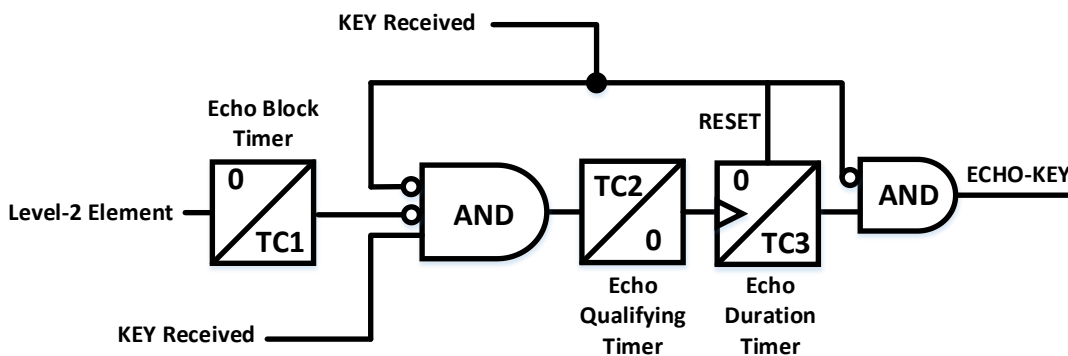

Figure 5-7: Typical Echo Logic [136, 145]

116

C- Weak infeed Logic

Weak infeed refers to a situation at which fault current contribution from one terminal is not sufficient to trigger the forward overreaching level-2 element. This condition prevents classical POTT scheme from operation. Echo logic discussed earlier allows only the strong terminal to trip at high speed. To allow the both terminals to trip at high speed, weak infeed logic must be added in combination with echo logic. Weak infeed logic uses phase undervoltage (27P) element, and zero sequence overvoltage (59N) element to detect weak infeed condition. As shown in Figure 5-8, weak infeed trip is issued to the weak terminal if the echo signal is issued, the phase undervoltage or zero sequence overvoltage picked up, the circuit breaker poles are closed, and no fault is detected in reverse direction.
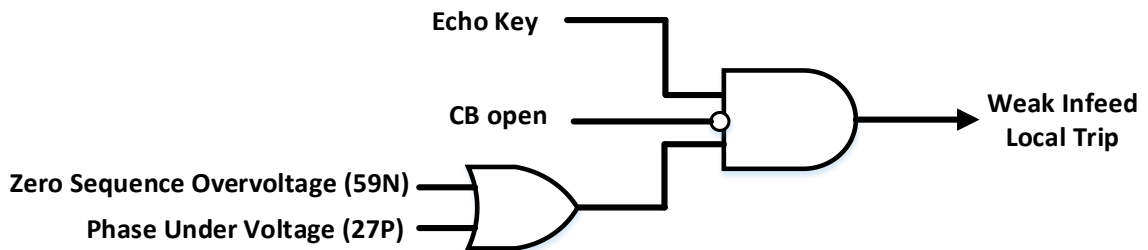
Figure 5-8: Typical Weak infeed logic [145]

Figure 5-9 shows a simplified logic diagram of the complete hybrid POTT scheme. In this thesis, SEL451-5 IED with built-in HPOTT logic will be used. The actual logic in this IED is little more complex and include more functionalities compared to the basic scheme shown in Figure 5-9.
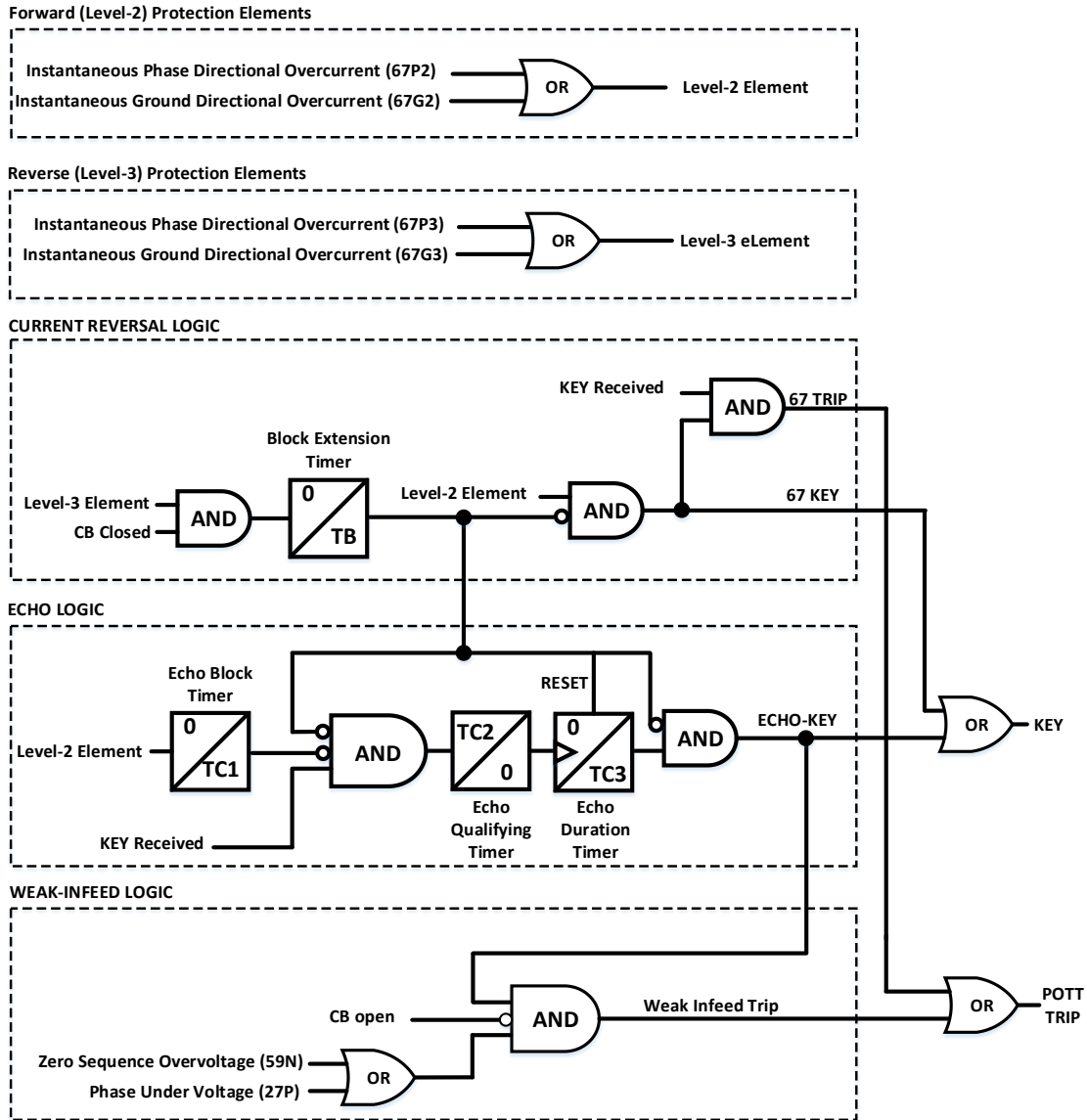
Figure 5-9: Simplified Hybrid POTT Logic [136, 145]

5.2.3 POTT scheme settings

Directional phase overcurrent (67P2, 67P3), and directional ground overcurrent element (67G2, 67G3) are used as the main pilot protection elements to operate the POTT scheme. For dependability reasons, the pickup settings of forward phase overcurrent pilot elements

(67P2) were set below the minimum phase-phase or three phase fault current at remote bus with proper margin to ensure the whole line length is covered. For security reasons, the pick-up setting is set above the maximum load and inrush currents through the line to avoid false tripping. The pickup settings of the forward ground overcurrent pilot element (67G2) was set below the minimum single line to ground fault on remote bus with proper margin to ensure the whole line length is covered. For security reasons, the pick-up setting is set above the maximum expected load unbalance, which was assumed to be 30 percent of maximum full load current of each line in each direction. The reverse directional (phase and ground) overcurrent elements (67P3, 67G3) are necessary to block high speed tripping for external faults and for proper operation of echo logic, weak infeed logic and current reversal logic. To ensure proper pilot coordination between level-2 and level-3 elements, the reverse level 3-elements shall always be set more sensitive (have longer reach) than the level-2 element at remote bus as shown in Figure 5-4. In this thesis, the pilot coordination margin between level-2 and level-3 elements were set to 2, i.e., the pickups of the reverse pilot blocking elements (phase and ground) were set equal to half the pickup of the forward (phase and ground) overcurrent pilot tripping elements at remote bus. For the weak-infeed voltage element settings, typical setting of the phase undervoltage element (27P) is 0.7–0.8 of the lowest expected operating voltage. On the other hand, the zero-sequence overvoltage element (59N) should be set to at two times the expected standing zero sequence voltage [136, 161].

5.3   Bus Protection Scheme

If a fault strikes the bus, the POTT scheme will not respond to the fault because it is outside its zone of protection. This causes the local backup protection to clear the fault after time

delay. To provide accelerated bus protection, separate bus protection technique is required. At medium voltage level, buses are normally protected using bus differential relays (ANSI number 87B). However, to avoid the extra cost of differential relays and current transformers, a fast bus tripping (FBT) scheme using IEC61850 GOOSE messages and existing IEDs is proposed in this thesis. In this scheme, each distribution line feeder, and generator feeder are equipped with directional phase and ground overcurrent elements (67P/67G). The directional elements must be configured to look into the bus. Since load feeders cannot detect reverse fault current, it is equipped with instantaneous phase and ground overcurrent protection (50P, 50G). A trip output is produced when all directional overcurrent functions detect the fault into the bus and none of the load protection relays operate. The trip output is published through GOOSE messages to all circuit breakers connected to the bus except load feeders. Figure 5-10 shows typical logic diagram for substation bus-1 as an example. When both directional overcurrent elements at CB10 and CB12 operate for a fault into the bus, and the load overcurrent protection did not operate, a trip signal is initiated to trip CB10 and CB12 using IEC61850 GOOSE protocol. If the load overcurrent protection detected the fault, bus tripping will be blocked for a specific time TD set by the coordination timer as shown in Figure 5-10. If the load overcurrent relay failed to clear the fault within the time TD, the bus directional IED will trip to provide backup protection. The multi-cast nature of GOOSE protocol facilitates sharing the directional overcurrent element status and trip signals among the IEDs, moreover, the highspeed transmission of GOOSE messages plays important role in enhancing the tripping speed. The main drawback of this approach is that bus fault must be cleared by time delayed local backup protection in cased of communication failures.
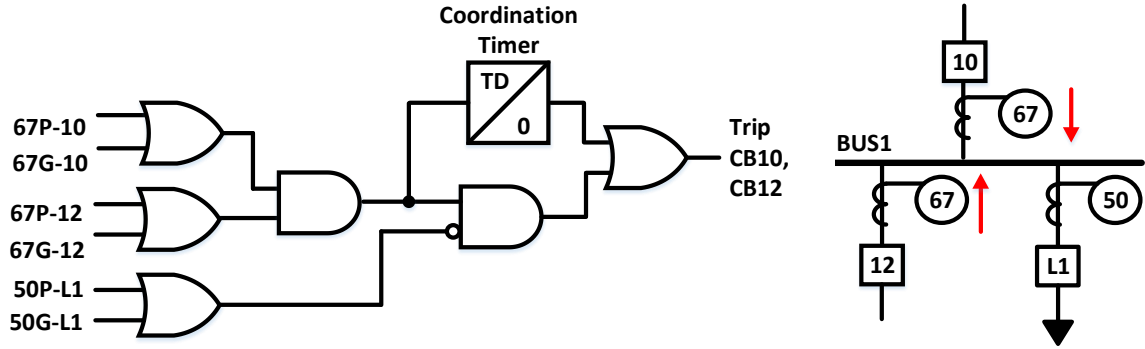
120

Figure 5-10: Example on Fast Bus Trip Scheme

5.4 Point of Common Coupling (PCC) Protection

Protection at the point of common coupling (PCC) is required to detect islanding condition (loss of main), moreover, it provides protection against faults at grid side and backup protection for faults at microgrid side. Islanding detection systems are classified as local based (passive, and active), and communication based [162]. In this paper, communication-based islanding is proposed as main and the local-passive islanding is proposed as backup. In the communication-based method, whenever the upstream IED issues a trip/open command to the upstream circuit breaker, a direct transfer trip (DTT) is sent simultaneously to the downstream circuit breaker at PCC through high speed IEC61850 GOOSE messages. The local-passive islanding scheme consists of time delayed under/over voltage (27/59), and time delayed under/over frequency (81O/U). The range of accepted time delays and thresholds are normally defined by international standards such as IEEE 1547 and based on utility interconnection requirements. In this paper, the IEEE 1547-2018 requirement is used as guide [41]. Table 5-1 shows the default setting range, and the allowable setting range for DG response to voltage disturbance as required by IEEE 1547-2018. Table 5-2 shows the default setting range, and allowable setting range for DG response to frequency disturbance. However, since IEEE 1547-2018 is based on 60Hz, the values in table-2 is

modified done by converting the 60Hz values to per unit, and then multiplying the result by 50Hz to match the frequency of the benchmark microgrid understudy. Figure 5-11 shows the corresponding fault ride through curve.

Table 5-1: PCC response to abnormal voltages [41]

Ranges of allowable setting		Default settings		
Voltage (p.u)	Clearing time (s)	Voltage (p.u)	Clearing time (s)	Relay operation time
fixed at 1.20	fixed at 0.16	1.20	0.16	0.095s= 4.75cycle
1.10–1.20	1.0–13.0	1.10	2.0	1.935=96.75cycle
0.0–0.88	2.0–21.0	0.70	2.0	1.935=96.75cycle
0.0–0.50	0.16–2.0	0.45	0.16	0.095s= 4.75cycle

Table 5-2: PCC response to abnormal frequencies [41]

Ranges of allowable setting (IEEE 1547)		Relays settings		
Frequency (Hz)	Clearing time (s)	Frequency (Hz)	Clearing time (s)	Relay operation time (s)
51.5–55.0	0.16– 1000.0	51.6	0.16	0.095s= 4.75cycle
50.83–55.0	180.0–1000.0	51.25	300.0	299.9s=14995cycle
41.66–49.16	180.0–1000.0	48.75	300.0	299.9s=14995cycle
41.66–47.5	0.16–1000	47.08	0.16	0.095s= 4.75cycle

Directional phase and ground overcurrent (67P, 67G) are used to clear faults on grid side and to provide backup protection for faults within the microgrid. Moreover, the PCC relay receives a DTT trip from the utility circuit breaker to provide to clear fault at high speed. For example, if a fault occurs at F1 in Figure 5-12, the upstream substation IED clears the fault faster since it sees higher fault current. Accordingly, a transfer trip signal is sent to

the PCC relay to trip the microgrid circuit breaker. A synchro check element is required to enable microgrid reconnection to utility after islanding. Figure 5-12 shows the structure of the proposed PCC protection.
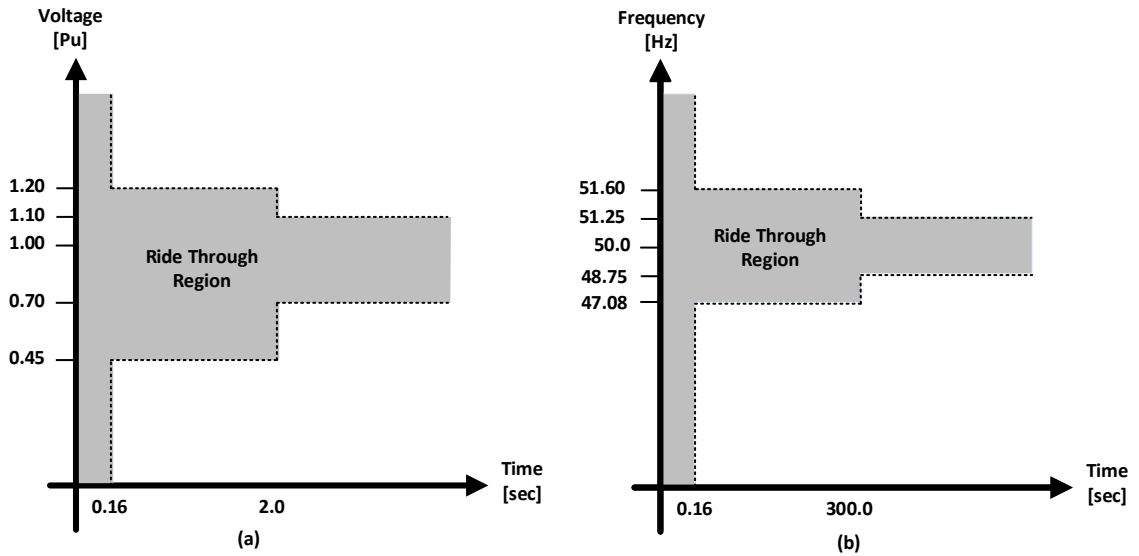

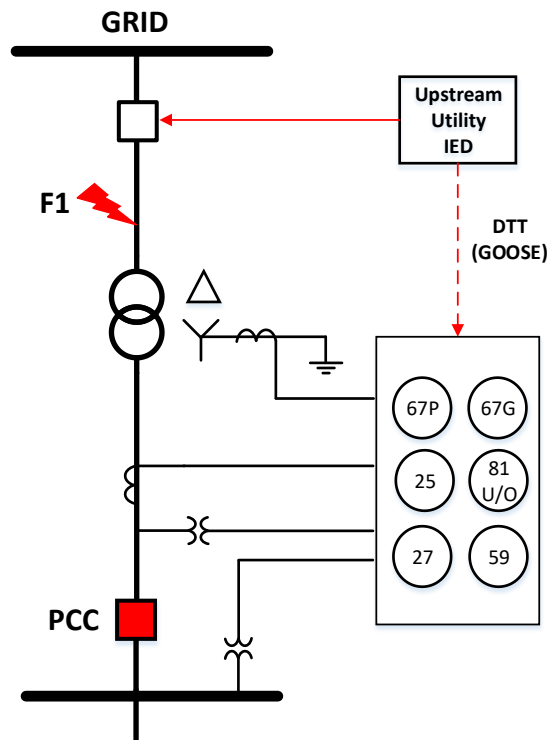**Figure 5-11: DER voltage and frequency fault ride through curves**

Figure 5-12: PCC Protection

123

5.5   Protection of Distributed Generators

Distributed generator protection consists of three parts, the self-protection, the Interconnection Protection Systems (IPS), and the islanding detection system [163]. DG self-protection against internal faults is not part of this paper scope. The IPS focuses on protecting the microgrid equipment from the adverse effects of DG response to faults within the utility. Moreover, it protects customer equipment from DGs that operate outside voltage and frequency limits. The islanding detection system is used to detect the loss of interconnection with main supply. In this paper, DGs will receive a direct transfer trip signal from other IEDs using IEC61850 GOOSE messages and/or hardwire connection. For example, in case of bus fault, the trip signal will be published to all IEDs connected to the bus to clear the fault. Time delayed over/under voltage (27/59), and time delayed over/under frequency (81 U/O) are use passive islanding detection system. The tripping thresholds and time delays are selected to coordinate with the islanding detection system installed at the PCC, i.e., it should be selected slower than the PCC islanding detection to enable successful islanding, moreover, it should be set slower than main protection to avoid DG over tripping for out of section faults [164]. Figure 5-13 shows the corresponding fault ride through curve. Table 5-3 and Table 5-4 shows the selected values for voltage and frequency elements. In addition to islanding detection system, the DGs will be equipped with directional phase, negative sequence, and ground overcurrent (67P, 67Q,67G) to provide protection against short circuit faults and load unbalance. A synchro check element is required to enable DG reconnection to Microgird. Figure 5-14 shows the structure and connection of the DG interconnection protection relay.

Table 5-3: DER response to abnormal voltages

Ranges of allowable setting (IEEE 1547)		Selected settings		
Voltage (p.u)	Clearing time (s)	Voltage (p.u)	Clearing time (s)	Relay operation time
fixed at 1.20	fixed at 0.16	1.20	0.2	0.135s= 6.75cycle
1.10–1.20	1.0–13.0	1.150	3.0	2.935=146.75cycle
0.0–0.88	2.0–21.0	0.80	3.0	2.935=146.75cycle
0.0–0.50	0.16–2.0	0.5	2.0	0.135s= 6.75cycle

Table 5-4: DER response to abnormal frequencies

Ranges of allowable setting (IEEE 1547)		Relays settings		
Frequency (Hz)	Clearing time (s)	Frequency (Hz)	Clearing time (s)	Relay operation time
51.5–55.0	0.16– 1000.0	52.6	1.0	1.935s=(96.75 cycle)
50.83–55.0	180.0–1000.0	52.25	500	499.9s=(24995cycle)
41.66–49.16	180.0–1000.0	47.75	500	499.9s=(24995cycle)
41.66–47.5	0.16–1000	46.08	1.0	1.935s=(96.75 cycle
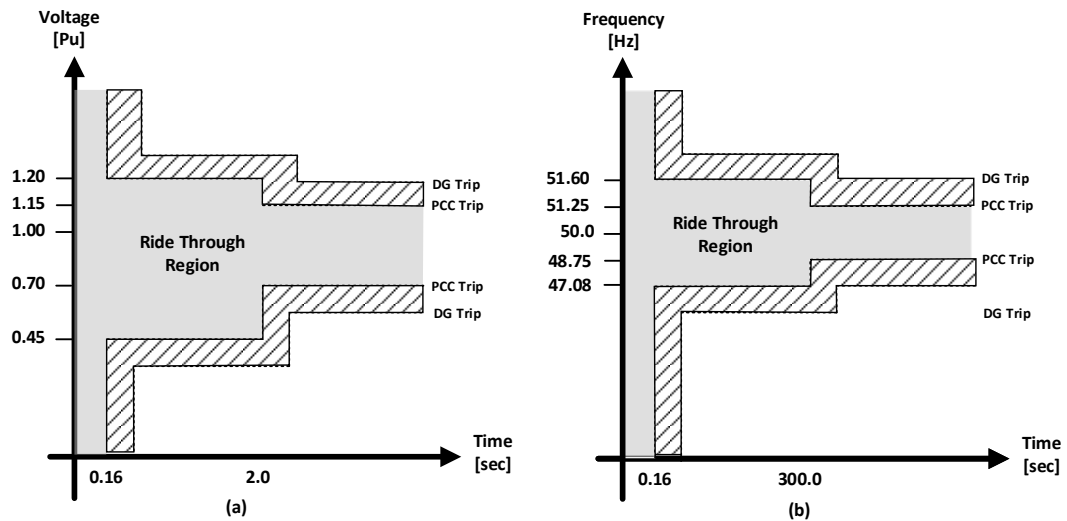
Figure 5-13: Microgrid fault ride through requirements
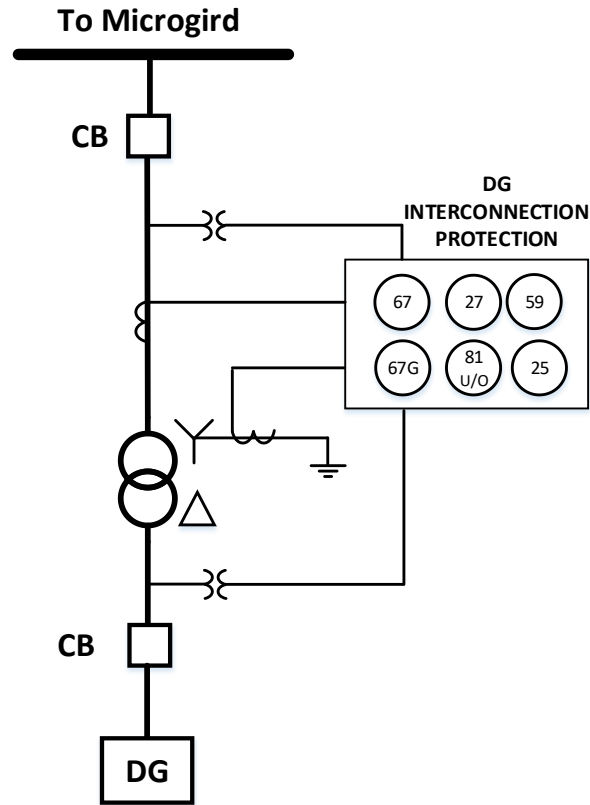
Figure 5-14: Structure of DG interconnection Protection

5.6 Load Protection

Loads are protected with simple non-directional overcurrent protection. In case of failure, back up protection can be provided by time delay overcurrent protection in the line and DG protection relays. If microgrid control system requires load shedding, then protective relay shall have the provision to receive load shedding signals from microgrid controller.

5.7 Adaptive Protection Method

As explained in chapter 2, the intermittent nature of DGs combined with the changes in microgrid mode of operation (grid connected and islanded modes) and the changes in network structure (open/close of tie switches) causes both the non-fault and fault currents

to change continuously in magnitude and direction. Consequently, conventional protection schemes with fixed protection settings become insufficient to meet protection requirement (selectivity, sensitivity, and speed) under such circumstances [8]. To tackle these problems, the concept of adaptive protection has been suggested. Adaptive protection can be generally defined as *"a protection philosophy which permits and seeks to make adjustments in various protection functions automatically in order to make them more attuned to prevailing power system conditions"* [165]. Despite the fact the proposed pilot protection strategy almost eliminates time coordination problems, the changes in fault current level impacts the sensitivity of directional overcurrent relays. Accordingly, the pickup setting must be adjusted according the prevailing network configuration to ensure the relay have maximum possible sensitivity under all operating conditions. Therefore, adaptive protection is required in this thesis.

To achieve adaptive protection in general, the relay must permit its protection settings and/or protection functions to be changed based on information received from outside world, or the relay itself seeks to make the adjustment within itself. Practically, such requirement can be achieved using modern microprocessor-based relays or IEDs (Intelligent Electronic Devices). Modern IEDs contain multiple protection functions with multiple instances (levels) of the same function, support multiple communication protocols, and have programmable logic. Moreover, modern IEDs contains multiple protection setting groups where each group contains complete relay settings and protection logic. However, one setting group can be active at a time. The active group setting can be changed manually, or automatically using external signals received though hardwire connection or using communication system. The switching between group setting can be

achieved via communication command, hardwire signal, or manually through relay local control panel. However, there are several dis-advantages to this approach:

- The number of group settings available in modern transmission/distribution system IEDs is approximately six [136]. However, this number is not enough to store protection setting that correspond to all possible operating scenarios.

- The switching between group settings require the relay to be disabled for a short period of time that range from a few milliseconds to a few cycles or seconds [166]. During this period, the relay will not respond to any fault. Switching circuit breaker is a common time for fault to occur, therefore, disabling the relay during this period present a risk and reduces the reliability of protection scheme.

Different from group setting method, the protection setting can be changed online by sending the setting file from external central unit [10, 15, 19, 128]. In this approach, the central unit calculates the protection setting in real-time and the resulting settings are sent to the relays directly, i.e., the old settings are overwritten. A communication protocol with automated messaging/file transfer capability such as IEC 61850 is required to write the files to the relay directly. This approach overcomes the limitation of setting group method by increasing the number of instances for which the settings must be changed. However, the speed at which this process occurs is critical to the protection system. The huge computational burden, the large data traffic, and the time required to write the new settings to the relay memory may introduce considerable time delay in the APS response. Moreover, implementation of this method is limited by the read/write capability of the relay's flash memory. Considering the intermittency of renewable based DG, and the limited number of read/write operation of flash memories, the relay life expectancy will be

reduced drastically. This thesis tries to fill this gap by proposing an alternative approach which utilize the capabilities of modern off-the-shelf commercial distribution system IEDs.

In this thesis, an adaptive setting management method is developed using the programmable logic available in modern IEDs. The salient feature of the proposed adaptive technique is that setting adaptation is achieved using the IED's programmable logic and math operators without changing the IED setting group. The developed logic therefore allows for larger number of change instances while making the change in protection settings instantaneous.

In the proposed APS, the first step is to conduct an offline short circuit analysis and load flow study for all possible operational, and topological scenarios. The study is necessary to calculate the pick-up settings of overcurrent relays under different operating conditions. It is found that the change in Microgird operation from grid connected to islanded mode has the largest impact on fault current level followed by the connection and disconnection of diesel generator. Inverter based DGs has relatively lower impact on fault current level due to their limited fault current capability. During online operation, the connection status of the DG's circuit breakers, and the circuit breaker at PCC are monitored in real time by the corresponding IEDs. Accordingly, the circuit breaker connection status is transferred to all adaptive relays in the network via IEC 61850 GOOSE communication network. The adoption of IEC 61850 with horizontal and vertical messaging structure made it possible to build a decentralized APS in which decision making is distributed over several IEDs instead of one central unit. Each adaptive IED uses the communicated information about circuit breaker status to activate the appropriate pickup settings which has been studied offline.

In modern distribution and transmission system IEDs, the pickup setting of overcurrent elements must be assigned a specific fixed value, it cannot be assigned as variable quantity based on equations. However, modern IEDs contain programmable logic which allows the user to define custom protection elements and custom protection logic. Therefore, in the proposed methodology, a customized instantaneous directional overcurrent element was created. The pickup setting in this customized overcurrent element is defined as a math variable rather than a constant value. Figure 5- 15 and Figure 5-16 shows custom logic used to create the instantaneous directional phase and ground overcurrent elements. These elements are associated with Level-2 and Level-3 elements of the HPOTT scheme. Analogue quantities, mathematical variables, logic variables, and comparators are used to create these protection elements. IAWM, IBWM, and ICWM are the measured fault currents. LIGFIM represent the zero-sequence current magnitude. F32P, and R32P are the forward and reverse phase directional elements. G32F, and G32R represent the forward and reverse ground directional elements. Finally, the PSV16-PSV23 are logical variable that store the status of protection elements. PMV01-PMV04 are protection math variable in which the adaptive pick up setting of directional overcurrent elements is stored.
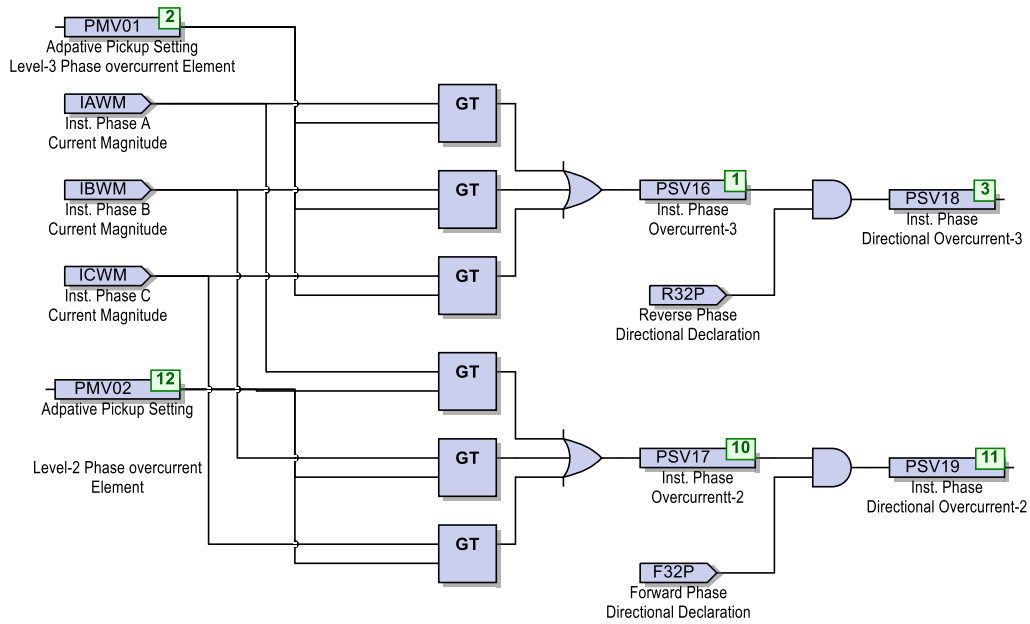
Figure 5-15: Directional Phase Overcurrent Element Using Programmable Logic
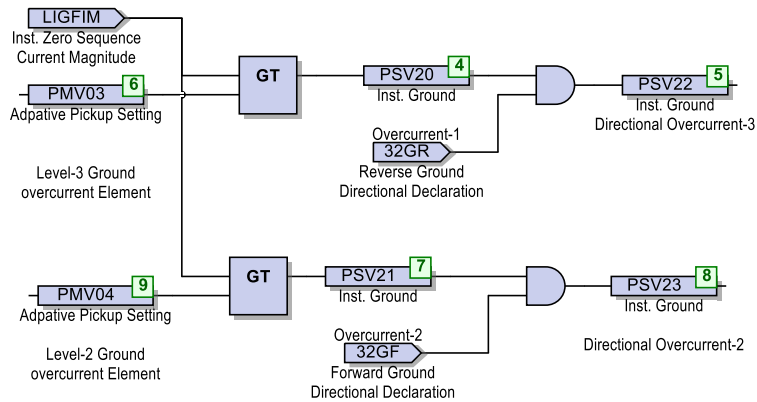
Figure 5-16: Directional Ground Overcurrent Element Using Programmable Logic

The control logic shown in Figure 5-17 is used to identify the current status of microgrid. The Relay word bits VB012-VB015 are virtual bits that represent the circuit breaker connection status of DGs and microgrid which are communicated using GOOSE messages. Each combination of circuit breaker status is stored in dedicated protection logical variable PSV01-PSV012. One of these logical variables will be active at a given time.

131
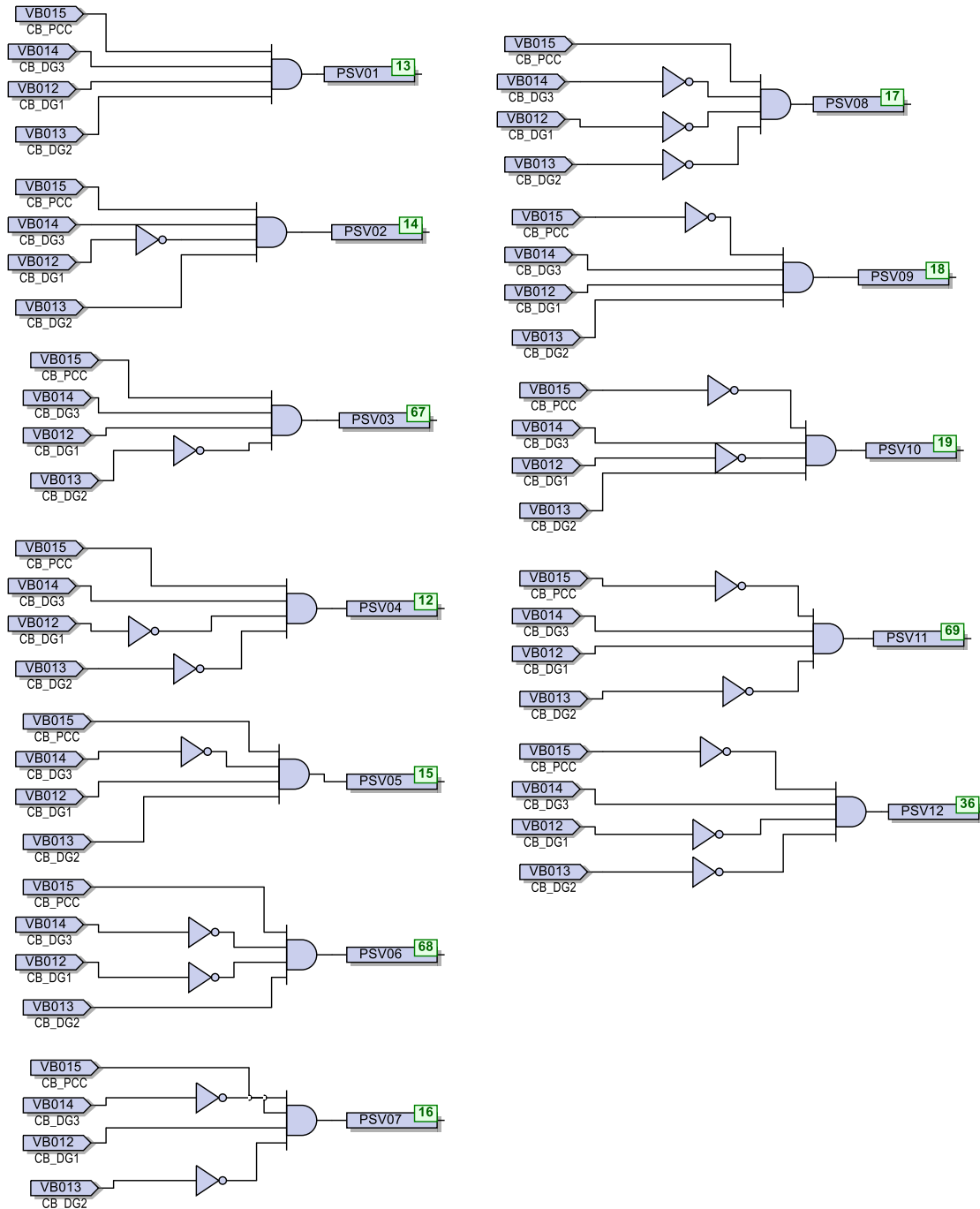
Figure 5-17: The logic used to identify Microgird operation state

The typical logic shown in Figure 5-18 is used to enable the pickup that matches the current configuration of microgrid. This is done by multiplying the logical variables PSV01-PSV012 with the corresponding pickup setting. The overall result will be added and stored

in a math variable. In this typical case, it is PMV01. This math variable represents the adaptive pickup setting of level-3 phase directional phase overcurrent element shown in Figure 5-15. The same logic is repeated for other protection elements to achieve adaptive pickup setting.
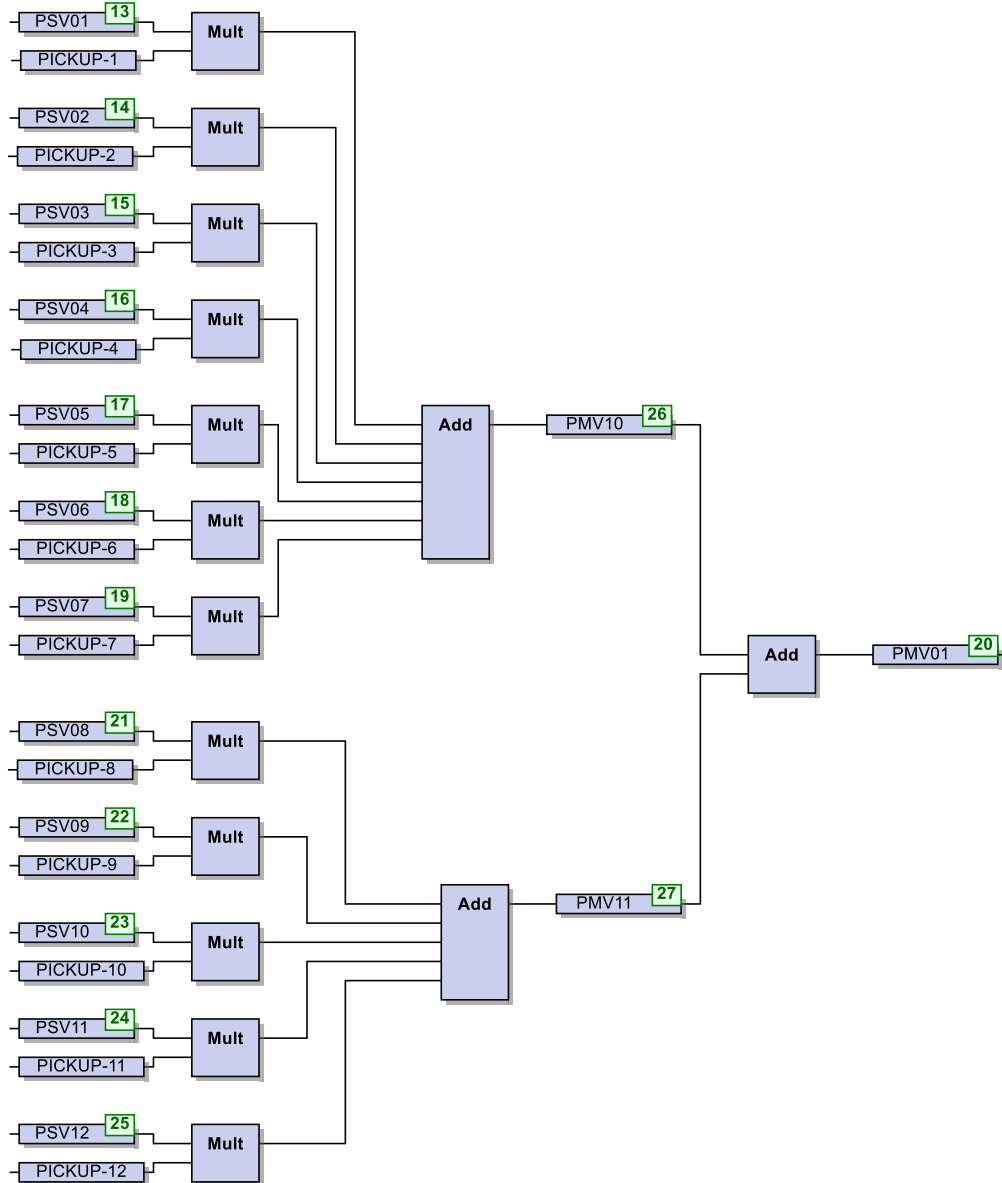
Figure 5-18: Typical logic used to select pickup setting based on Microgird and DG status

CHAPTER 6

IMPLEMENTATION IN RTDS

6.1 Relay Test Setup

Real time simulation presents an effective way to test physical protective relays. Since the simulation in RTDS runs in real time, the physical protection relays can be connected in closed loop with the microgrid model in RTDS. The interaction between RTDS and protection relays allows protection engineers to test the relay performance for all types of faults and operating conditions before putting them in real operation. In this thesis, a hardware in the loop test setup will be implemented to test the performance of the proposed adaptive protection strategy in real time using RTDS and commercial relays from Schweitzer Engineering Laboratory (SEL). This chapter describes the structure of the test setup, and the interface connection between RTDS and protection relays. The later includes the analogue output hardwired signal interface, the digital input/output hardwired signal interface, and IEC61850 based communication interface.

6.1.1 Structure of the test setup

Figure 6-1 shows the basic structure of the laboratory test setup.
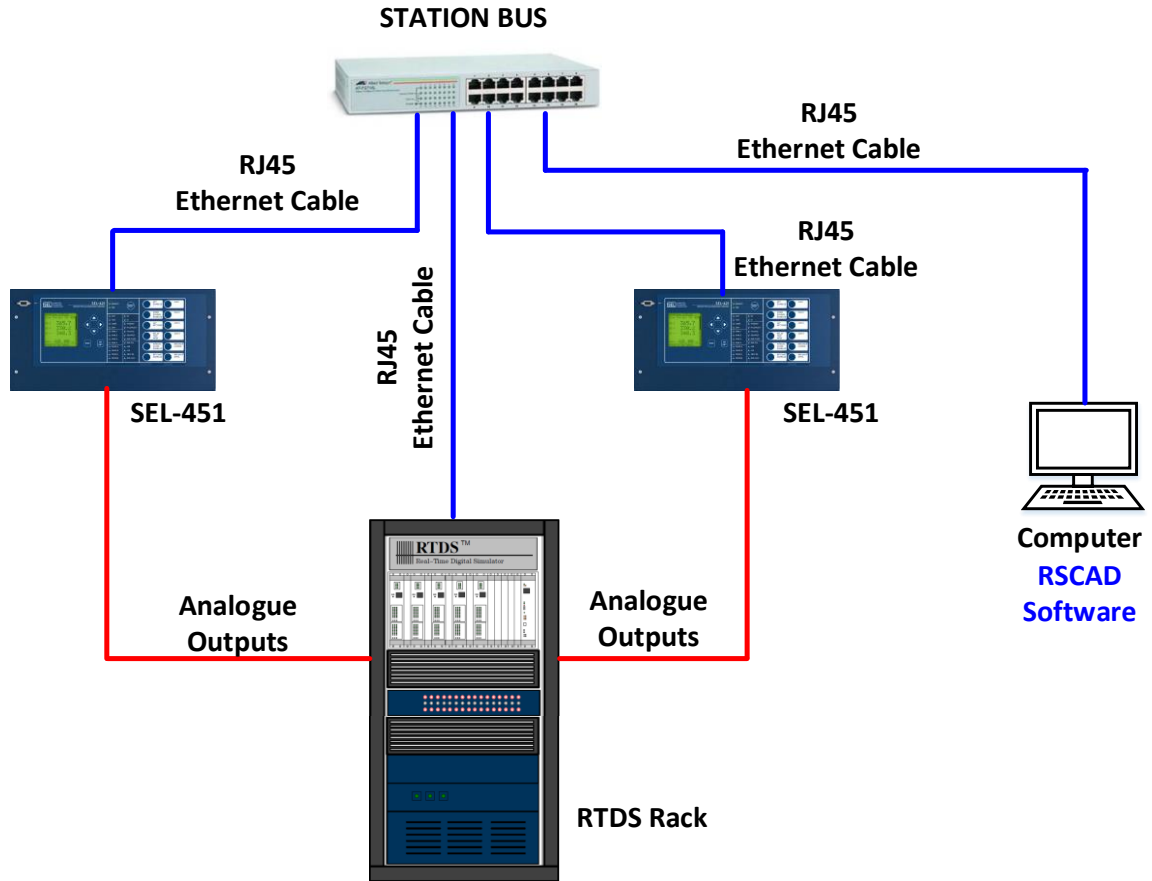
Figure 6-1: Basic structure of the laboratory test setup

The main components of the laboratory test setup are:

- **Real Time Digital Simulator (RTDS)**

- **Protection relays:** Two line-protection relays model number SEL451are used to protect the microgrid, the relays are from Schweitzer Engineering Laboratories (SEL). Each relay takes voltage and current signals from RTDS through analog outputs. GOOSE messages are used to send trip signal to RTDS as well as to receive the circuit breaker statuses from RTDS.

- **Ethernet switch**.

6.1.2 Interfacing RTDS and Protection Relays

The developed microgrid model in RTDS contains the microgrid model, the models of power system components (circuit breakers, current transformer, potential transformers, etc.), and the model of the control components which are not included in the physical relay under test such as fault control logic, and breaker control logic. Interface cards, analog and digital input and output cards of RTDS can be used to connect RTDS with protection relays [151]. The interface between physical relays and RTDS requires sharing three types of signals:

1- Analogue outputs from RTDS to Physical Relay: It includes the simulated power system voltages and currents.

2- Digital inputs from physical relays to RTDS: It includes the trip/reclose signals, block/permissive signals, and control signals.

3- Digital outputs from RTDS to physical relays: It includes the circuit breaker connection status (ON/OFF).

(1) Analog Output from RTDS to Physical Relay

Protection relays require analog voltage and current signals as inputs. The RTDS Gigabit Transceiver Analogue Output (GTAO) cards are used to export simulated voltage and current signals from RTDS to outside world. The GTAO card has a twelve, 16-bit output channels with output range of ±10 V. In practice, however, protection relays receive current and voltage signals form instruments transformers (CTs, and VTs) which are rated differently. The CT secondary is normally rated 5A or 1A and the VT secondary is normally rated 115 Vrms Phase-Phase. However, the GTAO card output cannot source

these power signals. To make the RTDS output compatible with the relay inputs, three approaches can be used:

- **Using the RTDS GTAO card and power amplifiers:** In this method, the GTAO outputs are inputted to power amplifiers to scales the voltage and current signal to a range that matches the relay's CT and VT inputs respectively. However, this option requires using power amplifiers that may introduced some distortion and delays to the original signal. Therefore, it will not be used in this thesis.

- **Using the RTDS GTAO card and relays low level test interface:** In this option, the external VT and CT inputs are bypassed, and the GTAO outputs signals are connected directly to the relay's analogue to digital converter board inside the relay. This option is available in SEL relays through low-level test interface. This option is simple and requires no expensive hardware, therefore, it will be adopted in this thesis.

- **IEC61850 Sampled value-based testing:** In this advanced option, the voltage and current signals are transferred to the relay through IEC61850 sampled values protocol by using the GTNET communication cards in the RTDS. This option requires ethernet switch, and IEC61850 compliant IEDs. In this thesis, however, this option will not be used because the available GTENT cards will be used for GOOSE communication.

(2) Low Level Connection

The low-level test interface can be accessed by opening the relay front cover, removing the original 34-pin ribbon cable from the main board J24 receptacle, and substituting it with the test 34-pin ribbon cable as shown in Figure 6-2.
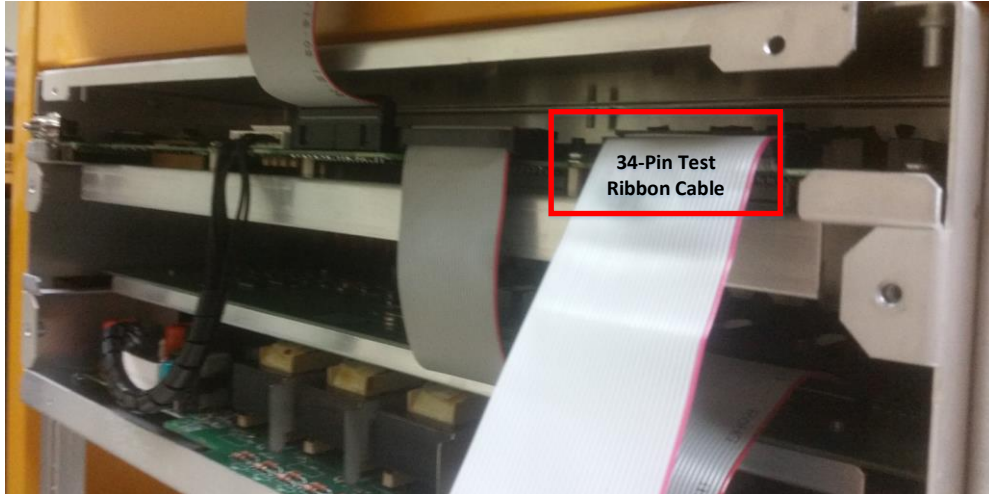
Figure 6-2: Low level interface of SEL 451-5 relay directly connected to RTDS with ribbon cables

GTAO Connection

Two GTAO cards are used in this research to send simulated voltage and current values to the relays. Figure 6-3 shows one of the GTAO card and its control cable connection. The GTAO has twelve optically isolated output channels.

Figure 6-3: GTAO Card

To establish interconnection between the 34-pin ribbon cable from SEL relays to the control cables coming from GTAO, a 34-pin header to terminal block adapter board is used as shown in Figure 6-4.
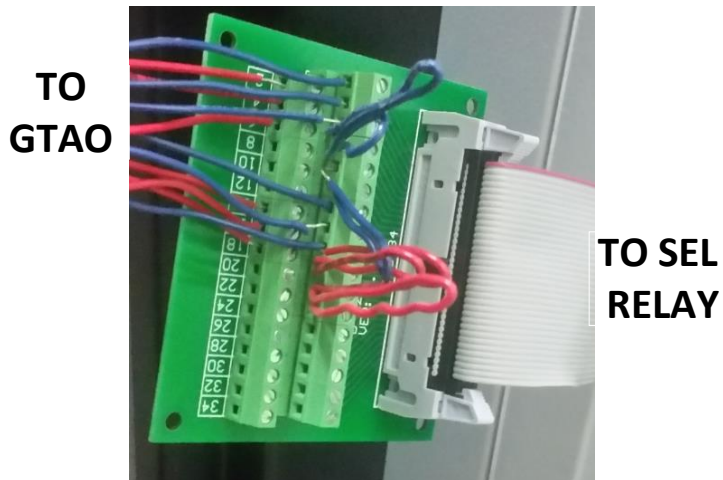
Figure 6-4: 34-pin header to terminal block adapter board

Sending Analogue signals from RSCAD to GTAO

Sending the simulated voltage and current signals to the RTDS GTAO card requires configuring the GTAO component in RSCAD. Fig. 6-5 shows the GTAO component in RSCAD. The desired analogue signals are given as input to the GTAO channels. Table 6-1 shows the channel assignment of each GTAO card.
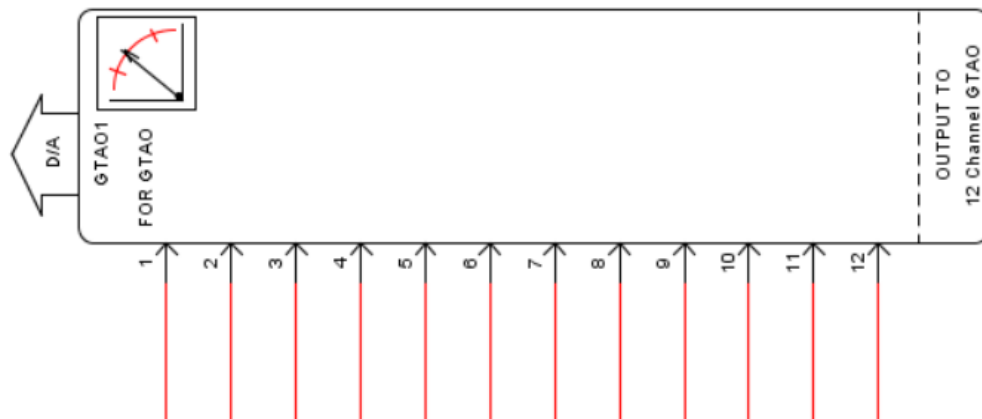
Figure 6-5: Sending out analogue signals using a GTAO

Table 6-1: Connections from GTAO cards to relays

GTAO card number	Channel number	Relay	Signal type
1	1-3	SEL 451 (1)	Line currents of relay at end-1: IA1, IB1, IC1
	4-6	SEL 451 (1)	Terminal of relay at end-1: VA1, VB1, VC1
	7-9	SEL 451 (2)	Line currents of relay at end-2: IA2, IB2, IC2
	10-12	SEL 451 (2)	Terminal of relay at end-2: VA2, VB2, VC2

The GTAO configuration is used to enabled/disable the channels, and to set the appropriate scaling factors. The full scale of the GTAO output voltage is 10 volts. The scaling factor is entered as a floating-point value which correspond to half scale, i.e. 5 volts. Figure 6-6 shows the relationship between GTAO input signal in RSCAD, and the output measured at GTAO card.
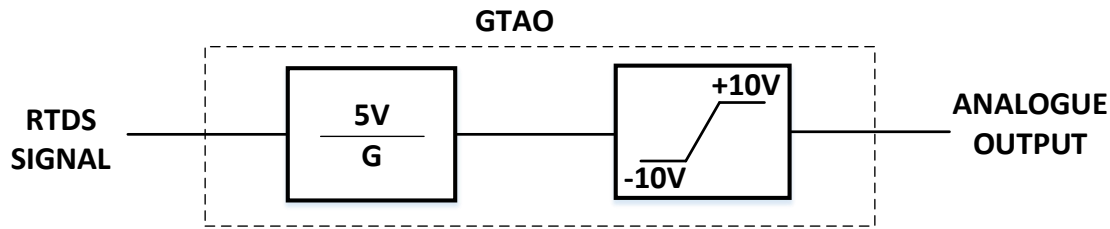
Figure 6-6: GTAO input/output voltage relation with scaling factor

The following equation shows the relationship between GTAO scaling factors and its output voltage:

$$Analogue\ Output = \frac{5V}{G} \times RTDS\ Signal \qquad (6.1)$$

Where G is the scaling factor. Solving equation 6.1 for G yields:

$$G = \frac{5V}{Analogue\ Output} \times RTDS\ Signal \qquad (6.2)$$

Scaling factors are used to scale GTAO channel's output voltage to a level compatible with the interfaced protective relays. SEL relays operation manual specify the required voltage input to the low-level test interface for both voltage input and current input. Figure 6-7 shows the low-level test interface connector information of SEL451 relays. This figure shows the pin assignment of voltage and current inputs as well. The relay has two voltage channels (Y and Z), and two current channels (W and X). In this thesis, one current channel (IAW, IBW, and ICW), and one voltage channels (VAY, VBY, and VCY) will be used. All other inputs will not be used. However, all GND terminals should be connected to ground even for unused terminals. Otherwise, some relay models may consider the board as disconnected, and may disable the relay.
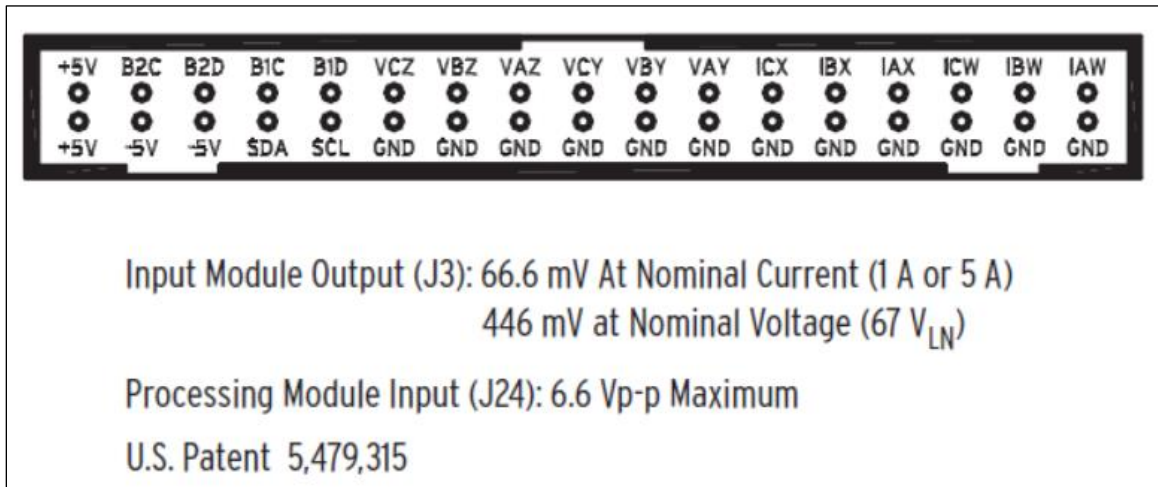
Figure 6-7: SEL 451 Low-Level Test Interface [136]

Using information from figure 6-7, and equation 6.2, the scaling factors can be calculated. In this thesis, all relay inputs are rated 1A, therefore the desired analogue input to the relay low-level interface is 66.6mV as per Figure 6-7. Accordingly, the scaling factor can be calculated from equation 6.2 as such:

141

$$G = \frac{5V}{66.6mv} \times 1 = 75.075 \qquad (6.3)$$

Similarly, the scaling factor for the voltage input is calculated as such:

$$G = \frac{5V}{446mv} \times 67 = 751.121 \qquad (6.4)$$

(3) RTDS Digital Inputs/Outputs

The digital input signals to the RTDS include the protective relay trip/reclose signals. The digital output from RTDS to the relay include the connection status of circuit breakers. In this thesis, two methods are used to transfer the digital input/output signals between RTDS and protective relays:

1- Conventional Hardwire connection methods using GTFPI Cards.

In this approach, trip signals and breaker status signals to and from RTDS are controlled with GTFPI card. The GTFPI card control two input/output panels. The low voltage I/O panel which operate at 5 VDC, and the HV Input/output panel that operate at voltages up to 250VDC.The digital outputs of SEL protection relays are voltage free contacts. The RTDS digital I/O panel can interface to inputs from voltage free contacts as it includes a built-in 1kΩ pull up resistors to a 5-volt supply [151]. Therefore, the trip/reclose signal from protective relay to the RTDS will be interfaced to the LV digital I/O panel as shown in Figure 6-8.
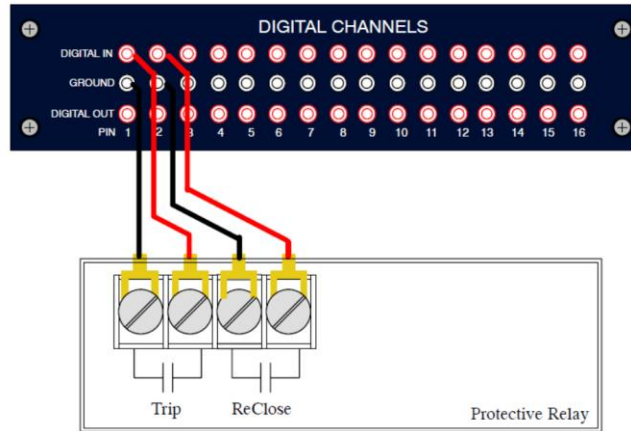
Figure 6-8: Dry Contact Connections to the Front Panel's Digital Input Port [151]

The digital inputs of the available SEL relays at KFUPM laboratory are rated at 125VDC, therefore, these signals cannot be interfaced to the RTDS LV digital I/O panel. Alternatively, the GTFPI HV patch panel will be used since it can accept voltages up to 125VDC. Figure 6-9 shows typical interconnection between the relay digital input and the GTFPI HV output. An external 125VDC supply is required.
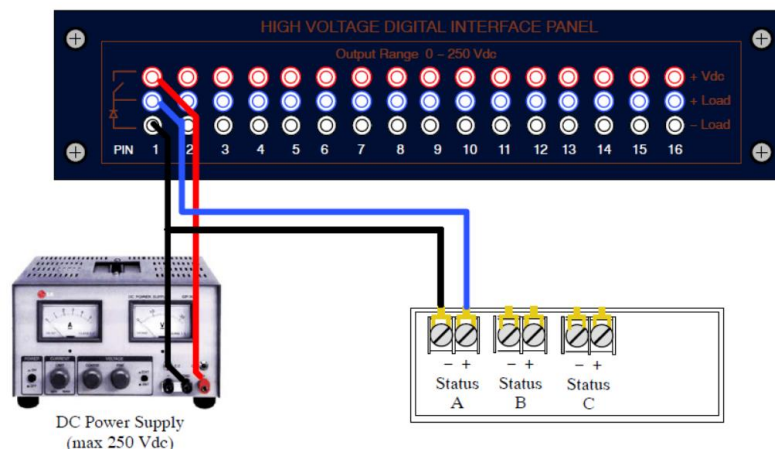
Figure 6-9: HV Panel Connection for Breaker Status Signals which require an external supply voltage[151]

Figure 6-10 shows the RSCAD component of the GTFPI card and its associated I/O panels. The upper portion is the LV I/O panel, and the lower portion is the HV I/O panel. Circuit breaker connection status are connected in the left side of the HV panel as shown, whereas

the trip signal from external relays are extracted from the right side of the LV panel. In this

thesis, the input of the LV panel, and the output of the HV panel are not used.
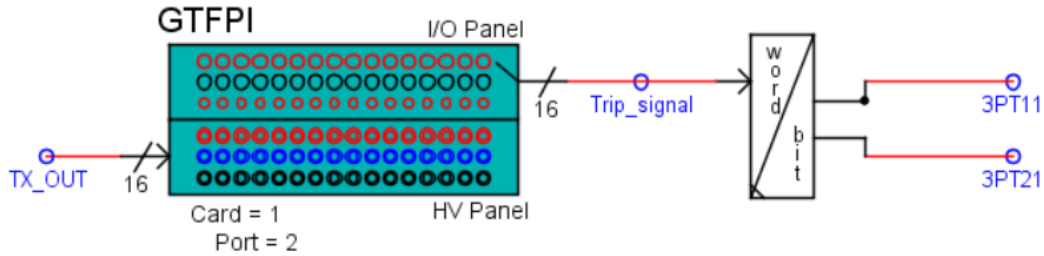
Figure 6-10: GTFPI Component in RSCAD

2- The second method is through GOOSE Messages using the GTNET Card

The GTNET network interface card support multiple communication protocols, one of

them is the IEC 61850 GOOSE protocol. GTNET card can support only one protocol at a

time [151]. Figure 6-11 shows GTNET card front and back view.

Figure 6-11: Front and back view of two GTNET cards

Figure 6-12 shown the interconnection interface between IEDs and the GTNET card

including the IP address, the subnet mask, and default gate way used. The GOOSE

messages are sent of the Ethernet LAN. The GTNET card can be thought of as a gateway

that accept the packets from the LAN, extract the data and send it to the processor card via

fiber optic cable. The configuration of GTNET card, and GOOSE message configuration

of IEDs will be presented in next section.

ETHERNET SWITCH

SEL-451
IP ADDRESS: 10.59.0.35
SUBNET MASK: 255.255.0.0
GATEWAY: 10.59.0.64

GTNET
IP ADDRESS: 10.59.0.26
SUBNET MASK: 255.255.0.0
GATEWAY: 10.59.0.64

SEL-451
IP ADDRESS: 10.59.0.36
SUBNET MASK: 255.255.0.0
GATEWAY: 10.59.0.64

Computer
IP ADDRESS: 10.59.0.37
SUBNET MASK: 255.255.0.0
GATEWAY: 10.59.0.64
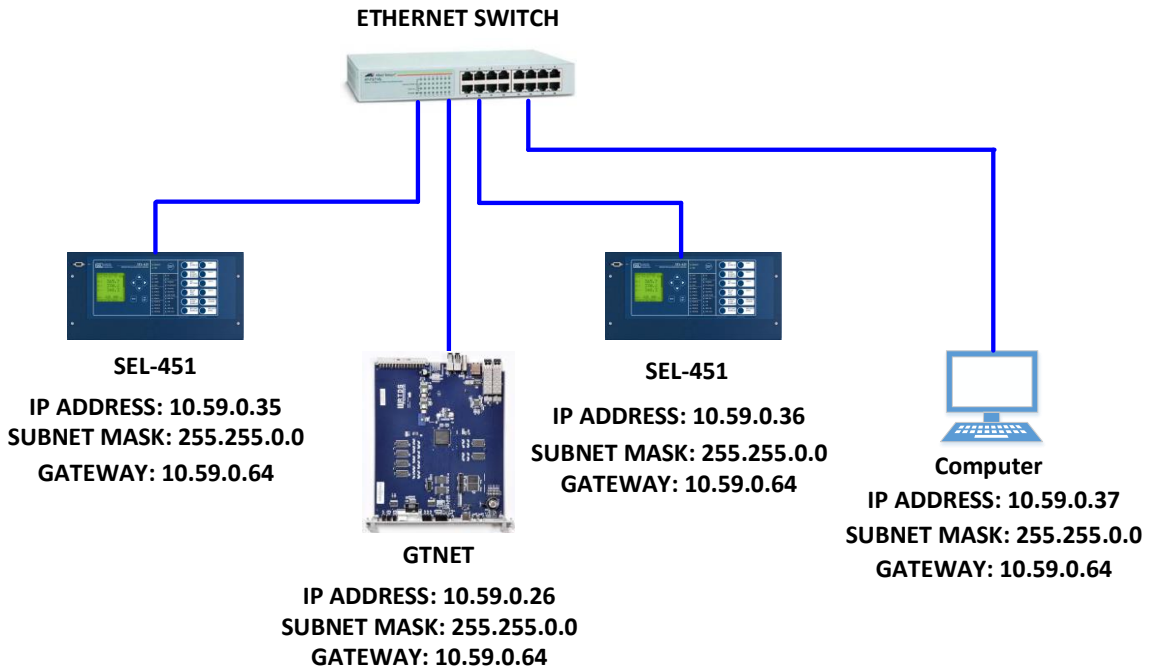
Figure 6-12: GTNET card Integration interconnection

In this thesis, the second method is used to obtain all simulation results (GOOSE Messages

using the GTNET Card). The first method is used for comparison and verification only.

CHAPTER 7

RESULTS AND DISCUSSION

This chapter demonstrates the effectiveness of the proposed adaptive protection strategy based on real time hardware in the loop testing. First, the effectiveness of the proposed HPOTT scheme will be tested during grid connected mode of operation by applying several types of faults and by changing the DG connection state. After that, the HPOTT scheme will be tested at islanded mode of operation for different types of faults and different DG connection states. Next, the effectiveness of bus protection scheme will be demonstrated by applying balanced and unbalanced faults at the main substation bus at grid connected mode. Figure 7-1 shows the structure of the network under test.

7.1 Grid connected mode of operation

In this section, the proposed scheme will be tested at grid connected mode by applying several fault types (three-phase, line to line, and single line to ground faults) with different DG connection states.

7.1.1 Fault on Distribution Line 1-2, and all DGs are connected

A- Three Phase Fault

A three phase, 10 cycle, bolted fault was applied on distribution line between CB12 and CB21. Figure 7-2 and 7-3 shows the SEL451_12 and SEL451_21 responses. These plots represent the relay event files which were extracted using the "*AcSELelator Analytic Assistant*" software from Schweitzer Engineering Laboratory. Each Figure contains the

146

fault current, the fault voltage, and a group of digital signals called Relay Word Bits (RWB). RWBs represent the status of protection element or logic results.
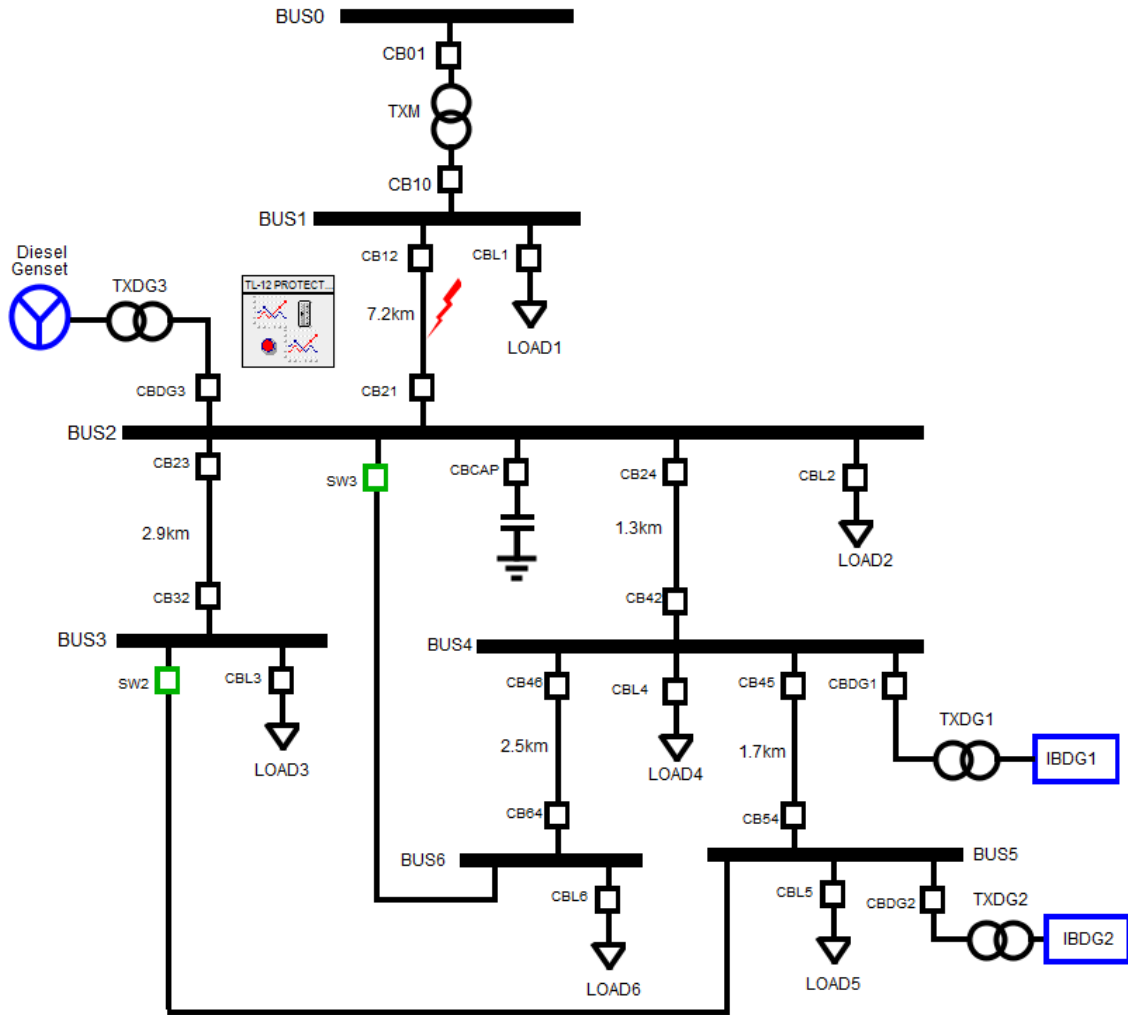
Figure 7-1: AC benchmark microgrid under test

In Figure 7-2 and 7-3, the relay word bits PSV19 and PSV23 are Protection logic variables that represent the status of phase and ground adaptive direction overcurrent elements. The relay word bit PT represents the permissive signal received from remote end. The relay word bit KEY represents the permissive signal initiated by the local overreaching element to the remote end. Finally, the relay word bit TRIP represents the three-pole trip signal initiated to trip the circuit breaker.
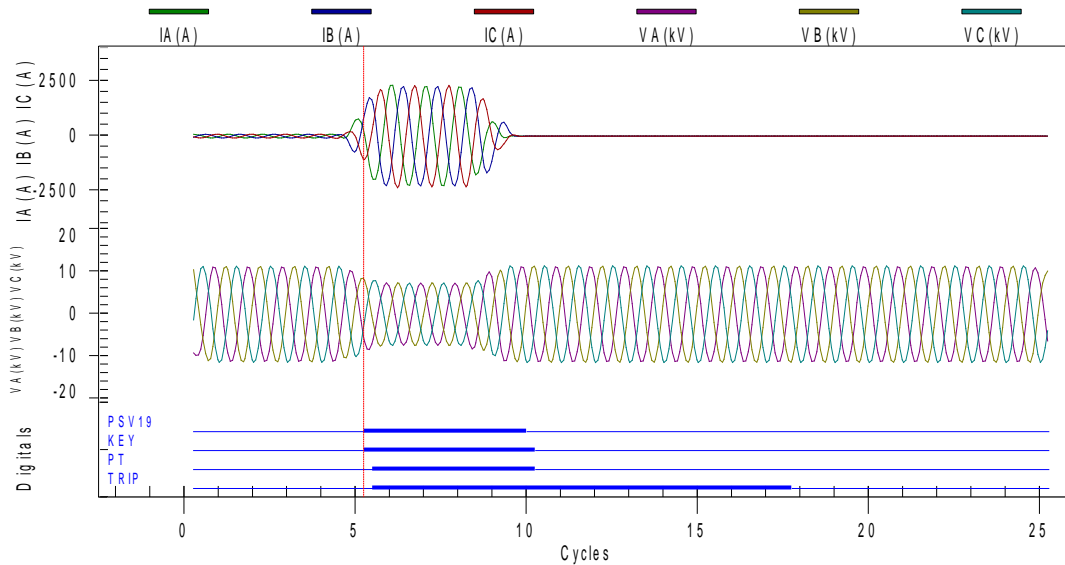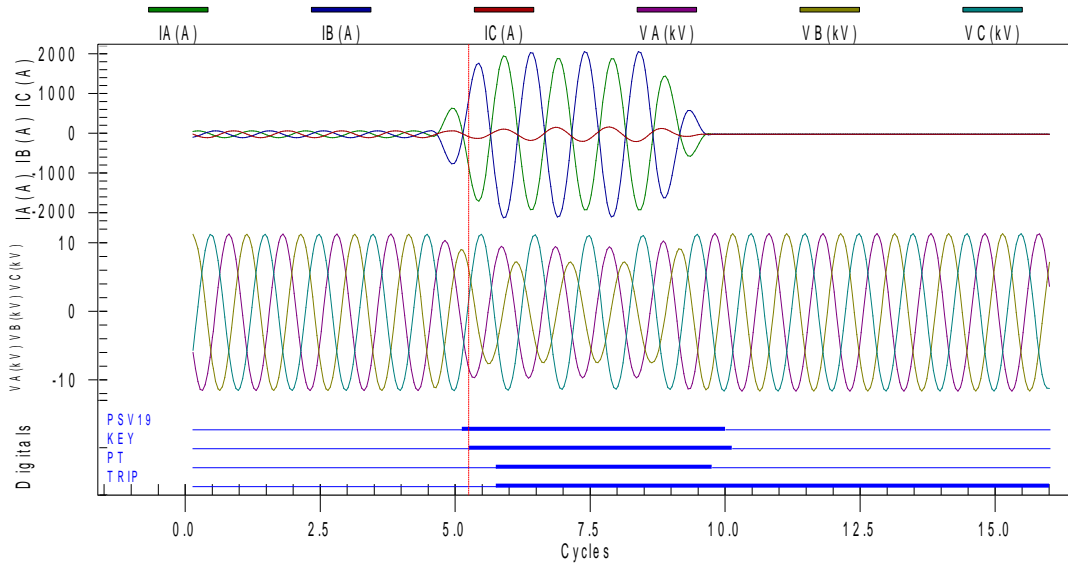
Figure 7-2: SEL451_12 response to three-phase,10 cycle fault on line 12. All DGs are connected.
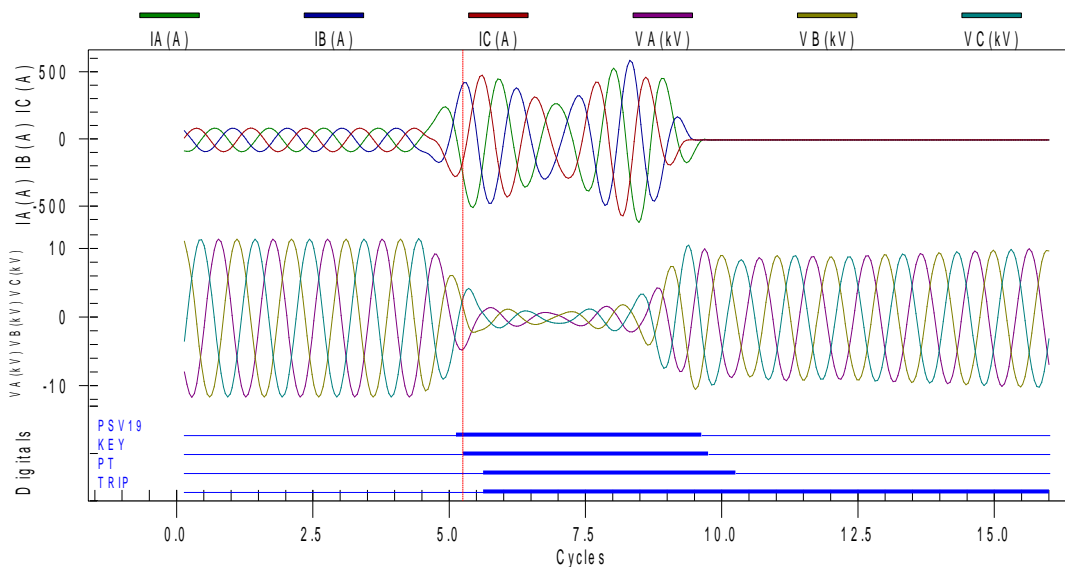
Figure 7-3: SEL451_21 response to three-phase,10 cycle fault on line 12. All DGs are connected.

From the recorded event in Figure 7-2 and Figure 7-3, after fault inception, the overreaching directional phase overcurrent (PSV19) elements operate. At the same time, the relay word bit KEY of the HPOTT scheme operates and a permission to trip signal is transmitted to the remote end via IEC61850 GOOSE communications. The PT relay word bit asserts indicating successful reception of the permissive trip signal from the remote end.

148

The relay word bit TRIP asserts to initiate local breaker tripping. The operation time of SEL451_12 is 17.47ms and that of SEL451_21 is 23.7ms.

B- Phase-Phase Fault

A phase-phase, 10 cycle-fault was applied on distribution line between CB12 and CB21. Figure 7-4 and 7-5 shows the SEL451_12 and SEL451_21 responses. The operation sequence is similar to the three-phase fault case. The operation time of SEL451_12 is 18.6ms and that of SEL451_21 is 22.58ms.
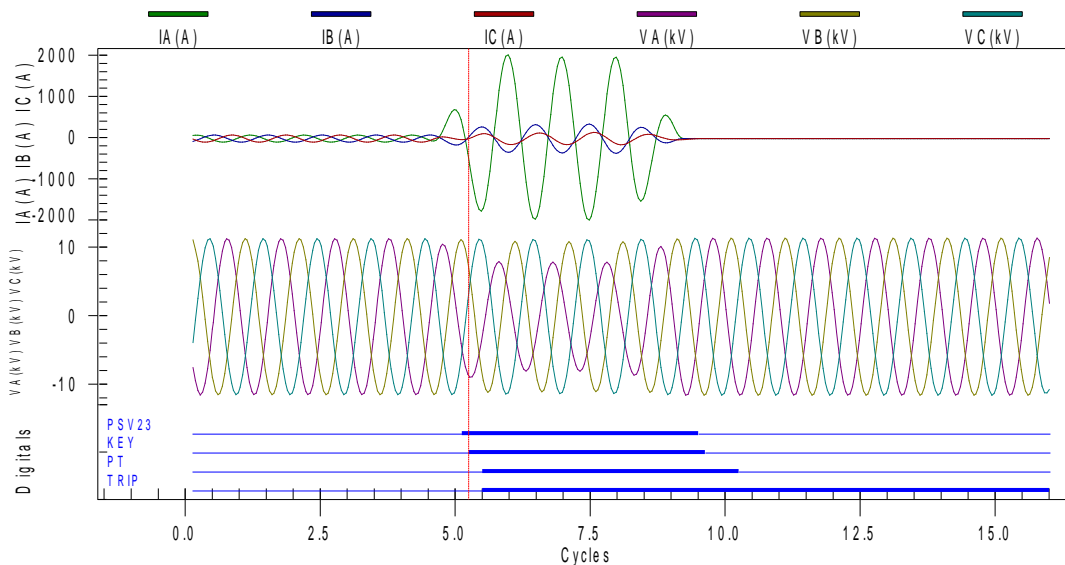

Figure 7-4: SEL451_12 response to phase-phase,10 cycle fault on line 12. All DGs are connected.
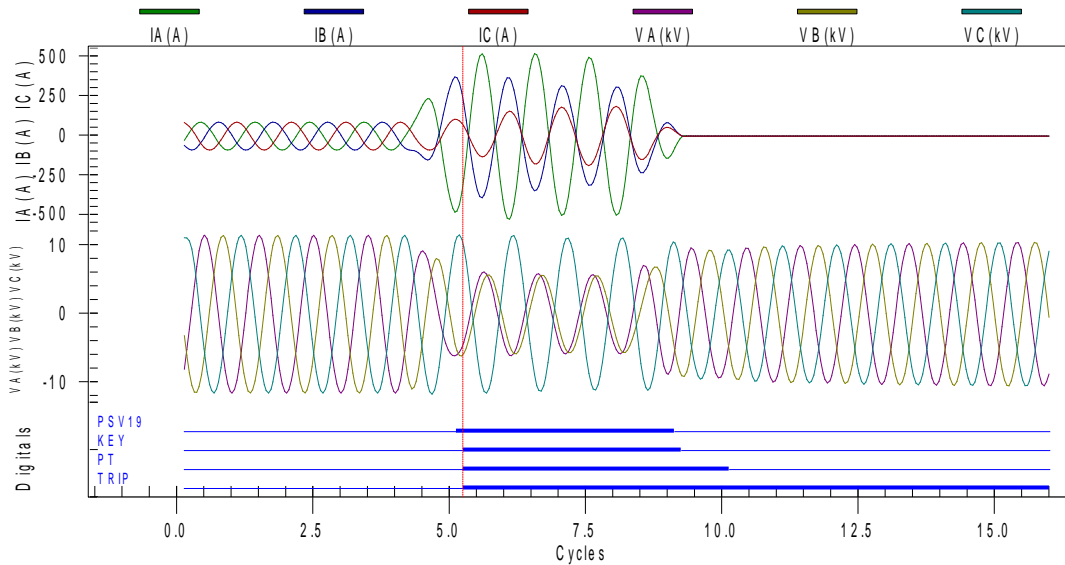
Figure 7-5: SEL451_21 response to phase-phase,10 cycle fault on line 12. All DGs are connected.

C- Single line to ground Fault

A single line to ground, 10 cycle-fault was applied on distribution line between CB12 and CB21. Figure 7-6 and 7-7 shows the SEL451_12 and SEL451_21 responses. The relay word bit PSV23 represent the pickup status of the overreaching directional ground overcurrent element (67G2). The operation sequence is similar to the previous fault cases. The operation time of SEL451_12 is 17.47ms and that of SEL451_21 is 22.72ms.

Figure 7-6: SEL451_12 response to single line to ground ,10 cycle fault on line 12. All DGs are connected.
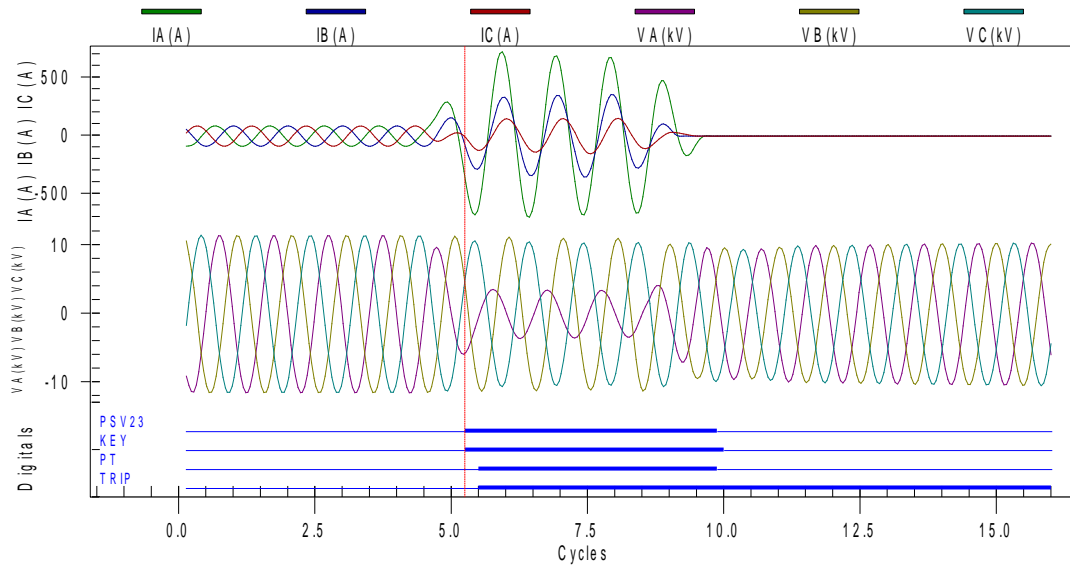
Figure 7-7: SEL451_21 response to single line to ground ,10 cycle fault on line 12. All DGs are connected.

7.1.2 Fault on distribution line 1-2, and diesel generator is out of Service

If the diesel generator is disconnected from the network at grid connected mode, the fault current contribution from CB21 will be reduced since it comes mainly from inverter based DGs (DG1 and DG2). On the other hand, the fault current contribution from CB12 side is relatively high since it come from utility grid. Therefore, in this situation, the hybrid POTT scheme response will be tested with one strong terminal and one weak terminal.

A- Three Phase Fault

A three phase, 10 cycle, bolted fault was applied on distribution line between CB12 and CB21. Figure 7-8 and 7-9 shows the SEL451_12 and SEL451_21 responses. It is noted from the event plot of SEL451_12 in Figure 7-8 that the overreaching directional phase overcurrent element (PSV19) have successfully operated. At the same time, the relay word bit KEY of the HPOTT scheme operated and a permission to trip signal is transmitted to the remote end via IEC61850 GOOSE communications. However, the PT relay word bit did not assert indicating that permissive to trip signal is not received from the remote end

151

(SEL451_21) at this moment. By observing the SEL451_21 event plot, it is noted that the overreaching directional phase overcurrent element (PSV19) did not pickup, and accordingly, the relay word bit KEY is not activated and no permission to trip is sent to the SEL451_12 at this moment. This occurs because the fault contribution from CB21 side which comes only from IBDGs (DG2 and DG3) is less than the full load current of line-12 in that direction. Since the pickup setting of 67P2 element is always set above the full load current, then only the strong terminal at CB12 detect forward fault using level-2 overreaching element. If conventional POTT logic is used, then the POTT scheme would fail to operate. However, because of the integrated echo logic and weak infeed logic, both terminals were able to trip at high speed. By observing the SEL451_21 event plot in Figure 7-9, it is noted that the phase under voltage relay word bit (marked as 27AWI, 27BWI, 27CWI) picked up to indicated weak infeed on that terminal. Moreover, the echo key relay word bit (marked as EKEY) is activated to indicated that the echo logic has successfully operate (since the breaker is closed, and no fault is detected in reverse direction). At this moment, the EKEY relay word bit is transmitted to the remote end via IEC61850 GOOSE message allowing it to trip at high speed. Simultaneously, the relay word bit ECTT operated, this internal bit indicates weak infeed trip command to local circuit breaker at the weak terminal (CB21). Therefore, the hybrid POTT scheme with echo logic and weak infeed logic allowed both terminals to clear the fault at high speed even when contribution at one terminal is less that overcurrent pickup settings. The operation time of SEL451_12 is 63.8ms, and the operation time of SEL451_21 is 58.1ms which is around 3 cycles. The extra two cycles are due to the echo qualifying timer which is set to delay the echo signal by 2 cycles.
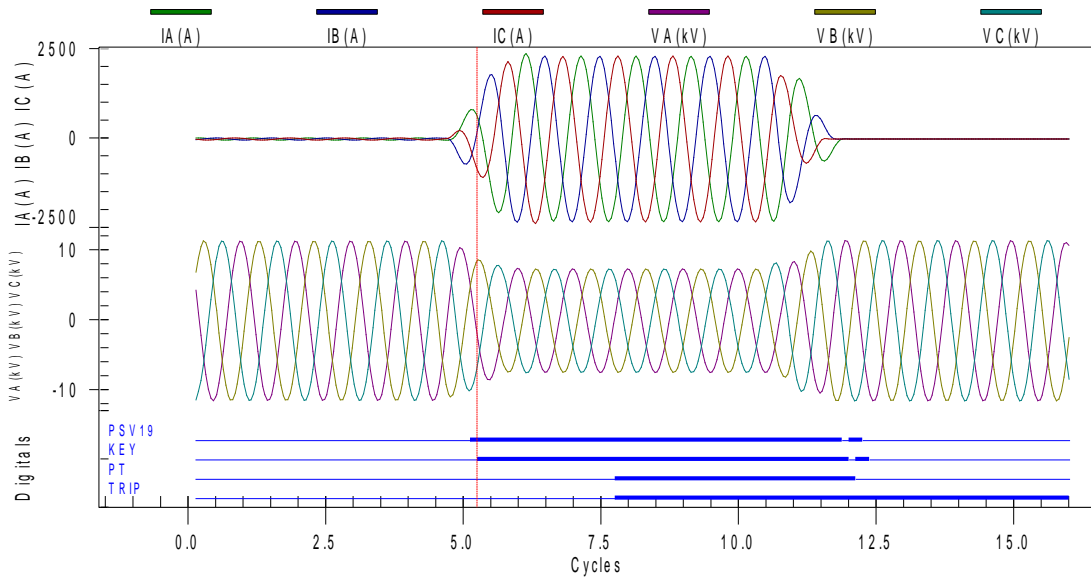
Figure 7-8: SEL451_12 response to three-phase,10 cycle fault on line 12. DG3 is Disconnected
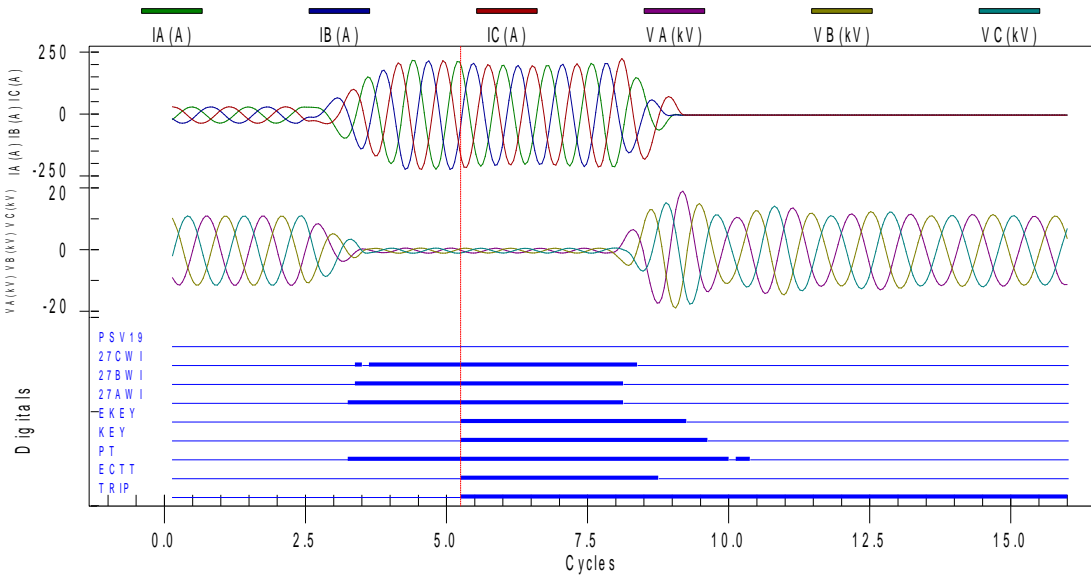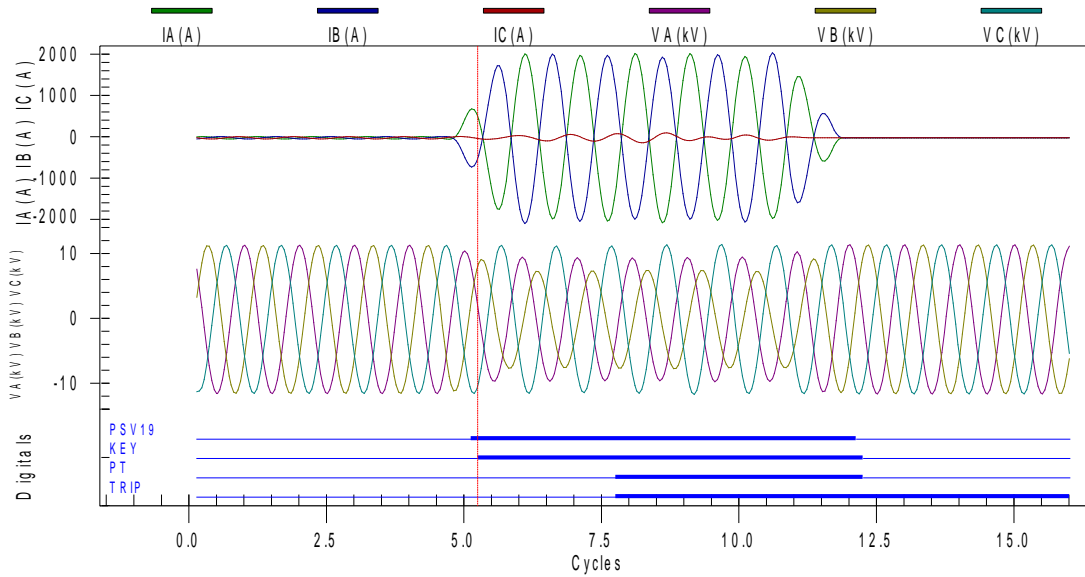

Figure 7-9: SEL451_21 response to three phase,10 cycle fault on line 12. DG3 is Disconnected

B- Phase-Phase Fault

A phase-phase, 10 cycle faults was applied on distribution line between CB12 and CB21. Figure 7-10 and 7-11 shows the SEL451_12 and SEL451_21 responses. The operation sequence is similar to the three-phase fault case, both line ends were able to clear the fault

after activation of echo logic and weak infeed logic. The operation time of SEL451_12 is 62.6ms and that of SEL451_21 is 58.0ms.
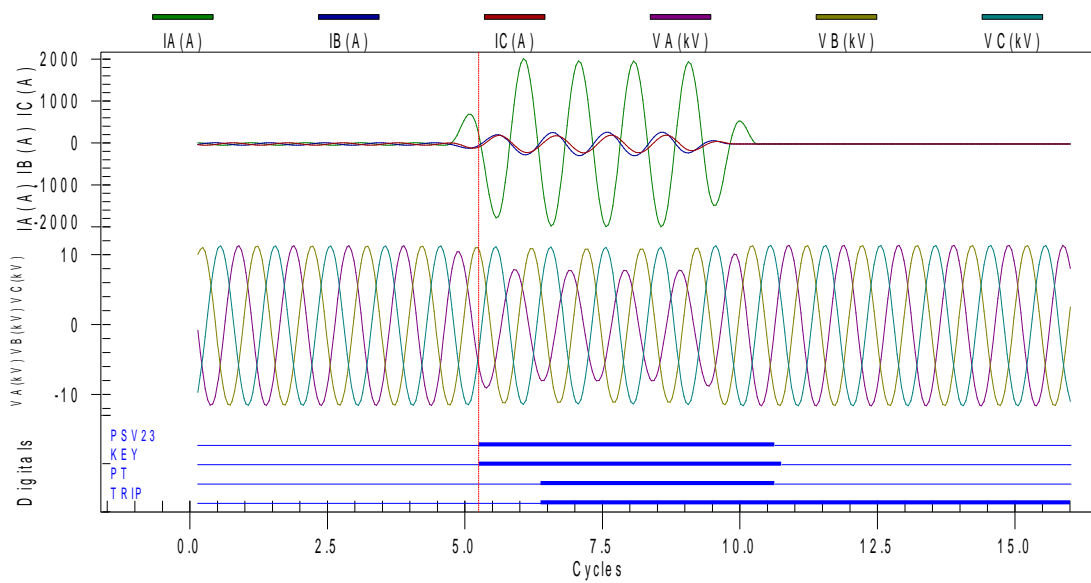

Figure 7-10: SEL451_12 response to phase-phase,10 cycle fault on line 12. DG3 is Disconnected
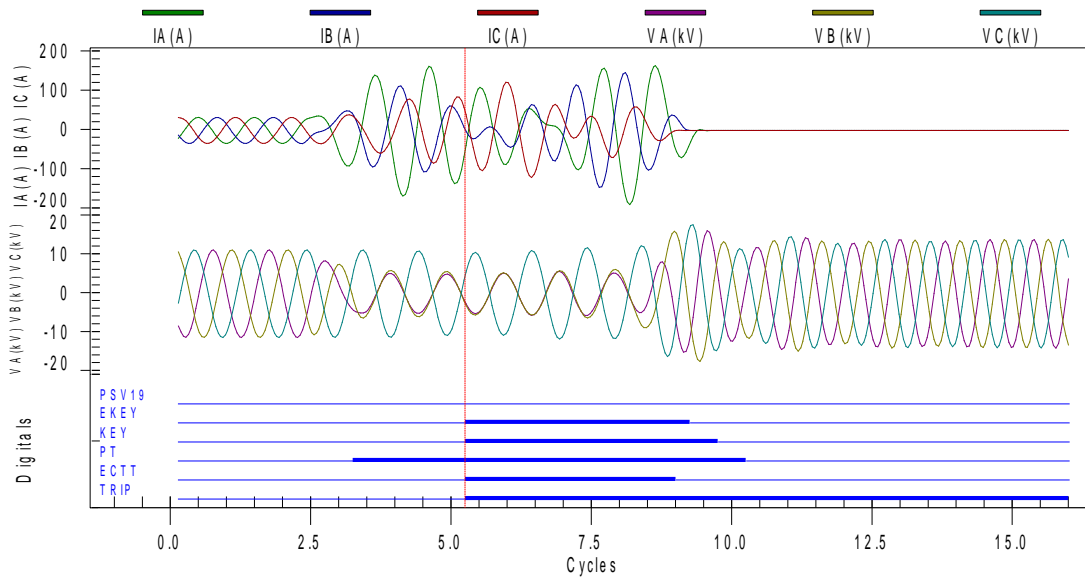
Figure 7-11: SEL451_21 response to phase-phase ,10 cycle fault on line 21. DG3 is Disconnected

C- Single line to ground Fault

A single line to ground, 10 cycle-fault was applied on distribution line between CB12 and CB21. Figure 7-12 and 7-13 shows the SEL451_12 and SEL451_21 responses. The relay word bit PSV23 represent the pickup status of the overreaching directional ground overcurrent element (67G2). Different from the previous cases (phase faults), since ground fault is normally set below full load current, single line fault from CB21 side is easily detected, and both relays tripped at high speed without echo/weak infeed logic. The operation time of SEL451_12 is 37.6ms and that of SEL451_21 is 33.1ms.

Figure 7-12: SEL451_12 response to single line to ground ,10 cycle fault on line 12. DG3 is Disconnected
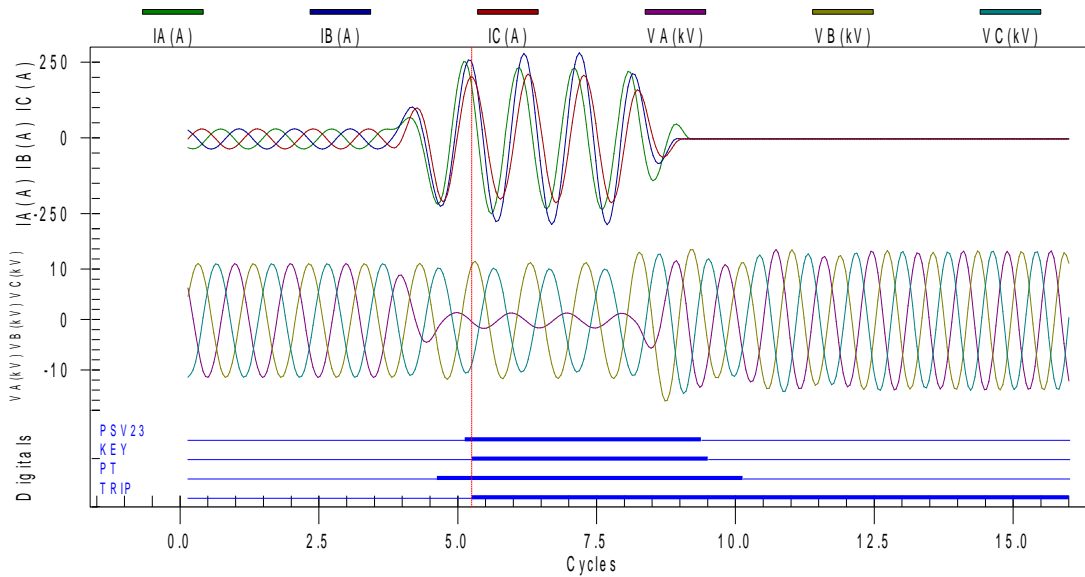
Figure 7-13: SEL451_21 response to single line to ground ,10 cycle fault on line 12. DG3 is Disconnected

7.1.3 Fault on Distribution Line 1-2, and all DGs are disconnected

If all DGs are disconnected from Microgird during grid connected mode of operation, fault current contribution will come only from gird side. The Line12 therefore changes from networked line in which fault is bidirectional to radial line at which fault is unidirectional. In this case, three-phase fault at line 12 will result in no fault contribution from terminal CB21 due to absence of DGs. However, it will be shown in this section that under such condition, the hybrid POTT scheme enabled double end disconnection at high speed without any modification.

A- Three Phase Fault

A three phase, 10 cycle, bolted fault was applied on distribution line between CB12 and CB21. Figure 7-14 and 7-15 shows the SEL451_12 and SEL451_21 responses. It is noted from the event plot of SEL451_12 in Figure 7-14 that the overreaching directional phase overcurrent element (PSV19) have successfully operated. At the same time, the relay word

156

bit KEY of the HPOTT scheme operated and a permission to trip signal is transmitted to the remote end via IEC61850 GOOSE communications. However, the PT relay word bit did not assert indicating that permissive to trip signal is not received from the remote end (SEL451_21) at this moment. By observing the SEL451_21 event plot in Figure 7-15, it is noted that no fault is contributed from this terminal due to DG disconnection, therefore, the overreaching directional overcurrent element PSV19 did not operate, and accordingly, no permission to trip signal is sent to the SEL451_12 at this moment. If conventional POTT logic is used, then the POTT scheme would fail to operate. However, because of the integrated echo logic and weak infeed logic, both terminals were able to trip at high speed. By observing the SEL451_21 event plot in Figure 7-15, it is noted that relay word bit EKEY has operated which indicates that the echo logic has successfully operated and a permission to trip is sent via IEC61850 GOOSE message to SEL451_12 allowing it to trip at high speed. Simultaneously, the relay word bit ECTT operated which indicate that weak infeed is detected and converted to trip command to open the local circuit breaker at the weak terminal (CB21). Therefore, the hybrid POTT scheme with echo logic and weak infeed logic allowed both terminals to clear the fault at high speed even when fault is contributed from terminal only, i.e., when the network has radial configuration. The operation time of SEL451_12 is 64.4ms, and the operation time of SEL451_21 is 60.2ms which is around 3 cycles. The extra two cycles are due to the echo qualifying timer which is set to delay the echo signal by 2 cycles.
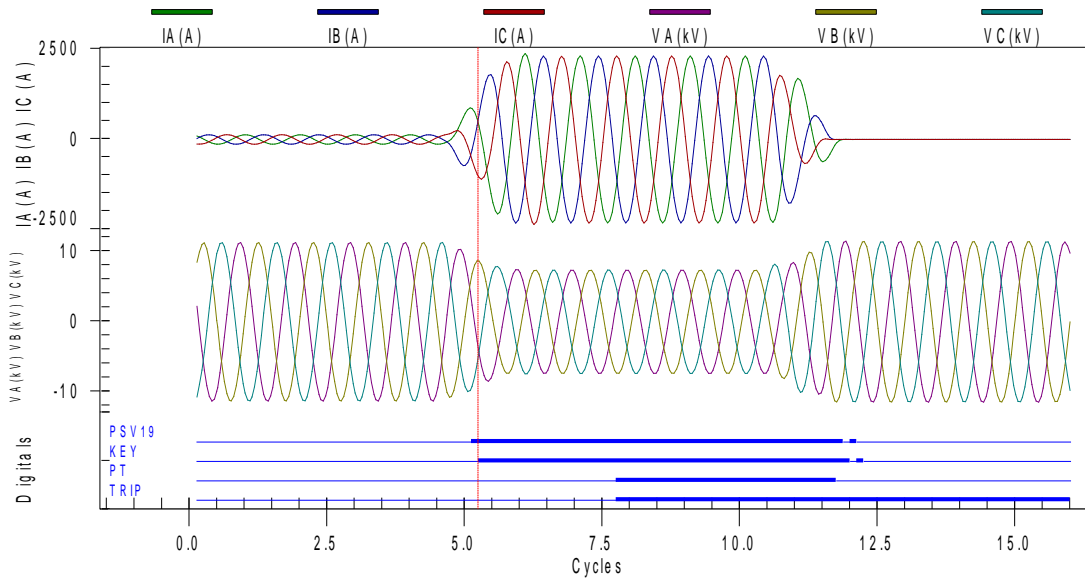
Figure 7-14: SEL451_12 response to three-phase ,10 cycle fault on line 12. All DGs are disconnected
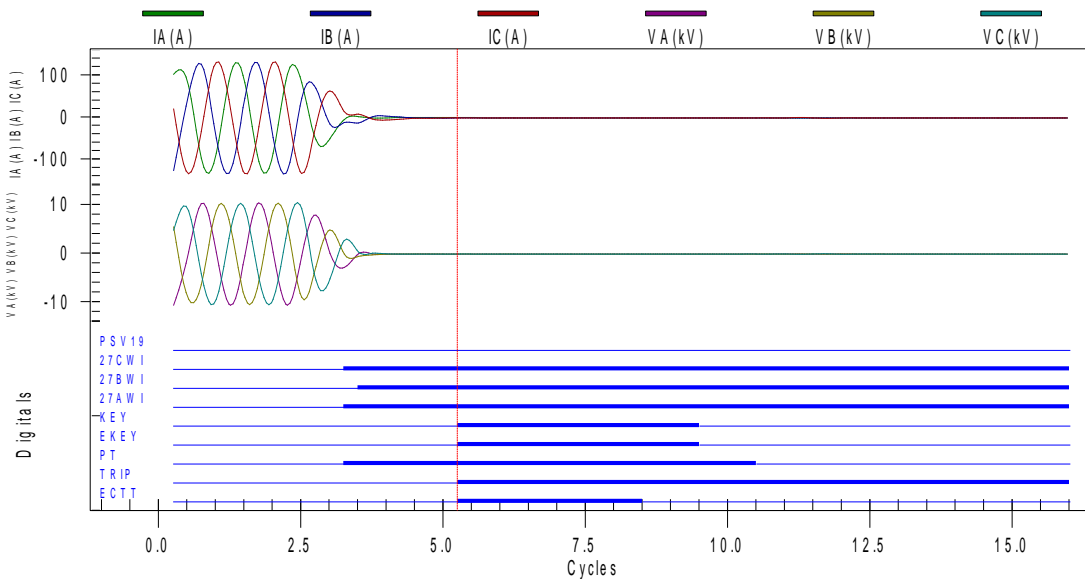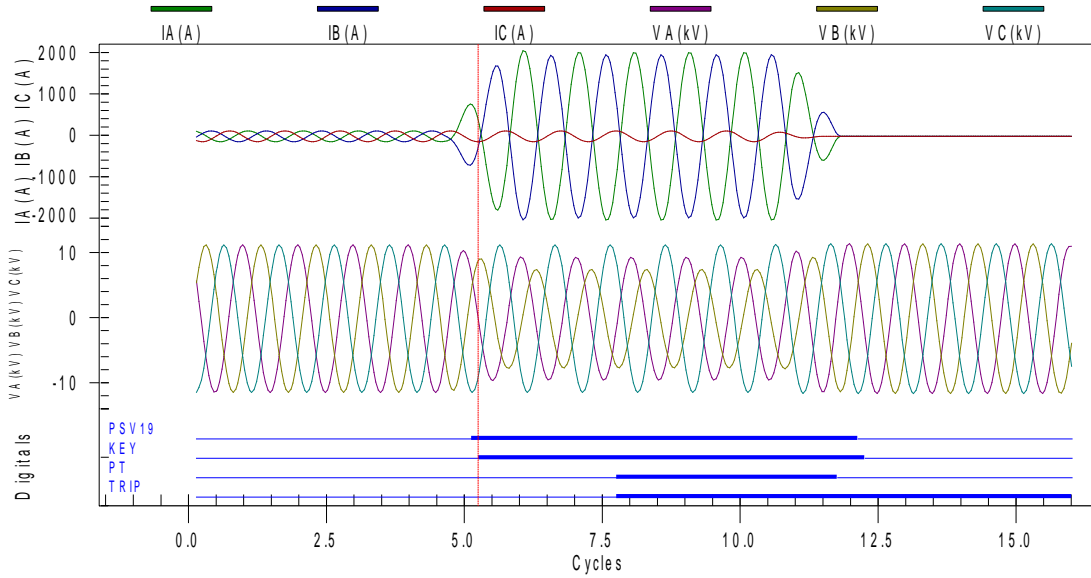

Figure 7-15: SEL451_21 response to three-phase,10 cycle fault on line 12. All DGs are disconnected

B- Phase-Phase Fault

A phase-phase, 10 cycle faults was applied on distribution line between CB12 and CB21.

Figure 7-16 and 7-16 shows the SEL451_12 and SEL451_21 responses. The operation

sequence is similar to the three-phase fault case, both line ends were able to clear the fault

158

after activation of echo logic and weak infeed logic. The operation time of SEL451_12 is 63.0ms and that of SEL451_21 is 59.4ms.

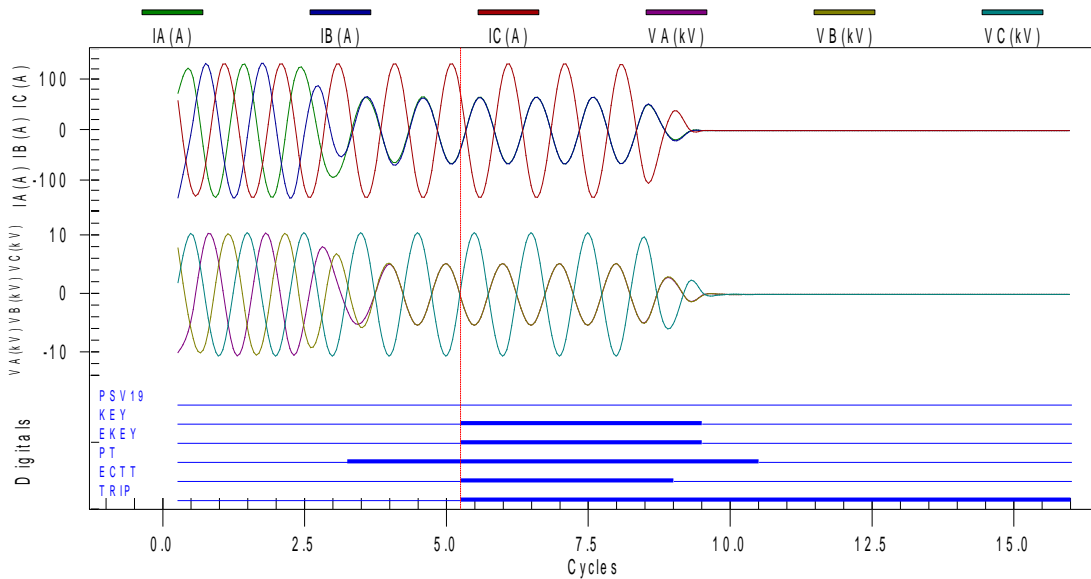**Figure 7-16: SEL451_12 response to phase-phase,10 cycle fault on line 12. All DGs are disconnected**

Figure 7-17: SEL451_21 response to phase-phase ,10 cycle fault on line 21. All DGs are disconnected

C- Single line to ground Fault

A single line to ground, 10 cycle-fault was applied on distribution line between CB12 and CB21. Figure 7-12 and 7-13 shows the SEL451_12 and SEL451_21 responses. The relay word bit PSV23 represent the pickup status of the overreaching directional ground overcurrent element (67G2). Different from the previous cases (phase faults), since ground fault is normally set below full load current, single line fault from CB21 side is easily detected, and both relays tripped at high speed without echo/weak infeed logic. The operation time of SEL451_12 is 37.6ms and that of SEL451_21 is 33.1ms.
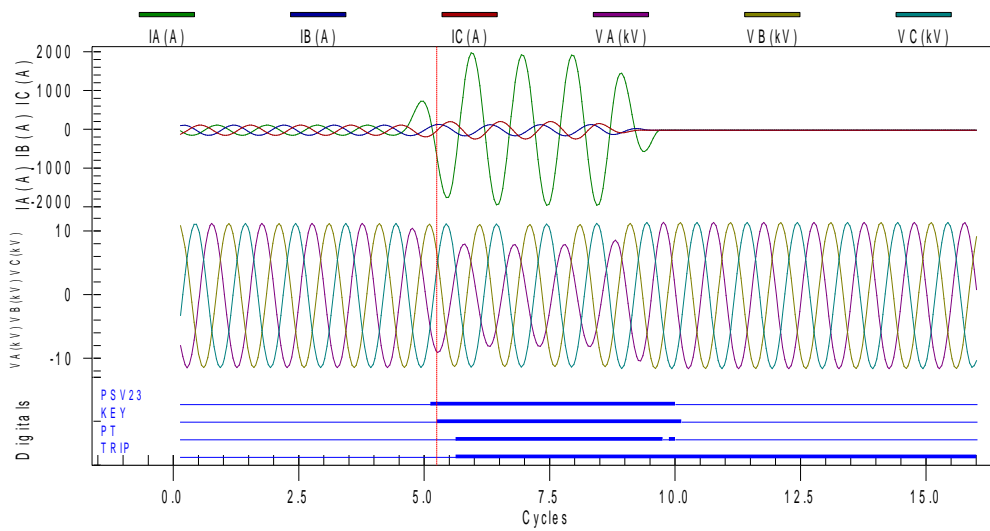

Figure 7-18: SEL451_12 response to single line to ground ,10 cycle fault on line 12. All DGs are disconnected
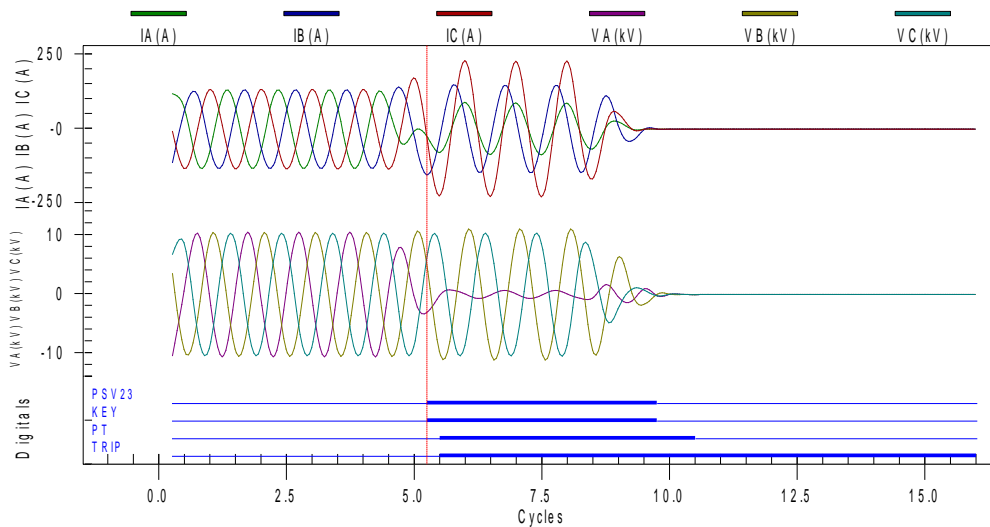

Figure 7-19: SEL451_21 response to single line to ground ,10 cycle fault on line 12. All DGs are disconnected

160

7.2   Islanded Mode of Operation

In this section, the proposed scheme is tested at islanded mode of operation. In this case, the utility connection is not available due to islanding. Therefore, there is no fault contribution from CB12 side, and fault current from CB21 side comes only from distributed generators.

7.2.1   Fault on Distribution Line 1-2, and all DGs are connected

A- Three Phase Fault

A three phase, 10 cycle, bolted fault was applied on distribution line between CB12 and CB21. Figure 7-20 and 7-21 shows the SEL451_12 and SEL451_21 responses. It is noted from the event plot of SEL451_21 in Figure 7-21 that the overreaching directional phase overcurrent element (PSV19) have successfully operated. At the same time, the relay word bit KEY of the HPOTT scheme operated and a permission to trip signal is transmitted to the remote end via IEC61850 GOOSE communications. However, the PT relay word bit did not assert indicating that permissive to trip signal is not received from the remote end (SEL451_12) at this moment. By observing the SEL451_12 event plot in Figure 7-20, it is noted that no fault is contributed from this terminal due to utility disconnection, and accordingly, the overreaching directional overcurrent element PSV19 did not operate. Therefore, permission to trip signal is not sent to the SEL451_21 at this moment. If conventional POTT logic is used, then the POTT scheme would fail to operate. By observing the SEL451_12 event plot in Figure 7-20, it is noted that the echo key relay word bit (marked as EKEY) has operated, this indicates that the echo logic has issued a permission to trip signal to allow SEL451_21 to trip at high speed. Simultaneously, the

relay word bit ECTT operated which indicate that weak infeed is detected and converted to trip command to open the local circuit breaker at the weak terminal (CB12). Therefore, the hybrid POTT scheme with echo logic and weak infeed logic allowed both terminals to clear the fault at high speed even when the network is islanded, and the fault is contributed from one terminal only. The operation time of SEL451_12 is 63.8ms, and the operation time of SEL451_21 is 68.6ms which is around 3 cycles. The extra two cycles are due to the echo qualifying timer which is set to delay the echo signal by 2 cycles.
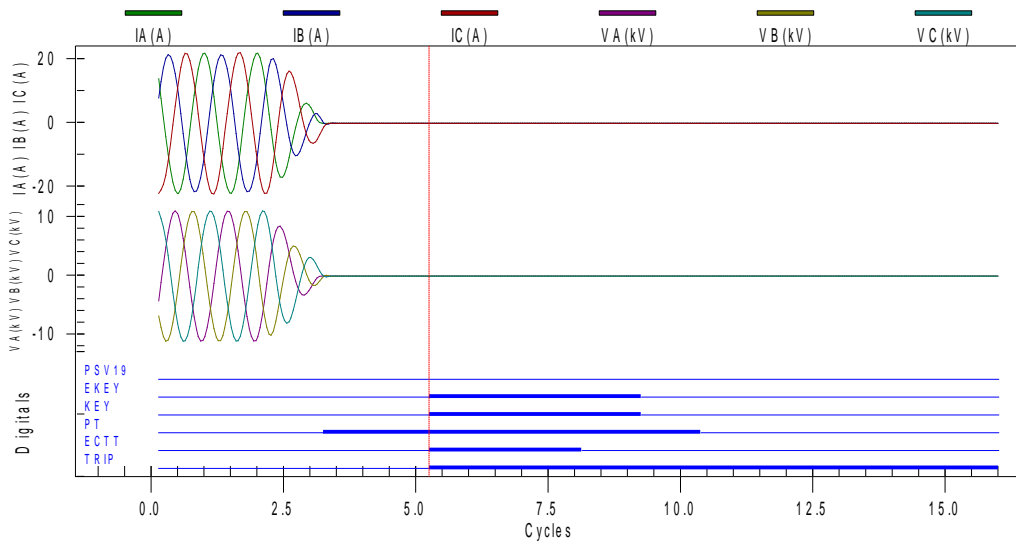

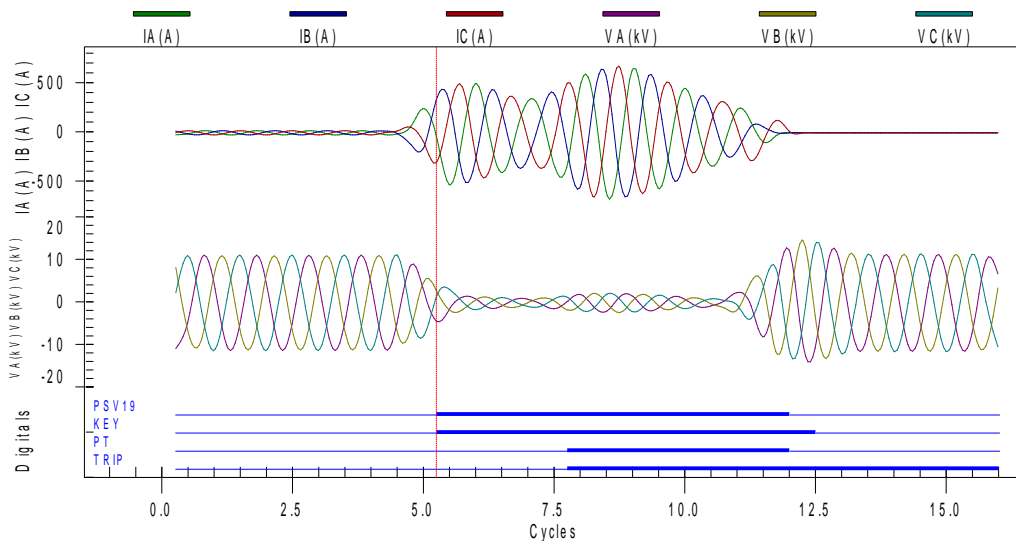**Figure 7-20: SEL451_12 response to three-phase ,10 cycle fault on line 12. All DGs are connected**

Figure 7-21: SEL451_21 response to three-phase,10 cycle fault on line 12. All DGs are connected

162

B- Phase-Phase Fault

A phase-phase, 10 cycle faults was applied on distribution line between CB12 and CB21. Figure 7-22 and 7-23 shows the SEL451_12 and SEL451_21 responses. The operation sequence is similar to the three-phase fault case, both line ends were able to clear the fault after activation of echo logic and weak infeed logic. The operation time of SEL451_12 is 70.5ms and that of SEL451_21 is 70.6ms.
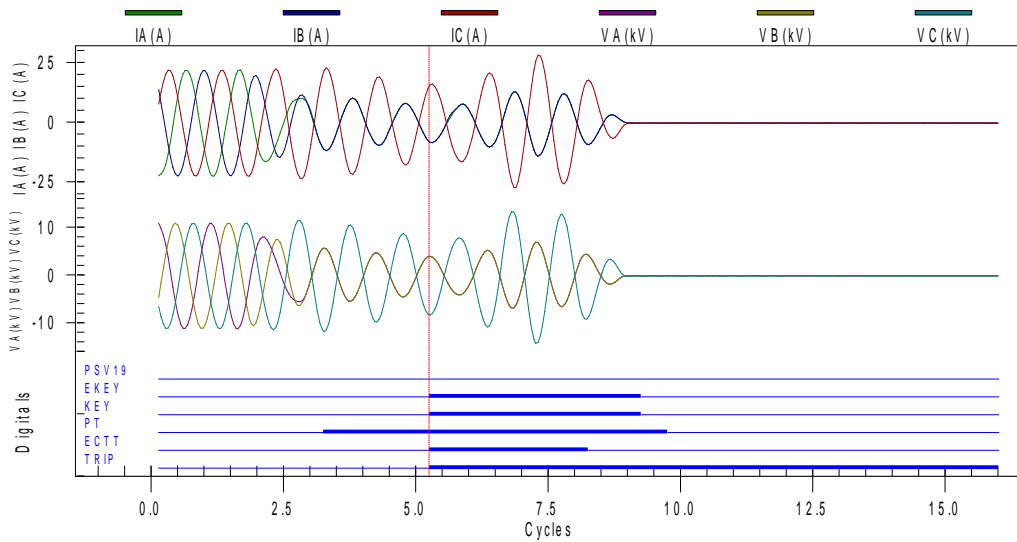

Figure 7-22: SEL451_12 response to phase-phase, 10 cycle fault on line 12. All DGs are connected
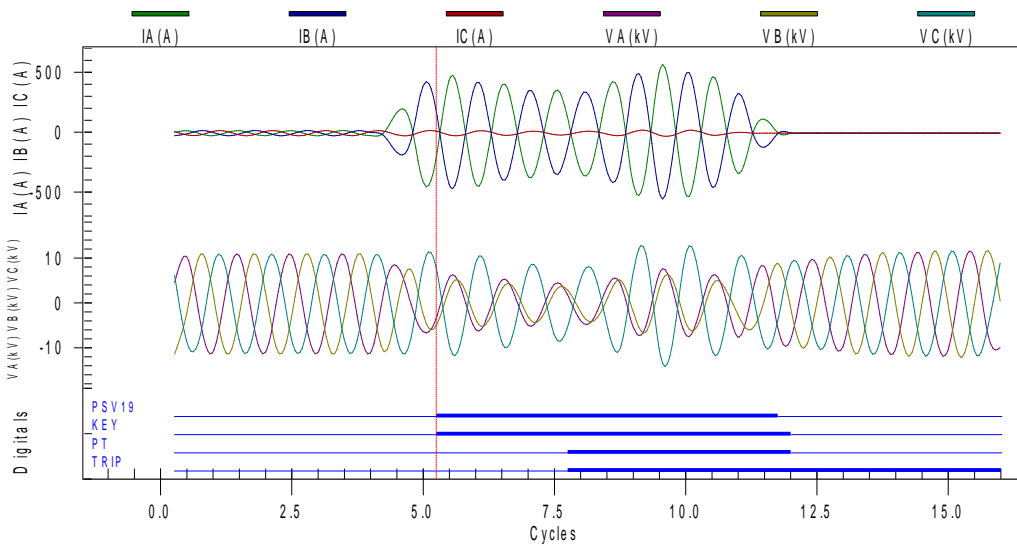

Figure 7-23: SEL451_21 response to phase-phase, 10 cycle fault on line 12. All DGs are connected

163

C- Single line to ground Fault

A single line to ground, 10 cycle-fault was applied on distribution line between CB12 and CB21. Figure 7-24 and 7-25 shows the SEL451_12 and SEL451_21 responses. The relay word bit PSV23 represent the pickup status of the overreaching directional ground overcurrent element (67G2). Different from the previous cases (phase faults), since ground fault is normally set below full load current, single line fault from CB21 side is easily detected, and both relays tripped at high speed without echo/weak infeed logic. The operation time of SEL451_12 is 24.7ms and that of SEL451_21 is 23.0ms.
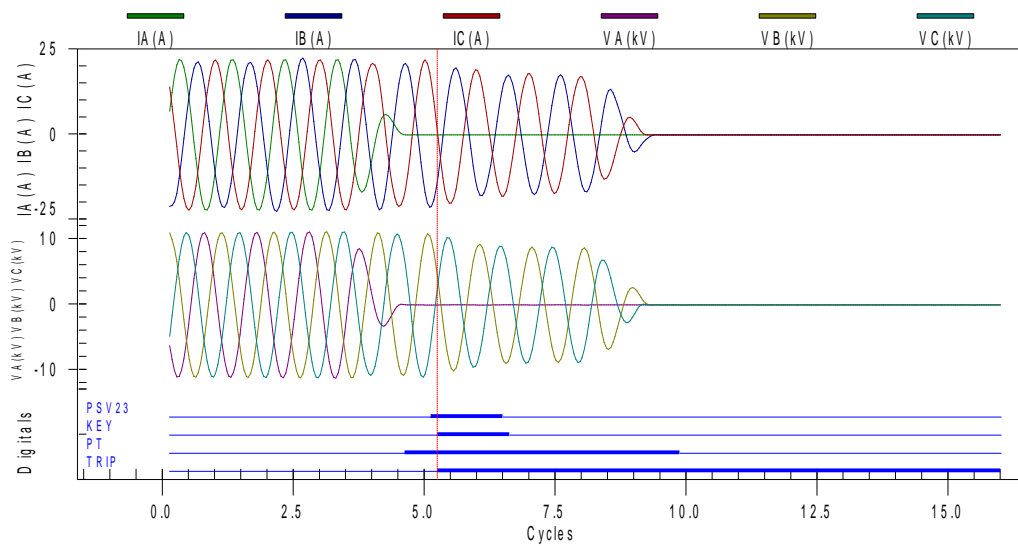

Figure 7-24: SEL451_12 response to single line to ground, 10 cycle fault on line 12. All DGs are connected
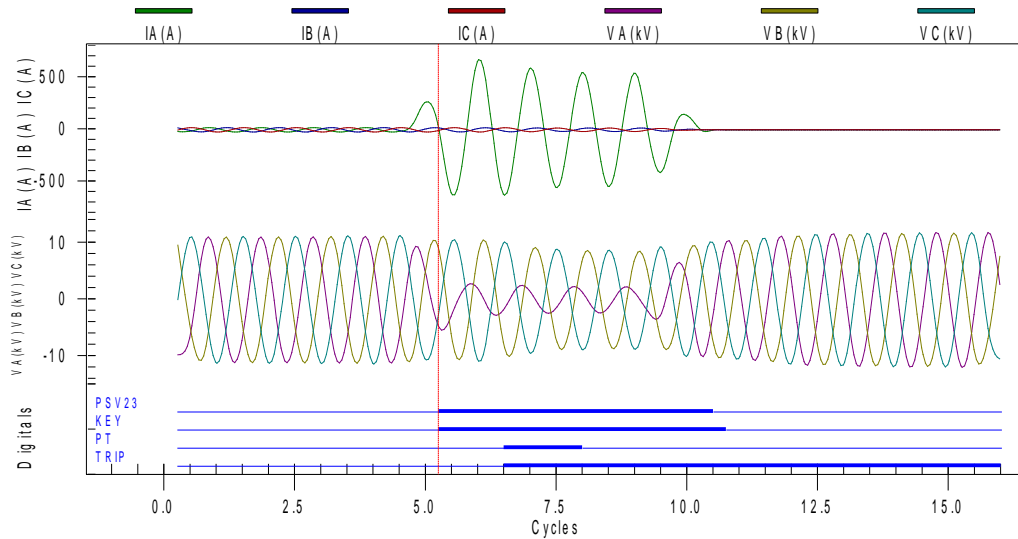
Figure 7-25: SEL451_12 response to single line to ground, 10 cycle fault on line 12. All DGs are connected

7.2.2 Fault on Distribution Line 1-2, and all IBDGs are disconnected

In this section, the proposed scheme is tested at islanded mode of operation with all IBDGs disconnected and only diesel generator in operation. The load at bus 4 and bus 5 are shed manually to achieve power balance. In this case, the utility connection is not available due to islanding. Therefore, there is no fault contribution from CB12 side. On the other hand, fault current from CB21 side comes only from diesel generator.

A- Three Phase Fault

A three phase, 10 cycle, bolted fault was applied on distribution line between CB12 and CB21. Figure 7-26 and 7-27 shows the SEL451_12 and SEL451_21 responses. It is noted from the event plot of SEL451_21 in Figure 7-27 that the overreaching directional phase overcurrent element (PSV19) have successfully operated. At the same time, the relay word bit KEY of the HPOTT scheme operated and a permission to trip signal is transmitted to the remote end via IEC61850 GOOSE communications. However, the PT relay word bit did not assert indicating that permissive to trip signal is not received from the remote end

(SEL451_12) at this moment. By observing the SEL451_12 event plot in Figure 7-26, it is noted that no fault is contributed from this terminal due to utility disconnection, and accordingly, the overreaching directional overcurrent element PSV19 did not operate. Therefore, permission to trip signal is not sent to the SEL451_21 at this moment. If conventional POTT logic is used, then the POTT scheme would fail to operate. By observing the SEL451_12 event plot in Figure 7-26, it is noted that the echo key relay word bit (marked as EKEY) has operated, this indicates that the echo logic has issued a permission to trip signal to allow SEL451_21 to trip at high speed. Simultaneously, the relay word bit ECTT operated which indicate that weak infeed is detected and converted to trip command to open the local circuit breaker at the weak terminal (CB12). Therefore, the hybrid POTT scheme with echo logic and weak infeed logic allowed both terminals to clear the fault at high speed even when the network is islanded, and the fault is contributed from the diesel generator only. The operation time of SEL451_12 is 64.0ms, and the operation time of SEL451_21 is 68.0ms which is around 3 cycles. The extra two cycles are due to the echo qualifying timer which is set to delay the echo signal by 2 cycles.
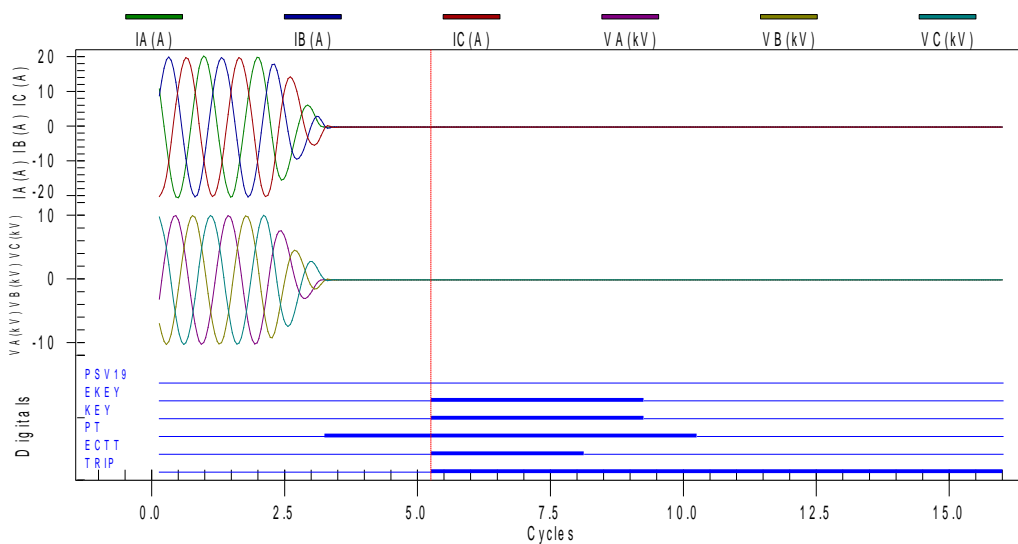

Figure 7-26: SEL451_12 response to three-phase ,10 cycle fault on line 12. DG2/DG3 are disconnected.
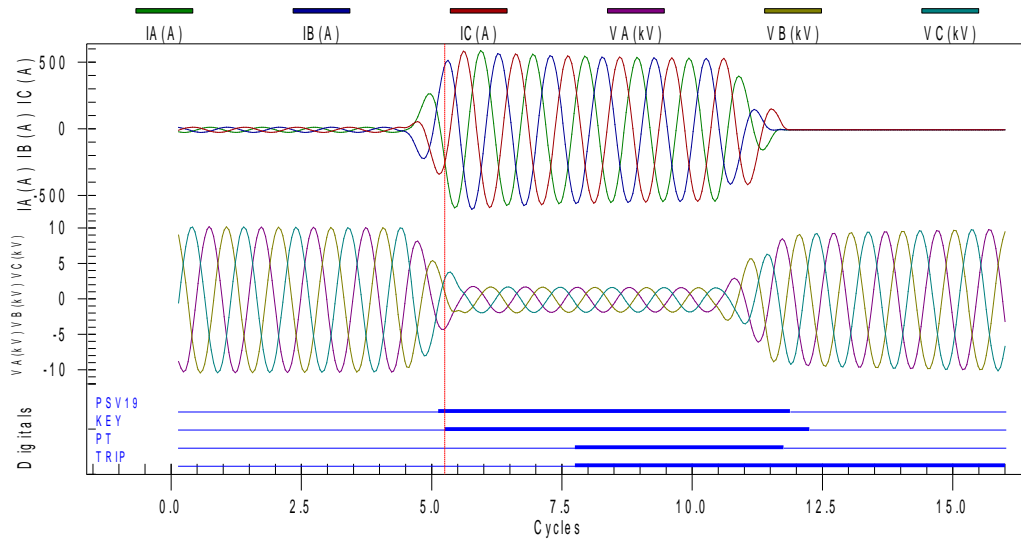
Figure 7-27: SEL451_21 response to three-phase,10 cycle fault on line 12. DG2/DG3 are disconnected.

B- Phase-Phase Fault

A phase-phase, 10 cycle faults was applied on distribution line between CB12 and CB21. Figure 7-28 and 7-29 shows the SEL451_12 and SEL451_21 responses. The operation sequence is similar to the three-phase fault case, both line ends were able to clear the fault after activation of echo logic and weak infeed logic. The operation time of SEL451_12 is 68.9ms and that of SEL451_21 is 73.5ms.
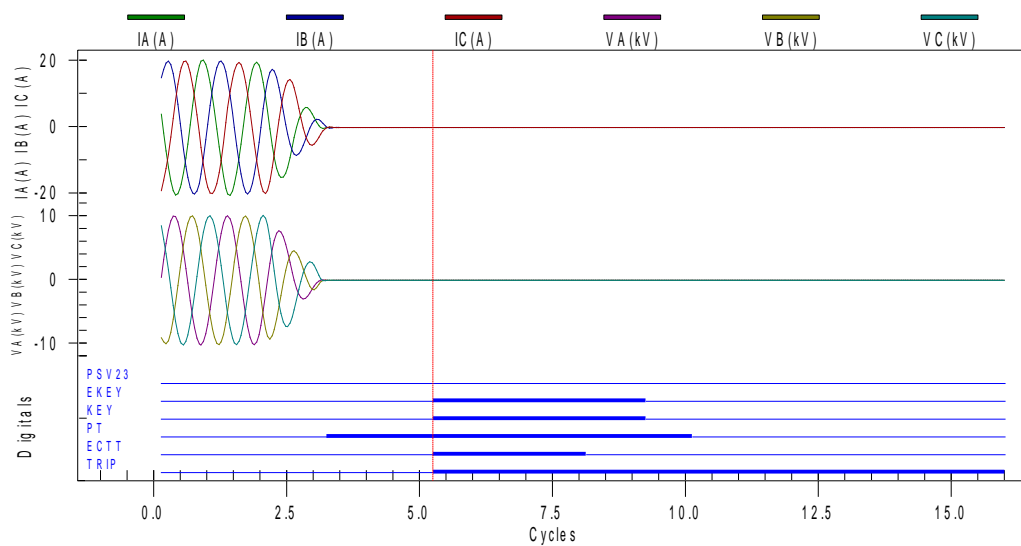

Figure 7-28: SEL451_12 response to phase-phase ,10 cycle fault on line 12. DG2/DG3 are disconnected.
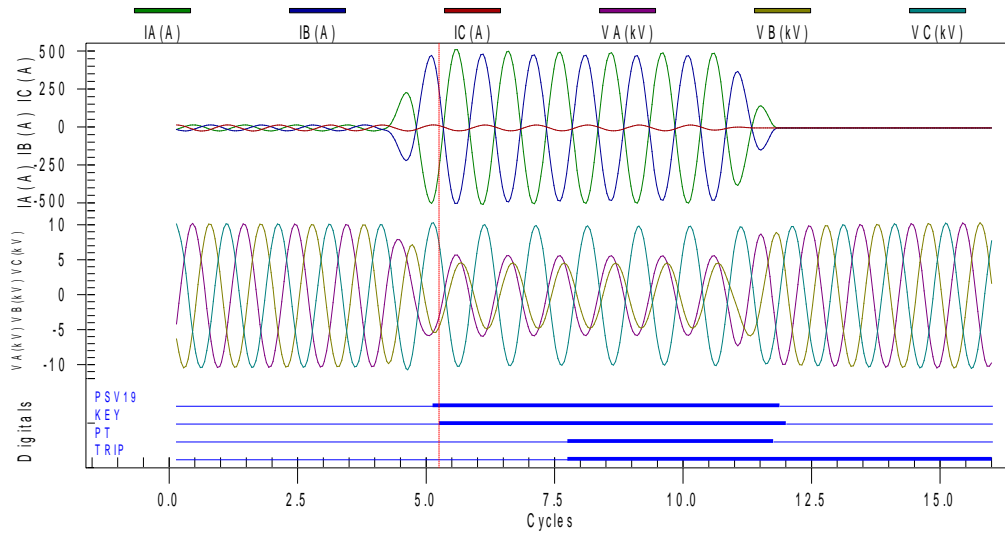
Figure 7-29: SEL451_21 response to phase-phase,10 cycle fault on line 120. DG2/DG3 are disconnected.

C- Single line to ground Fault

A single line to ground, 10 cycle-fault was applied on distribution line between CB12 and CB21. Figure 7-30 and 7-31 shows the SEL451_12 and SEL451_21 responses. The operation sequence is similar to the three-phase and phase-phase fault cases, both line ends were able to clear the fault after activation of echo logic and weak infeed logic. The operation time of SEL451_12 is 62.4ms and that of SEL451_21 is 68.1ms.
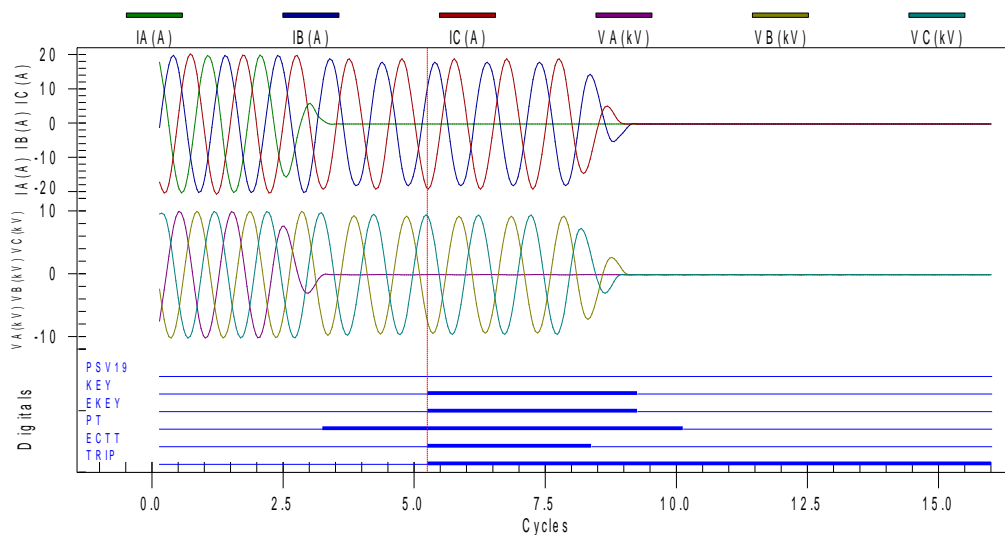

Figure 7-30: SEL451_12 response to single line to ground, 10 cycle fault on line 12. DG2/DG3 are disconnected.
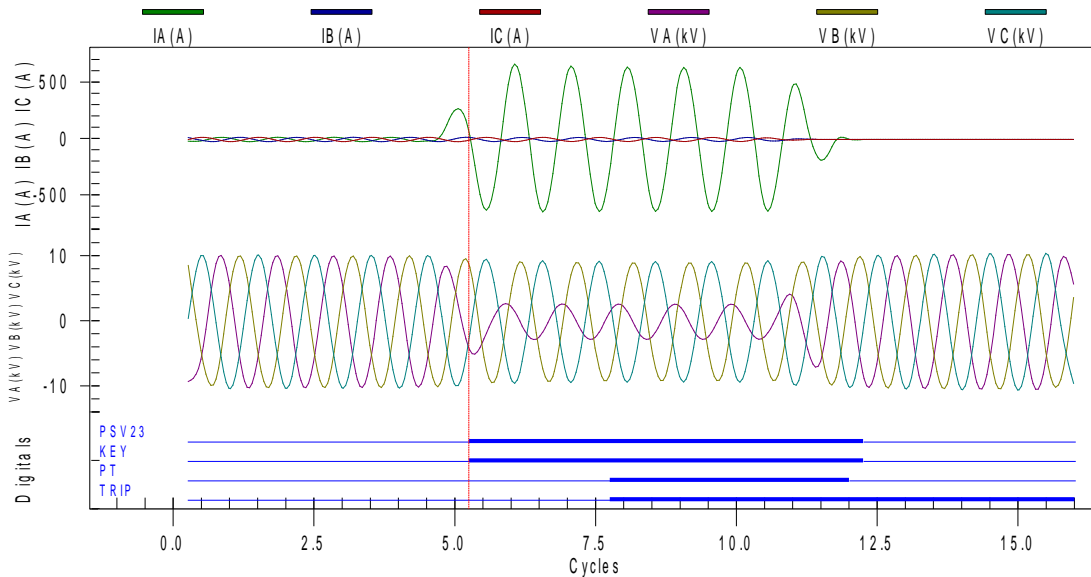
168

Figure 7-31: SEL451_21 response to single line to ground, 10 cycle fault on line 12. DG2/DG3 are disconnected.

7.3   Bus Faults

In this section, the performance of the proposed bus protection scheme is tested for one balanced against three-phase, phase to phase, and single line to ground fault at bus-1.

7.3.1   Fault on Substation Bus-1, and all DGs are connected

A- Three Phase Fault

A three phase, 10 cycle, bolted fault was applied on substation bus-1 between CB10 and CB12. Figure 7-32 and Figure 7-33 shows the responses of SEL451_10 and SEL451_12 against this fault. The relay word bit PSV34 represent the trip status of non-directional overcurrent protection element (50P) at load feeder relay (located at CBL1). The relay word bit PSV33 represents the trip status of directional phase overcurrent element (67P) from SEL451_12 relay. The relay word bit PSV31 represent the directional phase overcurrent element trip status at SEL451_10. It is observed from Figure 7-32 that the load feeder 50P element did not operate, whereas the 67P element of SEL451_10 and

SEL451_12 operated. This indicate that the fault is located on the bus, therefore a trip command is issued to CB10 and CB12 to clear the fault. The operation time of SEL450_10 is 24.15ms and the operation time of SEL451_12 is 30ms. This means that the bus protection scheme operated around 1-1.25 cycle.

Figure 7-32: SEL451_10 response to three-phase ,10 cycle fault on Bus-1

Figure 7-33: SEL451_12 response to three-phase,10 cycle fault on Bus-1

B- Phase-Phase Fault

A phase-phase, 10 cycle, bolted fault was applied on substation bus-1 between CB10 and CB12. Figure 7-34 and Figure 7-35 shows the responses of SEL451_10 and SEL451_12 against this fault. The operation sequence is similar to the three-phase fault case. The operation time of SEL450_10 is 24.97ms and the operation time of SEL451_12 is 30.83ms. This means that the bus protection scheme operated around 1-1.25 cycle.
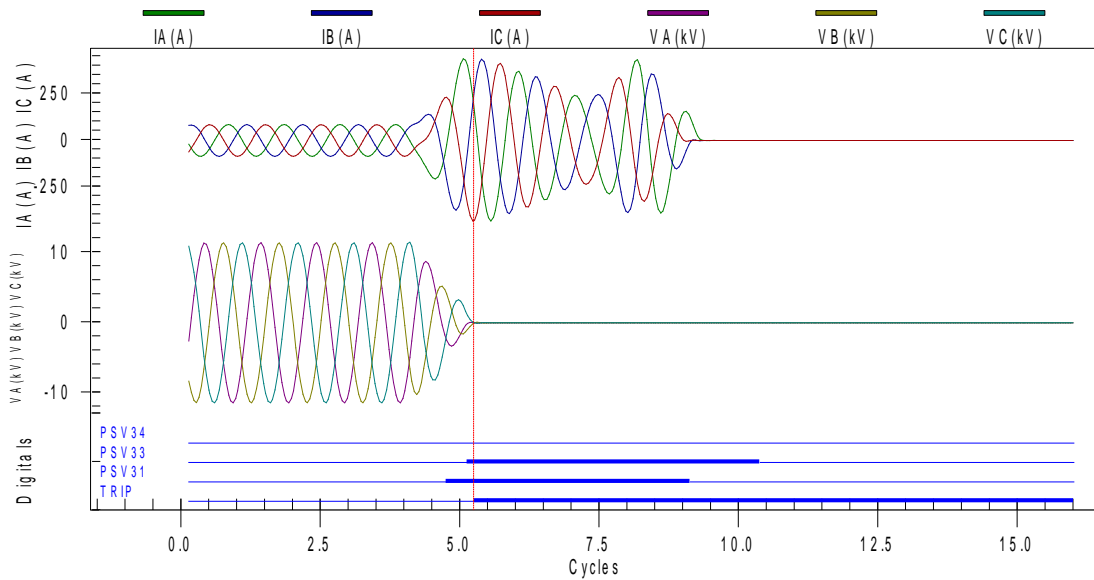

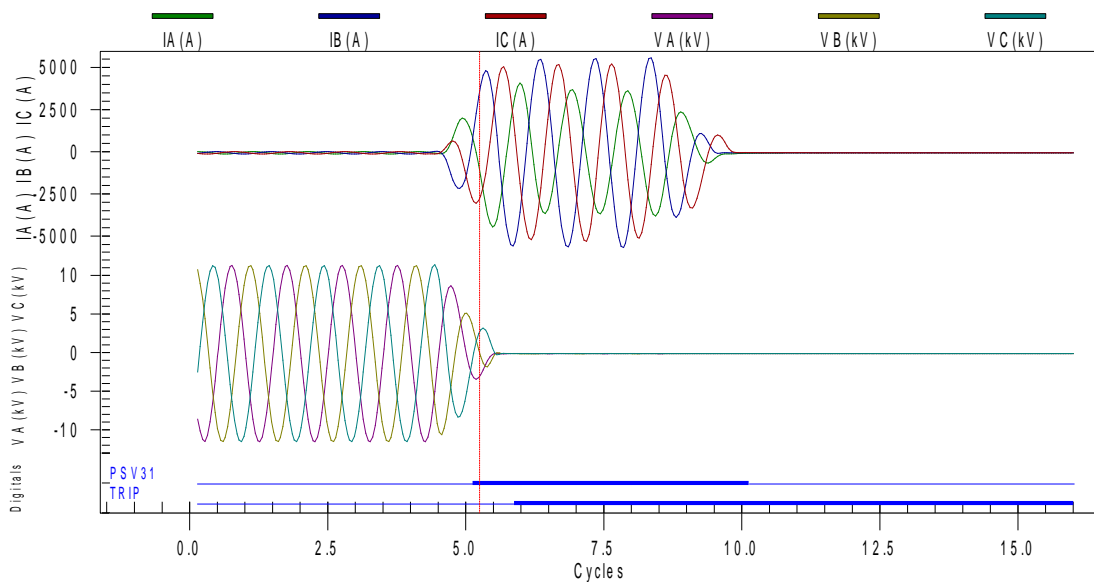**Figure 7-34: SEL451_10 response to phase-phase ,10 cycle fault on Bus-1**

Figure 7-35: SEL451_12 response to phase-phase,10 cycle fault on Bus-1

171

C- Single line to ground Fault

A single line to ground, 10 cycle, bolted fault was applied on substation bus-1 between CB10 and CB12. Figure 7-36 and Figure 7-37 shows the responses of SEL451_10 and SEL451_12 against this fault. The operation sequence is similar to the three-phase fault case. The operation time of SEL450_10 is 25.85ms and the operation time of SEL451_12 is 29.92ms. This means that the bus protection scheme operated around 1-1.25 cycle.
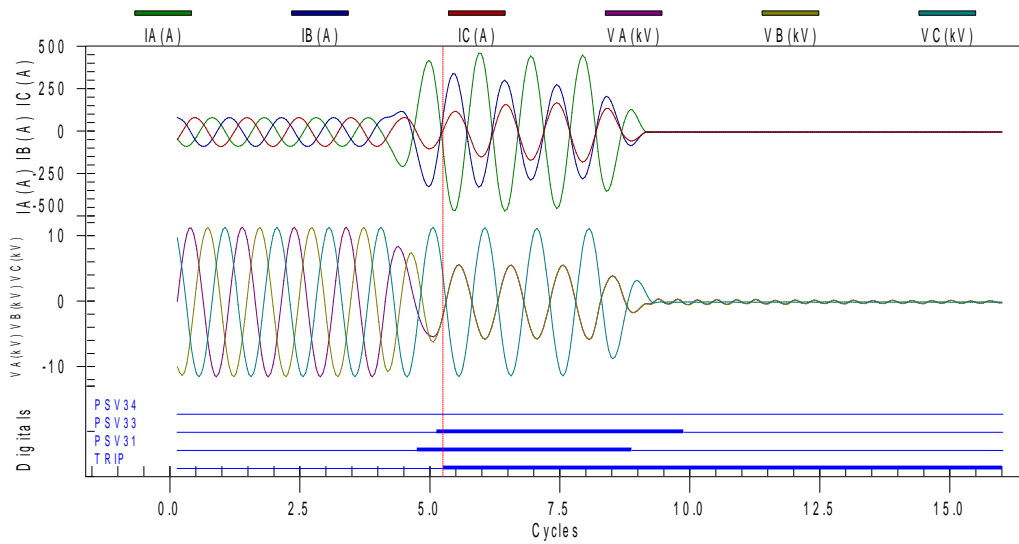

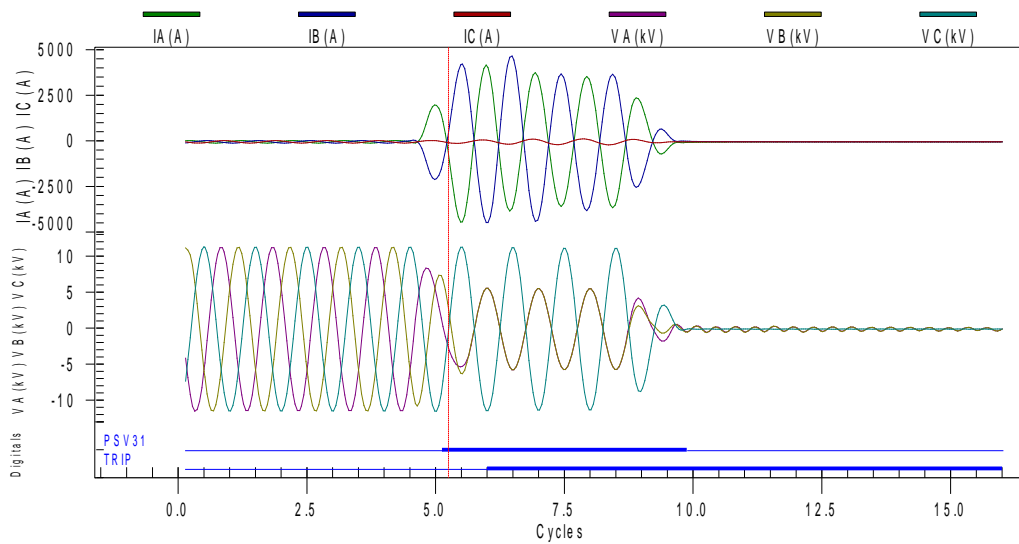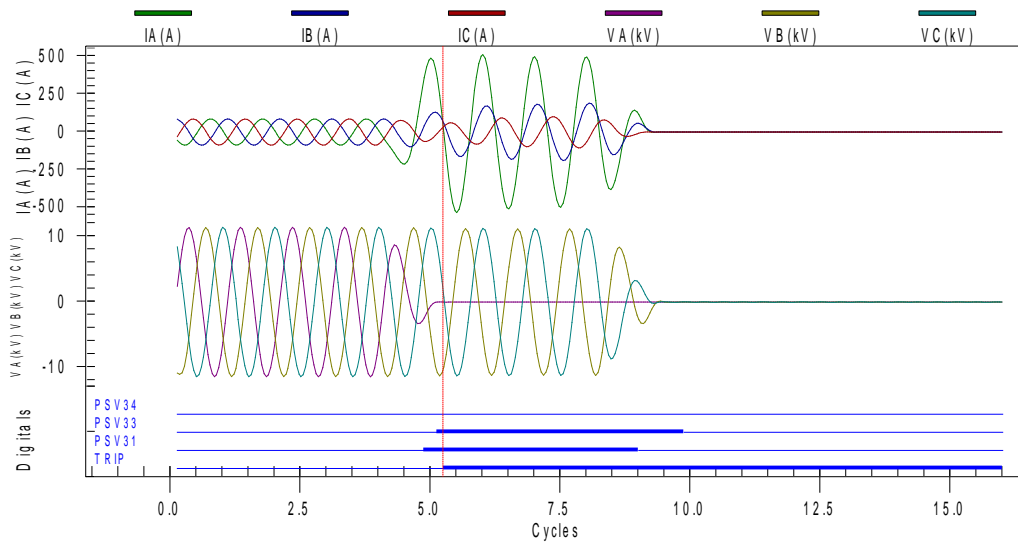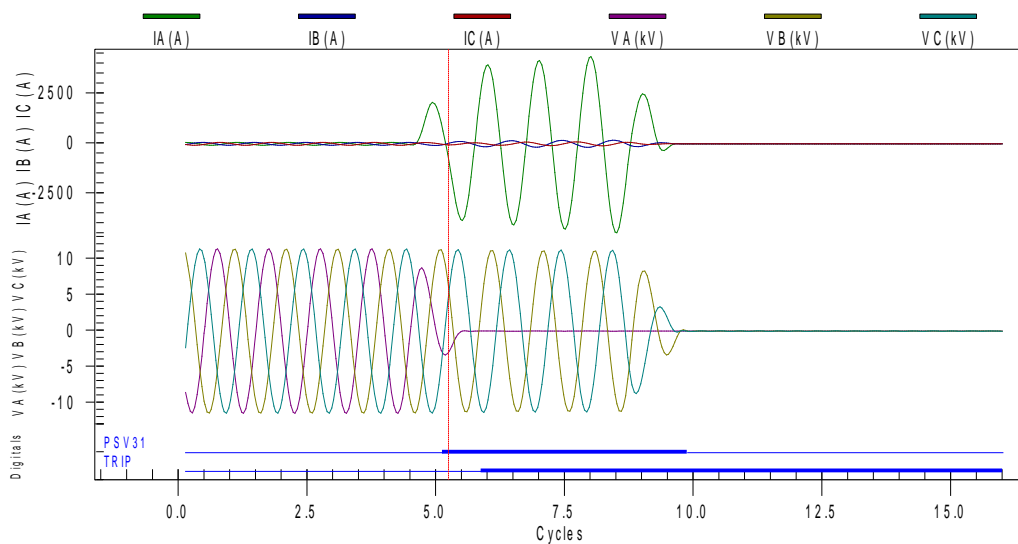**Figure 7-36: SEL451_10 response to single line to ground, 10 cycle fault on Bus-1**

Figure 7-37: SEL451_12 response to single line to ground, 10 cycle fault on Bus-1

172

CHAPTER 8

CONCLUSION & FUTURE WORK

8.1   Conclusion

In this thesis, a communication assisted decentralized adaptive protection strategy based on directional overcurrent relays is developed for MV AC looped microgrid with high penetration of rotating based and inverter based DGs. The main achievement of this thesis can be summarized as follows:

(1) A Hybrid Permissive Overreaching Transfer Trip (HPOTT) scheme and fast bus tripping (FBT) scheme for distribution line and substation buses protection has been proposed. A real-time hardware in the loop testing of the proposed scheme applied to MV AC microgrids using physical relays in the loop, physical communication infrastructure based on IEC61850, and Real Time Digital Simulator (RTDS) was conducted. The hardware in the loop testing results showed that the proposed scheme successfully cleared distribution line and bus faults at high speed in both modes of operation and for different connection states of DGs. The proposed HPOTT scheme operated in around one cycle without echo logic, and in 3 cycles when echo logic operated. The proposed bus protection scheme operated in around one cycle from fault inception. On the other hand, the simulation results showed that the proposed scheme enabled high speed double end disconnection under weak infeed, loss of infeed and remote open terminal conditions. The integrated weak infeed which used voltage-based

173

fault detection overcomes the limitation of overcurrent relay insensitivity to limited fault contribution from IBDGs. The weak infeed combined with echo logic allowed the weak terminal to trip at high speed, this is one of the main benefits of the proposed HPOTT scheme. It can be concluded therefore that proposed scheme provides high speed fault clearance for faults in both modes of operation and considering different connection states of DGs. Fast fault clearance enhances the microgrid stability and reduces the microgrid blackouts by avoiding unnecessary disconnection of DGs.

(2) A major contribution of this thesis is the development of an adaptive overcurrent element using programmable logic of microprocessor relays without the need for group setting change. The hardware testing results showed that the relay updates the pickup setting instantly according to the prevailing microgrid configuration which is communicated to the IEDs using IEC 61850 GOOSE protocol. Accordingly, group setting method which require disabling the relay during group setting change can be avoided. Moreover, the proposed adaptive overcurrent elements can be made to adapt to larger number of operational scenarios.

(3) The proposed scheme greatly simplified the problem of relay coordination commonly encountered in previous adaptive protection strategies. The HPOTT behaves similar to differential schemes, i.e., it responds to internal faults and restrains for external faults, therefore, coordination with other zones is greatly reduced especially in looped microgrids.

(4) The proposed methodology is practically feasible due to the following reason:

- The proposed scheme eliminates the need for the expensive bus differential relays and utilized the existing IED capabilities and the communication infrastructure

174

based on IEC61850 to implement a fast bus tripping scheme whose total operation time is around one cycle.

- The proposed methodology can be built using the existing off-the-shelf microprocessor-based relays of distribution systems. The methodology benefited from the current capability of distribution system IEDs and does not require new protection concepts or upgrading to transmission system IEDs. Since the fault detection is based on directional overcurrent relays, the capital cost of such IEDs is much lower compared to distance protection and differential IEDs. Therefore, great cost can be reduced by adopting the proposed protection strategy.

- The proposed HPOTT scheme requires transmitting one bit of information between the relays, the communication bandwidth requirement is greatly reduced compared to current differential for example. Therefore, the scheme can be implemented with lower communication infrastructure such as Licensed radio, Spread-spectrum radio, and Power Line Carrier (PLC).

(5) The proposed decentralized adaptive protection scheme is which the IEDs act independently from a master control unit enhances the reliability because it is not subject to single point failure. The impact of any failure will be localized and does not affect the total microgrid. Moreover, in case of communication failure, the relays can still operate using the time delayed back up protection elements which act independent from the communication scheme.

8.2   Future Work

The following topics are suggesting as future work:

(1) The future work can explore the application of other directional comparison logic such as DCB, DCUB, and PUTT schemes.

(2) The proposed methodology assumed a microgrid with rotating based and inverter based DGs. The MV synchronous based generators which contributes relatively high fault current at islanded mode facilitates fault detection and enabled the use of overcurrent protection to provide sufficient sensitivity at islanded mode. Inverter dominated microgrids are more challenging case. The future work shall explore the application of directional comparison-based protection schemes to IBDG dominated microgrids. Distance protection based directional comparison schemes which are independent of fault current is a potential solution to future microgrid with inverter-based DG.

(3) The proposed methodology can be expanded by applying automatic reclosing schemes, and fuse saving schemes which are commonly encountered in distribution systems.

(4) Protection solutions to distribution networks with extremely short lines and large number of feeders and laterals can be explored.

References

[1]   D. T. Ton and M. A. Smith, "The U.S. Department of Energy's Microgrid Initiative," *The Electricity Journal,* vol. 25, pp. 84-94, 2012/10/01/ 2012.

[2]   P. Asmus and M. Lawrence. (2016). *Market Data: Microgrids*. Available: https://www.navigantresearch.com/research/market-data-microgrids

[3]   N. Hatziargyriou, H. Asano, R. Iravani, and C. Marnay, "Microgrids," *IEEE Power and Energy Magazine,* vol. 5, pp. 78-94, 2007.

[4]   J. M. Guerrero, F. Blaabjerg, T. Zhelev, K. Hemmes, E. Monmasson, S. Jemei, *et al.*, "Distributed Generation: Toward a New Energy Paradigm," *IEEE Industrial Electronics Magazine,* vol. 4, pp. 52-64, 2010.

[5]   R. H. Lasseter, "Smart Distribution: Coupled Microgrids," *Proceedings of the IEEE,* vol. 99, pp. 1074-1082, 2011.

[6]   S. Parhizi, H. Lotfi, A. Khodaei, and S. Bahramirad, "State of the Art in Research on Microgrids: A Review," *IEEE Access,* vol. 3, pp. 890-925, 2015.

[7]   M. Stadler, G. Cardoso, S. Mashayekh, T. Forget, N. DeForest, A. Agarwal, *et al.*, "Value streams in microgrids: A literature review," *Applied Energy,* vol. 162, pp. 980-989, 2016/01/15/ 2016.

[8]   B. J. Brearley and R. R. Prabu, "A review on issues and approaches for microgrid protection," *Renewable and Sustainable Energy Reviews,* vol. 67, pp. 988-997, 2017/01/01/ 2017.

[9]   S. Teimourzadeh, F. Aminifar, M. Davarpanah, and J. M. Guerrero, "Macroprotections for Microgrids: Toward a New Protection Paradigm Subsequent to Distributed Energy Resource Integration," *IEEE Industrial Electronics Magazine,* vol. 10, pp. 6-18, 2016.

[10]   T. S. Ustun, C. Ozansoy, and A. Ustun, "Fault current coefficient and time delay assignment for microgrid protection system with central protection unit," *IEEE Transactions on Power Systems,* vol. 28, pp. 598-606, 2013.

[11]   O. V. G. Swathika and S. Hemamalini, "Prims-Aided Dijkstra Algorithm for Adaptive Protection in Microgrids," *IEEE Journal of Emerging and Selected Topics in Power Electronics,* vol. 4, pp. 1279-1286, 2016.

[12]   S. F. Zarei and M. Parniani, "A Comprehensive Digital Protection Scheme for Low-Voltage Microgrids with Inverter-Based and Conventional Distributed Generations," *IEEE Transactions on Power Delivery,* vol. 32, pp. 441-452, 2017.

[13]   K. G. R. S. Manson, and S. K. Raghupathula. (2016, Microgrid Systems: Design, Control Functions, Modeling, and Field Experience. Available: https://selinc.com/api/download/116957/

[14]   L. Che, M. E. Khodayar, and M. Shahidehpour, "Adaptive Protection System for Microgrids: Protection practices of a functional microgrid system," *IEEE Electrification Magazine,* vol. 2, pp. 66-80, 2014.

[15]   S. C. Hsieh, C. S. Chen, C. T. Tsai, C. T. Hsu, and C. H. Lin, "Adaptive Relay Setting for Distribution Systems Considering Operation Scenarios of Wind Generators," *IEEE Transactions on Industry Applications,* vol. 50, pp. 1356-1363, 2014.

[16]   A. M. Ibrahim, W. El-Khattam, M. ElMesallamy, and H. A. Talaat, "Adaptive protection coordination scheme for distribution network with distributed generation using ABC," *Journal of Electrical Systems and Information Technology,* vol. 3, pp. 320-332, 2016/09/01/ 2016.

[17]   V. A. Papaspiliotopoulos, G. N. Korres, and N. D. Hatziargyriou, "Protection coordination in modern distribution grids integrating optimization techniques with adaptive relay setting," in *2015 IEEE Eindhoven PowerTech*, 2015, pp. 1-6.

[18]   V. A. Papaspiliotopoulos, G. N. Korres, V. A. Kleftakis, and N. D. Hatziargyriou, "Hardware-In-the-Loop Design and Optimal Setting of Adaptive Protection Schemes for Distribution Systems With Distributed Generation," *IEEE Transactions on Power Delivery,* vol. 32, pp. 393-400, 2017.

[19]   M. Y. Shih, A. Conde, Z. Leonowicz, and L. Martirano, "An Adaptive Overcurrent Coordination Scheme to Improve Relay Sensitivity and Overcome Drawbacks due to Distributed Generation in Smart Grids," *IEEE Transactions on Industry Applications,* vol. 53, pp. 5217-5228, 2017.

[20]   H. Laaksonen, D. Ishchenko, and A. Oudalov, "Adaptive Protection and Microgrid Control Design for Hailuoto Island," *IEEE Transactions on Smart Grid,* vol. 5, pp. 1486-1493, 2014.

[21]   H. Lin, J. M. Guerrero, J. C. Vásquez, and C. Liu, "Adaptive distance protection for microgrids," in *IECON 2015 - 41st Annual Conference of the IEEE Industrial Electronics Society*, 2015, pp. 000725-000730.

[22]   Z. Liu, H. K. Hoidalen, and M. M. Saha, "An intelligent coordinated protection and control strategy for distribution network with wind generation integration," *CSEE Journal of Power and Energy Systems,* vol. 2, pp. 23-30, 2016.

[23]   M. Cintuglu, T. Ma, and O. Mohammed, "Protection of autonomous microgrids using agent-based distributed communication," in *2017 IEEE Power & Energy Society General Meeting*, 2017, pp. 1-1.

[24] Z. Liu and H. K. Høidalen, "A simple multi agent system based adaptive relay setting strategy for distribution system with wind generation integration," in *13th International Conference on Development in Power System Protection 2016 (DPSP)*, 2016, pp. 1-6.

[25] C. I. Ciontea, C. L. Bak, F. Blaabjerg, K. K. Madsen, and C. H. Sterregaard, "Decentralized adaptive overcurrent protection for medium voltage maritime power systems," in *2016 IEEE PES Asia-Pacific Power and Energy Engineering Conference (APPEEC)*, 2016, pp. 2569-2573.

[26] C. Liu, Z. H. Rather, Z. Chen, and C. L. Bak, "Multi-agent system based adaptive protection for dispersed generation integrated distribution systems," *Trans. Grid,* vol. 60, p. 20kV, 2013.

[27] M. A. Haj-ahmed and M. S. Illindala, "The Influence of Inverter-Based DGs and Their Controllers on Distribution Network Protection," *IEEE Transactions on Industry Applications,* vol. 50, pp. 2928-2937, 2014.

[28] N. E. Naily, S. M. Saad, R. E. Elsayed, S. A. Aomura, and F. A. Mohamed, "Planning &amp; application of distance relays coordination for IEC microgrid considering intermediate in-feed factor," in *2018 9th International Renewable Energy Congress (IREC)*, 2018, pp. 1-6.

[29] M. Monadi, M. Amin Zamani, J. Ignacio Candela, A. Luna, and P. Rodriguez, "Protection of AC and DC distribution systems Embedding distributed energy resources: A comparative review and analysis," *Renewable and Sustainable Energy Reviews,* vol. 51, pp. 1578-1593, 2015/11/01/ 2015.

[30] S. A. Gopalan, V. Sreeram, and H. H. C. Iu, "A review of coordination strategies and protection schemes for microgrids," *Renewable and Sustainable Energy Reviews,* vol. 32, pp. 222-228, 2014/04/01/ 2014.

[31] P. T. Manditereza and R. Bansal, "Renewable distributed generation: The hidden challenges – A review from the protection perspective," *Renewable and Sustainable Energy Reviews,* vol. 58, pp. 1457-1465, 2016/05/01/ 2016.

[32] A. A. Memon and K. Kauhaniemi, "A critical review of AC Microgrid protection issues and available solutions," *Electric Power Systems Research,* vol. 129, pp. 23-31, 2015/12/01/ 2015.

[33] E. O. Schweitzer, D. Finney, and M. V. Mynam, "Applying radio communication in distribution generation teleprotection schemes," in *2012 65th Annual Conference for Protective Relay Engineers*, 2012, pp. 310-320.

[34] A. Girgis and S. Brahma, "Effect of distributed generation on protective device coordination in distribution system," in *LESCOPE 01. 2001 Large Engineering Systems Conference on Power Engineering. Conference Proceedings. Theme: Powering Beyond 2001 (Cat. No.01ex490)*, 2001, pp. 115-119.

[35] A. Zamani, T. Sidhu, and A. Yazdani, "A strategy for protection coordination in radial distribution networks with distributed generators," in *IEEE PES General Meeting*, 2010, pp. 1-8.

[36] E. Coster, J. Myrzik, and W. Kling, "Effect of DG on distribution grid protection," in *Distributed generation*, ed: IntechOpen, 2010.

[37] J. Kennedy, P. Ciufo, and A. Agalgaonkar, "A review of protection systems for distribution networks embedded with renewable generation," *Renewable and Sustainable Energy Reviews,* vol. 58, pp. 1308-1317, 2016/05/01/ 2016.

[38] J. A. P. Lopes, J. Vasiljevska, R. Ferreira, C. Moreira, and A. Madureira, "Advanced Architectures and Control Concepts for More Microgrids," 2009.

[39] S. I. Turunen, "Protection of Microgrids and Distributed Energy Resources based on IEC 61850," 2016.

[40] P. Janssen and J.-C. Maun, "Monitoring, protection and fault location in power distribution networks using system-wide measurements," Ph. D. dissertation, Ecole Polytechnique de Bruxelles, 2013-2014, 2014.

[41] "IEEE Standard for Interconnection and Interoperability of Distributed Energy Resources with Associated Electric Power Systems Interfaces," *IEEE Std 1547-2018 (Revision of IEEE Std 1547-2003),* pp. 1-138, 2018.

[42] A. Hooshyar and R. Iravani, "Microgrid Protection," *Proceedings of the IEEE,* vol. 105, pp. 1332-1353, 2017.

[43] J. C. Boemer, B. G. Rawn, M. Gibescu, E. Coster, M. A. M. M. v. d. Meijden, and W. L. Kling, "Contribution of negative-sequence controlled distributed generation to power system stability under unbalanced faults: A discussion paper," in *2012 3rd IEEE PES Innovative Smart Grid Technologies Europe (ISGT Europe)*, 2012, pp. 1-8.

[44] J. Mohammadi, F. B. Ajaei, and G. Stevens, "Grounding the AC Microgrid," *IEEE Transactions on Industry Applications,* vol. 55, pp. 98-105, 2019.

[45] S. Conti, L. Raffa, and U. Vagliasindi, "Innovative solutions for protection schemes in autonomous MV micro-grids," in *2009 International Conference on Clean Electrical Power*, 2009, pp. 647-654.

[46] A. H. A. Bakar, B. Ooi, P. Govindasamy, C. Tan, H. A. Illias, and H. Mokhlis, "Directional overcurrent and earth-fault protections for a biomass microgrid system in Malaysia," *International Journal of Electrical Power & Energy Systems,* vol. 55, pp. 581-591, 2014/02/01/ 2014.

[47] H. M. Sharaf, H. H. Zeineldin, D. K. Ibrahim, and E. E. L. D. A. El-Zahab, "A proposed coordination strategy for meshed distribution systems with DG

considering user-defined characteristics of directional inverse time overcurrent relays," *International Journal of Electrical Power & Energy Systems,* vol. 65, pp. 49-58, 2015/02/01/ 2015.

[48] K. A. Saleh, H. H. Zeineldin, A. Al-Hinai, and E. F. El-Saadany, "Optimal Coordination of Directional Overcurrent Relays Using a New Time–Current–Voltage Characteristic," *IEEE Transactions on Power Delivery,* vol. 30, pp. 537-544, 2015.

[49] H. H. Zeineldin, H. M. Sharaf, D. K. Ibrahim, and E. E. A. El-Zahab, "Optimal Protection Coordination for Meshed Distribution Systems With DG Using Dual Setting Directional Over-Current Relays," *IEEE Transactions on Smart Grid,* vol. 6, pp. 115-123, 2015.

[50] S. A. Hosseini, H. A. Abyaneh, S. H. H. Sadeghi, F. Razavi, and A. Nasiri, "An overview of microgrid protection methods and the factors involved," *Renewable and Sustainable Energy Reviews,* vol. 64, pp. 174-186, 2016/10/01/ 2016.

[51] R. M. Chabanloo, H. A. Abyaneh, A. Agheli, and H. Rastegar, "Overcurrent relays coordination considering transient behaviour of fault current limiter and distributed generation in distribution power network," *IET Generation, Transmission & Distribution,* vol. 5, pp. 903-911, 2011.

[52] W. K. A. Najy, H. H. Zeineldin, and W. L. Woon, "Optimal Protection Coordination for Microgrids With Grid-Connected and Islanded Capability," *IEEE Transactions on Industrial Electronics,* vol. 60, pp. 1668-1677, 2013.

[53] E. Dehghanpour, H. K. Karegar, R. Kheirollahi, and T. Soleymani, "Optimal Coordination of Directional Overcurrent Relays in Microgrids by Using Cuckoo-Linear Optimization Algorithm and Fault Current Limiter," *IEEE Transactions on Smart Grid,* vol. 9, pp. 1365-1375, 2018.

[54] N. Jayawarna, C. Jones, M. Barnes, and N. Jenkins, "Operating MicroGrid Energy Storage Control during Network Faults," in *2007 IEEE International Conference on System of Systems Engineering*, 2007, pp. 1-7.

[55] K. O. Oureilidis and C. S. Demoulias, "A Fault Clearing Method in Converter-Dominated Microgrids With Conventional Protection Means," *IEEE Transactions on Power Electronics,* vol. 31, pp. 4628-4640, 2016.

[56] H. F. Habib, A. A. S. Mohamed, M. El Hariri, and O. A. Mohammed, "Utilizing supercapacitors for resiliency enhancements and adaptive microgrid protection against communication failures," *Electric Power Systems Research,* vol. 145, pp. 223-233, 2017/04/01/ 2017.

[57] H. Al-Nasseri and M. A. Redfern, "Harmonics content based protection scheme for Micro-grids dominated by solid state converters," in *2008 12th International Middle-East Power System Conference*, 2008, pp. 50-56.

[58]   Z. Chen, X. Pei, and L. Peng, "Harmonic components based protection strategy for inverter-interfaced AC microgrid," in *2016 IEEE Energy Conversion Congress and Exposition (ECCE)*, 2016, pp. 1-6.

[59]   H. Al-Nasseri, M. A. Redfern, and R. O. Gorman, "Protecting micro-grid systems containing solid-state converter generation," in *2005 International Conference on Future Power Systems*, 2005, pp. 5 pp.-5.

[60]   T. Loix, T. Wijnhoven, and G. Deconinck, "Protection of microgrids with a high penetration of inverter-coupled energy sources," in *2009 CIGRE/IEEE PES Joint Symposium Integration of Wide-Scale Renewable Resources Into the Power Delivery System*, 2009, pp. 1-6.

[61]   H. Al-Nasseri, M. A. Redfern, and F. Li, "A voltage based protection for micro-grids containing power electronic converters," in *2006 IEEE Power Engineering Society General Meeting*, 2006, p. 7 pp.

[62]   L. Xinyao, A. Dyśko, and G. M. Burt, "Application of communication based distribution protection schemes in islanded systems," in *45th International Universities Power Engineering Conference UPEC2010*, 2010, pp. 1-6.

[63]   H. Nikkhajoei and R. H. Lasseter, "Microgrid Protection," in *2007 IEEE Power Engineering Society General Meeting*, 2007, pp. 1-6.

[64]   H. J. A. Ferrer and E. O. Schweitzer, *Modern solutions for protection, control, and monitoring of electric power systems*: Schweitzer Engineering Laboratories, 2010.

[65]   "IEEE Standard Electrical Power System Device Function Numbers, Acronyms, and Contact Designations," *IEEE Std C37.2-2008 (Revision of IEEE Std C37.2-1996),* pp. 1-48, 2008.

[66]   E. O. Schweitzer and B. Kasztenny, "Distance protection: Why have we started with a circle, does it matter, and what else is out there?," in *Protective Relay Engineers (CPRE), 2018 71st Annual Conference for*, 2018, pp. 1-19.

[67]   J. M. Dewadasa, A. Ghosh, and G. Ledwich, "Distance protection solution for a converter controlled microgrid," in *Proceedings of the 15th National Power Systems Conference*, 2008.

[68]   M. Dewadasa, A. Ghosh, and G. Ledwich, "Line protection in inverter supplied networks," in *Power Engineering Conference, 2008. AUPEC'08. Australasian Universities*, 2008, pp. 1-6.

[69]   D. Uthitsunthorn and T. Kulworawanichpong, "Distance protection of a renewable energy plant in electric power distribution systems," in *2010 International Conference on Power System Technology*, 2010, pp. 1-6.

[70] H. Lin, C. Liu, J. M. Guerrero, and J. C. Vásquez, "Distance protection for microgrids in distribution system," in *IECON 2015 - 41st Annual Conference of the IEEE Industrial Electronics Society*, 2015, pp. 000731-000736.

[71] A. Sinclair, D. Finney, D. Martin, and P. Sharma, "Distance protection in distribution systems: How it assists with integrating distributed resources," *IEEE Transactions on Industry Applications,* vol. 50, pp. 2186-2196, 2014.

[72] V. C. Nikolaidis, C. Arsenopoulos, A. S. Safigianni, and C. D. Vournas, "A distance based protection scheme for distribution systems with distributed generators," in *2016 Power Systems Computation Conference (PSCC)*, 2016, pp. 1-7.

[73] A. M. Tsimtsios and V. C. Nikolaidis. (2018, Application of distance protection in mixed overhead-underground distribution feeders with distributed generation. *The Journal of Engineering 2018(15),* 950-955. Available: https://digital-library.theiet.org/content/journals/10.1049/joe.2018.0216

[74] M. Dewadasa, A. Ghosh, and G. Ledwich, "An inverse time admittance relay for fault detection in distribution networks containing DGs," in *TENCON 2009 - 2009 IEEE Region 10 Conference*, 2009, pp. 1-6.

[75] M. Dewadasa, R. Majumder, A. Ghosh, and G. Ledwich, "Control and protection of a microgrid with converter interfaced micro sources," in *2009 International Conference on Power Systems*, 2009, pp. 1-6.

[76] M. Dewadasa, A. Ghosh, and G. Ledwich, "Fold back current control and admittance protection scheme for a distribution network containing distributed generators," *IET Generation, Transmission & Distribution,* vol. 4, pp. 952-962, 2010.

[77] M. Dewadasa, A. Ghosh, G. Ledwich, and M. Wishart, "Fault isolation in distributed generation connected distribution networks," *IET Generation, Transmission & Distribution,* vol. 5, pp. 1053-1061, 2011.

[78] R. Majumder, M. Dewadasa, A. Ghosh, G. Ledwich, and F. Zare, "Control and protection of a microgrid connected to utility through back-to-back converters," *Electric Power Systems Research,* vol. 81, pp. 1424-1435, 2011/07/01/ 2011.

[79] E. Sortomme, S. S. Venkata, and J. Mitra, "Microgrid Protection Using Communication-Assisted Digital Relays," *IEEE Transactions on Power Delivery,* vol. 25, pp. 2789-2796, 2010.

[80] C. Yuan, K. Lai, M. S. Illindala, M. A. Haj-ahmed, and A. S. Khalsa, "Multilayered Protection Strategy for Developing Community Microgrids in Village Distribution Systems," *IEEE Transactions on Power Delivery,* vol. 32, pp. 495-503, 2017.

[81] X. Liu, M. Shahidehpour, Z. Li, X. Liu, Y. Cao, and W. Tian, "Protection Scheme for Loop-Based Microgrids," *IEEE Transactions on Smart Grid,* vol. 8, pp. 1340-1349, 2017.

[82] M. A. Zamani, T. S. Sidhu, and A. Yazdani, "A communication-based strategy for protection of microgrids with looped configuration," *Electric Power Systems Research,* vol. 104, pp. 52-61, 2013/11/01/ 2013.

[83] M. Dewadasa, A. Ghosh, and G. Ledwich, "Protection of microgrids using differential relays," in *AUPEC 2011*, 2011, pp. 1-6.

[84] T. S. Ustun, C. Ozansoy, and A. Zayegh, "Differential protection of microgrids with central protection unit support," in *IEEE 2013 Tencon - Spring*, 2013, pp. 15-19.

[85] N. El Halabi, M. García-Gracia, J. Borroy, and J. L. Villa, "Current phase comparison pilot scheme for distributed generation networks protection," *Applied Energy,* vol. 88, pp. 4563-4569, 2011/12/01/ 2011.

[86] S. A. Saleh, R. Ahshan, M. S. Abu-Khaizaran, B. Alsayid, and M. Rahman, "Implementing and Testing $ d $–$ q $ WPT-Based Digital Protection for Microgrid Systems," *IEEE Transactions on Industry Applications,* vol. 50, pp. 2173-2185, 2014.

[87] S. A. Saleh, "Signature-Coordinated Digital Multirelay Protection for Microgrid Systems," *IEEE Transactions on Power Electronics,* vol. 29, pp. 4614-4623, 2014.

[88] S. Kar and S. R. Samantaray, "Time-frequency transform-based differential scheme for microgrid protection," *IET Generation, Transmission & Distribution,* vol. 8, pp. 310-320, 2014.

[89] A. Gururani, S. R. Mohanty, and J. C. Mohanta, "Microgrid protection using Hilbert–Huang transform based-differential scheme," *IET Generation, Transmission & Distribution,* vol. 10, pp. 3707-3716, 2016.

[90] A. V. Masa, S. Werben, and J. C. Maun, "Incorporation of data-mining in protection technology for high impedance fault detection," in *2012 IEEE Power and Energy Society General Meeting*, 2012, pp. 1-8.

[91] S. Theodoridis and K. Koutroumbas, *Pattern Recognition*: Elsevier Science, 2003.

[92] E. Casagrande, W. L. Woon, H. H. Zeineldin, and N. H. Kan'an, "Data mining approach to fault detection for isolated inverter-based microgrids," *IET Generation, Transmission & Distribution,* vol. 7, pp. 745-754, 2013.

[93] D. P. Mishra, S. R. Samantaray, and G. Joos, "A Combined Wavelet and Data-Mining Based Intelligent Protection Scheme for Microgrid," *IEEE Transactions on Smart Grid,* vol. 7, pp. 2295-2304, 2016.

[94]   D. P. Mishra, "A Protection Scheme for Microgrids Using Intelligent Relays," McGill University, 2014.

[95]   E. Casagrande, W. L. Woon, H. H. Zeineldin, and D. Svetinovic, "A Differential Sequence Component Protection Scheme for Microgrids With Inverter-Based Distributed Generators," *IEEE Transactions on Smart Grid,* vol. 5, pp. 29-37, 2014.

[96]   S. Kar and S. R. Samantaray, "Combined S-transform and data-mining based intelligent micro-grid protection scheme," in *2014 Students Conference on Engineering and Systems*, 2014, pp. 1-5.

[97]   S. Kar, S. R. Samantaray, and M. D. Zadeh, "Data-Mining Model Based Intelligent Differential Microgrid Protection Scheme," *IEEE Systems Journal,* vol. 11, pp. 1161-1169, 2017.

[98]   M. Mishra and P. K. Rout, "Detection and classification of micro-grid faults based on HHT and machine learning techniques," *IET Generation, Transmission & Distribution,* vol. 12, pp. 388-397, 2018.

[99]   E. O. Schweitzer, B. Kasztenny, A. Guzmán, V. Skendzic, and M. V. Mynam, "Speed of line protection - can we break free of phasor limitations?," in *2015 68th Annual Conference for Protective Relay Engineers*, 2015, pp. 448-461.

[100]   X. Li, A. Dyśko, and G. M. Burt, "Traveling Wave-Based Protection Scheme for Inverter-Dominated Microgrid Using Mathematical Morphology," *IEEE Transactions on Smart Grid,* vol. 5, pp. 2211-2218, 2014.

[101]   S. Shi, B. Jiang, X. Dong, and Z. Bo, "Protection of microgrid," in *10th IET International Conference on Developments in Power System Protection (DPSP 2010). Managing the Change*, 2010, pp. 1-4.

[102]   X. Li, A. Dyśko, and G. Burt, "Enhanced protection for inverter dominated microgrid using transient fault information," in *11th IET International Conference on Developments in Power Systems Protection (DPSP 2012)*, 2012, pp. 1-5.

[103]   L. Yu, A. P. S. Meliopoulos, F. Rui, and S. Liangyi, "Dynamic State Estimation based protection of microgrid circuits," in *2015 IEEE Power & Energy Society General Meeting*, 2015, pp. 1-5.

[104]   S. Choi and A. P. S. Meliopoulos, "Effective real-time operation and protection scheme of microgrids using distributed dynamic state estimation," in *2017 IEEE Manchester PowerTech*, 2017, pp. 1-1.

[105]   M. E. Elkhatib and A. Ellis, "Communication-assisted impedance-based microgrid protection scheme," in *2017 IEEE Power & Energy Society General Meeting*, 2017, pp. 1-5.

[106] M. Elkhatib, A. Ellis, M. Biswal, S. Brahma, and S. Ranade, "Protection of Renewable-dominated Microgrids: Challenges and Potential Solutions," Sandia National Laboratories (SNL-NM), Albuquerque, NM (United States)2016.

[107] M. Elkhatib, A. Ellis, M. Biswal, S. Brahma, and S. Ranade, "Protection of Renewable-dominated Microgrids: Challenges and Potential Solutions," Sandia National Laboratories (SNL-NM), Albuquerque, NM (United States)2016.

[108] S. B. A. Bukhari, M. Saeed Uz Zaman, R. Haider, Y.-S. Oh, and C.-H. Kim, "A protection scheme for microgrid with multiple distributed generations using superimposed reactive energy," *International Journal of Electrical Power & Energy Systems,* vol. 92, pp. 156-166, 2017/11/01/ 2017.

[109] X. Wang, Y. Li, and Y. Yu, "Research on the relay protection system for a small laboratory-scale microgrid system," in *2011 6th IEEE Conference on Industrial Electronics and Applications*, 2011, pp. 2712-2716.

[110] M. A. Zamani, A. Yazdani, and T. S. Sidhu, "A Communication-Assisted Protection Strategy for Inverter-Based Medium-Voltage Microgrids," *IEEE Transactions on Smart Grid,* vol. 3, pp. 2088-2099, 2012.

[111] M. A. Zamani, T. S. Sidhu, and A. Yazdani, "A Protection Strategy and Microprocessor-Based Relay for Low-Voltage Microgrids," *IEEE Transactions on Power Delivery,* vol. 26, pp. 1873-1883, 2011.

[112] H. Wan, K. K. Li, and K. P. Wong, "An Adaptive Multiagent Approach to Protection Relay Coordination With Distributed Generators in Industrial Power Distribution System," *IEEE Transactions on Industry Applications,* vol. 46, pp. 2118-2124, 2010.

[113] H. F. Habib, T. Youssef, M. H. Cintuglu, and O. A. Mohammed, "Multi-Agent-Based Technique for Fault Location, Isolation, and Service Restoration," *IEEE Transactions on Industry Applications,* vol. 53, pp. 1841-1851, 2017.

[114] A. Hussain, M. Aslam, and S. M. Arif, "N-version programming-based protection scheme for microgrids: A multi-agent system based approach," *Sustainable Energy, Grids and Networks,* vol. 6, pp. 35-45, 2016/06/01/ 2016.

[115] R. M. Tumilty, M. Brucoli, G. M. Burt, and T. C. Green, "Approaches to Network Protection for Inverter Dominated Electrical Distribution Systems," in *2006 3rd IET International Conference on Power Electronics, Machines and Drives - PEMD 2006*, 2006, pp. 622-626.

[116] P. Mahat, Z. Chen, B. Bak-Jensen, and C. L. Bak, "A Simple Adaptive Overcurrent Protection of Distribution Systems With Distributed Generation," *IEEE Transactions on Smart Grid,* vol. 2, pp. 428-437, 2011.

[117] P. Mahat, Z. Chen, and B. Bak-Jensen, "A Hybrid Islanding Detection Technique Using Average Rate of Voltage Change and Real Power Shift," *IEEE Transactions on Power Delivery,* vol. 24, pp. 764-771, 2009.

[118] P. Mahat, Z. Chen, and B. Bak-Jensen, "Control and operation of distributed generation in distribution systems," *Electric Power Systems Research,* vol. 81, pp. 495-502, 2011/02/01/ 2011.

[119] H. Muda and P. Jena, "Real time simulation of new adaptive overcurrent technique for microgrid protection," in *2016 National Power Systems Conference (NPSC)*, 2016, pp. 1-6.

[120] U. Orji, C. Schantz, S. B. Leeb, J. L. Kirtley, B. Sievenpiper, K. Gerhard*, et al.*, "Adaptive Zonal Protection for Ring Microgrids," *IEEE Transactions on Smart Grid,* vol. 8, pp. 1843-1851, 2017.

[121] A. Oudalov, A. Fidigatti, T. Degner, B. Valov, C. Hardt, J. Yarza*, et al.*, "Advanced architectures and control concepts for more microgrids: Novel protection systems for microgrids," *IDeliverable DC2,* 2009.

[122] R. Sitharthan, M. Geethanjali, and T. Karpaga Senthil Pandy, "Adaptive protection scheme for smart microgrid with electronically coupled distributed generations," *Alexandria Engineering Journal,* vol. 55, pp. 2539-2550, 2016/09/01/ 2016.

[123] H. Muda and P. Jena, "Superimposed Adaptive Sequence Current Based Microgrid Protection: A New Technique," *IEEE Transactions on Power Delivery,* vol. 32, pp. 757-767, 2017.

[124] A. Oudalov and A. Fidigatti, "Adaptive network protection in microgrids," *International Journal of Distributed Energy Resources,* vol. 5, pp. 201-226, 2009.

[125] T. S. Ustun, C. Ozansoy, and A. Zayegh, "A microgrid protection system with central protection unit and extensive communication," in *2011 10th International Conference on Environment and Electrical Engineering*, 2011, pp. 1-4.

[126] T. S. Ustun, C. Ozansoy, and A. Zayegh, "Modeling of a Centralized Microgrid Protection System and Distributed Energy Resources According to IEC 61850-7-420," *IEEE Transactions on Power Systems,* vol. 27, pp. 1560-1567, 2012.

[127] T. S. Ustun, C. Ozansoy, and A. Zayegh, "Implementation of Dijkstra's algorithm in a dynamic microgrid for relay hierarchy detection," in *2011 IEEE International Conference on Smart Grid Communications (SmartGridComm)*, 2011, pp. 481-486.

[128] F. Coffele, C. Booth, and A. Dyśko, "An Adaptive Overcurrent Protection Scheme for Distribution Networks," *IEEE Transactions on Power Delivery,* vol. 30, pp. 561-568, 2015.

[129] H. Laaksonen and K. Kauhaniemi, "Smart protection concept for LV microgrid," *International Review of Electrical Engineering,* vol. 5, 2010.

[130] M. J. Daryani and A. E. Karkevandi, "Decentralized cooperative protection strategy for smart distribution grid using Multi-Agent System," in *2018 6th International Istanbul Smart Grids and Cities Congress and Fair (ICSG)*, 2018, pp. 134-138.

[131] R. Bansal, *Power System Protection in Smart Grid Environment*: CRC Press, 2019.

[132] H. J. Altuve, K. Zimmerman, and D. Tziouvaras, "Maximizing line protection reliability, speed, and sensitivity," in *Protective Relay Engineers (CPRE), 2016 69th Annual Conference for*, 2016, pp. 1-28.

[133] G. ALSTOM, "Network Protection and Automation Guide NPAG," *May,* 2011.

[134] S. H. Horowitz and A. G. Phadke, *Power system relaying* vol. 22: John Wiley & Sons, 2008.

[135] "IEEE Standard Inverse-Time Characteristic Equations for Overcurrent Relays," *IEEE Std C37.112-1996,* pp. 1-20, 1996.

[136] S. E. Laboratories, "SEL-421-4, -5 Relay Protection and Automation System Instruction Manual," S. E. Laboratories, Ed., ed: Schweitzer Engineering Laboratories, 2012.

[137] K. Zimmerman and D. Costello, "Fundamentals and improvements for directional relays," in *2010 63rd Annual Conference for Protective Relay Engineers*, 2010, pp. 1-12.

[138] A. Guzmán, M. V. Mynam, V. Skendzic, and J. L. Eternod, "Directional Elements – How Fast Can They Be?," in *72nd Annual Georgia Tech Protective Relaying Conference*, Atlanta, Georgia, 2018, pp. 1-16.

[139] A. H. A. Bakar, H. Mokhlis, H. A. Illias, and P. L. Chong, "The study of directional overcurrent relay and directional earth-fault protection application for 33kV underground cable system in Malaysia," *International Journal of Electrical Power & Energy Systems,* vol. 40, pp. 113-119, 2012/09/01/ 2012.

[140] A. Guzman, J. Roberts, and D. Hou, "New ground directional elements operate reliably for changing system conditions," in *23rd Annual Western Protective Relay Conference*, 1996.

[141] J. Roberts and A. Guzman, "Directional element design and evaluation," in *proceedings of the 21st Annual Western Protective Relay Conference, Spokane, WA*, 1994.

[142] J. L. Blackburn and T. J. Domin, *Protective relaying: principles and applications*: CRC press, 2014.

[143] K. Zimmerman and J. Mooney, "Comparing ground directional element performance using field data," in *20th Annual Western Protective Relay Conference, Spokane, Washington*, 1993.

[144] M. J. Thompson and D. L. Heidfeld, "Transmission line setting calculations - beyond the cookbook," in *2015 68th Annual Conference for Protective Relay Engineers*, 2015, pp. 850-865.

[145] W. Tucker, A. Burich, M. Thompson, R. Anne, and S. Vasudevan, "Coordinating dissimilar line relays in a communications-assisted scheme," in *2014 67th Annual Conference for Protective Relay Engineers*, 2014, pp. 111-124.

[146] R. Moxley and K. Fodero, "High-speed distribution protection made easy: Communications-assisted protection schemes for distribution applications," in *CIRED 2005 - 18th International Conference and Exhibition on Electricity Distribution*, 2005, pp. 1-5.

[147] "IEEE Guide for Protective Relay Applications to Transmission Lines," *IEEE Std C37.113-2015 (Revision of IEEE Std C37.113-1999),* pp. 1-141, 2016.

[148] O. Nzimako and A. Rajapakse, "Real time simulation of a microgrid with multiple distributed energy resources," in *2016 International Conference on Cogeneration, Small Power Plants and District Energy (ICUE)*, 2016, pp. 1-6.

[149] F. A. M. Moura, J. R. Camacho, J. W. Resende, and W. R. Mendes, "Synchronous generator, excitation and speed governor modeling in ATP-EMTP for interconnected DG Studies," in *2008 18th International Conference on Electrical Machines*, 2008, pp. 1-6.

[150] "IEEE Recommended Practice for Excitation System Models for Power System Stability Studies," *IEEE Std 421.5-1992,* p. 0_1, 1992.

[151] R. T. Inc., "Real time digital simulator, power system user's manual," December 2012.

[152] J. Peralta Rodriguez, "Dynamic Averaged Models of VSC-Based HVDC Systems for Electromagnetic Transient Programs," École Polytechnique de Montréal, 2013.

[153] N. Onyinyechi, "Real tIme simulation of a microgrid system with distributed energy resources," 2015.

[154] M. A. Hassan and M. A. Abido, "Optimal Design of Microgrids in Autonomous and Grid-Connected Modes Using Particle Swarm Optimization," *IEEE Transactions on Power Electronics,* vol. 26, pp. 755-769, 2011.

[155] K.-G. Masoud, "Enhanced Phase-Locked Loop," in *Enhanced Phase-Locked Loop Structures for Power and Energy Applications*, ed: IEEE, 2014, p. 1.

[156] M. A. Zamani, A. Yazdani, and T. S. Sidhu, "A Control Strategy for Enhanced Operation of Inverter-Based Microgrids Under Transient Disturbances and Network Faults," *IEEE Transactions on Power Delivery,* vol. 27, pp. 1737-1747, 2012.

[157] B. Li, J. Jia, and S. Xue, "Study on the Current-Limiting-Capable Control Strategy for Grid-Connected Three-Phase Four-Leg Inverter in Low-Voltage Network," *Energies,* vol. 9, p. 726, 2016.

[158] A. Yazdani and R. Iravani, *Voltage-Sourced Converters in Power Systems: Modeling, Control, and Applications*: Wiley, 2010.

[159] K. Strunz, E. Abbasi, R. Fletcher, N. Hatziargyriou, R. Iravani, and G. Joos, *TF C6.04.02 : TB 575 -- Benchmark Systems for Network Integration of Renewable and Distributed Energy Resources*, 2014.

[160] I. Commission, "IEC 60076-1: Power Transformers," *General, ed,* p. 96, 1999.

[161] A. Guzman, J. Roberts, and K. Zimmerman, "Applying the SEL-321 Relay to Permissive Overreaching Transfer Trip (POTT) Schemes," *SEL Application Guide,* 1999.

[162] K. G. Ravikumar, A. Upreti, and A. Nagarajan, "State-of-the-Art Islanding Detection and Decoupling Systems for Utility and Industrial Power Systems," in *proceedings of the 69th Annual Georgia Tech Protective Relaying Conference*, 2015.

[163] J. Mulhausen, J. Schaefer, M. Mynam, A. Guzmán, and M. Donolo, "Anti-islanding today, successful islanding in the future," in *2010 63rd Annual Conference for Protective Relay Engineers*, 2010, pp. 1-8.

[164] W. Edwards and S. Manson, "Using protective relays for microgrid controls," in *2018 71st Annual Conference for Protective Relay Engineers (CPRE)*, 2018, pp. 1-7.

[165] A. CIGRÉ, "protections and control–Final report," in *Working Group*, 1995.

[166] R. Moxley and F. Becker, "Adaptive protection — What does it mean and what can it do?," in *2018 71st Annual Conference for Protective Relay Engineers (CPRE)*, 2018, pp. 1-4.

APPENDIX-A

RSCAD Models of the Studied Microgrid

A.1   Main Grid Model

The main grid represents the sub-transmission network that feed the distribution test system. In this thesis, it will be represented as an ideal voltage source behind impedance. Figure A-1 shows the three line diagram of RSCAD model. The impedance parameters are given in section 4.3.2.
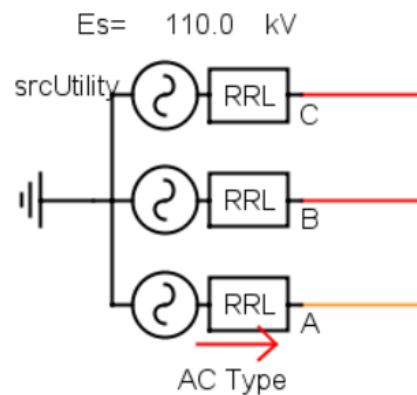
Figure 9-1: Sub-transmission grid mode as a source behind impedance

A.2   Transformer Model

RSCAD library includes many models of power transformers, in this thesis, two winding, three-phase power transformer with tap changer is used. The three-line diagram view of this component in RSCAD is shown in Figure A-2.
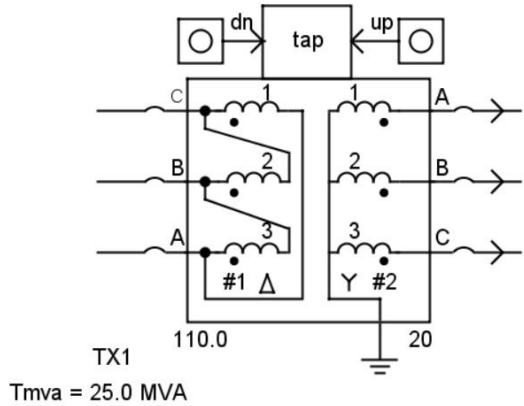
Figure A-2: RSCAD three-line diagram of Dyn1 transformer connection with tap changer

A.3 Distribution Line model

RSCAD contains two models for transmission lines, the travelling wave model which is based on distributed parameter representation, and the PI section model which is based on lumped parameter representation. However, according to RTDS manual [73], if the transmission line model is shorter than 15kM (which is the case in most distribution grids), PI section can model the line more accurately. Therefore, PI section model is adopted in this thesis. The RSCAD draft model requires entering the positive and zero sequence impedances.
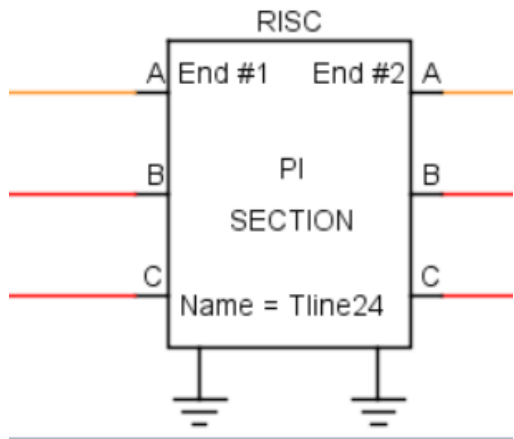
Figure A-3: Transmission line model

192

A.4 Load Model

Load is modeled using the RSCAD "Three phase RLC load with embedded breaker". This model allows the user to model the load and its circuit breaker and thus reducing the total number of nodes required. The load values have been modified to suit the purpose of this study after adding DG. The load schedule considered is presented in Table 4-7.

Name = Load4
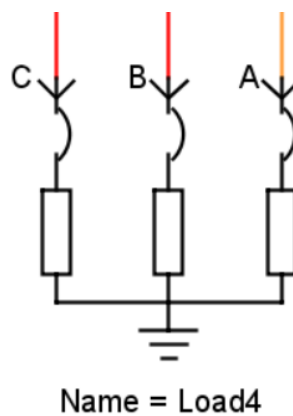
Figure A-4: Three phase RLC load with embedded breaker

A.5 Diesel Generator

The diesel generator model consists of synchronous generator, excitation system, automatic voltage regulator (AVR), diesel engine and speed governor. The complete model is shown in Figure A-5. The synchronous generator and step up transformer are taken directly from RSCAD library. The integrated transformer helps in reducing the number of nodes. The excitation system is based on IEEE type AC4 which has a built-in RSCAD model as shown in Figure A-5. The diesel engine and its speed governor block are based on the contribution from reference [150]. The internal component of tis block are shown in Figure A-6.
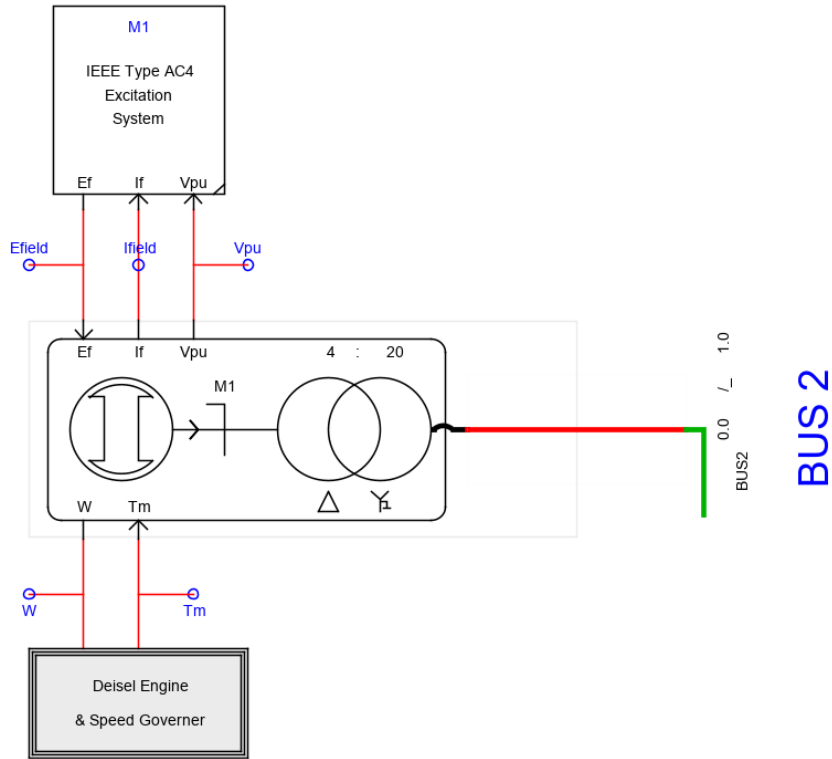
Figure A-5: Diesel Generator Model
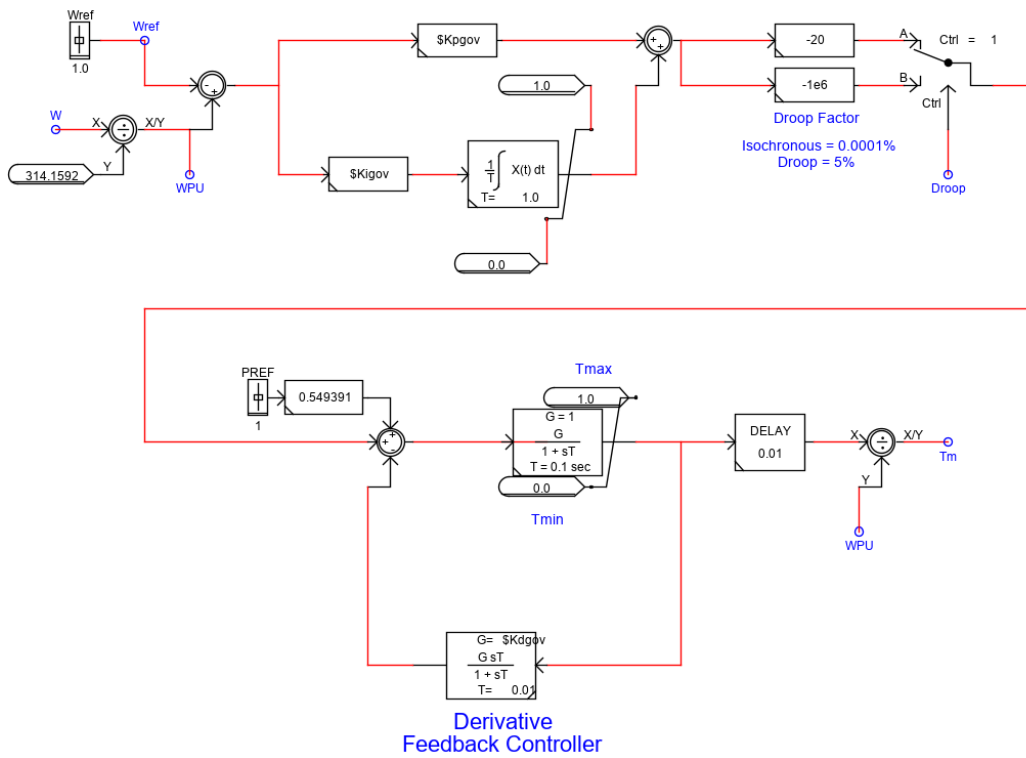
Figure A-6: Diesel Engine and Speed Governor Model

194

A.6 Inverter Based DG

The inverter-based DG source model is shown in Figure A-7. It consists of a DC source, an average value model of voltage source inverter, a DC bus capacitor, a step-up transformer, and the control system. All the components shown in Figure A-7 are based on built-in RSCAD models except for the control system block. The internal components of the control system block are shown in Figure A-8 to Figure A-16.
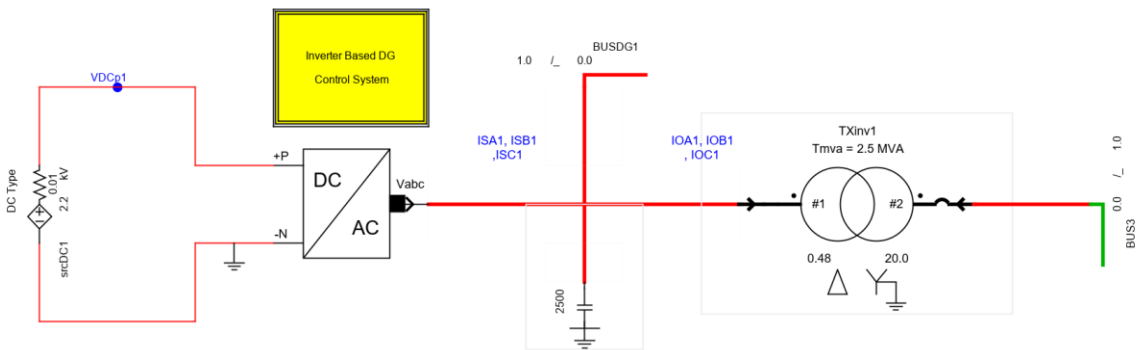
Figure A-7: Inverter Based DG Model
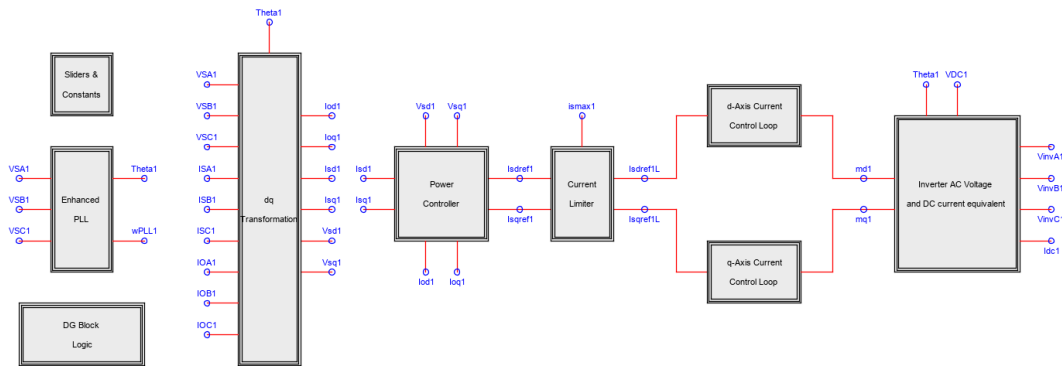
Figure A-8: Internal sub-components of Inverter Based DG control system
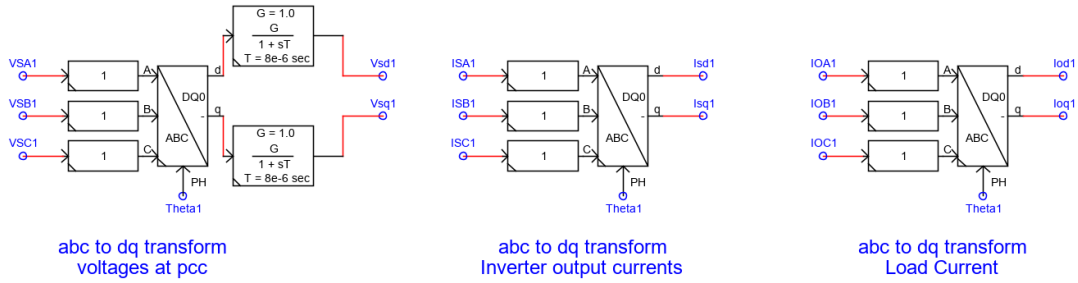
Figure 9-9: Internal components of dq-transformation block
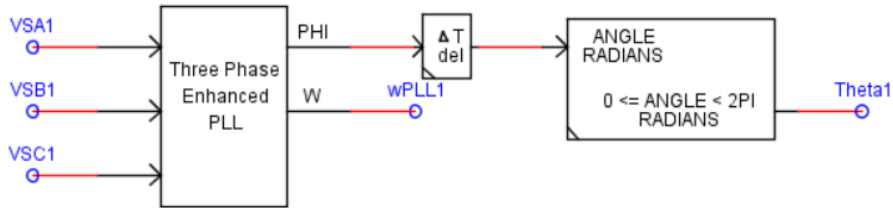
Figure A-10: Enhanced PLL Model
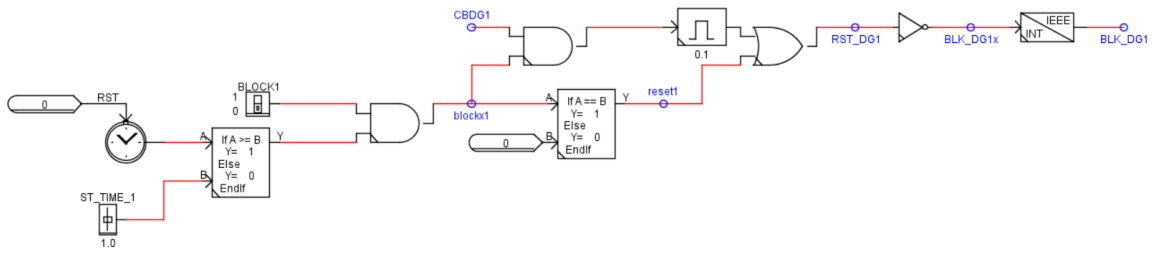
Figure A-11: Internal components of DG Block Logic
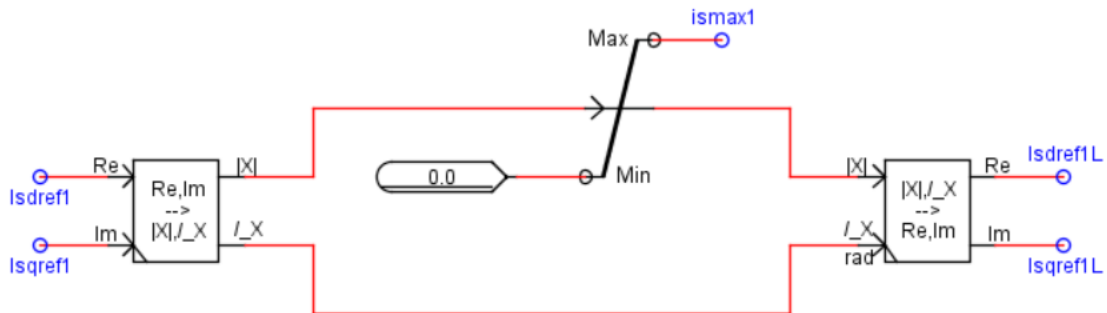
Figure A-12: Internal Component of Inverter Fault Current Limiter

196
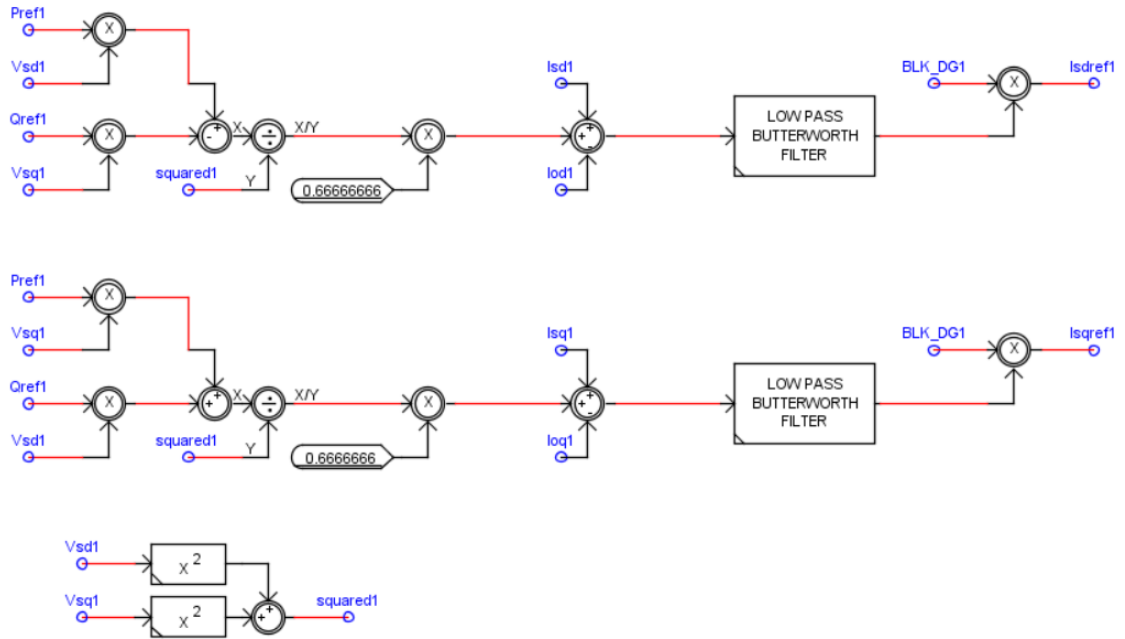
Figure A-13: Internal Component of Power Controller
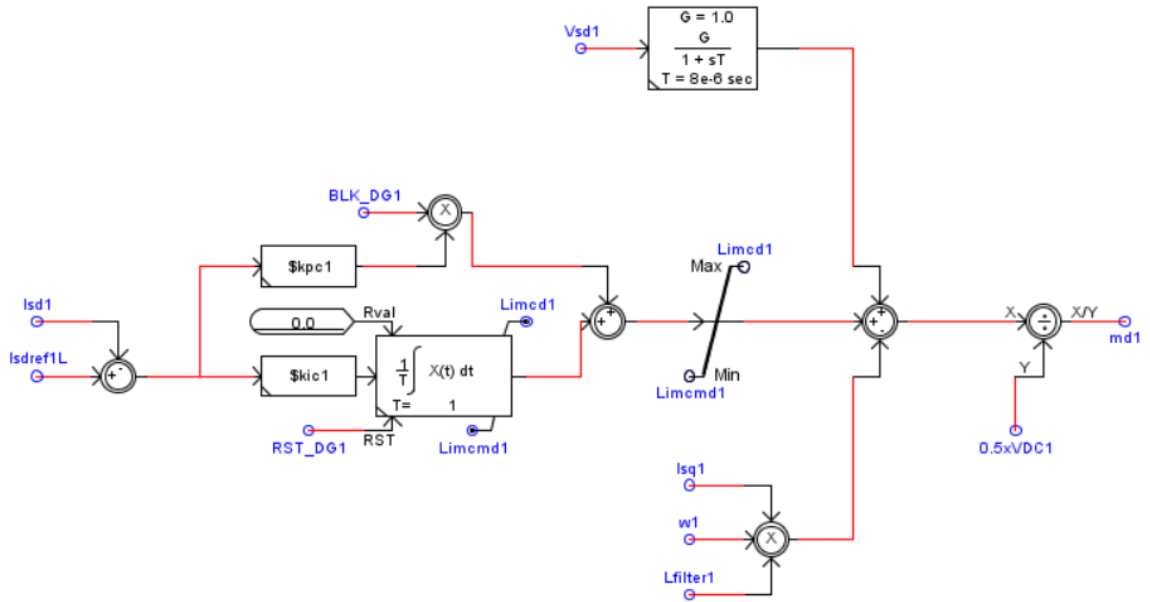
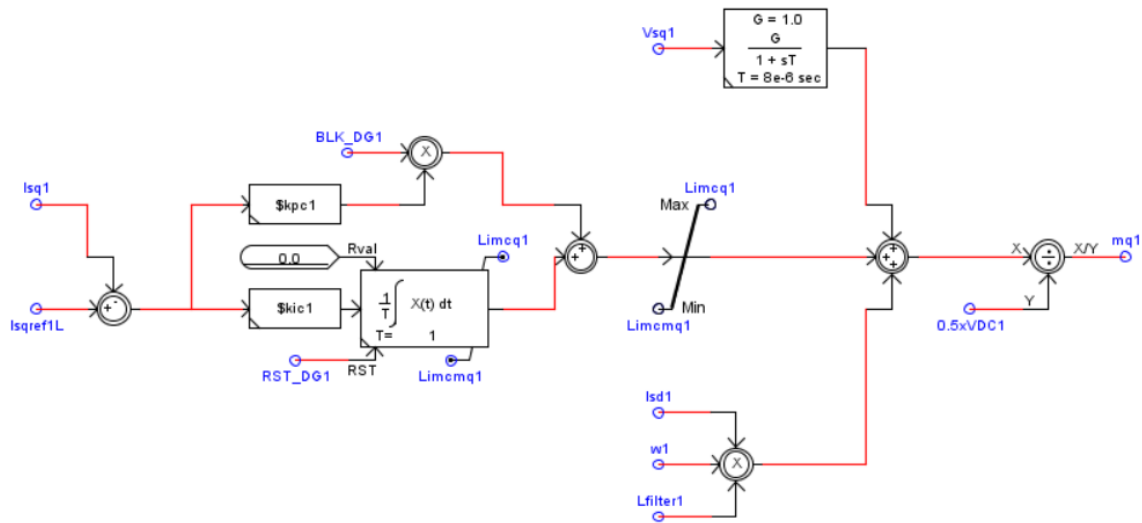**Figure A-14: Internal Component of d-Axis Current Control Loop**

197

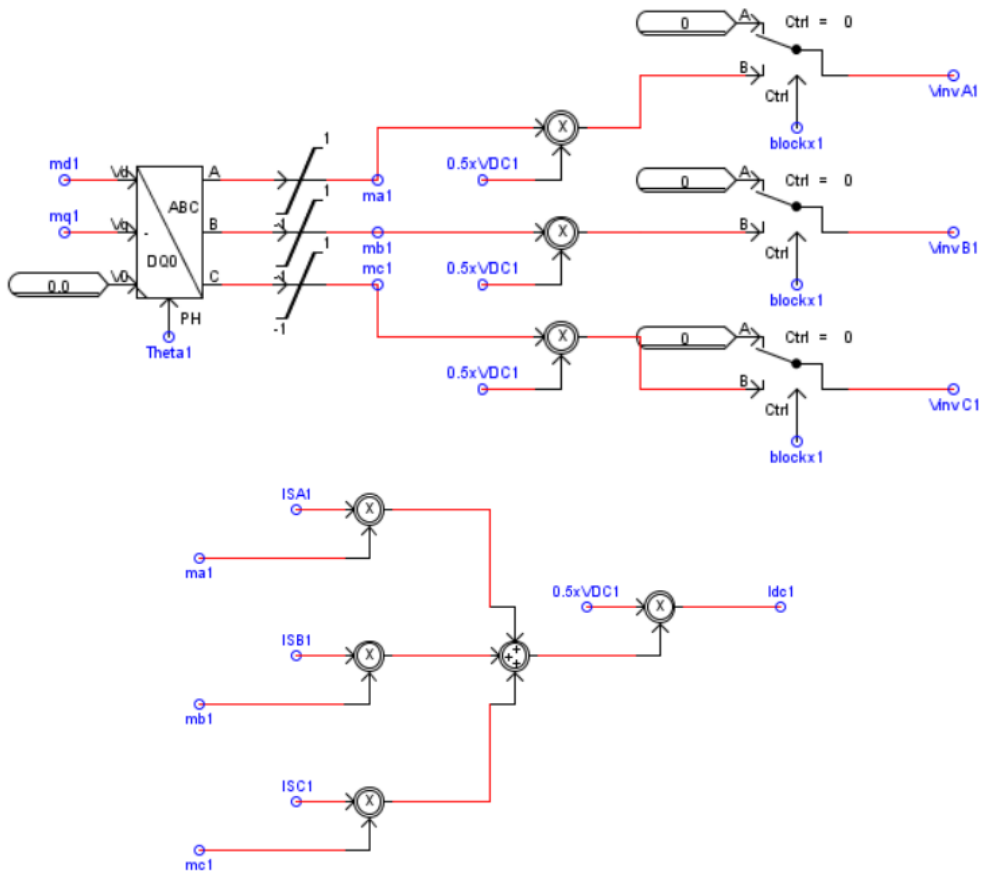**Figure A-15: Internal Component of q-Axis Current Control Loop**

Figure A-16: Internal component of Inverter AC side Voltage and DC side Current Equivalent Model

198

A.7   Circuit Breaker

Circuit breaker model is used directly from RSCAD library. The three-line diagram view is shown in Figure A-17.

Figure A-17: Three Phase Circuit Breaker Model from RSCAD library

A.8   Circuit Breaker Control Logic

Circuit Breaker control logic (trip/close) is shown in Figure A-18. The breaker Control block is a pre-built component from RSCAD library. The Circuit breaker can be controlled using the open/trip pushbutton or it can receive external trip commands.
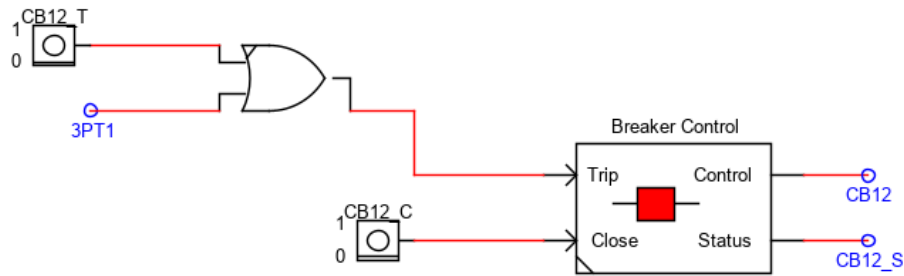

Figure A-18: Circuit Breaker Control

A.9   Fault Model

The fault model is built inside RSCAD library. Figure A-19 model is shown the three-line diagram view of this component. There are two fault models, one is line to line, and the other is line to ground.
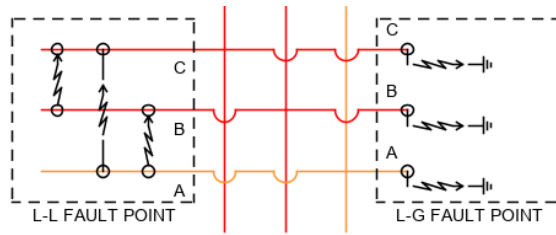
Figure A-19: Line to line and line to ground fault components from RSCAD library.

A.10 Fault Control Logic

The control circuit of Figure A-20 is used to control the fault duration, fault location, and fault resistance.
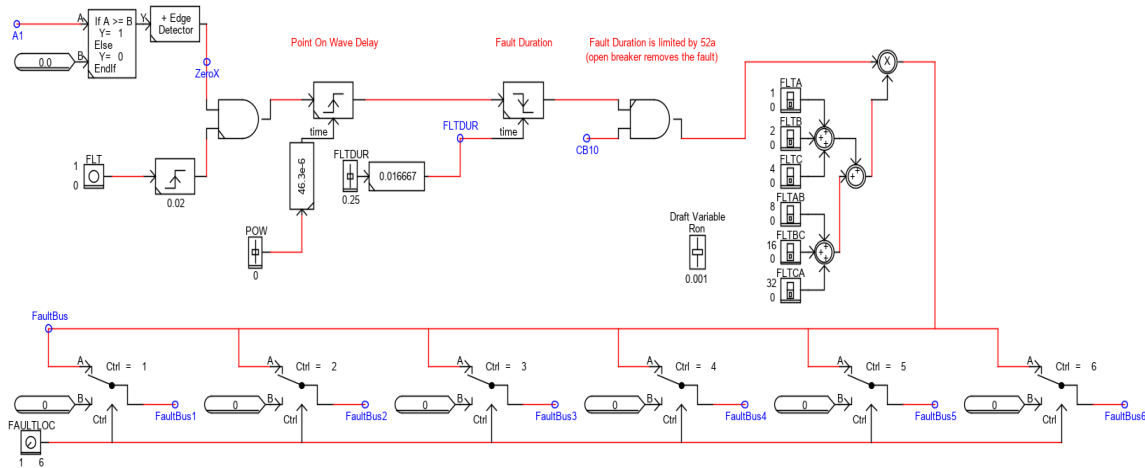

Figure A-20: Fault control logic.

A.11 Instrument Transformers

Instrument transformer models (current transformers and voltage transformers) are built inside RSCAD library and was directly used in this thesis. Figure A-21 shows the three-line diagram view of these components.
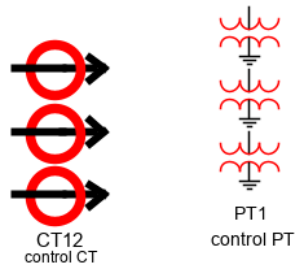
Figure A-21: Instrument Transformers Models

A.12 GTNET GOOSE Communication block

The GTNET-GSE component which is pre-built in RSCAD library is used for GOOSE communication configuration. Figure A-22 shows the GTNET-GSE component and typical input/output GOOSE message into and out from this component.
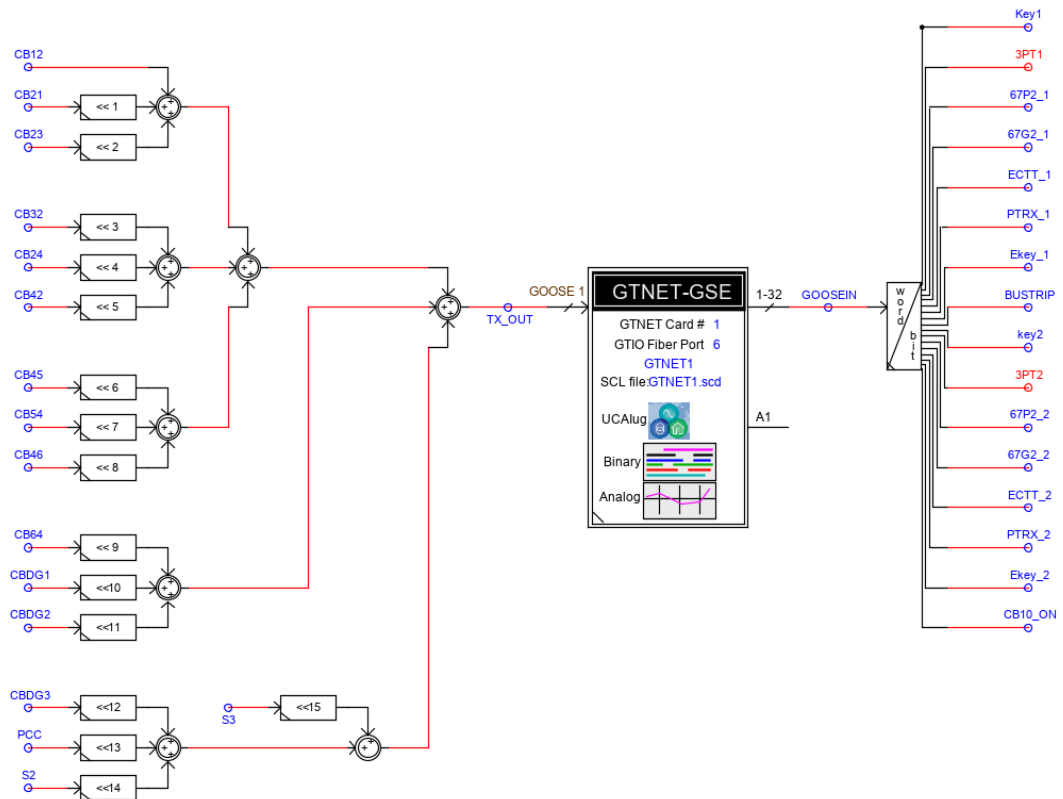

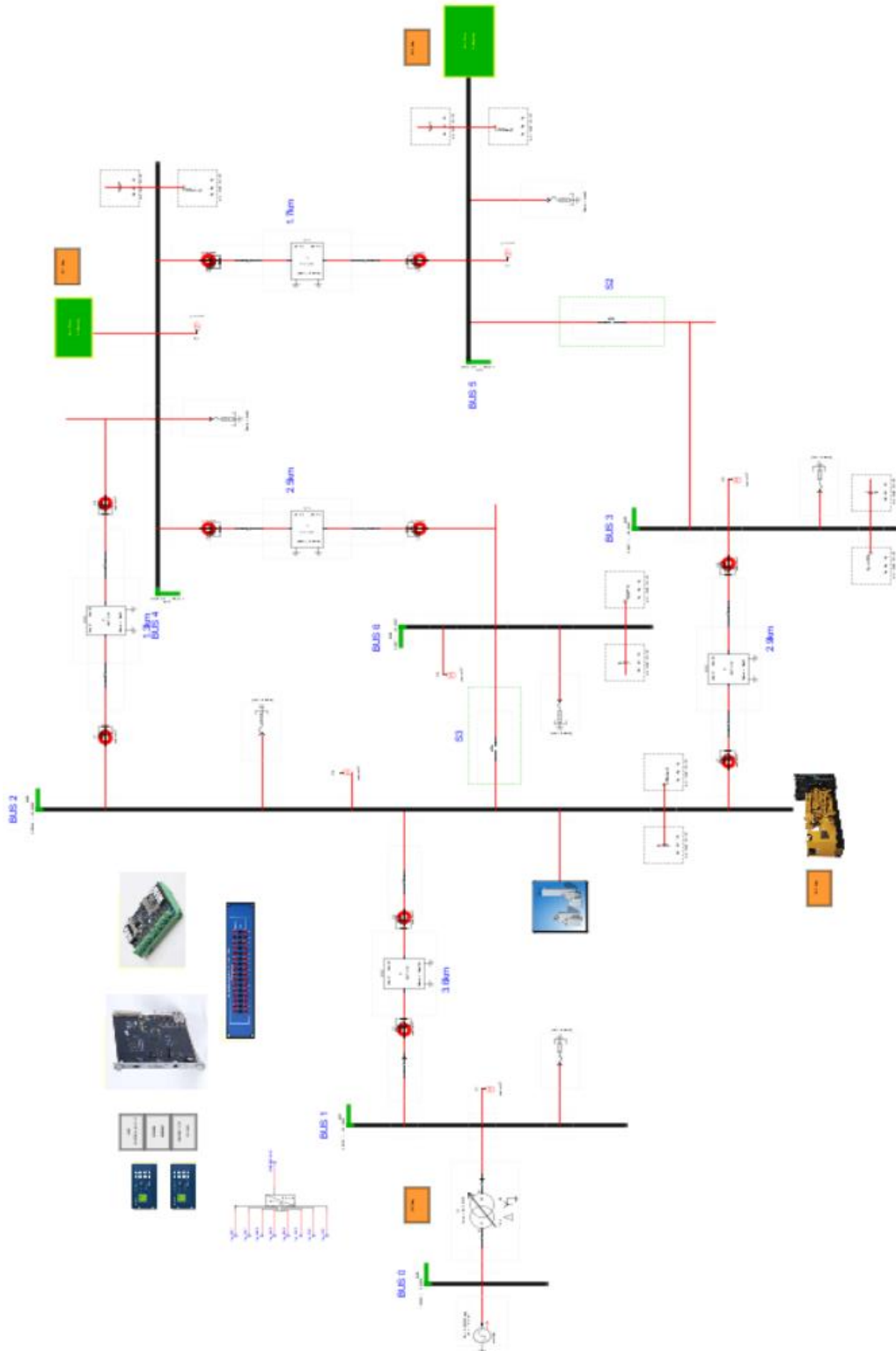**Figure A-22: GTNET-GSE model in RSCAD for GOOSE Configuration**

A.13 Microgird Model

Figure A-23: RSCAD single line diagram view of the test Microgrid.

Vitae

Name	:Muiz Muhyeddin Izzat Zaben
Nationality	:Jordanian
Date of Birth	:12/13/1988
Email	:muiz.zaben@gmail.com, sp3-muez@hotmail.com
Native Address	:Almazraa ash sharqia 652, Ramallah, West Bank, 00972IL
Academic Background	:**BSc in Electrical Engineering**
	May-2011
	Birzeit University
	Ramallah, PALESTINE,

Thesis Outcome

1. M. Zaben, M.A. Abido, "*A Pilot Based Adaptive Protection Scheme for Looped Microgrid*" (Under Preparation).

Work Experience

He is working as electrical design engineer at Wahah Electric Supply Company of Saudi Arabia (WESCOSA) since 2012. He is specialized in the design and manufacturing of LV/MV Switchgear, LV/MV Controlgear, HV relay panel, and LV distribution boards.